Final Technical Report

to

ASME Standards Technology, LLC

Gen IV/NGNP Materials Project: Task 8

DE-FC07-05ID14712

Task 8: Creep and Creep-Fatigue Crack Growth at Structural Discontinuities and Welds

Part I Task Report – Review and Assess Current Methodologies and Recommend NH Implementation

to

Mr. Jim Ramirez
Vice President, Business Development
ASME Standards Technology, LLC
Three Park Avenue
New York, NY 10016

from

Dr. F. W. Brust
Dr. G. M. Wilkowski
Dr. P. Krishnaswamy
Mr. Keith Wichman
Engineering Mechanics Corporation of Columbus (Emc^2)
3518 Riverside Drive, Suite 202
Columbus, OH 43221-1735

July 20, 2009

Executive Summary

The subsection ASME NH high temperature design procedure does not admit crack-like defects into the structural components. The US NRC identified the lack of treatment of crack growth within NH as a limitation of the code and thus this effort was undertaken. This effort is broken into two parts. Part 1, summarized here, involved examining all high temperature creep-fatigue crack growth codes being used today and from these, the task objective was to choose a methodology that is appropriate for possible implementation within NH. The second part of this task, which has just started, is to develop design rules for possible implementation within NH. This second part is a challenge since all codes require step-by-step analysis procedures to be undertaken in order to assess the crack growth and life of the component. Simple rules for design do not exist in any code at present. The codes examined in this effort included R5, RCC-MR (A16), BS 7910, API 579, and ATK (and some lesser known codes).

There are several reasons that the capability for assessing cracks in high temperature nuclear components is desirable. These include:

- Some components that are part of GEN IV reactors may have geometries that have sharp corners – which are essentially cracks. Design of these components within the traditional ASME NH procedure is quite challenging. It is natural to ensure adequate life design by modeling these features as cracks within a creep-fatigue crack growth procedure.
- Workmanship flaws in welds sometimes occur and are accepted in some ASME code sections. It can be convenient to consider these as flaws when making a design life assessment.
- Non-destructive Evaluation (NDE) and inspection methods after fabrication are limited in the size of the crack or flaw that can be detected. It is often convenient to perform a life assessment using a flaw of a size that represents the maximum size that can elude detection.
- Flaws that are observed using in-service detection methods often need to be addressed as plants age. Shutdown inspection intervals can only be designed using creep and creep-fatigue crack growth techniques.
- The use of crack growth procedures can aid in examining the seriousness of creep damage in structural components. How cracks grow can be used to assess margins on components and lead to further safe operation.

After examining the pros and cons of all these methods, the R5 code was chosen as the most up-to-date and validated high temperature creep and creep fatigue code currently used in the world at present. R5 is considered the leader because the code: (i) has well established and validated rules, (ii) has a team of experts continually improving and updating it, (iii) has software that can be used by designers, (iv) extensive validation in many parts with available data from BE resources as well as input from Imperial college's database, and (v) was specifically developed for use in nuclear plants.

R5 was specifically developed for use in gas cooled nuclear reactors which operate in the UK and much of the experience is based on materials and temperatures which are experienced in these reactors. If the next generation advanced reactors to be built in the US used these same materials within the same temperature ranges as these reactors, then R5 may be appropriate for consideration of direct implementation within ASME code NH or Section XI. However, until more verification and validation of these creep/fatigue crack growth rules for the specific materials and temperatures to be used in the GEN IV reactors is complete, ASME should consider delaying this implementation. With this in mind, it is this authors opinion that R5 methods are the best available for code use today.

The focus of this work was to examine the literature for creep and creep-fatigue crack growth procedures that are well established in codes in other countries and choose a procedure to consider implementation into ASME NH. It is very important to recognize that all creep and creep fatigue crack growth procedures that are part of high temperature design codes are related and very similar. This effort made no attempt to develop a new creep-fatigue crack growth predictive methodology. Rather examination of current procedures was the only goal. The uncertainties in the R5 crack growth methods and recommendations for more work are summarized here also.

1.0 Introduction

ASME Standards Technology, LLC is leading efforts to conduct research in support of the Generation IV/NGNP Materials project. A number of tasks have been completed and many efforts are ongoing in this program. These programs are a continuation of an existing Cooperative Agreement between ASME Standards Technology, LLC and The U.S. Department of Energy in support of the Generation IV/NGNP programs. The scope includes development of technical basis documents necessary to update and expand codes and standards for application in next generation reactor systems that operate at elevated temperatures. This is a multi-year agreement. A project structure is already in place that includes a Steering Committee, and subcontracted Task Investigators and Technical Advisors.

The GEN IV reactor concepts require structural components to operate at high temperatures in a regime where creep damage may occur and cracks may grow. The US Nuclear Regulatory Commission (NRC) has identified the lack of a quantitative methodology for evaluating creep and creep crack growth as a shortcoming of the ASME Subsection NH (Class 1 Components in Elevated Temperature Service) standard [1]. The development of elastic-plastic fracture mechanics methods and the concepts of leak-before-break (LBB) were led by the needs of the nuclear industry. These crack assessment methods are now well established and used routinely in PWR and BWR plant extension applications and new designs. Quantitative creep and creep-fatigue crack growth assessment procedures are now needed for these GEN IV developments.

The subsection ASME NH high temperature design procedure does not admit crack-like defects into the structural components. In fact, design codes generally consider defect free structures while assessment codes address flaws and their treatment. Therefore, from a code design perspective, the need for creep and creep-fatigue crack growth procedures within NH is not warranted. However, there are several reasons that the capability for assessing cracks in high temperature nuclear components is desirable. These include:

- Some components that are part of GEN IV reactors may have geometries that have sharp corners – which are essentially cracks. For instance, some of the heat exchanger designs consist of micro-process technology, which are diffusion bonded sheets with hole patterns strategically placed so as to make thousands of small passages and features. Due to the fabrication procedure, the features have sharp corners. Design of these components within the traditional ASME NH procedure is quite challenging. It is natural to ensure adequate life design by modeling these features as cracks within a creep-fatigue crack growth procedure.
- Workmanship flaws in welds sometimes occur. It can be convenient to consider these as flaws when making a design life assessment.
- Non-destructive Evaluation (NDE) and inspection methods after fabrication are limited in the size of the crack or flaw that can be detected. In fact, it can be said that every nuclear component has crack like defects of some size that cannot be detected due to limitations in NDE technology. It is often convenient to perform a life assessment using a flaw of a size that represents the maximum size that can elude detection.
- Flaws that are observed using in-service detection methods often need to be addressed as plants age. Shutdown inspection intervals can only be designed using creep and creep-fatigue crack growth techniques. While NH is meant to be a design procedure rather than a service assessment procedure, methods for crack growth analysis can be useful.

- The use of crack growth procedures can aid in examining the seriousness of creep damage in structural components. How cracks grow can be used to determine the ultimate or limit load of a component and margins on safety.

The focus of this work was to examine the literature for creep and creep-fatigue crack growth procedures that are well established in codes in other countries and choose a procedure to consider implementation into ASME NH. The currently established engineering methods for predicting creep and creep fatigue crack growth at discontinuities and welded components was thoroughly reviewed. For the most part, these procedures were developed in Europe and have been implemented into European codes. *It is very important to recognize that all creep and creep fatigue crack growth procedures that are part of high temperature design codes are related and very similar.* The differences, which are pointed out later, are mainly in how to estimate the appropriate creep crack growth parameters. As such, the choice of the procedure to implement within ASME NH is made based on applicability to nuclear components, validation data bases, ongoing support for the methods, maturity of the procedures, options for computer codes to apply the methods, among others.

These procedures examined in this effort include:

- British R5. The R5 standard [2], which was an extension of the low temperature crack assessment procedure R6, is the oldest and most established code procedure available. The procedures were developed in the 1980's in response to the need for high temperature crack assessment of UK reactor designs which operate at higher temperatures compared with the US PWR and BWR designs. R5 also has a crack initiation procedure, called Time Dependent Failure Assessment Diagram (TPFAD approach) also since crack initiation can be important for minimal fatigue conditions.
- The French RCC-MR (A-16) procedure [3]. This method, which is quite similar in concept to the R5 method and appears to have followed the philosophy of R5 from the beginning, has seen extensive development in the 1990's. The main difference to R5 is the methods used to estimate the reference stress methods used.
- API 579 approach. The API fitness for service (FFS) standard provides guidance for conducting FFS assessments using methods specifically prepared for equipment in the refining and petrochemical industry, although they are used in other industries as well [4]. The specific approach for creep and creep-fatigue crack growth has recently been implemented and a computer code has been developed for FFS assessment for both time dependent and time independent crack growth. The methods again are similar to the other approaches.
- BS-7910 code. The BS-7910 code, which is an advanced creep-fatigue crack growth assessment approach [5] similar to R5 and A16 (in fact many portions come from the R5 code), provides assessment and remaining life estimation procedure that can be used at the design stage and for in service situations.
- The German KTA method. KTA does not appear as well established as R5 or A16 as a creep-fatigue crack growth assessment code. The 2-criterion method regards crack initiation as the most important factor in life assessment and does not deal with the crack growth regime [6]. The flat-bottom-hole approach (FBH) represents a crack detection and characterization method. The approaches used in Germany follow along the lines the R5 and A16 approaches, and are not discussed further here. It is important to note that

crack incubation time can take up to 70% of the life, especially under conditions where fatigue is not important.

- Several other code approaches exist in other countries, many of which are summarized and compared in [7], also are available. However, these approaches either follow R5 or A16 or do not consider crack growth explicitly.

Damage based methods used in some industries such as the Omega Method can be quite valuable for creep-fatigue life assessment as well. The creep-crack code procedures discussed above are related to each other. Most currently established methods use variations of K, C* (C_t), and reference stress, all of which will be discussed. An engineering approach based on these parameters is natural since estimates are based on extensions of methods and solution handbooks on well-established elastic-plastic fracture. Hence, new users of the NH crack growth code that are familiar with elastic-plastic methods should adjust rather quickly. It is anticipated that a step-by-step procedure will be recommended for code implementation.

2.0 Creep and Creep-Fatigue Crack Growth Fundamentals and Engineering Methods

Damage nucleation usually begins with the development of small voids. These voids begin to grow via both diffusion mechanisms along the grain boundaries and with dislocation creep within the grains. At high stresses as occur near a material discontinuity or crack tip, a particle/matrix de-cohesion process with rupture could be predominant. Voids eventually link-up to produce micro-cracks and then macro-cracks. The treatment of crack growth, which eventually leads to component failure, is the purpose of this effort. These issues have been studied for more than 30 years and engineering methods for predicting creep crack growth now exist. Implementation of established crack growth methods is the purpose of this effort. However, before proceeding it is important to point out that more work is needed to reduce the conservatism in the current engineering methods of life prediction. Moreover, it is not clear that the current creep/fatigue crack growth procedures will perform adequately under GEN IV conditions and materials. While the engineering methods that have emerged to predict creep-fatigue crack growth lives are generally accepted it is important to point out that these methods are not appealing from a theoretical standpoint due to the assumptions made. The research needs to improve these methods will be discussed at the end of this report. This is especially true when trying to extend the well established R5 rules to conditions where experience and/or validation has not been made yet.

2.1 High Temperature Damage Progression and Crack Growth: Theoretical Considerations

Damage nucleation, growth, damage link-up, crack growth, and breakage are the typical progression of failure for components that operate at high temperature. Damage nucleation begins (see Figure 1 below) with the nucleation of a cavity at a size scale at the higher end of the nano-scale level (~50 to 500 nm, depending on the material). Early in the process, such nucleation and growth phenomenon is explained by diffusion of atomic flux from the cavities to the grain boundaries, along with grain boundary sliding (to a lesser extent)[1]. As time proceeds, nonlinear viscous flow (creep) occurs, and, depending on the local stress state, eventually overrides the diffusion growth process, especially as the neighboring voids approach each other. This is fortunate since engineering creep crack

[1] Practical engineering methods to account for diffusion based creep damage development and crack growth are in their infancy. Classical grain boundary cavitations' only can be predicted properly in an engineering assessment.

growth methods that exist today can only deal with nonlinear viscous flow type crack growth. This is also one reason that crack nucleation is very difficult to predict, as discussed later. As voids link, micro-cracks develop, link-up, and lead to a macro-crack.

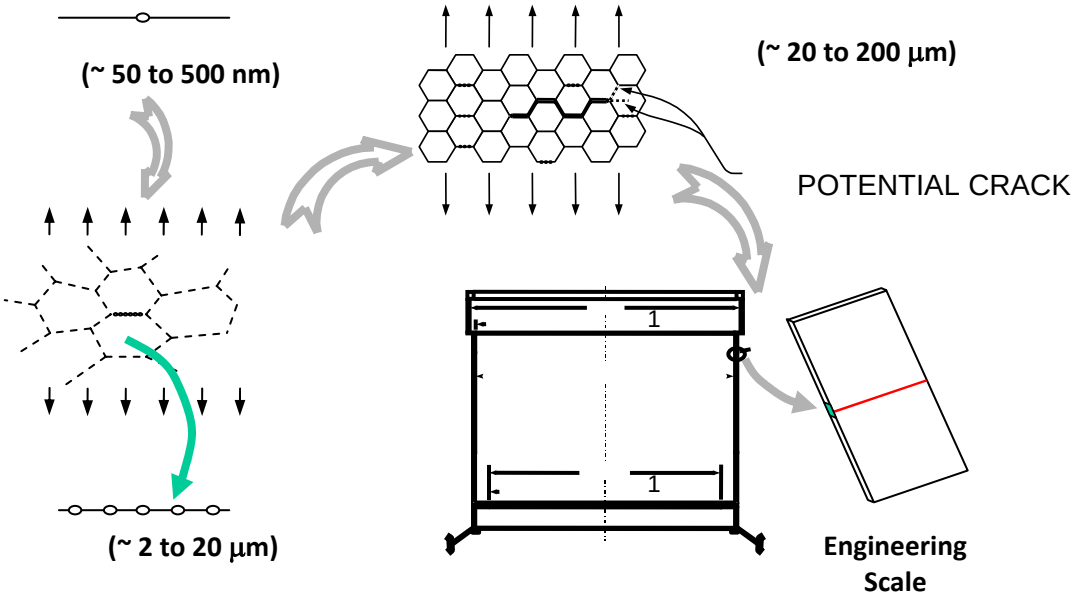

Figure 1. Scales of Creep Damage Development and Failure.

Depending on the operating conditions, the macro-crack can slowly grow during component operation, or fail quickly. The growth of this crack during high temperature cyclic load conditions is considered here.

Much of the general theoretical discussion provided above, along with limitations of current engineering approaches, was obtained through a long grant by the authors (1990 through 2003).[2] Many summary and technical papers were developed describing this work, which focused on creep-fatigue crack growth (both modeling and testing) under cyclic loading, weld modeling, high temperature cyclic constitutive modeling, and development of diffusion creep models (References [8 – 32] and many references sited therein. ***Deficiencies in the current engineering methods recommended here for possible implementation into NH, along with suggestions for further development work required to improve the present engineering creep-fatigue crack growth methods are presented at the end of this report.*** Despite the limitations, we recognize that conservatisms in the current engineering methods existing today are due to these unknowns. The methods considered are the best available today. Unfortunately, it is has not been established that the current code based methods are conservative for GEN IV conditions yet. Until enough data and validation is available for GEN IV conditions, current creep fatigue crack growth rules should be used only if an experimental validation program is undertaken.

2.2 Currently Established Engineering Methods for Creep Fatigue Crack Growth

[2] Department of Energy, Office of Basic Energy Sciences, DOE Grant No. DE-FG02-90ER14135 entitled, *An Investigation of the Effects of History Dependent Damage In Time Dependent Fracture Mechanics*, PI, F. W. Brust.

The engineering methods for predicting creep and creep fatigue crack growth are essentially an extension of engineering approaches which are used to predict elastic-plastic fracture. The methods are based on the concept that crack growth can be characterized by the strength of the asymptotic crack tip field. Creep crack growth rates can be correlated with the stress intensity factor (K), the C*-Integral, and the reference stress (used in R5) among other approaches. The forms of the creep crack growth laws typically are power-law relationships between crack growth rates and these parameters. Crack growth rates can correlate with K when creep is confined very locally to the crack tip; with C* when the creep zone is larger during secondary creep; and with C_t (or C(t)) when creep transients occur at the crack tip (C* and C_t are related); and with reference stress (which can also be related to C*). While reference stress methods are often used to estimate creep/fatigue crack growth parameters within the current code approaches, there is some evidence that these methods are not accurate for all crack shapes. This is the topic of research at present. However, finite element methods can always be used to obtain the crack growth parameters – although this may not always be practical. Most creep crack growth procedures used in worldwide codes are related to each other.

The C*-integral is the creep analogue of the elastic-plastic J-Integral which is used extensively to predict elastic-plastic fracture. For this reason, C*/C(t) approach is a natural parameter to use in ASME NH code procedures. The US NRC and utilities have developed a very large data base of solutions used to estimate the J-integral for through-wall and surface cracks in pipe, plate, vessels, and other nuclear power plant components. Once the creep material constants in the form of power-law fits of creep data are available, these estimation schemes can be used directly to obtain C* and provide predictions of creep crack growth. Moreover, most commercial finite element codes permit the easy calculation of both C* and C_t, so obtaining this parameter for a creep-fatigue crack growth prediction for cases where compiled solutions are not available is not difficult. It is our view that extension of the J-integral based methods for incorporation into NH based on C* is natural since NRC, contractors, and utilities are well versed in these methods and furthermore J-based solutions are also in the ASME Boiler and Pressure Vessel code (e.g., Section XI flaw evaluation procedures).

2.3 Creep Fatigue Crack Growth Methods for NH Code

For conditions where time-dependent deformation does not occur, fatigue crack growth rates can be correlated with K using the Paris law, the Forman equation (including mean stress effects), and many other fatigue laws. When creep deformation can occur at the crack tip, the fatigue crack growth rates are strongly affected. Hold times at load increase crack growth rates. A higher mean stress will increase crack growth rates, which can be important in and near welds or high-constraint cracks. The NH code has conservative procedures for combining the damage caused by fatigue and creep in un-cracked structures. For crack-growth predictions, the separation of creep and fatigue crack growth damage is also the accepted procedure with well established engineering rules within R5 for materials where validation results are available. We anticipate that rules of this form will serve as the basis of the new NH rules if and when they can be accepted for GEN IV conditions. It turns out that low-frequency creep conditions permit crack growth correlation with C*, and high-frequency fatigue correlates with ΔK. In the transition regime, the current rules must be shown to be adequate for code use. However, the precise implementation into ASME code NH or other division should be delayed until validation is made for GEN IV materials. Alternatively, R5 rules should only be permitted for materials and conditions where validation has been made. These conditions are mainly those experienced within the gas cooled reactors within UK. For low cycle fatigue, where there is non-negligible plasticity at the crack tip during reloading, the cyclic J-integral parameter may be more appropriate. Despite theoretical concerns with

Dowling ΔJ based low cycle fatigue crack growth predictions, it has performed reasonably well in engineering predictions.

3.0 Fracture Mechanics Basis for Engineering Creep-Fatigue Methods

The engineering creep/fatigue crack growth methods depend on both elastic and creep fracture mechanics parameters. These parameters are summarized in this section.

3.1 Elastic Fracture Considerations

Fracture mechanics began in the 1920's with the famous A. E. Griffith study of glass fracture. Griffith pondered the question as to why glass does not have the theoretical strength of the molecular bond and concluded that 'cracking' was the cause. George Irwin is the father of modern fracture mechanics with his definition of the stress intensity factor needed for his famous studies of naval fractures in the 1950's and 1960's. Irwin identified three 'modes' of fracture which are illustrated in Figure 2. Mode I type fracture is the opening mode defined by stresses which directly open the crack faces in the direction of the applied load. Modes II and III are shear modes with Mode III representing the 'tearing' type analogous to ripping a sheet of paper. All three modes of fracture are possible at the same time – however mode I type fracture often dominates. *In fact, all engineering creep crack growth methods available today require that Mode I crack growth dominates.*

Irwin applied the elasticity procedures of Westergaard to write the asymptotic solution of the

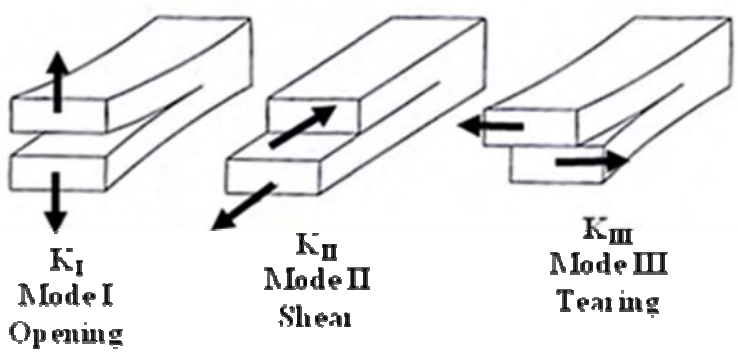

Elastic

$$\sigma = K_I \left[f(\theta) / \sqrt{2\pi r} \right] \qquad (1)$$

Figure 2. Elastic crack tip fields.

crack tip stress fields as (for Mode I type fracture) as seen in Figure 2, equation 1. Equation (1) then provides the stress field for every point (r, θ) near the crack tip. The figure inserted above Equation (1) illustrates the geometric definitions and 'r' represents the radial distance from the crack tip and 'θ' represents the angular distance around the crack for the radial coordinate system centered at the crack tip[3]. f(θ) is a known function of sine and cosine functions. K_I is called the stress intensity factor (mode one hence the designation 'I') since; if one knows its value (K_I units are psi-in$^{1/2}$, Mpa-m$^{1/2}$, etc.), then one can determine if the crack will be stable or grow. *If $K_I = \boldsymbol{K_c}$ then the crack grows, where $\boldsymbol{K_c}$ is obtained from tests on fracture specimen in the laboratory*. K_I depends on crack size, crack shape, material parameters, and loading conditions. Tables of K are available in all of the code methods, including R5 and A16. Alternatively, one can always calculate K using finite element methods for the geometry and load condition of interest. One can write similar equations for the other modes of fracture with the same conclusion: if one knows the stress intensity factor(s), then one knows if the crack will grow or not.

When time independent plasticity dominates near the crack tip, i.e., when the plastic zone at the crack tip is not embedded within the elastic crack tip fields, a nonlinear parameter called the J-integral is used to characterize fracture. As for the elastic case, J represents the strength of the asymptotic crack tip fields for a for a power law hardening material where the crack experiences proportional loading (replace 'C*' in equation (3) of Figure 4 by 'J'). For this case, the crack grows when $J = J_{IC}$, where J_{IC} is the measured fracture toughness. J-tearing theory applies for small amount of crack growth as well. The commercial nuclear industry in the US (and in many other countries) bases crack growth assessment and leak before break rules on J-Theory. In practice, especially in the nuclear industry, J-tearing theory is applied far beyond its theoretical basis into crack growth ranges and non-proportional load ranges that greatly violate the strict theoretical limits with success. The main reason it is accepted far beyond its theoretical limits is that extensive fracture test data in many geometries (specimens, pipe, vessels, elbows, etc.), and in many nuclear materials validates it use as a conservative predictive tool. This will be discussed later as well with regard to creep/fatigue fracture methods since the currently used methods violate the theory as well.

3.2 Fatigue Crack Growth

Fatigue of metals became a concern in the early 1950's when the British de Havilland Comet, the world's first commercial jet aircraft, experienced catastrophic service failures that were identified as metal fatigue. Structures are now designed to prevent fatigue failures throughout their expected life. There are two general philosophies of fatigue design, stress based and fracture mechanics based design.

Stress Based Fatigue Design. The standard ASME NH procedure for the fatigue portion of life in high temperature design is based on developing an 'S-N' or Goodman curve type of approach. 'S' represents the cyclic stress range of a structural part and 'N' represents the number of cyclic loads to failure. This is combined with creep damage and interaction in NH using the well known and validated procedures in [1].

Fracture Mechanics Based Fatigue Design. Another type of fatigue weld design philosophy is based on fracture mechanics. Paris and colleagues in the early 1960's observed that fatigue life can be correlated with the stress intensity as

[3] Note that this equation implies that the stress near a crack tip is infinite since 'r' is in the denominator. This is of course not possible. Actually, plasticity near the crack tip reduces the stress to a physically realistic value but is still characterized by the stress intensity factor.

$$\Delta a/\Delta N = C(\Delta K)^n. \quad (2)$$

Here ($\Delta a/\Delta N$) represents the amount of crack growth, 'Δa' that occurs for every load cycle, 'ΔN'. The sigmoidal curve plotted in Figure 3 in log scale mode illustrates this. From a laboratory cyclic fatigue test of a cracked specimen, one can plot the amount of crack growth per cycle versus the range of stress intensity factor, ΔK. This curve may be divided into three regions. At low stress intensities, Region A, cracking behavior is associated with a threshold value, below which the crack does not grow. In the mid-region, Region B, the curve is essentially linear. Finally, in Region C, crack growth rates are high and little fatigue life is expected. Most of the current applications of LEFM (linear elastic fracture mechanics) concepts to describe crack growth behavior are associated with Region B. In this region the slope of the log **$\Delta a/\Delta N$** versus log **ΔK** curve is approximately linear and lies roughly between 10^{-6} and 10^{-3} in/cycle, depending on the material. In equation (2), C and n are constants with n usually between 3

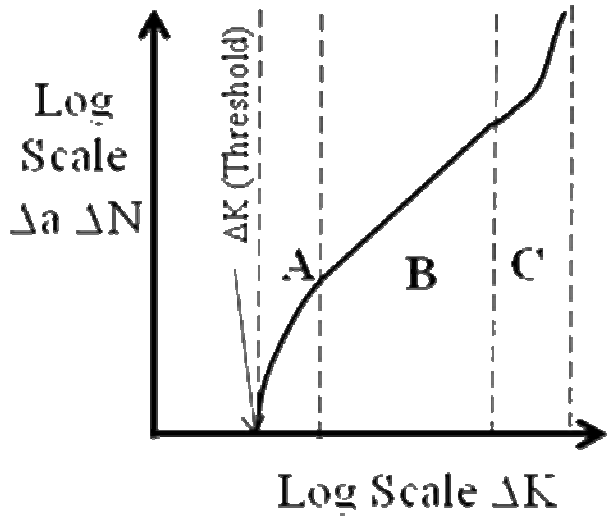

Figure 3 Fatigue Crack Growth Relationship.

and 4.

In using the fracture mechanics based philosophy to fatigue design, one models fatigue crack growth using equation (2) and failure is predicted when $K = K_c$, or when $J = J_c$ if plasticity is important. The fracture mechanics approach to fatigue life is used in industries which use a 'damage tolerant' approach to life design. A damage tolerant approach recognizes the fact that cracks are present in the structure and ensures that the crack will not grow to failure within the design life of the structures with a safety factor applied. This method is often used for aerospace and other high fidelity design applications where non destructive evaluation methods (such as ultrasonic methods) are used to measure and monitor crack growth during the life of the structure.

All of the creep-fatigue crack growth methodologies are based on interaction between the creep and cyclic crack growth. The fatigue relationship is obtained by testing at the temperature of interest. It is seen that the fracture mechanics and NH design approaches are analogous to each other.

3.3 Creep Crack Growth

Referring to Figure 4, for a power law type creep law, a creep zone will develop at the crack tip ('blue' zone in Figure 4) and grow with time even under constant load. During early times, or for low loading conditions, the creep zone may be small. For this case, the creep crack growth rates can be correlated with the stress intensity factor of section 3.1.

$$\sigma_{ij} = \left(\frac{C^*}{r}\right)^{\frac{1}{n+1}} f_{ij}(\theta, n) \qquad (3)$$

$$C^* = \int_\Gamma \left[\dot{W}\,dy - T_i\left(\frac{\partial \dot{u}_i}{\partial x}\right)ds\right] \qquad (4)$$

$$C(t) = \int_{\Gamma-0} \left[\dot{W}\,dy - T_i\left(\frac{\partial \dot{u}_i}{\partial x}\right)ds\right] \qquad (5)$$

$$\dot{W} \equiv \int_0^{\dot{\varepsilon}^c} \sigma\, d\dot{\varepsilon}^c$$

$\dot{W}$ is strain energy rate density

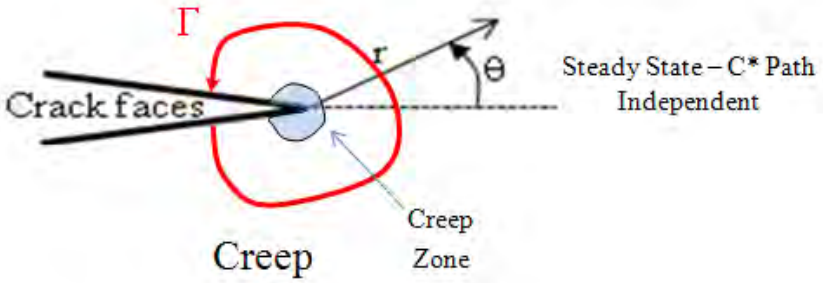

Figure 4 Asymptotic creep crack tip fields.

For steady state creep, where the creep zone is large and dominates the deformation, the asymptotic crack tip field can be written as the HRR field [33, 34] (Hutchinson, Rice, Rosengren) shown in equation (3) in Figure 4. Using the crack tip coordinate system shown in the illustration at the bottom of Figure 4, it is seen that the asymptotic stress field depends only on 'r' (the distance from the crack tip),'n'(the power law exponent on stress for the simple power creep law), other geometric parameters, and C*. Analogous to the discussion of the stress intensity factor, here the strength of the asymptotic field depends only on C*. If one can calculate C*, then the crack tip severity can be determined. For large scale creep and steady state conditions, C* can be calculated as a line integral, as seen in Equation

4. In Equation 4, C* is evaluated as a path independent integral along a path, Γ, which circles the crack tip as seen in the bottom illustration in Figure 4. Here 'x' is in the direction of crack growth, 'y' is perpendicular to this, T_i and u_i are tractions and displacements (i = 1; 'x', i = 2; 'y') calculated along Γ, and W is strain energy rate density, also defined in Figure 4. In practice, C* can be easily estimated or calculated using numerical methods. In practice, C* values are tabulated for many types of geometries for the engineering crack growth methods such as R5 and A16. Indeed, due the direct correlation between the HRR field for elastic-plastic fracture and creep fracture, any estimation technique or tabulation of the J-integral (used for elastic-plastic fracture) can be used directly to estimate C*. The last 20 years have seen many estimation methods and tabulations of J for nuclear type components (pipe, vessels, elbows, nozzles, etc.). Therefore, in practice, C* is not difficult to obtain without using numerical methods.

For regions where non-steady creep persist, the C(t) parameter shown in Equation (5) of Figure 4 is used. This is identical to C*, except that the path, Γ, is calculated in the limit as the size goes to zero. As with C* estimation, C(t) (or C_t), can be easily estimated using reference stress techniques, which are discussed later with regard to the R5 approach.

Therefore, the creep and creep-fatigue crack growth rates are calculated using these parameters. As with NH, interaction between fatigue and creep crack growth can be included. It is important to note that the engineering creep crack growth predictive methods are also valid for creep laws that are general, although the asymptotic interpretation of meaning is obscured. It is also claimed in the crack growth procedures that the methods are also applicable to creep laws that do not experience any secondary creep. Again for this case, the theoretical interpretation is lacking. Moreover, we are not certain that this is generally true. As will be summarized later, more work is needed to study this phenomenon. This is important since some new high temperature materials may not experience secondary creep for all temperatures.

4.0 Review and Summary of Current Engineering Methods

The currently established code based engineering methods for predicting creep and creep fatigue crack growth at discontinuities and welded components was thoroughly reviewed. All established creep-crack code procedures are related to each other and so the choice of method is difficult. The main difference is how crack initiation is treated. As summarized in the last section, all currently established methods use variations of K, C* (C_t), and reference stress as previously discussed to make creep and creep/fatigue crack growth predictions. The procedures used for elastic-plastic fracture analysis are much more established and have more clear differences in them compared with creep fracture so such a choice would be more difficult. An engineering approach based on the above parameters is natural since estimates are based on extensions of methods and solution handbooks on well-established elastic-plastic fracture. Hence, new users of the NH crack growth code that are familiar with elastic-plastic methods such as those in Section XI should adjust rather quickly. Some of the issues that were addressed in this code implementation study include the following.

- Rules for determination of creep-fatigue crack growth interaction must be incorporated.
- The ductility exhaustion method for estimating creep crack damage for multi-axial stress states and discontinuities other than cracks should be considered.
- Creep–fatigue crack initiation in initially defect free components and the growth of flaws by creep and creep–fatigue mechanisms.

- Possible shakedown effects for structural assessment and relaxation of residual stresses.
- Creep crack initiation time should be considered since, for some cracked structures, the time to incubation can be a large portion of the crack growth life. Neglecting crack initiation is conservative. For conditions where fatigue loading is important, neglecting crack initiation is warranted since initiation predictive methods under combined creep/fatigue are not considered to be always conservative.
- Multi-axial stress effects, tri-axial stress effects, and crack constraint effects (plane stress, and between conditions).
- The treatment of the effects of crack closure during creep-fatigue growth.
- For treatment of weld residual stresses, it is noted that weld residual stresses play a major role in some current issues of corrosion in nuclear plants. It is well known that creep cracks can nucleate from relaxation of weld residual stresses alone.
- Incorporate rules for inclusion of plasticity effects in combination with creep under some circumstances.
- Consider the effects of diffusion creep issues. It turns out that none of the engineering methods account for this effect adequately. Moreover, including a diffusion creep component is a considerable challenge for engineering assessments due to its complexity.
- Established procedures for testing and obtaining material parameters must be clear. This includes obtaining creep constants, creep crack growth laws, fatigue laws, and interactions.

Material properties need to include: elastic properties, elastic-plastic properties, tensile creep rate curves, and crack growth material parameters. Properties for many nuclear materials such as stainless steels and Cr-Mo steels are available in the literature. Some material data is available for IN 617 and 230 in the literature and there is much proprietary data for these materials (especially for IN 617), some of which may be available. Plans for incorporating material data into the creep crack growth portion of NH will be developed and outlined.

4.1 Overview of Engineering Creep Methods

Five different methods for creep-fatigue crack growth assessment were briefly summarized in Section 1.0, the introduction. These were R5, A16, API 579, BS 7910, and KTA. Here we provide a little more detailed description of R5, A16, and API579. The KTA method is very basic, has not been fully developed and is mainly concerned with crack initiation (although for some structures which experience no or little fatigue, crack initiation times dominate life). BS 7910 is very similar to R5 – in fact many parts of the standard were taken directly from R5.

R5 Approach

The R5 approach [2] was developed specifically for use in nuclear and fossil fueled power plants in the UK by British Energy. British Energy pioneered the development of a code approach for handling creep-fatigue crack growth in high temperature structures. Indeed, the theoretical development of the method is summarized in the book by Webster and Ainsworth, two of the main R5 code developers [35].

The basic ingredients required for an assessment are: (i) the operating conditions; (ii) the nature of the defects; (iii) materials data; and (iv) structural calculations to correlate materials data tests with the behavior of complex structures. This information may be used to assess whether a defect of a given size will grow to an unacceptable size in a given service life under a given loading history. A step-by-step procedure (discussed in the next section) is written in a form which addresses assessments of this type. Detailed methods for following each step are provided with further background information on

materials data and structural calculations being included in Appendices. Worked examples illustrating application of the procedure are given in Appendices as well. The procedure represents the current state of the art. The status of the procedures and areas where care needs to be exercised in implementation are also discussed. This includes a list of changes from previous issues of R5.

The procedure can readily be adapted to consider assessments of various types, perhaps for a sensitivity analysis:

(a) The loadings which give a life equal to a given service life.

(b) The initial flaw size which will just grow to the maximum acceptable size in a given service life (and hence the margin for a given flaw size).

(c) The combinations of materials properties, geometry and loadings for which crack tip behavior has a negligible effect on lifetime.

A separate procedure in R5 also assesses whether or not a small, defined crack extension will occur in the required service life. This is the new time dependent failure assessment diagram (TPFAD) approach, which can be used to predict crack initiation. The procedure uses a failure assessment diagram approach similar to that in R6, which has long been used in UK for elastic-plastic fracture. Another procedure uses the calculation of a stress at a small distance ahead of the crack tip, the σ_d approach, which is also part of A16 [3], to assess whether significant crack extension occurs in the required service life (crack initiation). If the predicted crack growth in service is unacceptable, then the choice is:

(i) to remove some of the uncertainties in the input data;
(ii) to use an alternative assessment procedure or
(iii) to take remedial measures.

One alternative assessment procedure is to rely on inspection to limit failures to statistically acceptable numbers. The approach is only acceptable when inspection is relatively easy and when there are large numbers of similar components which can be sampled. Another possible alternative approach is given where the probability of failure can be determined. This relies on knowledge of the probability distribution functions of the variable input parameters, such as creep crack growth rate and creep strain behavior.

Two different methods of calculating creep-fatigue crack growth are given in this procedure. The method to be applied depends on both the defect size and the type and severity of the applied loading. In Method I, cyclic and creep crack growth rates are calculated separately and the total rate of crack extension taken as the simple sum of the two rates. For cycles in which strict shakedown is achieved, and significant thermal shock loading is absent, it is adequate to base the fatigue assessment on the elastically calculated stress intensity factor range, ΔK. For certain cases in which the loading is more severe and cyclic plastic deformation occurs, the value of ΔK needs to be modified to take account of plasticity by means of the parameter ΔJ. Creep crack growth during the dwell is determined from the C^* parameter. In Method II, the defect is required to be sufficiently small to be embedded in a cyclic plastic zone, as for example for severe thermal cycling; the structure satisfies global shakedown as defined. A crack growth rate law is derived by combining the creep damage occurring during a dwell with a high strain fatigue crack growth law. This avoids the complication of having to define fracture mechanics

parameters such as ΔJ or C*. The high strain fatigue law can also be derived from continuous cycling endurance data corresponding to the initiation of a crack of a specific size in the defect-free structure. The approach assumes that creep influences the cyclic contribution to crack growth and that no explicit calculation of creep crack growth is then required. Guidance on the choice of appropriate method for calculating crack growth is given in this procedure. The basic deterministic procedures of R5 require an end-of-life margin to be determined but do not otherwise contain margins or reserve factors. Confidence in the assessment is obtained by the use of lower and upper bound materials data as appropriate and by introducing a measure of conservatism in the analytical calculations. Additional confidence should then be gained by assessing sensitivity of predicted life to variations of input parameters.

The R5 method is presented in a binder which details each step of a creep/fatigue life prediction. The procedure is obtained from British Energy for an original fee and yearly updates can be obtained for a much smaller yearly fee. A computer code can be obtained from British Energy which aids in R5 analyses. Limited material data is available in R5 so often the user must obtain their own data from tests or obtain it from the literature.

RCC-MR (A16)

The French A16 procedure is quite similar to R5 and in fact some of the procedures were taken directly from R5. The main difference is the way crack initiation is determined and the choice of the reference stress. A16 has detailed and complete procedures for determining the reference stress. As discussed later, the reference stress is a key ingredient in the estimation procedures. This procedure is also considered state of the art. Many of the specific differences between R5 and A16 can be seen in the recent summary work of S. Marie et al. [43], which spell out a number of stress intensity factor solutions and reference stress procedures. With the purchase of British Energy by the French utility Electricite De France (now called EDF Group), the merger of R5 with A16 is quite possible.

API-579 Approach

As with ASME, the API construction code does not provide rules to evaluate a component containing a flaw or damage that results from operation or after initial commissioning. Fitness-for-service (FFS) assessments in the petroleum industry are quantitative engineering evaluations that are performed to demonstrate the structural integrity of an in-service component containing a flaw or damage. API 579 was originally developed to evaluate flaws and damage associated with in-service operation. While API 579 FFS procedures were not originally intended to evaluate fabrication flaws (or 'design' flaws), these procedures have been used for this purpose by many Owner-Users of petroleum manufacturing and transportation products. The API fitness for service standard provides guidance for conducting FFS assessments using methods specifically prepared for equipment in the refining and petrochemical industry. As with many codes, three levels of assessment are possible, with higher level assessments (level 3) being the least conservative but requiring an expert engineer. API 579 requires a remaining life assessment to be made for the damaged component and this forms the basis for in service inspection intervals. As with many assessment codes, API 579 includes a step by step method with 8 steps for making a creep/fatigue crack analysis. The types of damage covered by API 579 include metal loss, corrosion and blistering, weld misalignment, assessment of crack-like flaws, including those operating in the creep regime of concern here.

A level 3 expert assessment permits the use of alternative FFS procedures including R-5, R-6, BS-7910, EPRI J- and C*-integral approaches, and other methods. As with other creep-fatigue fracture assessment codes such as R5, API 579 has appendices which provide stress intensity factor solutions and

reference stress solutions that are necessary to perform a creep crack growth assessment. The methods in API 579 for creep-fatigue crack growth assessment are rather newly implemented. These procedures could be used here but the methods are more suited for equipment used in the refining and petrochemical industries. R5 was specifically developed for use in the nuclear field.

4.2 Choice of Code Creep Crack Growth Procedure

All of the procedures were carefully examined by studying copies of the code and from a series of references. Moreover, direct discussion with some of the developers was made. With R5, face to face meetings with Kamran Nikbin of Imperial College in London (and some of his colleagues), as well as e-mail discussions with R. Ainsworth of British Energy were made. In particular, Nikbin has made direct comparison of R5 with all of the other approaches. Both have been intimately involved the development of R5 from the beginning in the 1980's. Discussions with C. Faidy of EDF Group regarding A16 and E. Keim (German code) were made as well. Faidy has made it clear that since EDF (French utility where Faidy works) has acquired British Energy, there will likely be more interaction between R5 and A16 in the future. In essence, R5, A16, API 579, and BS 7910 all work well and could have been chosen. It was a difficult choice. The most appropriate code choice for possible implementation of creep fatigue crack growth procedures into ASME NH is R5 for the reasons discussed below.

R5 was chosen because the code: (i) has well established and validated rules, (ii) has a team of experts continually improving and updating it, (iii) has software that can be used by designers, (iv) extensive validation in many parts with available data from BE resources as well as input from Imperial college's database. Some of the reasons for the choice of R5 are listed in the following bullets.

- ***A recent European project meeting called HIDA (High Temperature Defect Assessment) and also a follow on called FITNET concluded that R5 is likely to be most up to date and state of the art code for high temperature crack growth assessment compared to any of the other code procedures for creep crack growth assessment.***
- ***R5 has a team of experts who are continually improving and updating the code. This will continue into the foreseeable future.***
- ***R5 is used daily in BE plant to assess the integrity of nuclear components and it was developed with full emphasis on nuclear applications. However, it is used worldwide in other industries as well.***
- ***R5 properly deals with cracked components under the creep and creep/fatigue regimes.***
- ***R5 has methods to estimate crack nucleation (TDFAD approach).***
- ***Has an optional software system (R-code) which can be used to run the cracked high temperature code. This feature can make learning the code for new users simple. Moreover, a material data base exists in the code.***
- ***R5 has been extensively validated in many nuclear components, including piping, reactor vessels and nozzles, steam generator components, and valves.***
- ***Material data is available data from BE resources as well as input from Imperial College's database. Nikbin and Ainsworth have agreed to provide some data and more data can be obtained for a fee.***
- ***A draft A16 section used the R5 methodology to do exactly the same as R5 but only limited to the cases of interest in the French nuclear plant. It has its own database and reference stress solutions, and could be used as well. There may be some portions of A16 that may be appropriate to include in the NH implementation, especially limit load solutions.***

- ***The German code is very basic and has not really been developed. It uses a two criteria method only relevant to crack initiation. However, for some components, initiation life can dominate.***
- ***BS 7910 is essentially R5.***
- ***API 579 has just recently introduced creep crack growth. Again, it uses features within the philosophy of R5. However, the API 579 procedure has material data and methods for estimating material constants if they are not available. API 579 could be an equally good choice for possible implementation into ASME. Moreover, since there is already a relationship between ASME and API 579, it would be natural to implement API 579 procedures. However, since it follows R5 for the most part, it seems more appropriate to use R5.***
- ***The Japanese are interested in R5 but they follow ASME. They have some basic in house methods which are not developed as codes as such.***

Because the R5 approach (and all other approaches) are based on K, C*, (and their transient counterpart components (C(t), C_t) and reference stress methods, the assumptions underlying the methods need further scrutiny – especially for needs in the Gen IV program. R5 limitations, issues, and need for further information are summarized later in this report. Before R5 procedures can be implemented into ASME NH we recommend further study and validation of the methods under Gen IV loading, temperature, and material conditions.

4.3 US Nuclear Regulatory Commission (NRC) Interface

As discussed in the introduction, a main goal of this sub task of Task 8 is to assess the feasibility of addressing creep/fatigue crack growth at the design stage within NH, and at the service stage (perhaps within Section XI) as requested by NRC. As such, one task goal is to ensure that the NRC is having its needs met. This interaction with the NRC will continue. Some of the interface activities include the following activities.

- Ensure NRC agrees with approach.
- Estimates based on extensions of methods and solution handbooks used for well-established elastic-plastic fracture is natural. The NRC pioneered elastic-plastic fracture methods and implementation in the US. Since the Creep crack growth methods are related to established elastic-plastic methods, new users should adjust rather quickly.
- Consider establishing the relationship between current flaw evaluation and Leak Before Break (LBB) procedures for elastic-plastic fracture to creep fracture (SRP 3.6.3, NUREG's). While this is not a direct ASME need or requirement, it is a key important issue of concern to the NRC, nuclear plant builders, and utilities. For an LBB assessment, which is used to eliminate expensive plant equipment such as pipe whip restraint and jet impingement shields, well established procedures have been developed for elastic-plastic crack growth. For creep crack growth these procedures would be quite different. Some differences between elastic-plastic and creep fracture mechanics LBB concerns include crack instability calculations, leak rate methods through creep cracks, how to deal with an active degradation mechanism like creep (similar to the current with primary water stress corrosion cracking (PWSCC) in current PWR plants), among many other issues. Hence, while our efforts for ASME NH do not require LBB, keeping the issues in mind during NH implementation is an important issue for NRC.

5.0 The R5 Creep-Fatigue Crack Growth Method

The R5 procedure is an engineering approach to predict creep-fatigue crack growth in components which operate at high temperature. Here we provide a summary of the R5 approach, the material property needs and requirements, and a short summary of the process. An example problem is provided in the next section. Some of the description below is part of the R5 code (presented with permission of BE, Inc.).

5.1 The R5 Method

The procedure of R5 [2] is concerned with estimating the remaining safe life of a structure which is subject to creep-fatigue loading and which contains a crack or a postulated crack (for design purposes). The ASME NH code procedure does not permit a crack to be in the structural component being designed. The question then is how can this procedure be implemented within NH even if it was considered appropriate? This question is being addressed with the 2nd part of this program entitled 'ASME NH Code Implementation'. Essentially, there are several reasons why a creep-fatigue creep crack growth assessment might be desirable. These include (i) some GEN IV components may have unavoidable sharp corners (or crack like defects) from fabrication, (ii) workmanship flaws may be assumed (iii) it may be desirable to perform a life assessment with an initial flaw size defined by the maximum size non-detectable flaw that can persist after inspection, (iv) address in service observed flaws, (v) determine crack growth failure mode, and (vi) determine the amount of crack growth over a given operating period.

For the R5 approach, only Mode I loading is considered; mixed modes are not taken into account. The procedure concentrates components which operate within the global creep shakedown limit. The cyclic modes of crack propagation which occur during load changes and crack growth during dwell periods due to creep mechanisms are considered. However an indication of the approach for more extensive cyclic plastic deformation can also be accounted for. The R5 procedures were originally developed for austenitic and ferritic steels at but they have been used in recent years for super alloy materials. Some potential Gen IV materials include In 617 and other nickel base alloys. Experimental and finite element validation for a range of these materials is given in the Appendices of the R5 documentation. Defects are assumed to be in homogeneous parent or weld metal or in non-homogeneous weldments.

Crack behavior under both load-controlled and combined load- and displacement-controlled stress systems is considered. Particular advice is given in an Appendix for the cases of displacement control due to a constant applied displacement and for thermal loads acting alone. R5 does not address leak-before-break procedures for pressurized components so that LBB considerations would have to be developed separately by NRC, if desired in the future. However, LBB arguments may be constructed using, as a basis, using the failure assessment diagram procedure in an Appendix of R5.

Before proceeding it is important to point out that GEN IV applications are likely outside the validation range of R5 applications. Before R5 could be used with confidence within the ASME code framework, more validation is necessary for GEN IV applications. Section 6 will deal with this in more detail.

5.2 The R5 Step by Step Approach

Here a step-by-step procedure is set out whereby a component containing a known or postulated defect can be assessed under creep-fatigue loading. The general 13 step approach is provided in Figure 5. Both continuum damage accumulation and crack growth are addressed. The cases of insignificant creep and insignificant fatigue are included as special cases. The procedure may be applied to a component in the design stage, or where it has already experienced high temperature operation, as in an operating plant where damage has been observed or is postulated. In the case of addressing an aging nuclear component advice if given on the effect of the time at which the defect is assumed to form. Continuum damage failure (creep rupture) of an un-cracked body may be considered as a special case by omitting the steps covering crack growth and cyclic loading. However, ASME NH already addresses this. The steps in the procedure are listed below with a description. Please refer to reference [2] for the complete details of the R5 method, where many examples are provided.

STEP 1 - Establish the Expected or Actual Cause of Cracking and Characterize Initial Defect.

Establish the cause of the cracking to ensure that the procedures of this volume are applicable. The defect type, position and size should be identified. For a creep-fatigue design crack growth assessment, the expected crack size and location can be determined from the stress analysis where the highest stresses occur. The size would be the limit on the NDE confidence. For defects found in service, this process may require the advice of materials and non-destructive testing experts, particularly for the case of defects in weldments. Suitable sensitivity studies (Step 12) should be performed to address uncertainties. The detected defect should be characterized by a suitable bounding profile amenable to analysis. Defects which are not of simple Mode I type should be resolved into Mode I orientation.

STEP 2 - Define Service Conditions for the component

Resolve the load history into cycle types suitable for analysis. This includes all design cycles or for in service assessment, the historical operation and the assumed future service conditions. The service life should be defined. For the case of a component which is defect-free at the start of high-temperature operation, an estimate of the time at which the defect formed (or the crack nucleation time) can be determined. It is conservative to neglect this time. Suitable sensitivity studies should be performed to address uncertainty in the time of defect formation.

STEP 3 - Collect Materials Data

The material data needs to be defined and collected. The details of the material data necessary will be discussed in the next section. Define the materials relevant to the assessed feature including, in the case of weldments, the weld metal and heat-affected zone structures. The material properties must be appropriate over temperature range and in the correct cyclically-conditioned state. The effects of thermal ageing may also need to be considered for some materials – especially cast stainless steel. In practice, the requirements are influenced by the outcome of the tests for significant creep or fatigue in Step 6 below. Time-independent material properties are required for the stability analyses performed in Steps 5 and 11. It should be noted in particular that fracture toughness properties are required for creep-damaged material, if available. If not available, they must be estimated from creep undamaged material. It is important to mention that some materials that may be used for GEN IV applications may not have been validated for R5 assessment yet. This will need to occur before R5 can be used in NH.

STEP 4 - Perform Basic Stress Analysis

Elastic stress analyses of the un-cracked feature should be performed for the extremes of the service cycles. In the case of cyclic loading, a shakedown assessment of the un-cracked feature should

Step 1) Establish cause of cracking or expected cracking

- Define defect type, bounding size, incubation. Mode I required.

Step 2) Define service conditions

- Resolve loads into cycle blocks, desired service life (loads, temperatures, etc.)

Step 3) Define materials and properties

- cyclic, creep crack growth, temperatures: collect appropriate data

Step 4) Basic stress analysis (operating extremes)

- Shakedown assessment. If shakedown not established, inelastic analysis necessary.

Step 5) Check time independent stability

- Time independent fracture analysis (section XI type): failure predicted stop here

Step 6) Check significance of creep and fatigue

- Rules are checked to determine insignificance of creep or fatigue. Check if creep-fatigue interaction is important

Step 7) Calculate rupture life based on initial defect size

- Rupture life calculated based on cracked limit load stress. Ductility exhaustion methods may be needed

Step 8) Calculate crack incubation time

- Conservative to ignore this

Step 9) Calculate crack growth for the desired life time

- Integrate creep and fatigue crack growth expressions. Note both affect each other. Changes in reference stress during crack growth should be included.

Step 10) Recalculate rupture life for final crack size (Step 7)

- Continuum damage prediction after crack growth. Conservative to base this final crack size.

Step 11) Time independent stability check for final crack size

- This is actually performed during crack growth analysis in practice

Step 12) Assess significance of results

- R5 does not prescribe margins. ASME may require this.

Step 13) Report results

- Prescribe inspection intervals, etc.

Figure 5. Draft Step by Step Procedure (13 steps).

then be performed. The type of shakedown assessment is quite similar to NH and could be performed using NH procedures. It should be determined if the feature satisfies strict or global shakedown or not. In the case that shakedown cannot be demonstrated, it is necessary to justify the use of the methods of this volume using. For example, inelastic analysis methods, including finite element analysis, may be required. If shakedown is demonstrated, the crack depth should be such that the compliance of the structure is not significantly affected.

STEP 5 - Check Stability under Time-Independent Loads

The cracked component must be checked to ensure time-independent mechanisms under fault or overload load conditions at the initial defect size does not occur. R5 suggests using R6 [36]. However, for ASME NH purposes and the US NRC, this can be performed using Section XI procedures or a J-Tearing assessment. If failure occurs due to time independent effects alone at this step, then the assumptions in the analysis should be revisited and remedial design action taken. Only if sufficient margins can be justified is it permissible to continue to Step 6 to justify future service life or the design.

STEP 6 - Check Significance of Creep and Fatigue

The checks for insignificant creep should be made using ASME NH or R5 procedures. If creep is insignificant then the assessment becomes one of fatigue loading alone and Steps 7 and 10 below are omitted. Conversely, if fatigue is judged to be insignificant then the assessment becomes one of steady creep loading alone and further consideration of cyclic loading is not required. A further test determines if creep-fatigue interaction is significant. If it is not, simplified summation rules for combining creep and fatigue crack growth increments may be adopted (Step 9).

STEP 7 - Calculate Rupture Life based on the Initial Defect Size

The time to continuum damage failure (creep rupture) must be calculated based on the initial crack size from Step 1. If this is less than the required service life, it may not be necessary to perform crack growth calculations and the NH procedure alone suffices. The estimate of rupture life is based on a calculated limit load reference stress (discussed in the appendices) and, for predominately primary loading, the material's creep rupture data. For damage due to cyclic relaxation and due to the relaxation of welding residual stresses, ductility exhaustion methods are more appropriate. The particular requirements for defects in weldments are also addressed. For the case of short defects close to stress concentrations such as notch radii or weld toes, special considerations must be followed to ensure that the reference stress is conservatively calculated.

STEP 8 - Calculate Crack Nucleation or Incubation Time

Typically it takes some time for a crack in a nuclear component to begin growing. For some components, crack initiation may consume the bulk of the life and when crack growth commences, failure occurs quickly. The crack nucleation or incubation time is the time from the start of the of high-temperature operation to crack growth start. Depending on the cause of cracking, its location within a weldment and the type of loading it may be possible to calculate a non-zero incubation time. *It is always conservative to ignore this period and assume that crack growth occurs on first loading*. The cause of cracking will influence the determination of an incubation time. For example, a naturally-occurring creep defect, such as some weld defects, may not experience an incubation period prior to macroscopic crack growth. There are several procedures for calculating crack incubation time within R5 including TDFAD and the two criteria approach (similar to A16).

STEP 9 - Calculate Crack Growth for the Desired Life Time

The crack size at the end of the design period of operation is calculated, following the procedures of R5 based on K, C*, reference stress, and the appropriate estimation schemes laid out. Finite element analysis can also be used. This is done by integrating the appropriate creep and fatigue crack growth expressions. This incremental process is simplified in some cases, depending on the outcomes of the significance creep and fatigue tests determined in Step 6. Changes in reference stress due to crack growth should be included in the calculations. Integration is required because all parameters (K, C*, C(t)) and reference stress change with time as the crack proceeds.

STEP 10 - Re-Calculate Rupture Life after Crack Growth

The time to continuum damage failure should be re-calculated taking into account the increased crack size from Step 9. Crack growth calculations should not be performed in practice beyond an acceptable rupture life. It is conservative to base the estimate of rupture life on the final crack size as this neglects slower accumulation of creep damage when the crack size is smaller during growth.

STEP 11 - Check Stability under Time-Independent Loads after Crack Growth

In practice, this step is carried out in conjunction with the crack size calculations of Step 9. The crack growth calculations of that step should not be performed beyond a crack size at which failure by time-independent mechanisms is conceded at fault or overload load levels using the R6 procedure [36]. For ASME purposes, this assessment could be made using ASME section XI methods.

STEP 12 - Assess Significance of Results

The uncertainties in loads, material properties, defined crack location, etc., need to be assessed. Margins against failure are not prescribed in R5 and are left to the user to set. The sensitivity of the results of the preceding steps to realistic variations in loads, initial flaw size and location, and material properties should be assessed as part of a sensitivity study. The various modeling assumptions made can also be revisited with a view to reducing conservative assumptions in the analysis if unacceptable margins are determined. If this still fails to result in an acceptable crack growth life the options of new design, or for service assessment, of reducing future service conditions, or repair or replacement of the defective components should be considered. For NRC needs, this may require placing the procedure within a probabilistic framework.

An alternative to the quantitative assessment of margins using the deterministic approach of this section is to use probabilistic methods to directly determine failure probabilities. A procedure for doing this is set out in one of the Appendices but requires estimates of the distributions of variable quantities.

STEP 13 - Report Results

The results of the assessment, including margins determined, and the details of the materials properties, flaw size, loads, stress analysis calculations, etc, used in the assessment should be comprehensively reported. This facilitates both verification of the particular assessment and repeatability in future assessments. Each of these steps is summarized in great detail within the large volume of material provided within R5. This includes some material data along with extensive examples of the use of the method. A simple example calculation of the procedure is provided in the Section 6.

5.3 Comments on R5 Application for ASME

From the flow chart description and 13 step procedure described above, it must appear that there are a number of judgments, interpretations and supporting properties data required to sort through the

various behavioral regimes and to make an eventual design assessment. For near term HTGR applications as described above, it is not possible to narrow down the options and simplify the procedure. To do so would make the assessments too conservative to be used as a practical design tool within NH. Also, the goal of Code design rules is to have requirements that can be implemented consistently such that the design assessment will not be dependent on the individual/organization doing the assessment. To ensure that the creep/fatigue assessment procedures are properly applied, organizations using the procedure must ensure that the staff is properly trained. The use of the procedure (and all other methods) requires an experienced user. Therefore, the R5 procedure may not be ready for generally applicable design rules within NH but may be more suitable to regulatory requirements and licensing review. This last point requires further discussion and cannot be answered at this point.

5.4 The R5 Material Data Requirements

The material requirements for R5 crack growth analyses are summarized here in this section. The material data testing requirements are well established in R5. In addition to the typical high temperature properties required for an ASME NH design life assessment, the following material data is needed.

1. Creep rate material properties and the constitutive law. The constitutive law could be a classical law (power law) or other type of law depending on the material and temperature (including hyperbolic laws and even tertiary laws). Validation examples are provided in the next section.
2. Creep crack growth constants are required to predict the creep crack growth portion of the analysis. Figure 6 provides an example of the creep crack growth data that is required. As seen in Figure 6, a compact tension specimen shown in the insert at the top is tested at temperature. The test can be done under applied load or displacement. The crack growth is monitored, along with the loads and displacements. From this, the crack growth rate can be plotted as a function the C* integral, as seen in Figure 6. Since this plot is logarithmic, the relation between crack growth rates and C* is typically a power law. *It is very important to note that this data can be estimated using a simple procedure within R5 if creep crack growth data is not available. This estimate is based only on knowledge of the tensile creep properties and the estimates are made to be conservative.*
3. Fatigue crack growth constants are needed as spelled out in R5. This data is obtained at the temperature of interest using one of a number of fracture specimens including the compact tension type specimen shown in Figure 6. Again, a power law relationship between crack growth per cycle and the change in stress intensity factor (ΔK) is generally obtained.
4. Creep ductility properties along with elastic and elastic-plastic fracture properties at temperature.

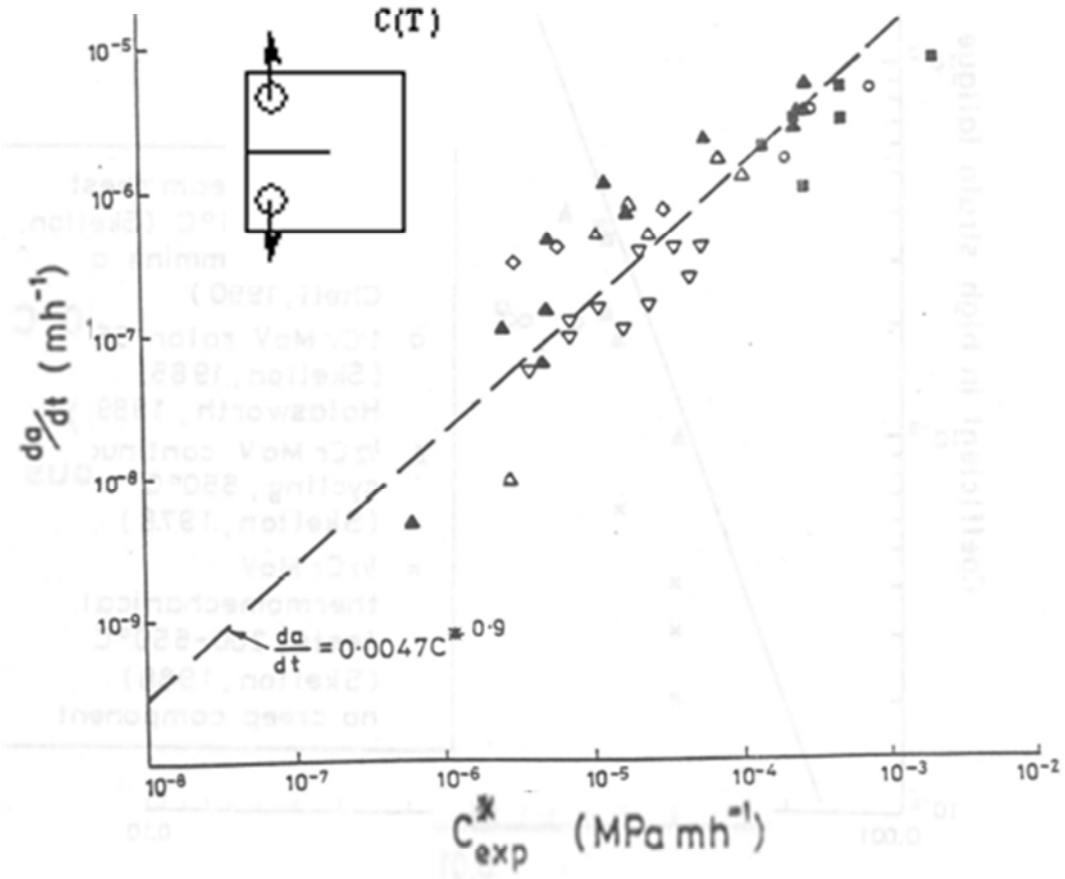

Figure 6. Example of creep crack growth data.

Many of the high temperature materials within NH are included in R5 and have been validated for creep-fatigue crack growth using the R5 approach. Figure 7 provides a comparison of materials that are supported within NH and those within R5. From Figure 7 it is seen that both NH and R5 support 2 1/4Cr-1Mo steels across nearly the same temperature ranges. For stainless steels, R5 has not been used much for temperatures higher than about 650 C while NH goes to 815C. However, R5 has been used for a larger variety of austenitic steels, including 347. BE says that R5 has been used outside this temperature range, but only on a spot basis, and it is not possible to document the specifics here. From the middle of Figure 7 it is seen that R5 has not been used for alloy 800H. As noted in Figure 7 though, it has been used for some other super alloys for a steel similar to IN 617. Also, 9Cr-1Mo-V steel has not been used, mainly since these steels are not used in any BE plants. Because of the success of R5 for other Cr-Mo steels, there is no reason to suspect that R5 cannot perform for this steel. At the bottom of Figure 7 some steels that have been supported by R5 are listed which are not supported within ASME NH.

NH:	**2 1/4Cr-1Mo steel (Grade 22 Class 1)** Stress intensity values to 1100F (575C) for 300,000 h .
R5:	**2 1/4 CrMoV, 1/2CrMoV and 1CrMoV** in the range 500-565C
NH:	**304H stainless steel** Stress intensity values to 1500F(815C) for 300,000 h.
NH:	**316H stainless steel** Stress intensity values to 1500F (815C) for 300,000 h.
R5:	**Various stainless steels and weldments (304, 316, 316H, 321, 347 weld, 316 weld)** in the range 525-650C
NH:	**Alloy 800H** Stress intensity values to 1400F (750C) for 300,000 h.
R5	**No Alloy 800 H**. However, BE has used R5 for super alloys up to 800C (similar to IN617)
NH:	**9Cr-1Mo-V steel (Grade 91)** Stress intensity values to 1200F (650C) for 300,000 h.
R5:	**No 9Cr-1Mo-V steel (Grade 91)**
R5:	**CMn** steels in the range 360-390C
R5:	**P22, P91 and some P92 ferritic steels**

Figure 7. Comparison of materials within NH and R5. BE has used R5successfully outside these temperature ranges also – to lower and higher temperatures especially in austenitic steels.

5.5 Summary of The R5 Material Data

Some of the material data required was summarized above. Sources for data are available in the literature. BE (Ainsworth) and Imperial College (Nikbin) can compile this data into a coherent library and this should be considered by ASME. The current sources for data needed for R5 assessments are:

- *R66 (Materials Data Handbook for R5), BE, is not available in general since some of the data is proprietary. The data is from a number of sources. However, some of this data that is not proprietary could be made available by BE.*
- *BE is willing to supply some of the data that is in the public domain*
- *Much is compiled in the R5-Code software, which can be licensed*
- *API 579 has a fair amount of data*
- *Some data for materials (including IN 617) is available from the German database.*

In summary, a large data base exists but much of it proprietary. Methods exist for estimating crack growth law without the necessary data. This is convenient and provides conservative estimates of

the properties. Finally, Nikbin (Imperial College) and Ainsworth (BE) will compile a data base of non-proprietary data for a fee**.** Material data required creep/fatigue crack growth assessments using R5 is not available for some GEN IV materials.

6.0 R5 Validation and Example Problems

Here we provide some material that illustrates the validity of R5 along with an example which shows how to use it. First an example problem is illustrated which shows the step-by-step procedure for applying the method for a cracked nuclear plant component (pipe). Here we leave out some of the details for brevity, but the full example problem can be found in Appendix A8 of [2]. Next we discuss some validation of the methods which address some of the concerns discussed earlier.

6.1 Example problem – surface crack pipe.

Figure 8 illustrates a practical problem concerning the life estimate of a nuclear power plant component. The pipe is made of 316 stainless steel with an inner radius of 300 mm and thickness of 100 mm. This is a thick pipe of the type often welded to and near nozzles in nuclear plants. The pipe has a 3mm deep, 360-degree crack in it. This size crack was chosen based on the limit of NDE capability at this particular plant. As seen in Figure 8, the pipe is to operate at 600 C. The design life is 1.5 million years with 500 equal cycles with 3000 hour dwell times. Figure 9a illustrates the elastic stresses that result from the internal pressure loading of 16 Mpa. It is seen that hoop and radial stresses vary from the pipe ID to OD while the axial stresses are constant at 20.57 Mpa. The pipe experiences a thermal gradient at temperature which produces tensile stresses on the pipe ID and compression at the OD (Figure 9b). The stresses in the pipe are initially zero and are zero at shutdown (which is the minimum of the load cycle). Therefore, the cause of cracking during service (creep-fatigue), geometries, and load have been defined constituting completion of steps 1 and 2 of Figure 5.

The material properties are shown in Figure 10. At the top of Figure 10, the creep material law is listed. This law represents a combination of primary and secondary creep. The primary creep law is an exponential time hardening law while the secondary law is a classical Norton type creep law. All material parameters are shown in Figure 10 as well. In addition, the fatigue crack growth law is shown at the bottom of Figure 10, with the material constants listed for 316SS at 600C. Note that the 'effective' stress intensity factor range (ΔK_{eff}) is used. This accounts for a concept called crack closure in fracture mechanics based fatigue crack growth. Essentially, the crack will not grow when it is closed and methods for calculating the effective value of K are shown in R5. Finally, the bottom of Figure 10 lists the creep crack growth law used, also with material constants. These represent the materials required in step 3.

Axis-symmetric surface crack pipe

- Ainsworth book example [35]– also part of R5 example case in Appendix
- 316 SS pipe: $R_i = 300mm$, $t = 100mm$
- Desired Life: 1.5×10^6 hours: 500 equal cycles with 3000 hour dwells at 600C
- $a_0 = 3mm$: Based on maximum size flaw eluding detection

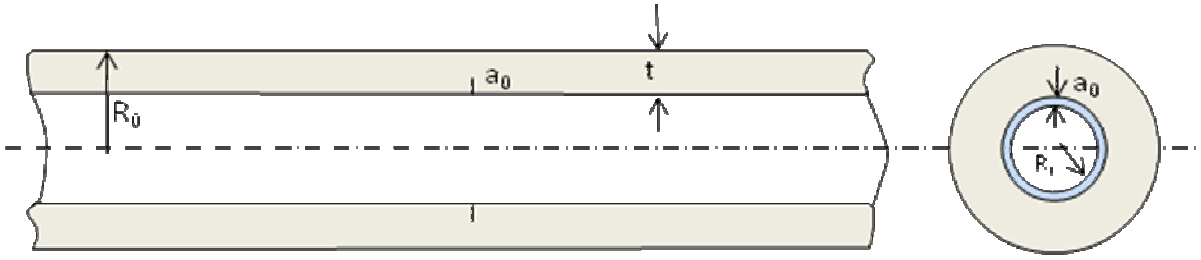

Figure 8. R5 example problem – surface crack pipe.

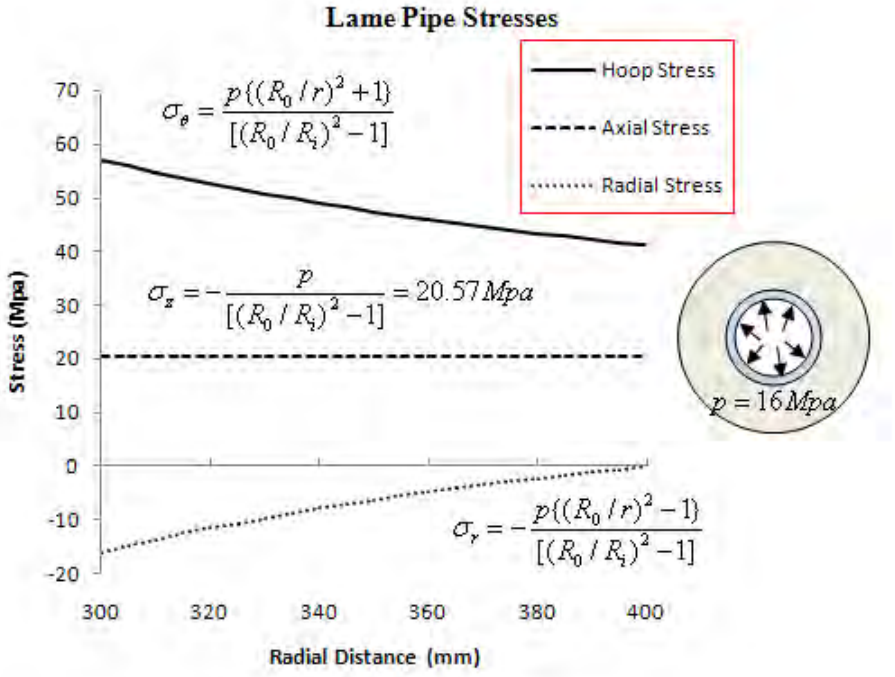

Figure 9a. Pipe Stresses due to pressure.

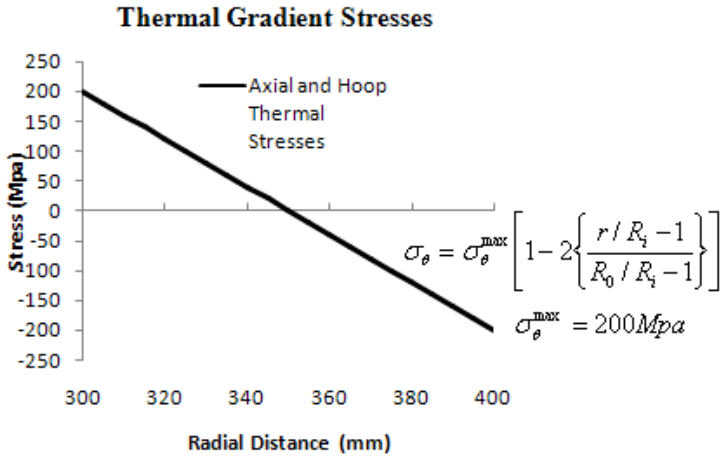

Figure 9b Pipe Stresses due to thermal gradient.

Primary Creep Rate

$$\dot{\varepsilon}_c = \varepsilon_p r\mu t^{\mu-1}\exp(-rt^{\mu}) + \dot{\varepsilon}_s$$

$$\varepsilon_p = A'\sigma^{m(\theta)}\exp\{-P/(\theta+273)\}$$

$m(\theta) = \alpha - \gamma\theta$, where θ is temperature (C)

Secondary Creep Rate

$$\dot{\varepsilon}_s = B\sigma^n\exp\{-Q/(\theta+273)\}$$

Creep constitutive law

r	2.42×10^{-2}
μ	0.64
A'	1.632×10^{35}
P	9.292×10^{4}
α	16.32
γ	0.02044
B	5.184×10^{-6}
Q	1.97×10^{4}
n	4

$$\left[\frac{da}{dN}\right]_f = C\left[\Delta K_{eff}\right]^{\lambda}$$ C=2×10^{-9} m/cycle, $\lambda = 3$ (316 SS at 600C) — Fatigue Law

$$\left[\frac{da}{dt}\right] = A\left[C^*\right]^q$$ A=.0197 ; q=0.89 (m/hr) — Creep Law

Figure 10. Material laws and properties

Step 4 involves determining whether the structure is operating within the strict shakedown or global shakedown limit. The procedures used to assess shakedown are performed without consideration of fracture mechanics, and details are omitted here (see Appendix A8 of [2]). The R5 shakedown procedure is similar to the ASME NH procedure, and is not summarized here (see [2]) for details. For this pipe structure, strict shakedown conditions are satisfied. The shakedown analysis is used to determine the re-distributed stresses caused by creep that are actually used for the crack growth analysis. The loads are low and the crack is small so the component easily passes the time independent fracture check in step 5. We are now ready to predict life using the fracture methods discussed earlier.

The parameters necessary for the crack growth and life prediction are the stress intensity factor, K, and C* (and the transient C(t)). C* is calculated using the reference stress and the stress intensity factor also. The stress intensity factors for this cracked pipe case can be determined from fracture mechanics handbooks. For complicated geometries, or for cases where K is not available, it can be easily determined from finite element methods. For an axis-symmetric crack in a pipe, K is:

$$K = \{F_m \sigma_m + F_b \sigma_b\} \sqrt{\pi a}$$

$$C^* = \left[\frac{K}{E'}\right]^2 \frac{E \dot{\varepsilon}_c}{\sigma_{ref}}$$

Where F_m and F_b are functions of a/t (crack depth over thickness), and σ_m and σ_b represent the membrane and bending, stresses, respectively. Since the crack depth changes with time, K changes throughout the crack growth phase of the analysis. The value of C* is calculated using the equation above where σ_{ref} is the reference stress and $\dot{\varepsilon}_c$ is the creep strain rate calculated at the reference stress value. Since the crack depth constantly changes, the reference stress and stress intensity factor constantly change throughout the analysis. As such, both the creep and fatigue portions of crack growth must be integrated (or summed) throughout the time life of the component. The reference stress is a simple well established function crack depth, thickness, pipe size, and yield stress for a pipe containing an axis-symmetric crack, and is listed in the R5 code. For this case, at the initial crack depth, the initial reference stress is 80.1 Mpa and at shakedown, it is 57.6 Mpa. The reference stress values within R5 are being improved at present. It is always possible to perform finite element analyses to obtain K and C* (C(t)) but it is more convenient to use reference stress estimates if they can lead to conservative estimates. Conservative estimates of these parameters using the reference stress approach are not always guaranteed. This is the subject of improvements being implemented into R5 at present and is discussed in the next section.

The creep response for the constitutive law shown in Figure 10 is shown for two constant levels of stress (100 and 150 Mpa) in Figure 11. For the 3000 hour dwell times, it is seen that primary creep is expected to play an important rule. Hence, using the equations and material parameters in Figure 10 with the stresses defined earlier.

Crack Growth Calculation. The total crack growth per cycle is obtained by summing the cyclic and creep contributions. The crack extension over the design life of 1.5 million hours is calculated iteratively using a computer program. The main features of the procedure are as follows.

1. Calculate the creep crack growth for the dwell period in the first cycle. The creep crack growth and strain rates are assumed constant over short time periods (a Newton scheme can also be used, but it is not necessary). The new crack depth and accumulated creep strain are then updated and new values of reference stress and creep strain rate are obtained using the creep law in Figure 10. The value of C* can then be obtained with K evaluated for the new crack depth, leading to a new value of crack growth rate.

2. Calculate the cyclic crack growth for the first cycle and increment the crack depth by this amount.

3. Repeat these calculations for subsequent cycles. This can automatically be performed with the R-code, although for this example, a simple FORTRAN code can be written.

The crack growth versus time is shown in Figure 12, which is taken from [2] (Figure A4.14 with permission of R5 authors). It is seen that this component is designed to handle the required lifetime in this example.

6.2 Theoretical Issues and Concerns with Engineering Creep Crack Growth Methods.

The state of the art engineering creep and creep-fatigue crack growth predictive methodologies are based on characterizing the crack growth rates using parameters (K, C*, C(t)) that measure, in theory, the strength of the asymptotic crack tip fields, as discussed in section 3. There are a number of theoretical concerns regarding this approach. Perhaps the main concern is that the asymptotic crack tip fields can only be developed for simple creep constitutive laws (such as power law types). Moreover, the methods formally break down once crack growth occurs, non-proportional stressing occurs, and cyclic loads are experienced when a creep crack grows in service.

For a creep/fatigue crack growth predictive methodology to be valid, the measured values of the parameters (here C*, C(t)) must be related to crack growth events. Experiments on fracture specimen are performed by measuring far field parameters (load, load point displacement (or crack opening displacement), and crack size). These parameters are then properly integrated to obtain the crack characterizing parameters. A fundamental question that must be answered in any fracture mechanics based approach is whether these far field measurements can properly characterize the near crack field events. Traditionally, with fracture mechanics, this characterization is made because the asymptotic crack tip fields, which characterize growth, can be related to far field measurements. For instance, with elastic-plastic fracture, far field events can be related to near crack tip field fracture events through the use of a path independent integral (J-integral). For creep crack growth, this relationship is only strictly valid for full scale creep for a stationary crack and for simplistic constitutive laws. When crack growth occurs, or more importantly, when both crack growth and cyclic loading occur, the asymptotic interpretation of the crack tip events to far field measurements, breaks down. *In fact, for cyclic loading of a stationary crack, the asymptotic crack tip fields depend strongly on the form of the constitutive law being used and these fields can change for each cycle of loading [15] and Appendix A!* This makes establishing the link between near field crack events, which drive crack growth and fracture, and far field events (where measurements are made to characterize material properties) quite challenging. Today, despite the fact that engineering creep/fatigue crack growth procedures based on R5 type methods have been used with success for years, controversy over the general nature of the methods persists. Indeed, while R5 has been established and validated for materials and operating conditions

within BE plants, it is not certain whether these methods will carry over in a straight forward fashion to GEN IV conditions. Hence, even if R5 approaches were implemented within NH, validation under GEN IV conditions is necessary. This issue is discussed further in the next section.

More theoretically sound creep and creep-fatigue crack growth parameters have been proposed which are based on energy considerations. Atluri [37, 38] summarized quite general crack parameters for all types of nonlinear materials, including creep, which is based on energetic principles. Brust and Nakagaki [8, 9, and 39] more recently summarized some of these parameters and discuss applications of the use of these parameters. These parameters represent 'the energy deposited into a finite sized crack tip region (and crack growth wake region) per crack growth increment' [39]. Moreover, there remains controversy over the appropriate general nature of these energetic parameters. Even so, these methods are not amenable to simple engineering application approaches at present since calculation of the energetic crack parameters requires the use of numerical methods and fine meshes. Hence, since asymptotic approaches break down under cyclic creep crack growth conditions and energetic approaches are either not practical or controversial, the engineering methods of R5 need to be established with validated field experience when being used under conditions outside their range of validity. More details of these theoretical issues are discussed in Appendix A.

The engineering creep-fatigue methods used in all codes today, including R5, are used outside their range of validity. Despite this, the methods have shown to provide reasonable predictions of creep-fatigue life, albeit conservative – perhaps sometimes too conservative. Here we provide some discussion of the estimation of these parameters when used for creep constitutive laws and used under conditions outside the theoretical range of validity. Most of this summary comes from the R5 manual [2], Ainsworth's book [35], and a recent paper by Kim et al [40]. It is this author's belief that continued development of more fundamentally sound creep-fatigue life predictive methods must continue while we continue to use the engineering approaches in R5.

6.3 Validation and Creep Constitutive Laws.

Essentially, the theory behind the R5 engineering method (and all other methods) is summarized in the book by Webster and Ainsworth [35] and it is based on earlier asymptotic solutions for creep emanating from an initially elastic field (or plastic HRR field) within a creeping zone (both primary, secondary, and combined primary and secondary creep). Herman Riedel, in his classic treatise in 1987 [41], summarizes all of this. Riedel bases his work on earlier work when he was working with Rice, Bassani and colleagues work, etc (see [44 – 55]. So a firm theoretical foundation based on the asymptotic interpretation of crack tip fields does exist and it is clear.

In practice though, these conditions are violated - often severely. The creep response very near the crack tip (high stresses) cannot be represented by power laws. Once the crack grows beyond a small amount, the asymptotic interpretation becomes unclear, and we can go on and on. As Hoffelner [56] points out, the linear life fraction rules used in NH today have no real basis. However, from an applications standpoint all these simplified rules and laws do a very good job for design provided you build in the necessary safety margins. The same can be said for R5. Nothing would ever be built if we kept waiting for the perfect theory. There are no perfect theories in the fracture field. The conservatisms built into the methods were done so with these issues in mind. They were then validated with mock-ups, and service experience over the years. As such, we must start with the R5 approach, see how well it performs for GEN IV conditions, and improve on these methods or develop new methods as required. We must keep in mind, that in practice, J-Tearing theory for elastic-plastic fracture is used far beyond its theoretical validity routinely - with success and it can guarantee conservative results.

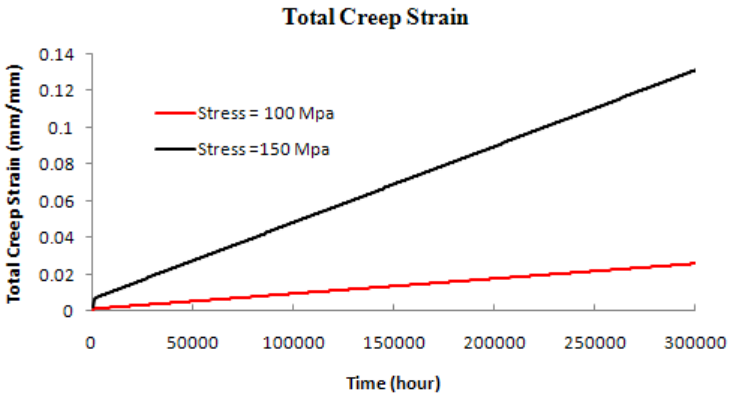

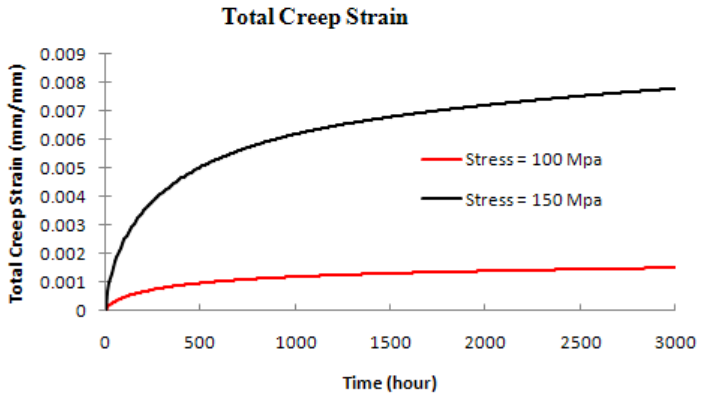

Figure 11. Material laws and properties

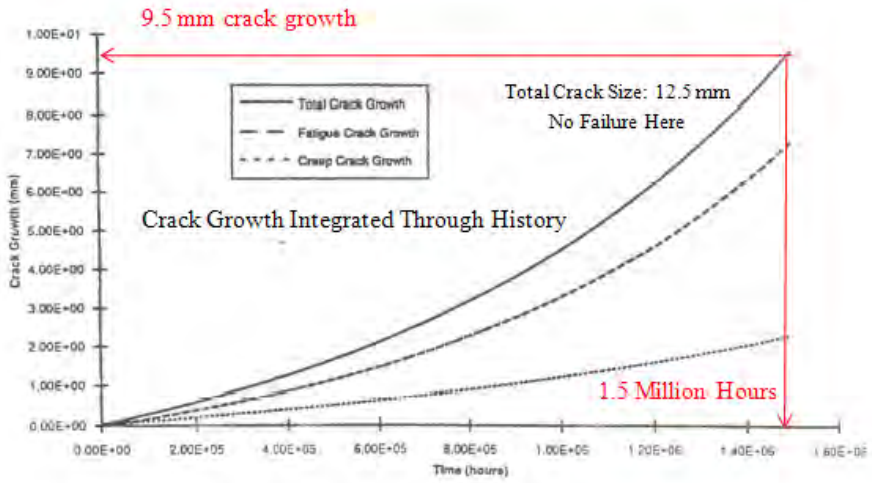

Figure 12. Crack growth versus time.

The original theoretical development of the R5 method required the constitutive theory to be of the power law type (Norton secondary creep, power primary creep). The classical treatise by Riedel [41] summarizes the theory and limitations. R5 was originally developed to be applicable for materials which are characterized by a more general creep law. Consider three different creep laws, as illustrated

Norton Power Law (Stress in Mpa, time in hours)

$$\dot{\varepsilon}_s = A\sigma^n \quad A = 10^{-16}; n = 5$$

Theta Projection (Stress; Mpa, time; hours, T; Kelvin)

$$\varepsilon_c = \theta_1(1 - \exp(-3600\theta_2 t)) + \theta_3(\exp(3600\theta_4 t - 1)$$

$$\log\theta_i = a_i + b_i T + c_i\sigma + d_i\sigma T; i = 1,4$$

$a_1 = -8.736; b_1 = .004604; c_1 = -.04489; d_1 = 0.6814E-4$

$a_2 = -2346; b_2 = .02225; c_2 = .02195; d_2 = -.1951E-4$

$a_3 = -1.869; b_3 = -.002034; c_3 = -.05497; d_3 = 0.799E-4$

$a_4 = -1643; b_4 = .009149; c_4 = -.04723; d_4 = 0.719E-4$

Primary-Secondary (RCC-MR)

$$\varepsilon_c = B\sigma^m t^p : t \le t_{fp}$$

$$\varepsilon_c = B\sigma^m t_{fp}^p + A\sigma^n (t - t_{fp}) : t \ge t_{fp}$$

$B = 2.2243E-14; m = 4.3056; p = 0.44633$

$A = 1.7122E-25; n = 8.2; t_{fp} = 2.75366E19\sigma^{-7.0337}$

Figure 13. Creep laws tested.

in Figure 13. The material constants are also presented there. The creep laws are quite different from each other. The Norton law is the classic law wherein many of the creep theories were developed from. The theta projection law is more of a secondary-tertiary creep law. The theta projection model constants in Figure 13 were developed for Cr-Mo-V steel at 565 C [42]. The RCC-MR law is a combination of primary and secondary creep. The RCC-MR material constants shown in Figure 13 are for 316 stainless steel at 565C [3]. The response of the three material models can be seen in Figure 14 where the vastly different response of the material laws can be easily seen.

As mentioned earlier, because the original theory for R5 (and all other engineering creep fracture laws) was based on power law creep laws, there is a question as to how accurate the estimation of the C* and C(t) parameters are within R5. Here this is addressed by showing comparison of the estimates of these parameters with finite element calculations. Such validation comparisons are provided in the R5 manual as well as reference [35]. Here we show some more recent validation examples developed in [40]. In [40] a number of different fracture specimens were considered for validation cases including center crack tension plate, compact tension specimen, single edge notch, and axially cracked cylinder. In addition, and of direct relevance to nuclear components, both circumferentially through wall cracked and surface cracked pipe were considered. Many of the estimation scheme methods for C(t) compared quite well with the finite element predictions, although some were overly conservative. Here we briefly

summarize the through-wall crack pipe validation case of [40]. Figure 15 shows the comparison of C(t) estimated using the procedure of R5 (called RSM or 'reference stress method') with finite element predictions for RCC-MR and the theta projection laws. It is seen that using the reference stress method to estimate C(t) over the time history is actually non-conservative in that it under predicts. An enhanced reference stress method (ERSM) proposed in [40] is seen in Figure 15 to provide better estimates of C(t) throughout the time domain.

Reference stress methods to estimate creep fracture parameters (C*, C(t)) were developed to simplify the calculation procedure. This can avoid the need for finite element calculations. In general, the RSM estimation methods are meant to be conservative in the sense that they overestimate the actual value of the parameter. Webster and Ainsworth [35] and the R5 manual [2] provide many examples where the estimate of C(t) using reference stress methods are quite accurate and conservative. Figure 15 illustrates a counter example where the current reference stress methods may not be conservative.

One of the main differences between the R5 and A16 are the methods used to estimate reference stress. Reference [43] summarizes some of the new reference stress solutions developed for A16.

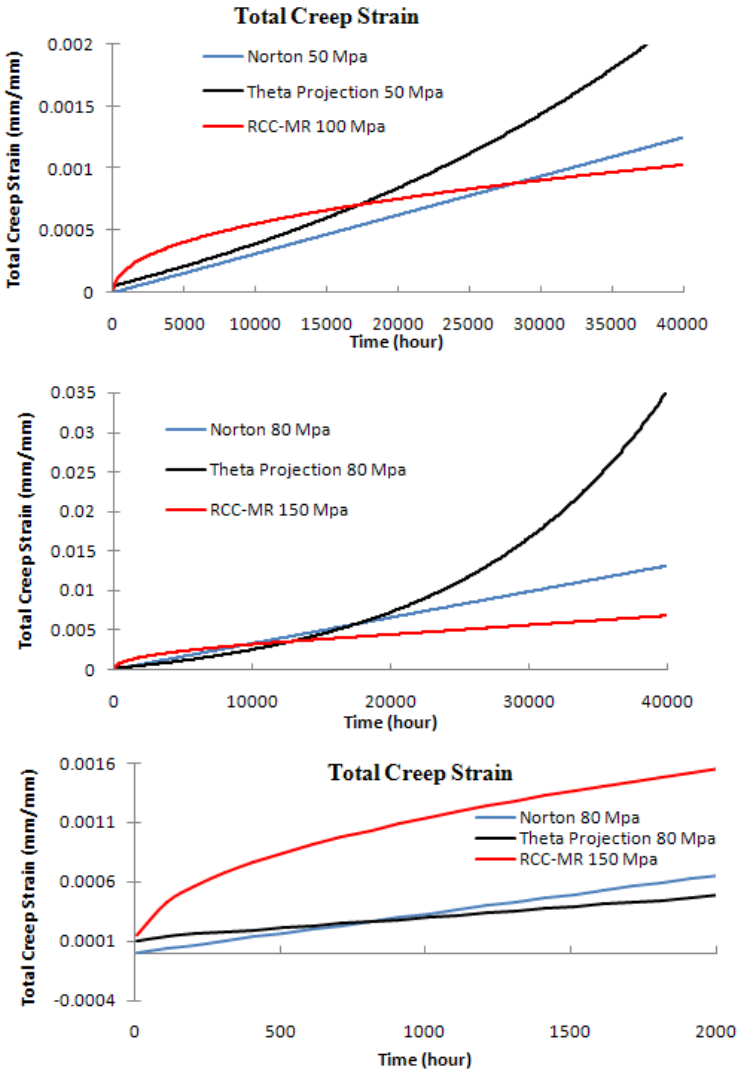

Figure 14. Total creep strain different creep laws.

Wasmer, Nikbin, and Webster [57] also show some examples where reference stress methods may not always be conservative in calculating creep fracture parameters. The R5 code is currently re-evaluating the RSM methods and improved formulae will be appearing in the code soon. However, it is always good to perform finite element calculations for some spot cases to verify the accuracy of RSM methods during an R5 assessment. In fact, if doubt exists, finite element solutions are recommended for calculating the creep/fatigue fracture parameters in order to ensure accuracy. Likewise, Samuelson et al [60] show examples of application of R5 to creep crack growth in welds and conclude that "… determination of creep crack growth rates in welds based on the C* value only may result in uncertain estimates". The weld mismatch effect can lead to uncertainties in R5 predictions. Therefore, while R5 is certainly the best code procedure available for creep/fatigue crack growth predictions, there is more validation work necessary, even for materials that are qualified for R5 assessment.

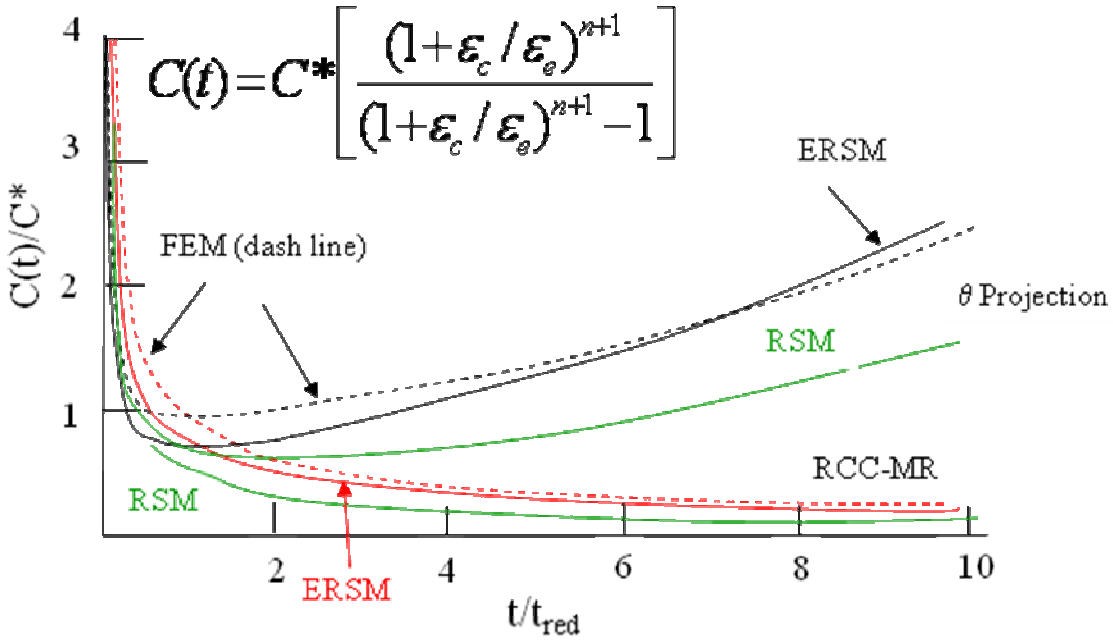

Figure 15. Comparison of C(t) estimates to FEM predictions.

7.0 Discussion of GEN IV and R5

7.1 R5 as a Possible ASME NH Rule Set

The R5 creep/fatigue life cycle crack growth prediction code represents the state-of-the-art procedure for assessing the life of cracked components operating in the creep regime. The method has a theoretical foundation which is based on rather simple constitutive laws and in practice, these assumptions are violated. This is not uncommon in the fracture mechanics field. J-tearing theory, which is used for predicting elastic-plastic fracture, likewise has a theoretical basis that is routinely violated in practice and is used far beyond its basis, with success. The success is possible by obtaining confidence in the procedures through validation with mock-up tests and service experience. Likewise, the success with R5 is based on a similar series of mock-up validations and service experience – mainly for the materials and operating conditions within British Energy HTGC reactors.

As such, the R5 procedure is a semi-empirical procedure (as is ASME NH) that needs qualification for materials and operating conditions that will be experienced in GEN IV. Certainly, the stainless steels and Cr-Mo steels are qualified for creep/fatigue crack growth assessment for a range of operating conditions in R5. We cannot recommend implementation of R5 procedures outside this range until further qualification for GEN IV materials is made. R5 is an assessment procedure rather than a design procedure in its present form. An assessment procedure attempts to accurately predict crack growth response while a design procedure involves built-in safety factors and conservatism. This is the case with all creep/fatigue crack growth procedures. Hence, if R5 were implemented to the high temperature design procedure of NH in the future, safety factors would have to be introduced.

Certainly there is ample data in the literature which supports the use of R5 outside the range of qualification. References [58-60] illustrate the use of this approach for nickel base alloys. The Petten database provide material constants for alloy 617 and 800H, and the method has been used to assess creep/fatigue lives in these materials. However, the method must be fully qualified for these materials and others that may be used in GEN IV applications – including ferritic vessel materials that may operate near the negligible creep range. For the near term, the gas outlet temperature for GEN IV has been reduced to 750 – 800C which means that alloy 617 may not be required for hot gas exposed structures. In addition to which, the only potential code boundary exposed to the hot gas will be the primary to secondary hot gas heat transfer interface. And, even there, the safety consequences of minor leakage across the interface may not be consequential. On the other hand, the reactor pressure vessel (and crossover duct in some concepts) will normally operate at nominally 350C, either below the conventional creep threshold or in the "twilight zone" between the creep regime and the negligible creep regime. For the near term, the material(s) of choice are SA533/508. These components can also potentially see quite limited off normal conditions roughly within the scope of Code Case 499, i. e. 800 – 1000F. From that perspective, R5 procedure may have to be qualified for vessel materials as well.

Finally, the issue of crack initiation must be dealt with. There is ample recent work examining crack initiation under creep/fatigue conditions. References [61, 62] discuss recent efforts on accurately predicting initiation under creep conditions. The recent thesis by Davies [63] (out of Imperial college, advised by Nikbin) summarizes the recent work relevant to R5 future implementations. For some structures and operating conditions, crack initiation may dominate life. However, the predictive methods are not robust enough and fully qualified to be used under creep/fatigue conditions. While conservative, Ainsworth, the main author of R5 over the years, recommends neglecting this phase for R5

since it will be conservative. However, it may be too conservative for use as a design criteria within NH.

7.2 Theoretical Issues with R5 Needing Resolution

Sections 1, 2, and 3, briefly summarized some of the theoretical concerns with the C* based engineering methods for creep/fatigue crack growth prediction. While possibly controversial, Appendix A summarizes these concerns in detail through the use of experimental, analytical, and numerical studies. For these reasons, despite the fact that R5 is the best available code procedure in use today for creep/fatigue crack growth life prediction, it must be qualified for GEN IV applications since the application use will be outside the window of R5 qualification.

7.3 Concluding Remarks on the R5 Approach

Fracture mechanics methods have proven a valuable practical tool to predict life of structures which develop cracks. The aerospace industry has adopted a 'damage tolerant' design approach which permits the presence of cracks. The structures are maintained by specifying sufficient inspection intervals so that a crack will not grow to a critical length between inspection intervals. Despite the fact that ASME does not permit cracks, they will be present and a procedure for assessing them is important to have. Some of the statements below must be kept in mind as we consider R5 for possible implementation into NH in the future.

1. A commitment to a fracture mechanics approach for components operating at high temperatures can only be on the basis of existing parameters (K, J, C*, C(t), TDFAD, 2-criteria concepts).

2. Each of these concepts has clear limitations which we have to live with. Bear in mind that also for the currently used linear life fraction rule in NH, no real physical justification exists and that we are using static stress-strain curves for materials undergoing cyclic softening etc. Moreover, elastic-plastic fracture mechanics methods are used routinely far beyond their theoretical validity with success since the methods are suitably 'qualified' from test data.

3. There are some doubts about the existence of a secondary creep stage for nickel-based alloys, which may find their way into GEN IV structures. It may be acceptable to "interpret" a secondary creep phase into the creep curves. Investigations [56-59] on nickel base alloys demonstrated that different sample geometries (CT, SENT, SENB, DENT) gave very comparable results based on C*.

4. The use of a reference stress for determination of C* (and C(t)) might bear some uncertainties as discussed earlier. Finite element calculations would be better and should be used for critical applications.

5. When crack extension up to 0.5 mm is considered as crack initiation then it may be sufficient to consider only this phase (TDFAD or 2-criteria) for some components. This may be too conservative for design purposes. Moreover, neglecting the crack initiation phase will always be conservative.

6. Creep-fatigue is certainly an ambitious field which still needs improvement and clarification. However, this is not only true for the fracture mechanics approach but is also true for the current design approach in NH.

7. Negligible creep should probably also re-visited with respect to crack growth (K-controlled crack growth may be applicable for some materials and service conditions).

8. A clear definition of the requirements for a fracture mechanics treatment of safety issues in an HTGR has to be agreed upon within NH (or Section XI if these procedures belong there). Should fracture mechanics be used for design, for safety considerations, or to set NDE and maintenance schedules?

In conclusion, in future HTGRs the influence of stress raisers like notches, production flaws, welding defects, developing cracks etc. should be considered for safety and/or NDE purpose, a fracture mechanics concept (for creep, fatigue and creep-fatigue) is needed. It is certainly a valid approach to use the methods, procedures and data developed within the R5 for that purpose, certainly as a starting point until the procedures are qualified for GEN IV conditions. Either the complete R5 procedure or only parts of it should be used depends on the demands and NRC's requirements and concerns.

8.0 Summary, Conclusion and Suggestions for Additional Work.

8.1 Summary

The subsection ASME NH high temperature design procedure does not admit crack-like defects into the structural components. The US NRC identified the lack of treatment of crack growth within NH as a limitation of the code and thus this effort was undertaken. This effort is broken into two parts. Part 1, summarized here, involved examining all high temperature creep-fatigue crack growth codes being used today and from these, choose a methodology that is appropriate for possible implementation within NH. The second part of this task is to develop design rules for possible implementation within NH. This second part is a challenge since all codes require step-by-step analysis procedures to be undertaken in order to assess the crack growth and life of the component. Simple rules for design do not exist in any code at present. The codes examined in this effort included R5, RCC-MR (A16), BS 7910, API 579, and ATK (and some less known codes).

After examining the pros and cons of all these methods, the R5 code was chosen for consideration. R5 was chosen because the code: (i) has well established and validated rules, (ii) has a team of experts continually improving and updating it, (iii) has software that can be used by designers, (iv) extensive validation in many parts with available data from BE resources as well as input from Imperial college's database, and (v) was specifically developed for use in nuclear plants. Further reasons for the choice of R5 are listed in Section 4.2.

There are several reasons that the capability for assessing cracks in high temperature nuclear components is desirable. These include:

- Some components that are part of GEN IV reactors may have geometries that have sharp corners – which are essentially cracks. Design of these components within the traditional ASME NH procedure is quite challenging. It is natural to ensure adequate life design by modeling these features as cracks within a creep-fatigue crack growth procedure. Figure 16 illustrates some types of components that may be part of GEN IV that fall into this category.
- Workmanship flaws in welds sometimes occur. It can be convenient to consider these as flaws when making a design life assessment.

- Non-destructive Evaluation (NDE) and inspection methods after fabrication are limited in the size of the crack or flaw that can be detected. It is often convenient to perform a life assessment using a flaw of a size that represents the maximum size that can elude detection.
- Flaws that are observed using in-service detection methods often need to be addressed as plants age. Shutdown inspection intervals can only be designed using creep and creep-fatigue crack growth techniques.
- The use of crack growth procedures can aid in examining the seriousness of creep damage in structural components. How cracks grow can be used to assess margins on components and lead to further safe operation.

The focus of this work was to examine the literature for creep and creep-fatigue crack growth procedures that are well established in codes in other countries and choose a procedure to consider

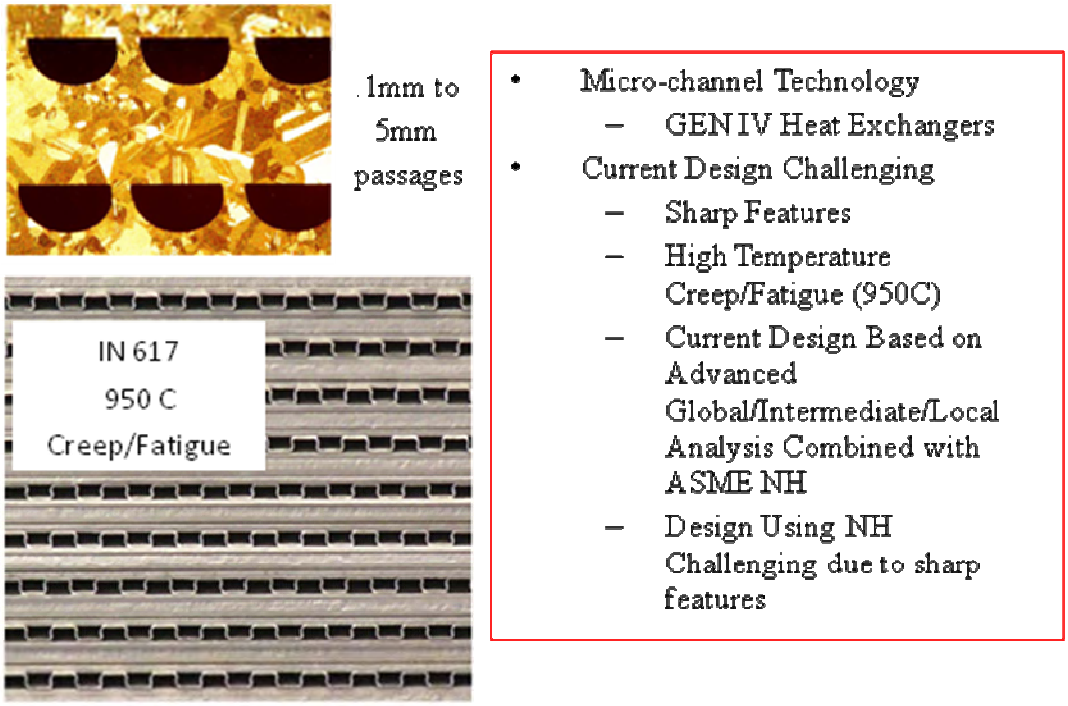

Figure 16. Example of possible GEN IV type heat exchangers. These illustrations are from "Heat Exchangers for the Next Generation of Nuclear Reactors" by Li, Le Pierres , and Dewson, J., Heatric Division of Meggitt (UK) Ltd., Proceedings of ICAPP '06, Reno, NV USA, June 4-8, 2006, Paper 6105.

implementation into ASME NH. It is very important to recognize that all creep and creep fatigue crack growth procedures that are part of high temperature design codes are related and very similar. This effort made no attempt to develop a new creep-fatigue crack growth predictive methodology. Rather, examination of current procedures was the only goal.

8.2 R5 Usage

Some details of R5 acquisition, training, and use are listed here.

- R5 can be obtained for $1700 for 1-year and $300 for future yearly renewal. This includes support. The methods are also well established to the point where one can learn the procedures from open literature publication such as in [35].
- Material libraries are available in the code.
- Methods exist for estimating crack growth laws from only knowing tensile properties if data is not available.

- Much data is available in the open literature.
  - BE willing to supply some of the data that is in the public domain (might charge for compilation)
  - Much is compiled in the R5-Code software, which can be licensed.
  - Nikbin also has data – he will charge a fee to compile it. This may be worth consideration by DOE/ASME since this represents a small investment to obtain a large database.
  - API 579 has some data that can be used.

8.3 Uncertainties in R5 and All Creep-Fatigue Crack Growth Methods

Creep-fatigue crack growth methods for design are now well established in Europe. In fact, many European countries ***require*** organizations to consider creep crack growth as part of the design process. While the methods in R5 are now well established and have been used on a daily basis for more than 15 years now, there remain a number of modeling uncertainties which must be kept in mind when using the methods. These include the following, which also are true for every method examined in this report.

- Crack Nucleation. The methods for predicting the onset of crack growth from an assumed or existing flaw are not considered to be fully robust by this author. One can always neglect this process and the assessment will be conservative.
- Material Properties for the R5 often have inherent statistical scatter. While this is also the case for current NH material properties, this results in additional sources of uncertainty.
  - The creep constitutive relationship for high temperature crack life assessment can be complicated, especially for new very high temperature materials. While R5 claims to be useful for all material laws, this remains to be seen in general.
  - The creep crack growth relationship is obtained by plotting the creep crack growth parameter (C(t), C*) on log-log paper to obtain a power law relationship. There is often scatter in these results so a lower bound curve is often taken. Moreover, it is not certain that a power law relationship will persist for new materials.
  - The fatigue crack growth relationship is likewise fraught with the similar uncertainties discussed for creep crack growth.
  - The creep-fatigue crack growth interaction equations are also subject to material variability and uncertainty.
  - The performance of the methods for very high temperature performance and for new materials will need to be established.
- There are also uncertainties that persist within the modeling and estimation assumptions used.
  - The estimation of the reference stress which is required to estimate the parameters for an engineering assessment of crack growth are difficult to determine for complicated cracked components. This can lead to overly conservative estimates of life. While finite

element analysis is always possible, this can make the crack life assessment time consuming.
    - The constraint at the growing crack tip can be difficult to determine. Moreover, the constraint can change as the crack grows. Figure 17 illustrates the elastic-plastic fracture toughness for different types of crack geometries and loadings. This same type of effect can affect the creep crack growth relationship and is a source of uncertainty.
    - Estimates of C(t) for complicated constitutive relationships using equations such as those shown in Figure 15 can be overly conservative.

8.4 Recommendations Regarding Additional R&D Needs and Testing Requirements

Some additional research and development needs for creep and creep-fatigue crack growth modeling are listed in the following bullets.

- Material data tests required for new materials (e.g. IN617) and operating conditions for GEN IV.
- Reference Stress Approach Needs More Validation for complicated geometries. These include more work for:
    - High constraint crack geometries.
    - Complex Crack Geometries (e.g. nozzles, advanced heat exchangers, etc.).
    - Materials without secondary creep regime (or minimal regime). The methods appear to have difficulties for materials that do not attain a secondary creep regime. The estimation schemes (such as the equation in Figure 15) apparently require this despite claims made by the R5 developers. More work is clearly needed here.
    - Validity for transient creep conditions needs more work. The current estimation schemes are too conservative for cases where extensive transient creep crack growth occurs.
    - Validity for advanced constitutive laws required – R5 developed to work for materials which exhibit complex creep response. However, we have not seen extensive validation and generality for new material and higher temperature operation.
    - Assumptions tend to result in extensive conservatism – Should re-evaluate these.
    - Others areas of research needs will be developer during the part II effort.
- Finite element methods should be used for situations where the accuracy of reference stress method is in doubt.
- Enhancement and further development of theory is necessary for new materials and higher temperature cyclic application. As discussed in Sections 2, 7, and Appendix A, the theory underlying R5 (and all other methods) is quite old and is fraught with issues that need to be studied more thoroughly. This can lead to a more fundamentally sound theory which can enhance the method, reduce conservatism, remove some uncertainties, and lead to more confidence in life predictions.
- Engineering methods to predict diffusion creep are needed.

R5 should be qualified for materials and operating conditions of GEN IV before implementation into NH. In the meantime, R5 procedures (for Cr-Mo and stainless steels) where qualification within R5 has been made, can be recommended.

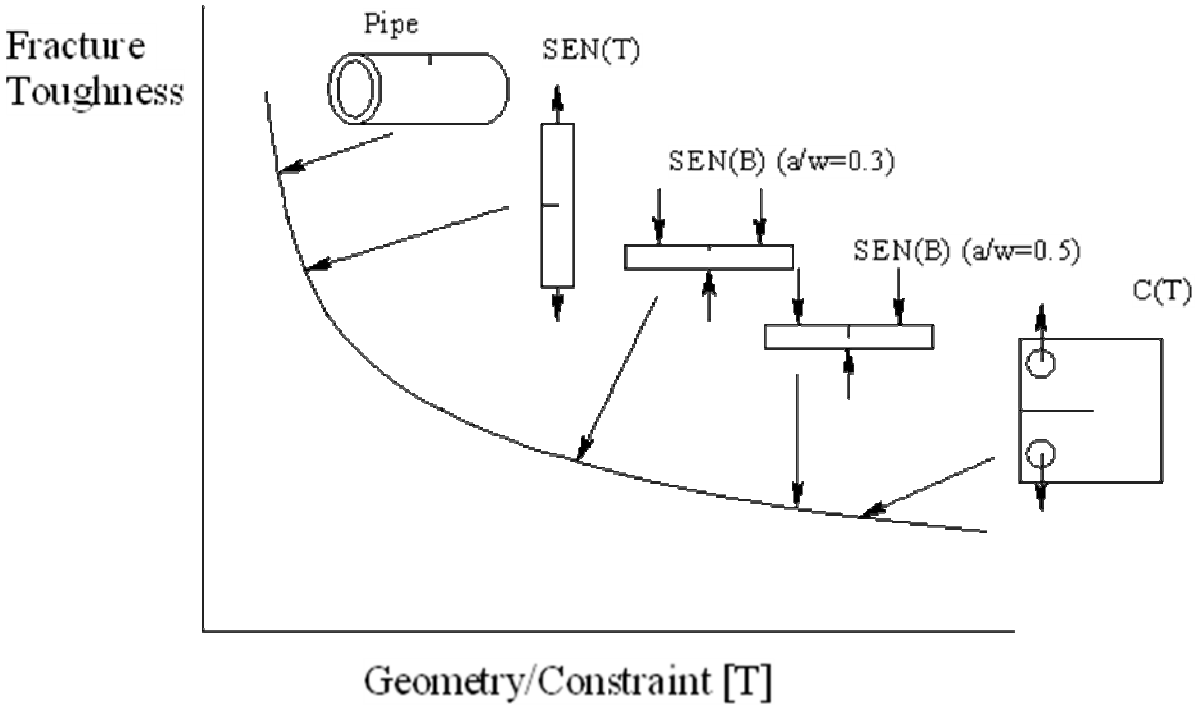

Figure 17. The effect of constraint on fracture toughness.

Acknowledgements

The author would like to thank ASME and DOE for funding the study presented within this report. In particular, Mr. James Ramirez of ASME and Ken Balkey of Westinghouse (DOE program manager) are thankfully acknowledged. Dr. Sam Sham of Oak Ridge National Laboratory, Mr. Robert Jetter, ASME NH chair, and Dr. Wolfgang Hoffelner of PSI, Switzerland provided excellent comments of the draft report which were implemented into this final version. Useful discussions with Dr. Bilal Dogan of EPRI are thankfully acknowledged as well.

9.0 References

1. ASME, *Case of ASME Boiler and Pressure Vessel Code*, 3NH Class 1 Components in Elevated Temperature Service, 2004, New York: American Society of Mechanical Engineers.
2. BEGL, *An Assessment Procedure for the High Temperature Response of Structures*, British Energy Generation Ltd., R5 Issue 3, 2008.
3. RCC-MR, *Design and Construction Rules for Mechanical Components of FBR Nuclear Islands and High Temperature Applications, Appendix A16: Guide for Leak Before Break Analysis and Defect Assessment*, AFCEN, Appendix A16, 2002.

4. API, *Recommended Practice for Fitness-For-Service*, American Petroleum Institute, Washington, D. C., 2008.
5. British Standard, *BS 7910: Guide on Methods for Assessing the Acceptability of Flaws in Metallic Structures*, BSI, London, 1999.
6. Ewald,J, and Keienburg, K. H., “A Two Critera Diagram for Creep Crack Initiation, Int. Conf. Creep, Tokyo, April, 1986.
7. ECC Recommendations – Volume 9, Part II, *High Temperature Component Analysis Overview of Assessment and Design Procedures*, Prepared by ECC Working Group 4, 8/31/05.
8. F. W. Brust and S. N. Atluri, "Studies on Creep Crack Growth Using the T* Integral," *Engineering Fracture Mechanics*, Vol. 23, No. 3, pp. 551-574, 1986.
9. F. W. Brust and M. Nakagaki, "Integral Parameters for Thermal Fracture," *Engineering Fracture Mechanics*, Vol. 33, No. 4, pp. 561-579, 1989.
10. F. W. Brust and B. N. Leis, "A New Model for Characterizing Primary Creep Damage,”, *Int. Journal of Fracture*, Vol 54, pp 45-63, 1992.
11. F. W. Brust and B. N. Leis, "Primary Creep Crack Growth at Room Temperature in Surface Cracked Pipes", *Int. Journal of Pressure Vessels and Piping*, Vol. 52, pp 273-298, 1992.
12. Leis, B. N., and Brust, F. W., "Validation of Room-Temperature Primary Creep Crack-Growth Analysis for Surface Cracked Pipes, *Nuclear Engineering and Design*, Vol. 142, pp. 69-75, (1993).
13. F. W. Brust and B. N. Leis, "A Model for Predicting Primary Creep Damage in Axial Cracked Cylinders, Part I, Theory," *Engineering Fracture Mechanics*, Vol. 43, No. 4, pp. 615-627, 1992.
14. F. W. Brust and B. N. Leis, "A Model for Predicting Primary Creep Damage in Axial Crack Cylinders, Part II, Applications", *Engineering Fracture Mechanics*, Vol. 43, No. 4, pp. 615-627, 1992.
15. Brust, F. W., "Investigations Of High Temperature Damage And Crack Growth Under Variable Load Histories," *International Journal Of Solids And Structure*, Vol. 32, No. 15, pp. 2191-2218, 1995.
16. Brust, F.W., 1999, “Classical and Emerging Fracture Mechanics Parameters for History Dependent Fracture with Application to Weld Fracture”, PVP-Vol. 393, ASME.
17. KRISHNASWAMY, P., Brust, F. W., AND GHADIALI, N. D., "A Finite Element Algorithm To Study Creep Crack Growth Based On The Creep Hardening Surface," *Intl. Journal For Numerical Methods in Engineering*, Vol. 38, No. 6, pp. 969-988, March, 1995.
18. MOHAN, R., AND Brust, F. W., "Analysis of Void Growth in Elastic-Nonlinear Solids Under Creep and Cyclic Creep Conditions" ASME Journal of Engineering Materials and Technology, Volume 122, July 2000, pp. 283-294.
19. RAHMAN, S. AND Brust, F. W., “Approximate Methods for Predicting J-integral of a Circumferentially Surface-Cracked Pipe Subject to Bending,” *International Journal of Fracture*, Vol. 85, No. 2, October 1997, pp. 111-130.
20. J. ZHANG, P. DONG, F. W. Brust, W. J. SHACK, M. MAYFIELD, M. MCNEIL, “Modeling of Weld Residual Stresses in Core Shroud Structures”, International Journal for Nuclear Engineering and Design, Volume 195, pp. 171-187, 2000.
21. Brust, F. W., “The Effects of Load History on Creep Damage Evolution”, Proc. ASME PVP Hawaii Conference, PVP Vol. 305, pp. 403-410, July, 1995.

22. Brust, F. W., *Numerical Modeling and Experiments of Creep Crack Growth Under Cyclic Loading*, ASTM Special Technical Publication 1256, Fracture Mechanics: 26th Symposium, pp. 304-331, 1995.
23. Brust, F. W. AND MAJUMDAR, B. S., "Load History Effects On Creep Crack Growth," *Engineering Fracture Mechanics*, Vol. 49, No. 6, pp. 809-837, December, 1994.
24. Brust, F. W., AND DONG, P., "Welding Residual Stresses and Effects on Fracture in Pressure Vessel and Piping Components: A Millennium Review and Beyond", Transactions of ASME, J. Of Pressure Vessel Technology, Volume 122, No. 3, August 2000, pp329-339.
25. MOHAN, R., AND Brust, F. W., "Effect of Elastic Accommodation on Diffusion Controlled Cavity Growth in Metals", ASME Journal of Engineering Materials and Technology, Volume 122, July 2000, pp. 294-300.
26. MOHAN, R., AND Brust, F. W., "On Void Growth in Elastic-Nonlinear Viscous SolidsUnder Creep and Cyclic Creep Conditions", to appear Journal of Pressure Vessel Technology, 2001.
27. OH, J., KATSUBE, N., AND Brust, F. W., "Unresolved Issues With Regard to Creep and Creep Fatigue Life Prediction", ICES'2K, Proceedings of the International Conference on Engineering Sciences, August, 2000, Ed. S. N. Atluri and F. W. Brust, pp. 1174-1182.
28. MOHAN, R., AND Brust, F. W., "An Analytical Study of Void Growth in Viscoplastic Solids", *Fatigue and Fracture of Engineering Materials & Structures*, Vol. 21, pp. 569-581, 1998.
29. MOHAN, R., ZHANG, J., AND Brust, F. W., *ASME PVP Volume PVP-391, Advances in Life Prediction Methodology*, pp. 201-207, Boston, August 1999.
30. BRUST, F. W., "The Importance of Material Fabrication History on Weld Durability and Fracture", *Fracture, ASTM STP 1644*, W. G. Reuter and R. S. Piascik, Eds., American Society for Testing and Materials, West Conshohocken, PA, 2001.
31. Oh, J., Brust, F. W., "*Studies on Effect of Cyclic Loading on Grain Boundary Rupture Time*", *Journal of Engineering Materials and Technology*, pp. 1-10, Volume 129, January, 2007.
32. Oh, J., Katsube, N., and Brust, F. W., "*Numerical Analysis of the Effect of Diffusion and Creep Flow on Cavity Growth*" Computers, Materials, and Continua CMC, vol.183, no.1, pp.1-29, 2008.
33. Hutchinson, J. W., *Singular behavior at the end of a tensile crack in a hardening material*, J. Mech. Phys. Solids, Vol. 16, pp 13-31.
34. Rice, J. R., and Rosengren, G. F., *Plane strain deformation near a crack tip in a power law hardening material*, J. Mech Phys. Solids, Vol. 16, pp 1-12.
35. Webster, G. A., and Ainsworth, R. A., *High Temperature Component Life Assessment*, Chapman & Hall Publishers, London, UK, 1994.
36. R6 Revision 4, Assessment of the integrity of structures containing defects, BEGL Procedure (2008).
37. Atluri, S. N., *Path Independent Integrals in Finite Elasticity and Inelasticity with Body Forces, Inertia, and Arbitrary Crack Face Conditions*, Engineering Fracture Mechanics, Vol. 16, pp 341-364, 1982.
38. Atluri, S. N., Editor, *Computational Methods in the Mechanics of Fracture*, in Monograph Series "Mechanics and Mathematical Methods, North Holland Press, 1983.
39. Brust, F. *W., The T*-Integral: Definition and Use for Predicting Damage Accumulation and Fracture*, in book *Contemporary Research in Engineering Science*, ed. R. C. Batra, pp. 118-140, Springer, November, 1995. Written and Presented in honor of S. N. Atluri, the 1995 A. C. Eringen Medal Awardees of the Society of Engineering Science.

40. Kim, You-Jae, et. al., *Engineering C-integral Estimates for Generalized Creep Behavior and Finite Element Validation*, Int., J. of Pres. Vessels and Piping, Vol. 79, pp 427-443, 2002.
41. Riedel, H., *Fracture At High Temperatures*, Springer-Verlag, 1987.
42. Evans, R. W., and Wilshire, B., *Creep of Metals and Alloys*, Institute of Metals, London, UK, 1985.
43. Ainsworth, R. A., 'Flaw Analysis in the French RSE_M and RCC-MR code appendices', five papers presented in special issue of *The International Journal of Pressure Vessels and Piping*, S. Marie et al authors, Vol. 84, 2007, pp 589-695.
44. Hui, C. Y., and Wu, K. C., "The Mechanics of a Constantly Growing Crack in an Elastic Power-Law Creeping Material", *Intl J of Fracture*, **31**, p 3-16, 1986.
45. Hawk, D. E., and Bassani, J. L., "Transient Crack Growth Under Creep Conditions", *J Mechanics and Phys of Solids*, **34** (3), p 191-212, 1986.
46. Hawk, D. E., and Bassani, J. L., presented at the 4th International Conference on Numerical Methods in Fracture Mechanics, San Antonio, TX, March 23-27, 1987.
47. Riedel, H., and Wagner, W., "The Growth of Macroscopic Cracks in Creeping Materials", *Advances in Fracture Research*, Proceedings of the Fifth International Conference on Fracture, Cannes, Ed. D. Francois, Pergamon Press, New York, NY, Vol. 2, p. 683-690, 1981.
48. Hui, C. Y., "The Mechanics of Self-Similar Crack Growth in an Elastic Power-Law Creeping Material", *Intl J of Solids and Structures*, **22** (4), p 357-372, 1986.
49. Riedel, H., "Crack-Tip Stress Fields and Crack Growth Under Creep-Fatigue Conditions", ASTM STP 803, p I-505 - I-520, 1983.
50. Riedel, H., in *Creep in Structures*, Proceedings of the 3rd IUTAM-Symposium, Leicester, UK, 1980, Ponter and Hayhurst (eds.), Springer-Verlag, p 504-519, 1981.
51. Hui, C. Y., ASTM STP 803, American Society for Testing and Materials, Shih and Gudas (eds.), p. I-573 - I-593, 1983.
52. Bassani, J. L., in *Creep and Fracture of Engineering Materials and Structures*, B. Wilshire and D.R.J. Owen (eds), Pineridge Press, p. 329-344, 1981
53. Chang, T. C., Popelar, C. H., and Staab, G. H., "A Damage Model for Creep Crack Growth", *International Journal of Fracture*, **32**, p. 157-168, 1987.
54. Wu, F. H. Bassani, J. L., and Vitek, V., "Transient Crack Growth Under Creep Conditions Due to Grain-Boundary Cavitation", *J of Mechanics and Phys of Solids*, **34** (5), p. 455-475, 1986.
55. Chung, J. O., Yu, J., and Hong, S. H., "Steady State Creep Crack Growth by Continually Nucleating Cavities", *J Mechanics and Phys of Solids*, **38** (1), p. 37-53, 1990.
56. Hoffelner, W., Private Communication to ASME NH Group, e-mail, 5/11/2009.
57. Wasmer, K., Nikbin, K. M., and Webster, G., A Sensitivity Study of Creep Crack Growth in Plates to Reference Stress Formulae', ECCC Creep Conference, 21-23 April, Zurich.
58. Auerkari, P., et al., "Developments in Assessing Creep Behavior and Creep Life of Components", Materials at High Temperatures, Vol. 21, No. 1, pp 61-64, 2004.
59. Nazmy, M., Hoffelner, W., and Wuthrich, C., "Elevated Temperature Creep-Fatigue Crack Propagation in Nickel-Base Alloys and 1Cr-Mo-V Steel, Metallurgical Transactions A, Volume 19A, pp 855-862, April, 1988.
60. Samuelson, L. A., Segle, P., Andersson, P., and Storesund, J., "Creep Crack Growth in Welded Components – A Numerical Study and Comparison with the R5 Procedure", I. Jour. Pres Ves and Piping, Volume 78, pp 995-1002, 2001.
61. O'Donnell, M. P., "Comparison of Crack Initiation Life Estimation Procedures Under Creep-Fatigue Conditions", Nuclear Engineering and Design, Volume 235, pp 1989-2001, 2005.

62. Wasmer, K., Nikbin, K. M., and Webster, G. A., “Creep Crack Initiation and Growth in Thick Section Steel Pipes Under Internal Pressure”, Submitted to Int. J. Pressure Vessels and Piping, March, 2009, under review.
63. Davies, C. M., Crack Initiation and Growth at Elevated Temperatures in Engineering Steels”, PhD thesis, Imperial College, London, Advisor K. Nikbin, May, 2006.

Appendix A

Investigations Of High Temperature Damage And Crack Growth Under Variable Load Histories

DOE Summary Report, 1995, Grant DE-FG02-90ER14135.

Also

International Journal Of Solids And Structure, Vol. 32, No. 15, pp. 2191-2218, 1995.

Pergamon

Int. J. Solids Structures Vol. 32, No. 13, pp. 2131–2218, 1995
Copyright © 1995 Elsevier Science Ltd
Printed in Great Britain. All rights reserved
0020-7683/95 $9.50 + .00

0020-7683(94)00249-5

INVESTIGATIONS OF HIGH TEMPERATURE DEFORMATION AND CRACK GROWTH UNDER VARIABLE LOAD HISTORIES

F. W. BRUST
Battelle, 505 King Avenue, Columbus, Ohio 43201-2693, U.S.A.

(*Received 29 October 1993; in revised form 24 September 1994*)

Abstract—Time dependent deformation and crack growth behavior under variable load conditions are investigated in this study. Experimental observations of load/unload effects in cracked creeping bodies are first discussed. Then a detailed analysis of a typical test result is presented. The potential of integral parameters, including the T^*-integral, to characterize this complex response, is shown.

1. INTRODUCTION

The demands for structural systems to perform reliably under severe operating conditions continue to increase. Time dependent deformation and corresponding damage development can be the limiting design feature for engineering structures that operate at high temperatures. This is true for both monolithic and composite materials. Time dependent degradation may also be a contributing factor to reducing life even at room temperatures and below [see, for instance, Brust and Leis (1992)].

Most of the studies of time dependent or creep crack growth have been concerned with simplified load conditions and constitutive relations. The methods developed by Riedel (1987) and extended into useful and practical engineering methods by Saxena (1991) are all based on simplified constitutive relations. Indeed, creep fracture parameters such as C^*, C_t^* (Riedel, 1987), C_t (Saxena, 1991), Q^* (Yokobori, 1984), $C(t)$ (Bassani, 1981), and others, are based on the assumptions of strain hardening primary creep law and/or Norton creep. Moreover, simple creep-fatigue engineering approaches rely on Miner's Rule, where the effects of creep crack growth and fatigue are considered separately for predictive purposes, as typified by Jaske's (1984) approach.

The approaches described above can provide useful engineering predictions of creep crack growth, especially under constant load conditions. However, for structural components that operate in a severe thermal environment, including thermal load-history effects in the analysis procedure is essential for accurate crack growth predictions. Indeed, the series of papers recently produced out of the AFWAL Materials Laboratory at Wright–Patterson Air Force Base [see Nicholas and Weerasooriya (1985, 1986) and the references therein] have clearly identified the importance of load history on crack growth behavior. This work, mainly applied to crack growth in the turbine disks of advanced military gas turbine engines made of IN100, consisted of a series of experiments and corresponding numerical analyses of this problem. The numerical analyses included more appropriate constitutive relations than the simple power law type theories discussed above. Useful design models to enable the Retirement for Cause philosophy to be used were developed for handling the creep/fatigue interactions for the turbine disk problem.

Kim *et al.* (1988, 1992) have been studying creep crack growth behavior under severe operating conditions as part of the NASA Hot Section Technology program. They have found that near field integral parameters have the ability to characterize creep crack growth under complex thermal mechanical loading conditions. The other simplified parameters discussed above could not characterize the behavior.

With the above comments in mind, this paper presents an investigation of the fundamental processes that develop in cracked bodies which experience history dependent loading. The paper begins by discussing some general considerations regarding cyclic creep

and experimental observations of this process. A detailed analysis of one of the experiments is then described. As part of this discussion, the importance of proper constitutive laws on response, discussion of asymptotic approaches, and the ability of integral parameters to characterize the response is provided.

2. GENERAL CONSIDERATIONS

The phenomena of creep response under *stress reversals* may be explained as follows. If a uniaxial (metal) bar is heated to a temperature in the materials creep range and then loaded, the following response may be observed [see Gittus (1975) or Murakami and Ohno (1982) for instance]. As creep deformations advance, dislocations lose their mobility as they pile up at obstacles or owing to the formation of various networks, i.e. hardening is induced. These dislocations consist of two parts:

(i) a reversible part, which recovers mobility upon stress reversals; and
(ii) an irreversible part, which has formed irreversible networks.

When the stress in the bar is reversed from tension to compression, or from compression to tension, the reversible dislocations of type (i) remobilize in a direction directly opposite to those previously immobilized. This induces a significant creep strain rate, which may be attributed to material softening. With time, after the stress reversal, the (i) dislocations again become immobilized, and they again start to form irreversible dislocation networks.

If a structural component, or a portion of a component experiences stress reversals, significant creep strain rates are reintroduced. These strain rates cannot be neglected. Moreover, classical creep constitutive laws such as Norton's law or strain hardening laws do not account for this effect.

When a cracked component is loaded in the creep regime, creep strains accumulate from the crack tip outward. When the component is unloaded globally to zero load or even a net positive load, a region of compressive stresses *always* develops near the crack tip. That is, the tensile stresses in the crack tip region at the end of the load-hold period reverse sign upon unloading. This happens because of elastic stress recovery that occurs in the crack tip region where a localized creep zone has developed during the load-hold period. These compressive stresses cause large compressive creep strain rates in the crack tip region. Upon reloading, these compressive stresses that develop during the unload-hold period again reverse sign to tension. This again induces large tensile creep strains, which emanate outward from the crack tip region.

Thus, it is seen that cyclic loading in the creep regime in cracked bodies causes significant creep strain rate reversals, and corresponding increased crack tip strain development. The size of the zone of stress reversals depends on several factors, including load magnitude and amount of creep strain. Under severe conditions (which are increasingly being demanded of structural components), this effect is very important.

The next section describes some of the consequences of this stress reversal effect on the creep crack growth process. This is done by observing the response of creep crack growth specimens that are subjected to variable loads. The analysis sections will also show vivid examples of the above-described processes.

3. EXPERIMENTS OF VARIABLE LOAD CREEP

Before reporting the experimental observations, a description of the experimental procedure is provided.

3.1. *Experimental procedure*

All specimens are standard 1T compact tension specimens with a nominal thickness of 25.4 mm and width (W) of 50.8 mm, which were machined and fatigue precracked prior to testing. The specimens had approximately 20% side grooves machined into them to enforce straight crack growth. During the initial testing phase, one specimen experienced

failure of one of the electric potential (EP) leads that measure crack growth rates, which led to incomplete crack growth data. Two separate EP leads were then used for all other tests.

For the variable load tests, the experimental technique is automated, with the load history programmed on an Instron Servohydraulic machine. This required development of a novel spring-loaded extensometer system. Data acquisition was triggered by load changes. This resulted in rapid data acquisition after load changes, and slower data acquisition during the load-hold periods, which is desired for testing the analysis results. Figure 1 provides a view of the test set-up.

3.2. *Experimental observations regarding variable load creep*

Experimental results on three 9 Cr–Mo tests that were subjected to three different load/unload sequences are described here. Tests have also been performed on 316 stainless steel at two different temperatures, with results indicating the same trends as are to be reported here. [Some of these results may be found in Brust *et al.* (1993) and Brust and Majumdar (1994), and other results will be reported soon.]

Let us first examine some of the general conclusions that can be made regarding history dependent loading in the time dependent deformation regime. Figure 2 illustrates a load versus time sequence that was applied to one of the 9 Cr–Mo compact tension specimens at 538°C. All were fatigue precracked prior to testing. As seen in Fig. 2a, an initial load period of 36 h was made to ensure the development of an initial creep zone in the specimen. The unload-hold times and subsequent reload times were continually decreased until about 90 h, after which 4-h hold periods and 1-h unload periods were maintained until the specimen failed. This assured a truly variable load history.

An enlargement of the displacement versus time history for this experiment between 325 and 365 h, after beginning the test, is illustrated in Fig. 2b. This specimen failed after about 400 h. Another specimen was loaded to the same load level and was identical in all other ways to the above-described specimen except for a slightly larger initial crack. However, this specimen was held for 320 h before unload/reload occurred, and only one cycle was applied. Figure 3 illustrates the displacement versus time history for this test. Note that this test failed at more than 600 h.

Several important general conclusions can be drawn from these results, as follows.

- During the unload-hold period, load-point displacement recovery occurs (Fig. 2b). This is due to the compressive stresses that develop at the crack tip during unload. This zone of compressive stresses near the crack tip can be quite large, as was verified through computational studies, even though the global load is never less than zero. The compressive stress zones will be illustrated later.
- After reload, the displacement rates increase as compared with the rates during the previous loading period. This is clearly seen in Figs 2b and 3. Note also that the displacement just after reloading is always smaller than the corresponding value just before unloading.
- Load history effects significantly decrease life as compared with the nearly constant load (only one unload) test, i.e. in this case the constant load test lasted nearly 1.5 times as long.

Further evidence of this behavior can be seen by observing the results of another test on 9 Cr–Mo steel, also at 538°C. However, the applied load was smaller than in the above tests, and the load sequence is as illustrated in Fig. 4a. As seen, the unload-hold times were only 5 min (as compared with the minimum hold time of 1 h in Fig. 2a). Figure 4b illustrates the load-point displacement response of this specimen before crack growth began. This was a long test, taking over 30 days, and crack growth began at about 192 h after the test began. Figure 4b shows that, as with Figs 2b and 3, the load-point displacement rates (i.e. slope of the curve) increase after an unload compared with the rates before unloading, even before crack growth begins. However, as seen in Fig. 4c, the change in displacements after

an unload/load sequence becomes greater as time proceeds. This particular test has been completely analyzed, and the results will be presented later.

4. ANALYSIS RESULTS

This section will provide several types of analysis results that illustrate the effect of load history on time dependent crack growth and fracture. The first topic discussed involved observations of asymptotic fields that develop under cyclic creep. This is interesting, since most work to date and most practical approaches to the creep crack problem are based on asymptotic solutions using very simple constitutive relations. Here we compare some asymptotic solutions using several types of constitutive laws, including classical and more advanced creep models, which are capable of adequately predicting cyclic response under creep conditions. The second topic briefly examines some integral parameters that are being examined regarding their ability to characterize variable load creep crack growth. The final analysis topic presents the results of the third creep crack problem illustrated in Fig. 4. This test was analyzed throughout the entire 700 h test by using an appropriate constitutive law. The performance of the integral parameters, as well as comparisons with experimental data, is illustrated. Before this, a brief discussion of the computational tools used to develop these solutions is provided.

4.1. *Constitutive laws and finite element code*

The creep behavior of metals under a constant sustained load is classified into three phases: primary, secondary, and tertiary creep. In this work, which considers creep crack growth under variable loads, tertiary creep is not considered, since it occurs only in a small process region near the tip. The influence of the constitutive model used to represent time dependent materials on the stress and strain fields in the vicinity of a crack tip has been shown to be significant (Leung *et al.*, 1988), *even for constant sustained load*. As discussed in Section 2, upon stress reversal, a temporary increase in strain rate has been observed that was due to strain softening. Classical time or strain hardening (S-H) creep laws, upon which most of the current engineering approaches to predicting creep crack growth are based, are incapable of predicting these phenomena. The next section will clearly illustrate this. In the Inoue benchmark problems (Inoue *et al.*, 1991), a model developed by Murakami and Ohno (1982) and improved by Ohno *et al.* (1985) provided as good or better predictions of a complex load response in the creep regime than more than ten different models. The Murakami–Ohno (M–O) law has the advantage of having very simple material property requirements. The mathematical structure and the complicated effort required to obtain material properties for other recently proposed constitutive models render their use in numerical analyses of the creeping crack problem cumbersome.

The constitutive law used for most of the creep crack growth analyses presented here is based on the concept of a creep hardening surface (CHS) developed by Murakami and Ohno (1982, 1985). This model is quite convenient since the material property requirements consist of only the classical time hardening material constants (A, n, m), and the two Norton law constants [A_1, n_1; see eqn (1)].

For the general multi-axial case, the creep strain rate in this model is given by:

$$\dot{\varepsilon}^c_{ij} = C(\sigma, q)S_{ij} = \tfrac{3}{2}m(A)^{1/m}(\sigma)^{(n-m)/m}(q)^{(m-1)/m}S_{ij} + \tfrac{3}{2}A_1(\sigma)^{n_1-1}S_{ij}, \tag{1}$$

where S_{ij} and σ are the deviatoric and equivalent stress, respectively. In eqn (1), q is given by:

$$q = \rho + \left(\frac{\varepsilon^c_{ij} - \alpha_{ij}}{\sigma}\right)S_{ij}. \tag{2}$$

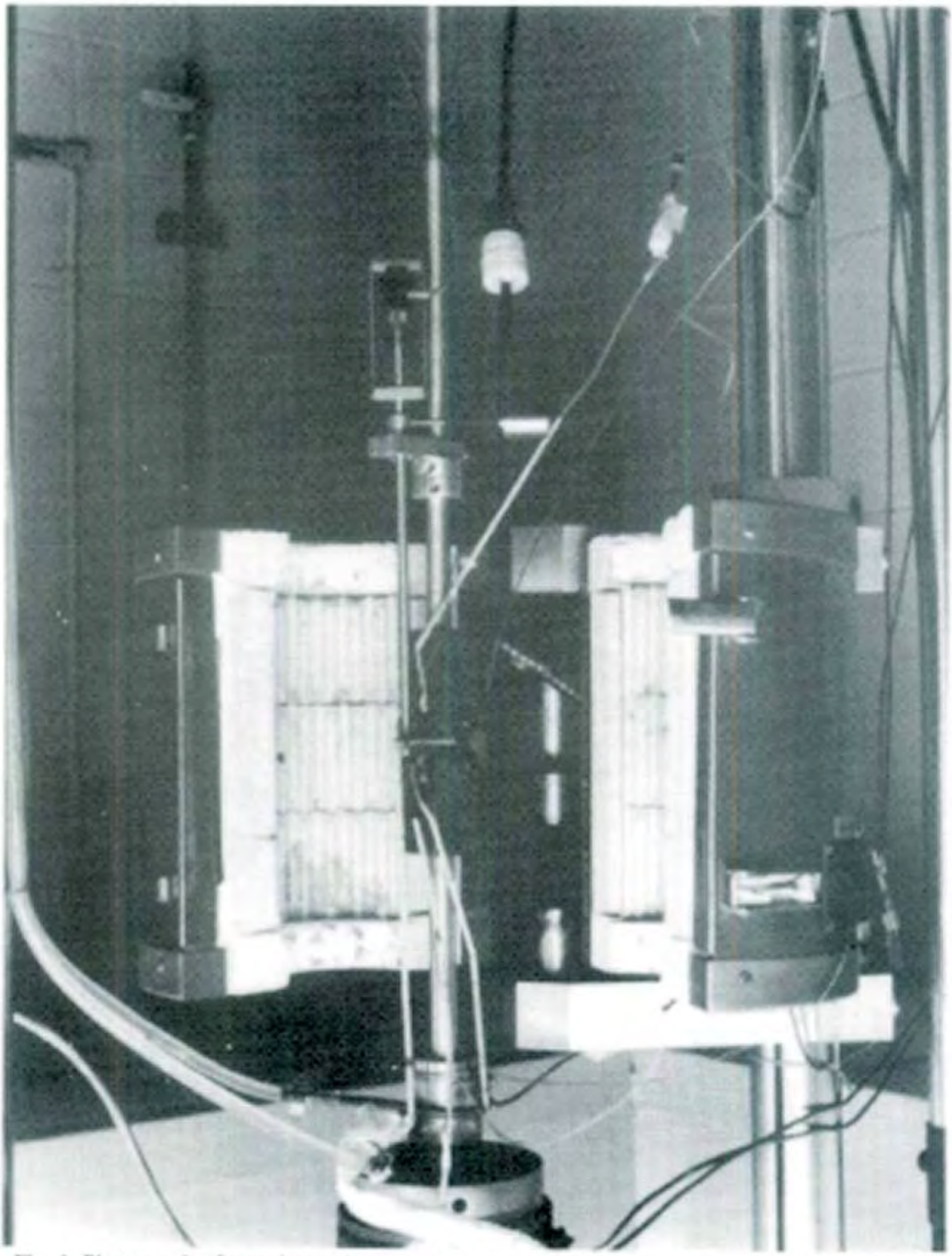

Fig. 1. Photograph of experimental set-up. An instrumented compact tension-specimen is shown here. The load pins go through the specimen. Note the spring-loaded extensometer entering the furnace from the top. This was used to measure crack opening displacements.

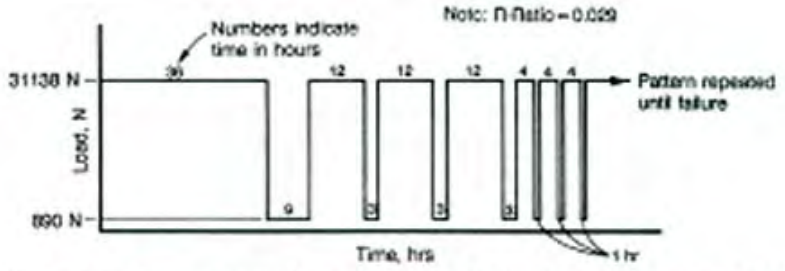

Fig. 2a. Load–time sequence applied to the first 9 Cr–Mo test. The initial crack size (a_0) was 26.75 mm, and $a_0/W = 0.527$.

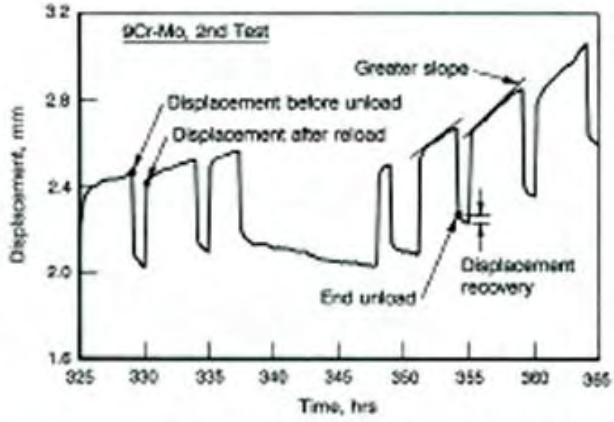

Fig. 2b. Displacement–time history for first 9 Cr–Mo test between 325 and 365 h.

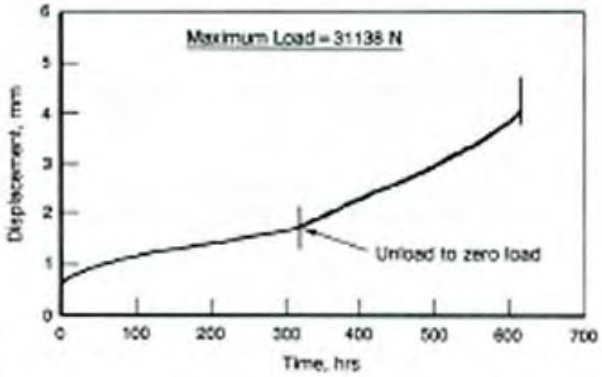

Fig. 3. Displacement–time history for second 9 Cr–Mo test. The load magnitude was identical to the load of Fig. 2a, but only one unload at time of about 320 h occurred. The initial crack size, a_0, was 27.23 mm with $a_0/W = 0.536$.

The evolution equations for the center of the yield surface α_{ij} and radius ρ are given by:

$$\dot{\alpha}_{ij} = \dot{\rho} = 0 \quad \text{if} \quad g < 0 \quad \text{or} \quad \frac{\partial g}{\partial \varepsilon^e_{ij}} \dot{\varepsilon}^e_{ij} \leq 0 \tag{3}$$

with

$$\dot{\alpha}_{ij} = \tfrac{1}{2}(\dot{\varepsilon}^p_{kl}\eta_{kl})\eta_{ij}; \quad \dot{\rho} = \frac{1}{\sqrt{6}}\dot{\varepsilon}^p_{ij}\eta_{ij} \quad \text{if} \quad g = 0 \quad \text{and} \quad \frac{\partial g}{\partial \varepsilon^e_{ij}} \dot{\varepsilon}^e_{ij} > 0, \tag{4}$$

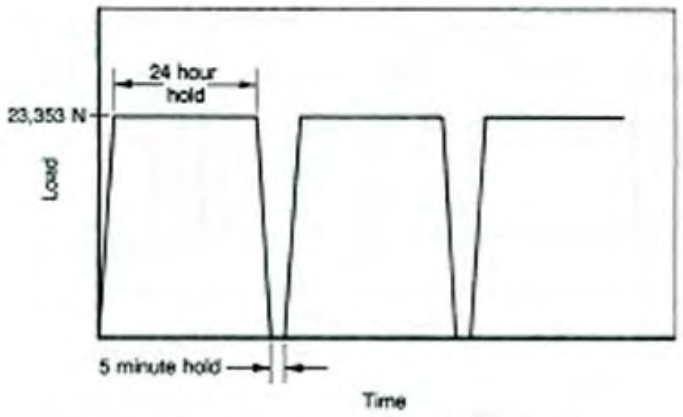

Fig. 4a. Load–time sequence for the third 9 Cr–Mo test.

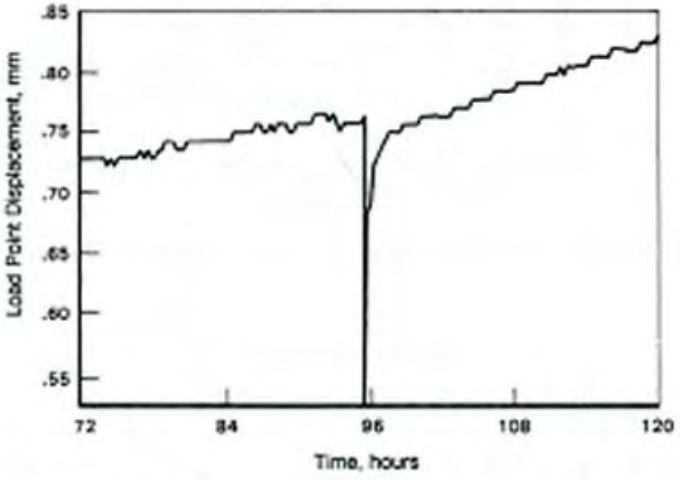

Fig. 4b. Load-point displacement versus time behavior between 72 and 120 h. Note in this specimen crack growth began at about 192 h (a_0 = 23.75 mm).

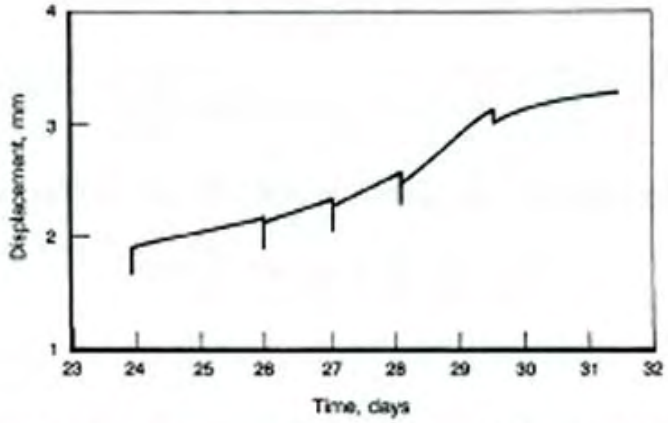

Fig. 4c. Displacement–time record for third test between the 24th and 30th days.

where η_{ij} is the outward normal vector to the CHS defined as

$$\eta_{ij} = \frac{\varepsilon^c_{ij} - \alpha_{ij}}{\{(\varepsilon^c_{kl} - \alpha_{kl})(\varepsilon^c_{kl} - \alpha_{kl})\}^{1/2}}. \tag{5}$$

The CHS is given as

$$g = \tfrac{2}{3}(\varepsilon^c_{ij} - \alpha_{ij})(\varepsilon^c_{ij} - \alpha_{ij}) - \rho^2 = 0 \text{ on CHS} \tag{6}$$

and

$$< 0 \text{ inside.}$$

The radius and center of the CHS therefore change only when the material state is on the CHS ($g = 0$) and remain the same when the state of creep strain is inside the CHS ($g < 0$).

From the evolution equations, it can be easily shown that q becomes $\bar{\varepsilon}^c$ (the equivalent creep strain) when stress reversals do not occur. Thus a principal advantage of this theory is that it coincides with classical creep constitutive laws when they apply. All material constants are therefore easily obtained from uniaxial creep data, which exist for most materials.

When a stress reversal occurs, q of eqn (2) becomes small, which renders the creep strain rates predicted in eqn (1) large. This accounts for large increases in creep strain rates observed experimentally during stress reversals [see Murakami and Ohno (1982, 1983) and Krishnaswamy *et al.* (1994)]. Classical laws upon which most creep fracture theories are based cannot account for this effect. Plasticity is included in this model by assuming that these strains occur over a very short time in evaluating the creep material constants.

A finite element (FE) algorithm using an implicit scheme has been developed for the Ohno and Murakami constitutive model and discussed by Krishnaswamy *et al.* (1993, 1994). The implicit method used here has the advantage of ensuring a convergent and stable solution for large time step sizes, unlike explicit integration schemes. The details of the algorithm have been omitted here and may be found in the cited references. Numerous comparisons using the implicit algorithm are compared with experimental data and with strain hardening theory and are also presented by Krishnaswamy *et al.* (1994) with good results.

The computational model for all analyses consisted of eight-noded isoparametric elements using plane stress or plane strain assumptions. Crack growth was modeled by using a node release technique whereby the nodal forces at both nodes in the particular element through which the crack is growing are released simultaneously over a period of time. The integral fracture parameters were calculated by using existing element shape functions and nodal averaged field quantities using a direct approach (i.e. a domain integral approach, which is convenient for three-dimensional problems, was *not* used). The analysis of the third experiment (Fig. 4) required a great deal of effort on a Cray computer system.

4.2. *Asymptotic observations*

Most practical methods for predicting the lives of cracked structural components that operate at temperatures at which creep occurs are based on a series of asymptotic solutions. These solutions were developed by using simple constitutive laws and are, for the most part, strictly valid for monotonic load-hold conditions [see Goldman and Hutchinson (1975), Riedel (1981), Riedel and Rice (1980), and the summaries provided by Riedel (1987)]. [Note that Riedel (1987) does provide an asymptotic solution for cyclic loading by using Norton's creep law, but the usefulness of this solution is unclear since Norton creep is inaccurate under cyclic load conditions.] Saxena and Han (1986) and Saxena (1991) (and many references cited therein) then developed engineering methods based on parameters that characterize the strength of these fields. In the following examples, we illustrate that the structures of these near tip fields change with time and load cycles, precluding the use of a single asymptotic strength parameter for cyclic load applications.

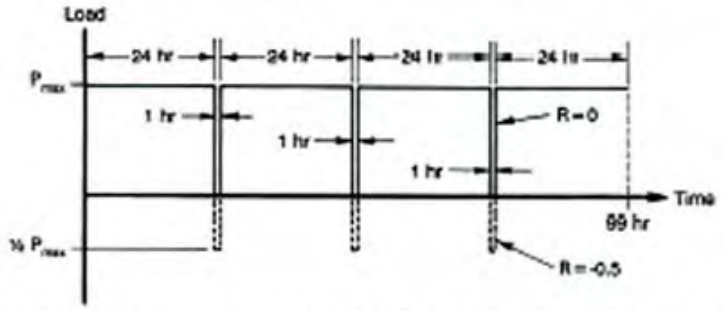

Fig. 5. Load spectra applied to asymptotic problem. Both $R = 0$ and $R = -0.5$ were considered. $P_{max} = 10$ kN for the 304 SS analysis, and $P_{max} = 23.353$ for the 9 Cr–Mo analysis.

Asymptotic solutions. The stress and strain fields near a crack tip are evaluated by using both the classical strain hardening creep law and the Murakami–Ohno (M–O) law [eqn (1)], the former of which is a special case of the M–O law. Cyclic loads are considered and the solutions are developed numerically by using the above-described finite element methodology. Only the first terms in eqn (1) are used since the primary creep term dominates during load changes.

Consider a standard compact tension specimen with crack length $a = 23.75$ mm and uncracked ligament length $c = 27.05$ mm. A finite element analysis of this specimen was performed by using creep properties of both 9 Cr–Mo Steel at 538°C and 304 stainless steel (SS) at 650°C. The applied load spectrum is shown in Fig. 5. Note from Fig. 5 that an $R = 0$ and an $R = -0.5$ spectrum were both used. This spectrum was applied up to 99 total hours. This means that the ends of the load-hold periods were 24, 49, 74, and 99 h while the *ends* of the unload-hold periods were 25, 50, and 75 h (four load and three unload periods). The material properties are:

$$A = 7.09 \times 10^{-15}, \quad n = 5.6, \quad m = 0.24 \quad (9\,\text{Cr–Mo})$$

$$A = 3.10 \times 10^{-19}, \quad n = 7.2, \quad m = 0.54 \quad (304\,\text{SS})$$

for stress in MPa and time in hours. These same constants are used for a strain hardening law and for the Murakami–Ohno cyclic creep law.

The symmetric finite element mesh was a focused mesh with ten rings of six-noded isoparametric triangular elements surrounding the crack tip and eight-noded elements elsewhere. The element size at the crack tip is about 0.00048 c, which is about two-and-one-half times more refined than the mesh used by Shih and German (1981) in their studies of HRR field dominance.

Figure 6(a) provides a plot of the shear creep strain rates just after two of the unload periods for the 304 SS with the $R = 0$ spectrum. This is a plot of $\dot{\varepsilon}_{r\theta}$ as a function of angle, θ, at a constant radius of 0.086 mm from the crack tip (standard crack tip polar co-ordinate definitions are used, with $\theta = 0$ ahead of the crack tip, and $\theta = \pi$ along the crack faces). This distance corresponds to about the seventh ring of elements away from the crack tip. Immediately afterwards the unloads occur at the first unload (time = 24+h) and third unload (time = 74+h), large stresses develop, which emanate from the crack tip. These stresses are relaxed with rather large creep strain rates. From Fig. 6(a), the maximum shear strain rates occur at an angle of about $\pi/2$, and it is clear that using a classical strain hardening creep law greatly underpredicts these strain rates. Figure 6(b) shows the shear creep strain rates at the end of the 1-h unload-hold period. Note that the position of maximum strain rate has shifted to about 1 radian. The strain rates have relaxed significantly; however, the rates from the Murakami–Ohno law are still higher than those of the classical law. All other components of creep strain rate exhibit a similar behavior at this location, and at all other locations.

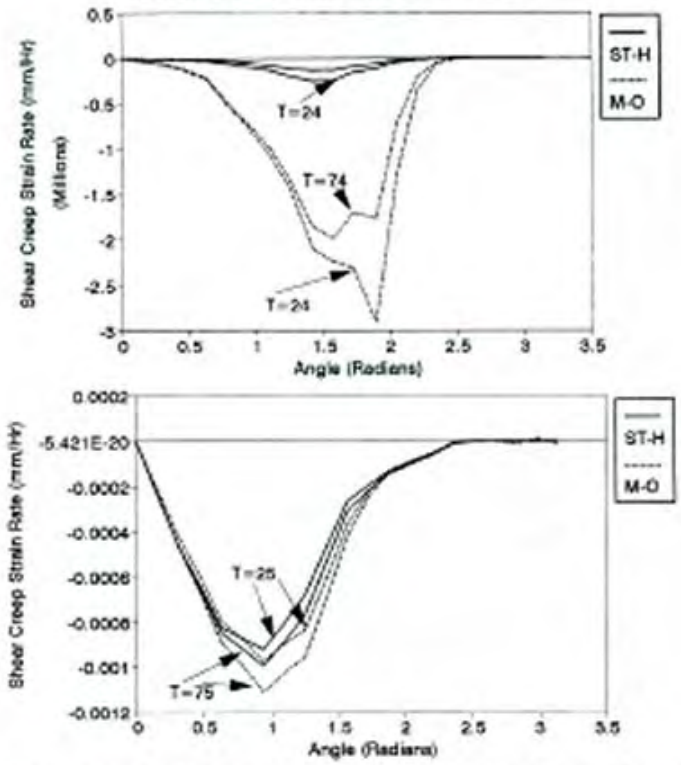

Fig. 6. Shear creep strain rates ($\dot{\varepsilon}_{r\theta}$) at a constant value of radius, 0.086 mm from the crack tip. (a) Just after the first and third unloads ($t = 24$, 74 h). (b) At the end of the hold times ($t = 25$, 75 h).

Figures 7(a)–7(c) show the θ component of stress at an angle of zero, also as a function of distance ahead of the crack tip. Figures 7(a)–7(c) show the stresses at the end of the hold times for 304 SS; $R = 0$, 304 SS; $R = -0.5$, and 9 Cr–Mo; $R = 0$ cases, respectively. Note that these plots show stresses versus $\log(r)$. The solutions for the Murakami–Ohno case, which has much better capability for modeling stress reversals, appear linear on these plots. Although certainly not proven here, it appears that the asymptotic fields behave as:

$$\sigma = C_1 \log (C_2 r). \tag{7}$$

In fact, this apparent logarithmic singularity appears to dominate over a very large distance, and, at least for these cases, does not change with cycle. On the other hand, the stress field when a strain hardening law is used appears to vary as a function of cycle number. Note also that the differences between the S–H and M–O solutions increase as the cycle number increases.

Figures 8a and 8b show the accumulated strains (ε_θ at $\theta = 0$) for the 9 Cr–Mo case, at the end of the unload-hold periods (times 25, 50, 75 h), and at the end of the load-hold periods (times 24, 49, 74 h), respectively. The differences between the S–H and M–O solutions increase as the number of cycles proceeds. Moreover, the strains at the end of the load-hold times are close, independent of the number of cycles for the S–H model. Note that these are the total accumulated creep strains, obtained by integrating the creep strain rates throughout the load history, as appropriate. An interesting observation can be made regarding the results of Figs 6–8. The stresses tend to be higher when a strain hardening law is used than when the Murakami–Ohno law is used, whereas the creep strains are lower. This can be explained as follows. During the load changes, the creep strain rates are greatly under-predicted by using a strain hardening law, whereas they are adequately predicted by using the Murakami–Ohno law. Because of this, the stresses do not relax after load path

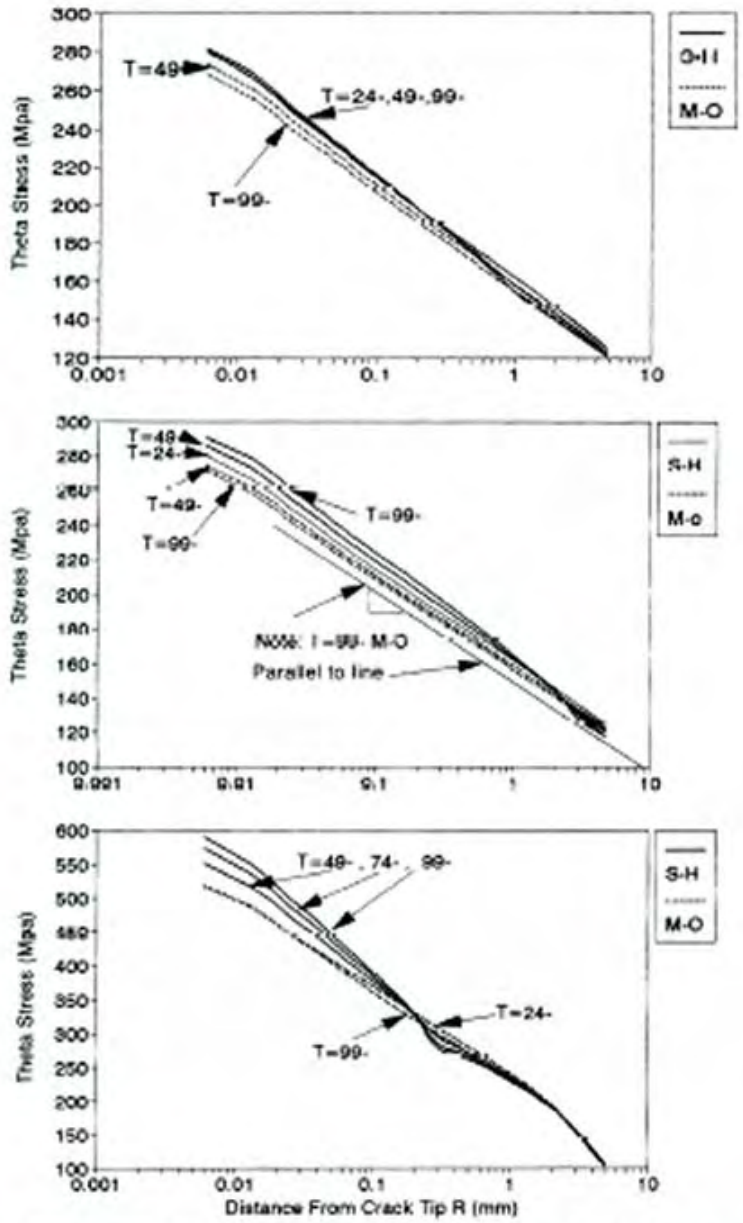

Fig. 7. σ_θ Stresses plotted as a function of distance from the crack tip for $\theta = 0$. Results are for times of 24, 49, and 99 h, i.e. after reload-hold sequences. (a) 304SS, $R = 0$ case. (b) 304SS, $R = -0.5$ case. (c) 9 Cr–Mo, $R = 0$ case.

changes as much as they should when a strain hardening law is used. At the same time, the corresponding creep strains do not accumulate as rapidly as they should when strain hardening theory is used.

Further comments are in order regarding Figs 7 and 8. It is well known [see Riedel (1981, 1987)] that the asymptotic stresses and strains are of $O\{[1/(n+1)]$ and $O\{(n/(n+1)\}$, respectively. When Figs 7 and 8 are plotted on a log–log scale, this means that the stresses and strains will plot as straight lines with a slope of $[1/(n+1)]$ and $\{n/(n+1)\}$, respectively. These slope values are indeed observed before unloading occurs, i.e. at time less than 24 h. At the end of the unload/reload sequences (times = 49, 74, 99 h), the stresses when a Murakami–Ohno creep law is used are not inconsistent with a slope of $[1/(n+1)]$

4.3. *Energetic or integral fracture parameters*

Making a choice as to which fracture parameters to focus on when attempting to characterize variable load or history dependent creep crack growth is difficult. We can label the different types of approaches as asymptotic approaches, damage or local approaches, and energetic or integral approaches. Asymptotic approaches are not considered here for reasons summarized above. Local or damage-based approaches, summarized in the recent book by Lemaitre and Chaboche (1990) and the numerous references cited therein, are very useful for predicting crack nucleation for all types of problems, including creep. For crack problems, however, there appears to be a difficulty. The procedure for both coupled and uncoupled damage theories consists of (i) developing the critical material parameter, D_c (scalar or tensor), and (ii) determining a critical length parameter, l_c, i.e. the degree of finite element refinement near the crack tip, so that experimental behavior is predicted. This same critical dimension is required for all other analyses. Because damage localizes at the crack tip, one finds that predicted results become more and more conservative as the mesh becomes more refined. This is because the finer the mesh, the greater are the stress and strain magnitudes and gradients near the crack tip become [see Giovanola and Kirkpatrick (1992) for example]. This type of behavior renders such methods, in the view of this author, to be insufficiently general to extend their use to history dependent creep fracture problems. The approach considered here is based on integral parameters. A general summary of this type of approach has been provided by Kim and van Stone (1992) and for creep problems by Brust and Majumdar (1994). For completeness, a summary of integral approaches is provided here.

Integral parameters. A number of integral parameters have been defined in recent years for application to non-linear fracture mechanics. Blackburn (1972) defined an integral, J_B, the J-integral was defined by Kishimoto *et al.* (1980), and other integral parameters have been suggested by McClintock (1971), and Watanabe (1985). Cherepanov (1967) first defined the Γ-integral, which was later called ΔT^* and T^* integrals by Atluri (1982), Nishioka and Atluri (1983), Brust *et al.* (1985, 1986), Brust and Atluri ((1986), and Brust and Majumdar (1994) in the context of creep fracture). A review of these integrals has recently been provided by Cherepanov (1989), and a review of a number of other integral parameters has recently been provided by Kim and Orange (1988) and Brust *et al.* (1989) in the context of thermal gradients.

The definition of the integrals in the notation defined below is:
Blackburn (1972):

$$J_B = \int_{\Gamma_c} (\tfrac{1}{2}\sigma_{ij}\varepsilon_{ij}n_1 - t_i u_{i,1})\,d\Gamma; \tag{8}$$

Kishimoto *et al.* (1980):

$$J = \int_{\Gamma_c} (W_e n_1 - t_i u_{i,1})\,d\Gamma; \tag{9}$$

Cherepanov (1967), Atluri (1982), Nishioka (1983), Nakagaki (1985), and Brust (1985):

$$T^* = \int_{\Gamma_c} (W n_1 - t_i u_{i,1})\,d\Gamma; \tag{10}$$

McClintock (1971):

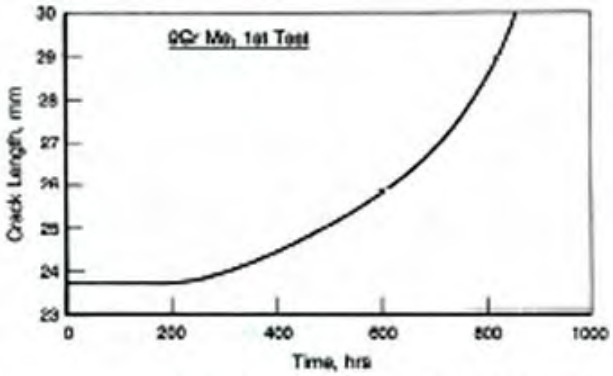

Fig. 9. Crack length versus time behavior for the test in Fig. 4a. The finite element model was forced to follow this crack growth relation.

$$J_M = \int_{\Gamma_\varepsilon} (-t_i u_{i,1})\, d\Gamma; \tag{11}$$

Watanabe (1985):

$$J_W = \int_{\Gamma_\varepsilon} (W n_1)\, d\Gamma. \tag{12}$$

In eqns (8)–(12), the integrals are integrated along a line path defined as Γ_ε. The path shape and other practical considerations are discussed by Brust and Atluri (1986) and Brust and Majumdar (1994), and in many references cited therein. In eqns 8–12, σ, ε, and $\hat{n}$ are the stress, total strain, and unit normal to the path, respectively, with x_1, and x_2 parallel and normal to the crack growth direction, respectively; t_i is the traction at the path point $(\hat{n}\cdot\sigma)$, $\mathbf{u}$ are displacements, and W is the stress work. The parameter W_e in eqn (9) is the elastic stress work. Note that $T^* = J_M + J_W$ always.

The physical interpretation of the T^*-integral is as an approximation of energy flux to the crack tip region and, as such, depends on the size of the path chosen, i.e. Γ_ε. Detailed discussion regarding the physical significance of the integrals, the path size, and other important considerations is provided by Brust and Majumdar (1994) and Brust *et al.* (1985).

4.4. *Analysis of an experiment*

The experiment discussed above and illustrated in Fig. 4 was modeled in its entirety. The load spectrum of Fig. 4(a) was applied. The experimentally determined crack growth versus time relationship shown in Fig. 9 was also imposed. The finite element mesh utilized is illustrated in Fig. 10. The side groove depth in these specimens was 20% of the thickness. (The nominal thickness was 25.4 mm.) Plane stress solutions were performed, since the creep zones were large here. The loads illustrated in Fig. 4 are the total applied load. The adequacy of this degree of mesh refinement was verified in two ways. First, several constant load cases were analyzed, and the C^*-integral and the C_t^*-integral [respectively, for analyses using the second and first terms of eqn (1) only] were evaluated numerically and compared with handbook solutions. Secondly, two identical analyses were performed by using the extremely refined mesh used to produce the asymptotic solutions for Section 4.2, and the mesh of Fig. 10 over the first 192 h of this test, before crack growth began. The crack initiated 192 h after the test began. All of the integrals discussed above were evaluated on numerous paths for both meshes. The numerical values of the integrals compared within 1% for path sizes greater than 0.3 mm. By observing Fig. 10(b), this means that we can expect numerically accurate results outside a buffer zone of about two elements outside the crack tip.

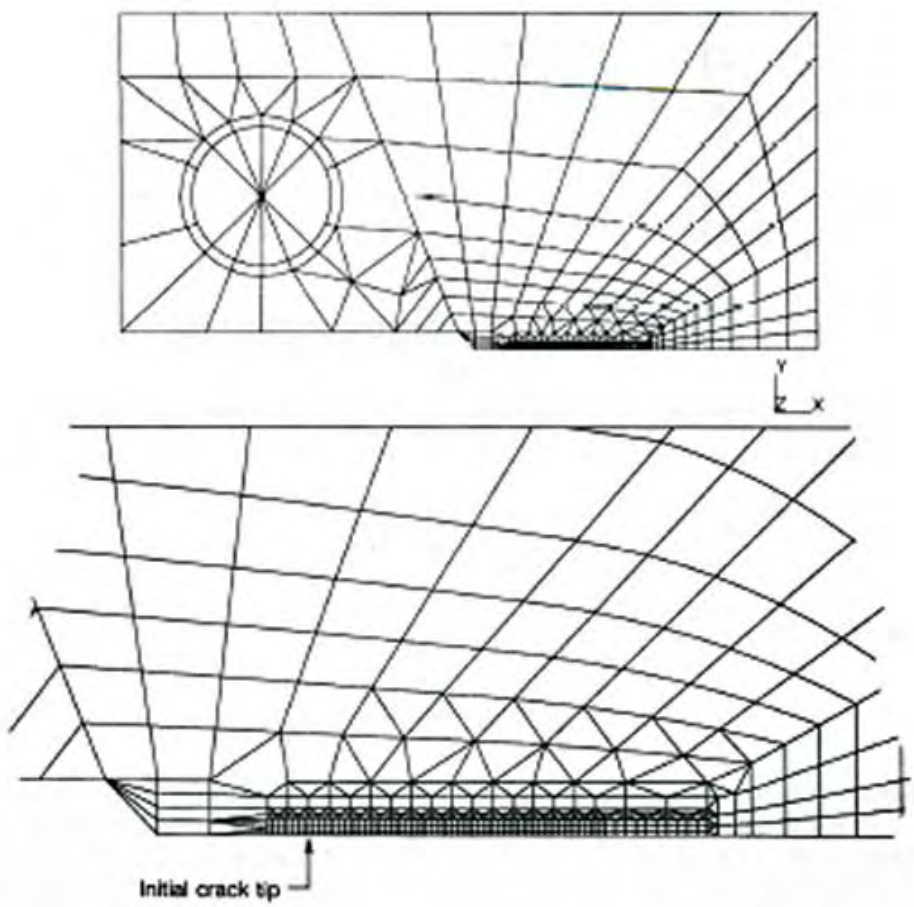

Fig. 10. Finite element mesh used to model test. (a) Overall mesh. (b) Mesh blow-up near the crack tip. The elements near the crack tip are 0.15-mm-square elements.

The material properties were those listed in Section 4.2 for the 9 Cr–Mo steel at 538° C. The two other constants needed to utilize eqn (1) are:

$$A_1 = 1.362 \times 10^{-56}, \quad n_1 = 18.86$$

for stress in Mpa and time in hours.

Figure 11(a) shows the compressive stress immediately after unloading at $t = 343$ h, i.e. before stress relaxation occurs. The finite element grid is shown so that the reader can obtain a feel for the size scales involved. Recall that the elements near the crack tip are square with a side length of 0.15 mm. The contour levels shown in these figures represent the magnitudes at the *outside edge* of the shading (the large stress gradients should be clear). Figure 11(b) shows the stresses after creep relaxation has occurred after the 0.1-h unload-hold period. Note the significant size of the compressive zone. Comparing compressive residual stress zone sizes at later times and comparing these with Fig. 11, one observes that the magnitudes of the compressive stresses after relaxation are continually increasing as the crack size increases, as expected.

Figure 12 shows the size of the compressive σ_x zone behind the wake of the growing crack at a time of 628 h. This is at a time when the full load is on the specimen, and the crack has just completed growing through an element. Such a compressive wake zone is known to exist for elastic–plastic growing cracks [see, for instance, Rice *et al.* (1980)], and here it is shown to occur for growing creep cracks. The known asymptotic solutions for growing cracks using simple constitutive laws also exhibit this compressive wake zone feature [(see Riedel (1987), for instance)] for plane stress, but not for plane strain. The

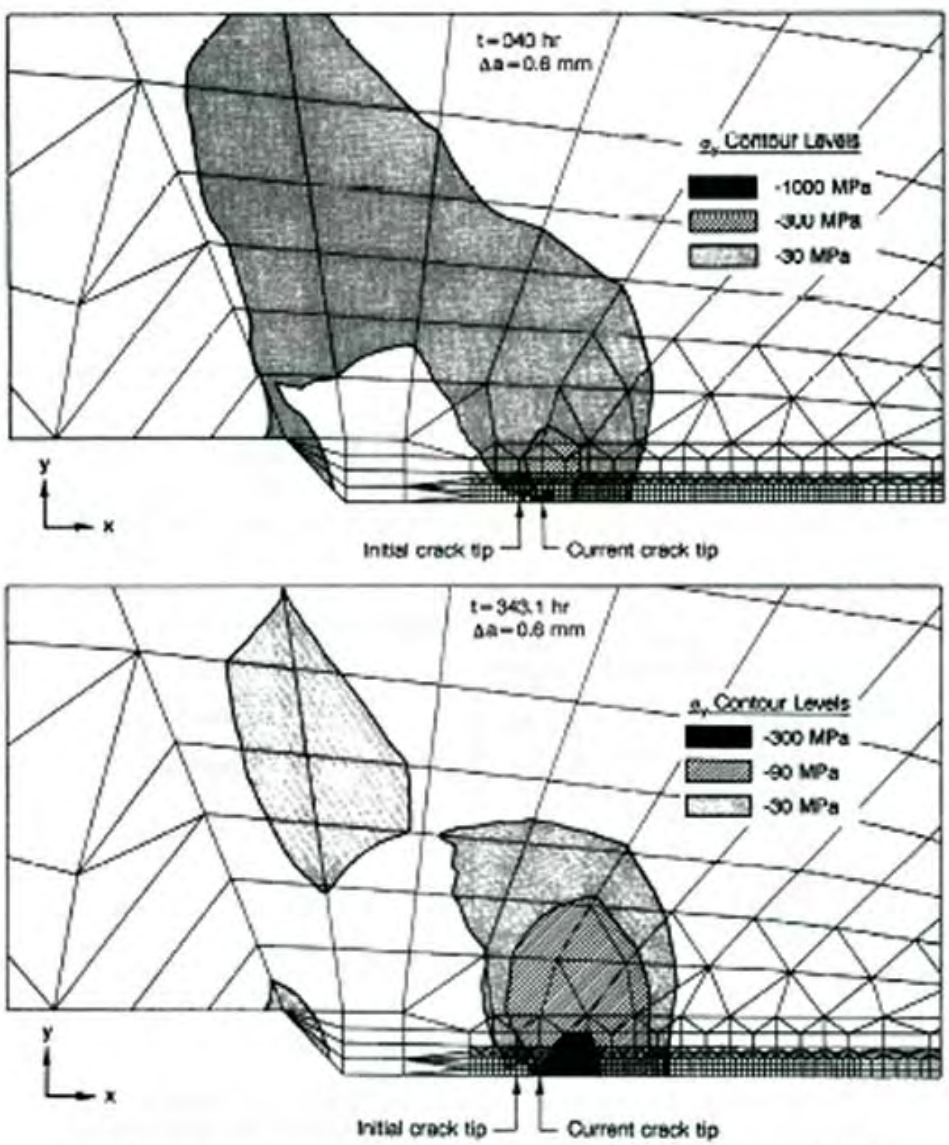

Fig. 11. Contour plots of σ_y near the time of 343 h. The contour levels represent the values at the outermost border of the shade. The size of the elements along the crack growth direction near the tip is 0.15 mm along the side. (a) Stresses just after unloading, before stress relaxation occurs. (b) Stress after the 0.1-h unload-hold period of relaxation has occurred.

compressive zone size seen here is much larger than that predicted from asymptotic solutions. The stresses in this zone are not insignificant, with a maximum stress in the compressive wake shown in Fig. 12 of −300 Mpa.

Displacement comparisons. The experimental and analytically predicted displacements are compared over the first 192 h of the test, before crack growth begins, in Fig. 13. The extremely refined mesh used in Section 4.2 was used for these predictions. The experimental results are slightly higher than the predicted values. Note that, for the analysis, the crack was assumed to begin growing at a time of 192 h after the beginning of the test. However, as indicated in Fig. 13, small amounts of crack growth actually occurred before this time, which, in part, accounts for the underprediction of the analysis. An analysis assuming a constant load is also plotted here, showing that there is a continual drift upward of

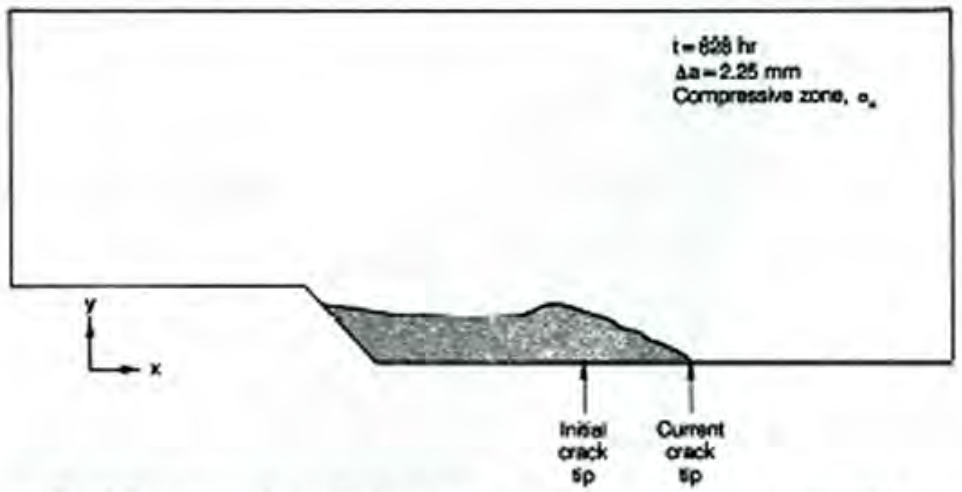

Fig. 12. Compressive wake zone for the growing creep crack. The maximum stress is −300 MPa in this region.

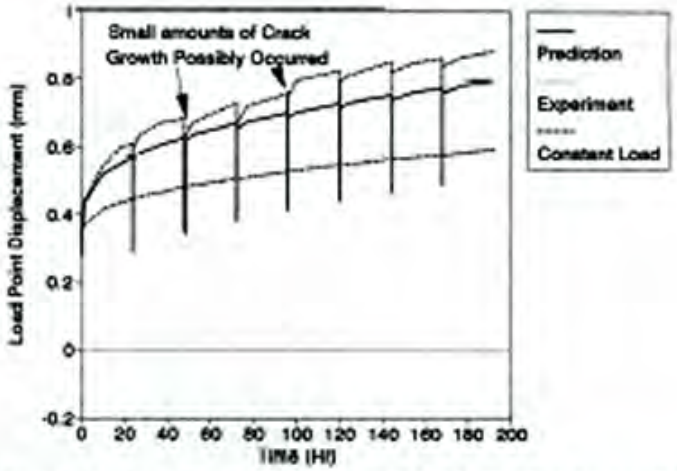

Fig. 13. Comparison between experimental and predicted load point displacements for the 9 Cr–Mo test before crack growth. The lower curve represents results for the constant load case.

the variable load solution owing to the increased strain rates that develop after each cycle.

Figures 14(a)–14(c) show some of the details of the displacement comparisons over shorter time periods. Figure 14(a) shows what happened very early in the test. The precise load history shown in Fig. 4 was not strictly followed in this particular test. There were a few times during the test where the load was held longer than 24 h before unloading. (It will be clear in some of the later figures when this occurred.) At the beginning of the test, some differences also occurred. A load of 19.94 kN was first applied to the specimen and held for 0.05 h. The specimen was then unloaded and held for 0.033 h before loading to 23.353 kN and following the general sequence of Fig. 4. (This was done to provide a check on the experimental set-up.) This means that the first unloading actually occurred about 5 min after the start of the test. Figure 14(a) details the displacements over the first 2 h of the test. Note the effect of the first unload cycle on the displacement predictions. It is also clear here that the displacement rates due to the first cycle of load increase significantly compared with having no cycle. Figure 14(b) details the displacements between 110 and 180 h after the test began. Note that the displacement rates after an unload cycle are greater than those before the unloading. This effect becomes more important after crack growth

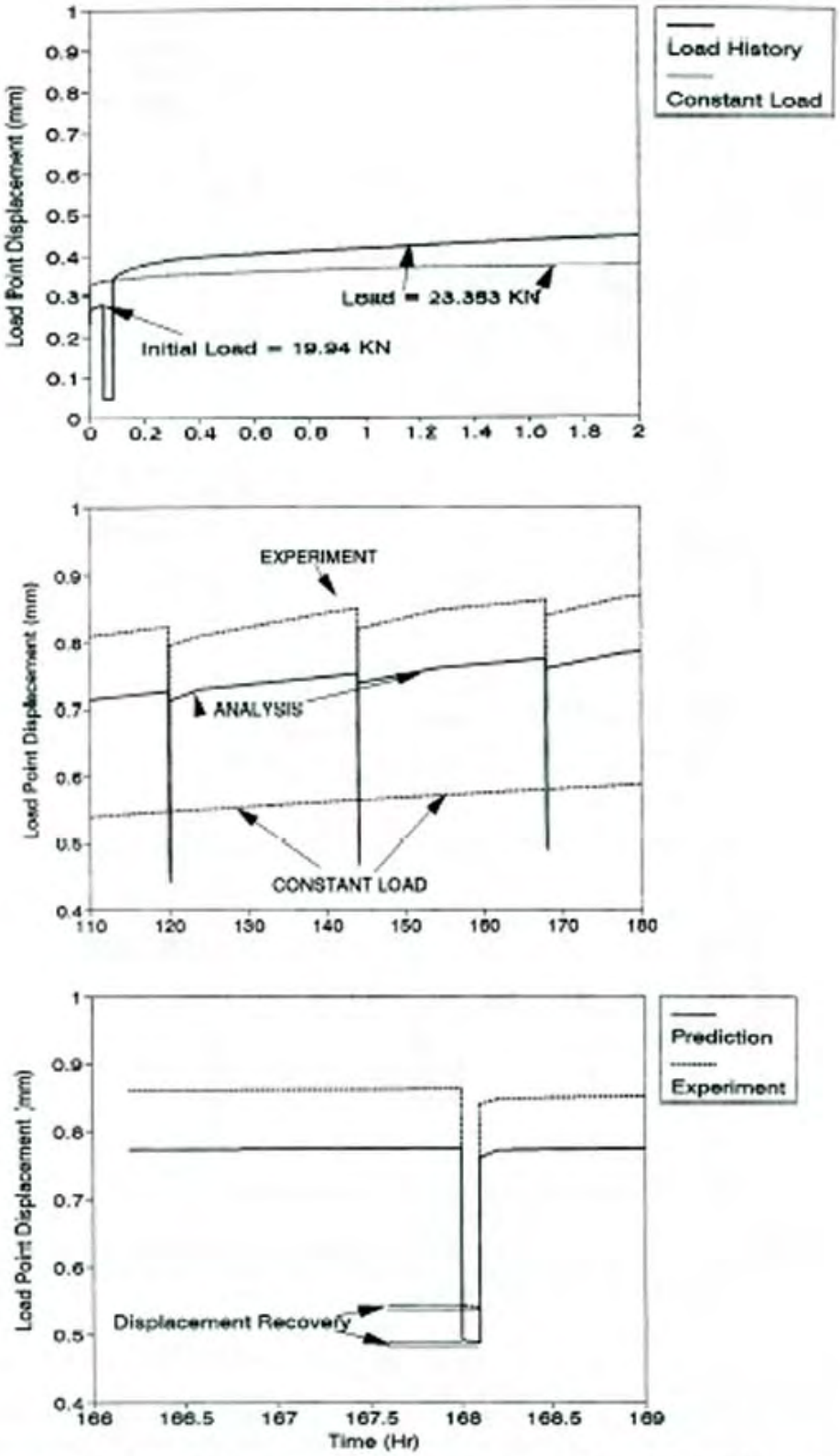

Fig. 14. Details of displacement versus time comparisons at specific times before crack growth begins. (a) Comparison of predicted results for variable load and constant load cases. (b) Detailed comparison of three unload cycles between 110 and 180 h. (c) Comparison of displacements during the load at time of 168 h.

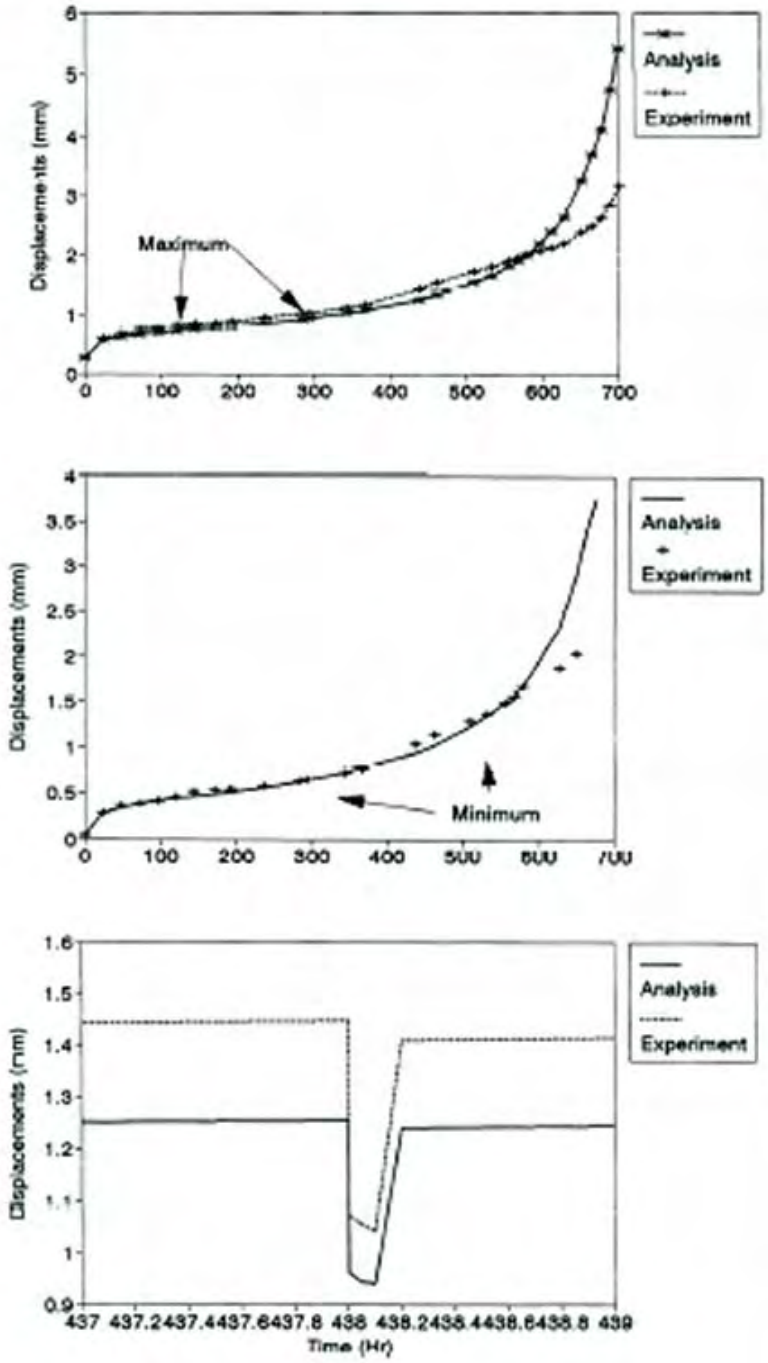

Fig. 15. Comparison of displacements for 9 Cr–Mo test. (a) Maximum displacements at the end of the reload-hold times. (b) Minimum displacements at the end of the unload-hold times. (c) Displacement comparison for the unload–reload cycle at time = 438 h.

commences, as will be shown shortly, and was discussed relative to Figs 2 and 4. Figure 14(c) shows displacement recovery at a time of 168 h.

Figure 15 shows the predicted and experimentally determined displacements over the entire test. Figure 15(a) shows the maximum displacements, i.e. at the end of reload and hold periods, throughout the entire test. The experimental and predicted displacements compare quite well until about 600 h. After this time, the predicted displacements overpredict the experimental values. This overprediction after 600 h essentially means that

failure was predicted a little earlier analytically than the experimental results showed. The experiment showed that the displacements began to rise sharply at about 650 h, prior to failure at about 710 h. This difference between the analysis and experiment may be due, in part, to the use of a plane stress assumption for the analysis. Figure 15(b) provides a comparison of the minimum displacements, i.e. at the end of the unload-hold periods. Again the comparison is quite reasonable. Figure 15(c) shows a detail of predicted and experimental displacements during the unload that occurred in the 438th hour of the test. Here the displacement recovery and the reduced displacement compared with the values before unloading, and the increased displacement rates due to the cycle are evident. Note from Fig. 15(a) that this comparison at a time of 438 h is made for the time when the difference between prediction and analysis is nearly the maximum for times less than 600 h. The results of Fig. 15 give us confidence that the numerical model compares reasonably with experimental data. The predictions provided next for the integral parameters are therefore likewise considered to be reasonably accurate.

Integral parameters. The behavior of the integral parameters is somewhat different before and after crack growth. Let us first look at the behavior for a constant load case with no crack growth before providing the predictions of the integrals for this particular test. Consider loading the compact tension specimen to 23.353 kN and holding it for 2000 h. The integral parameters should be path independent in the region of dominance of the asymptotic fields if the fields are separable and if terms like $\sigma \cdot \dot{\varepsilon}$ are of $O(1/r)$ [see Willis (1975) and Moran and Shih (1987)]. Figure 16(a) shows the behavior of the T^*-integral evaluated on four paths of radius $R = 0.3, 0.45, 0.6$, and 0.8 mm. These paths are circular in shape and traverse the stationary crack tip. (The refined focused mesh used for the asymptotic studies was used for this constant load case only.) This figure suggests that the integrals are independent of path. In fact, all the integral parameters behave this way, including J_W and J_M, even though these two integrals are not path-independent even for the elastic problem. This suggests that the region of dominance of the asymptotic fields is quite large. This observation of a large zone of dominance for the asymptotic field was also made in Section 4.2, which examined the asymptotic fields themselves. Indeed, this is an alternative technique to determine the region of dominance of the asymptotic fields. Observing Figs 16(b) and 16(c), however, note that both T^* and J_W are not path-independent. Figure 16(b) is actually a blow-up of Fig. 16(a) over the first 10 h. The initial load is applied elastically, this being followed by the relaxation of the elastic singularity via creep deformation. Apparently, the conditions for path independence discussed above are violated for a very short period of time (less than about 0.05 h). One can see that the integrals are path-dependent for early times, and then the same difference between the paths is maintained over the rest of the analysis. Since:

$$T^* = \int_0^t \dot{T}^* \, dt \tag{13}$$

throughout the entire load history, it is clear that the integral rates are path-dependent for a short period after application of the load, after which the rates of the integrals become path-independent. This effect was checked by using several different mesh refinements, and several different degrees of time step refinement, and appears to be real.

Now we return to the analysis of the experiment of Fig. 4 and discuss the behavior of these integral parameters during cyclic loading. Figure 17a shows the behavior of the J_W-integral for the variable load case, also evaluated along four different-sized circular paths emanating from the stationary crack tip. These plots show the first 192 h of the test analysis results, before crack growth commences. Several interesting observations can be made. (i) After each change in load path, a step function increase in the integral occurs. (Note here that the first unload actually occurred after only 0.05 h of testing; hence, large differences between the paths are observed early.) Such a step function change suggests that the unloads induce increased damage to the crack tip region. (ii) The value of the integral is larger as

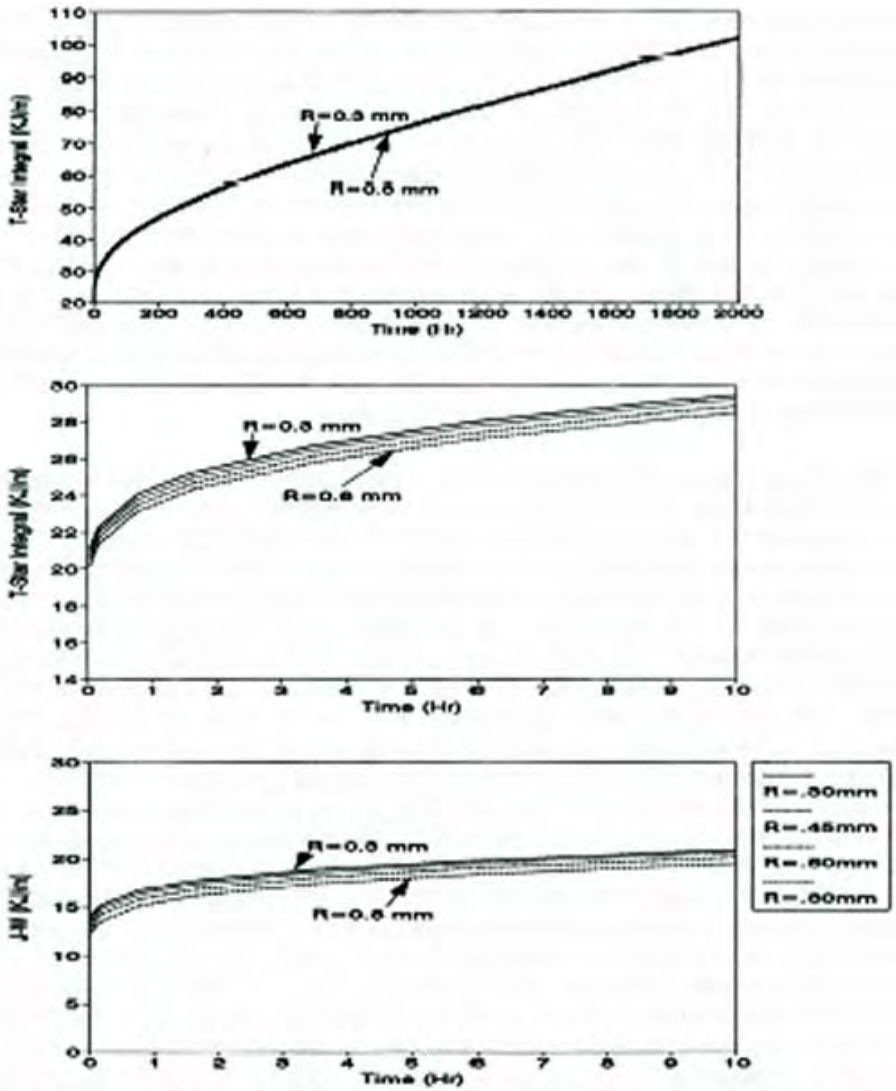

Fig. 16. Behavior of the integral parameters evaluated along different-sized circular paths (R = 0.3, 0.45, 0.60, and 0.80 mm) for the constant load case. (a) T^*-integral over the entire time period. (b) T^*-integral from 0 to 10 h. (c) J_w-integral from 0 to 10 h.

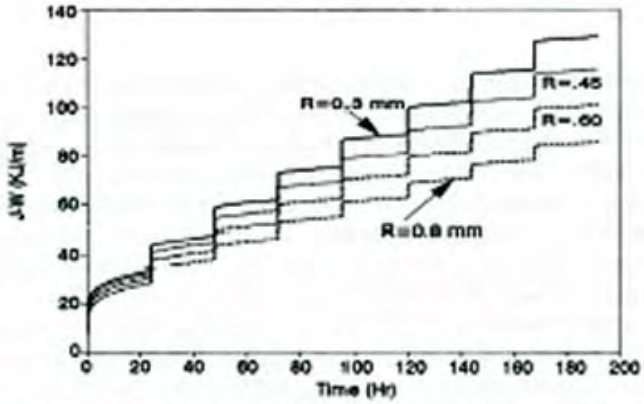

Fig. 17a. J_w-integral plotted as a function for the variable load test before crack growth begins; R is the radius of the circular path emanating from the crack tip.

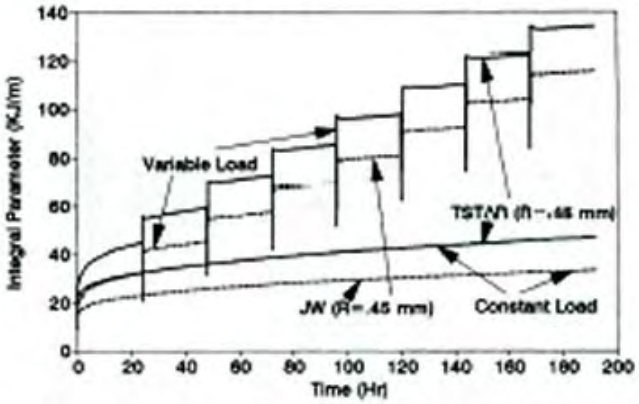

Fig. 17b. T^*- and J_w-integrals. Comparison between the constant load and variable load cases. The path size, R, is 0.45 mm.

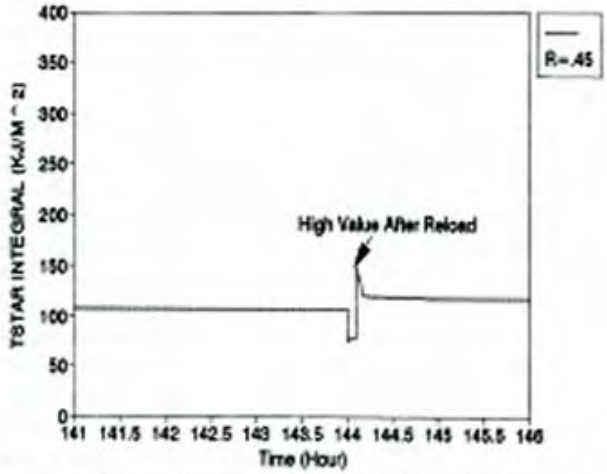

Fig. 17c. Behavior of T^*-integral for unloading at $t = 144$ h. Crack growth has not begun as yet.

the size of the path *becomes smaller*. In addition, it is clear that the integral is becoming more and more path-dependent, further suggesting that the asymptotic fields change, perhaps with each cycle, and further violate the conditions for path-independence in the region of asymptotic fields (i.e. separable fields, etc.). It should also be mentioned that the rates of J_w are also path-dependent even near the end of each of the reload-hold (24-h) periods. Clearly, these results, coupled with those presented in Section 4.2, suggest that the classical approach to creep fracture, i.e. the search for the strength of an asymptotic field, may not be practical under variable load conditions since the crack tip fields change significantly as unloads take place. *The trends illustrated in Fig. 17a occur for all five integrals considered here.*

Figure 17b shows the T^*- and J_w-integrals for a path radius of 0.45 mm for both the variable load and the constant load cases. Note that the T^*-integral decreases during an unload (see also Fig. 17c), whereas J_w does not. The constant load values of the integrals are also shown in Fig.17b. The effect of the unloads is to increase the crack tip severity if these integrals are crack tip characterization parameters. Finally, the behavior of the T^*-integral after an unload/reload sequence can be observed in Fig. 17c. Figure 17c shows an enlargement of the unload performance of the T^*-integral at a time of 144 h. Immediately after reloading, the integral attains a large value, which reduces very rapidly over short times to a steadily increasing value. All integrals behave in this way for the stationary crack problem. For the growing crack, this effect is not seen. It is believed that this is an artifact of the Murakami–Ohno constitutive law used. The plots of the integrals as a function of

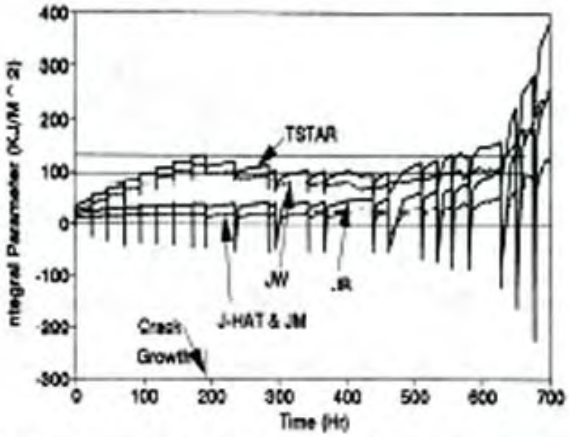

Fig. 18. Integral parameters plotted against time for complete analysis of test.

time do not include these large spikes, which occur over very short times after reloading. Rather, the first integral value plotted is typically after about 0.1 h after the reload-hold time begins to eliminate this artifact.

Figure 18 compares all the integral parameters as a function of time. This is for a value of the path size equal to 0.45 mm. Brust and Majumdar (1994) discuss the practical evaluation of these parameters in detail for the growing crack problem. The T^* and J_W integrals both experience a step jump after each cycle, as discussed earlier, before crack growth begins. The J_R-, $\hat{J}$-, and J_M-integrals also do so, but to a much smaller extent. Note that the J_M and $\hat{J}$ parameters are almost identical. This is because the W_e term in $\hat{J}$, which is the elastic stress work, is very small, as it is for nearly all non-linear problems [see eqn (9)]. Also observe that the experimental scheme of Fig. 4 is not strictly adhered to, since several times 48 h elapsed, and once 72 h, before an unload cycle. Further note that the T^*-integral attains a nearly constant value (close to the nucleation value) throughout the entire time history (between 100 and 130 kJ/m^2, as indicated by the lines in Fig. 18). This suggests that a constant value of T^* may characterize crack growth under creep fatigue conditions. The same comment applies to J_W.

The T^*- and J_W-integrals are plotted as a function of the path size in Figs 19a and 19b, respectively. These figures show the values of the integrals at the end of the hold periods only. It may be seen that, before crack growth occurs, the paths closest to the crack tip maintain larger magnitudes than the larger paths. After crack growth, however, a trend in the opposite direction begins, with the larger paths giving slightly larger values. The larger values after crack growth are expected because of the interpretation (discussed in Section 4.3) of the integrals as an energy loss per unit crack extension, to a finite-sized region (i.e. the value of the path size R) in the vicinity of the growing crack tip. The larger R is, the greater is the energy that may be deposited into the crack tip region. Values for the path size of $R = 0.3$ mm, which is probably too close to the crack tip, and subject to numerical errors, were not plotted here. The values of the integrals, especially after crack growth begins, are nearly independent of the path size. This is a very important result because it suggests that we may choose any value of R for our definition of the resistance curve, as long as R is small enough to capture the energy losses due to the crack only. For practical application of these parameters, the largest value of R that is feasible is desired in order to minimize computational costs.

It is also important to comment that the values of these integrals are independent of the finite element grid size chosen. For instance, if the same analysis is performed by using a grid twice as refined as the mesh used here, and the integrals are calculated on the same size of paths as those used here (i.e. $R = 0.45$, 0.6, etc.), the same resistance curve is obtained. This was shown here for the stationary crack portion of the analysis by using the meshes of Section 4.2 and Fig. 10 and was demonstrated by Brust *et al.* (1985), using four different meshes for the elastic–plastic crack growth problem.

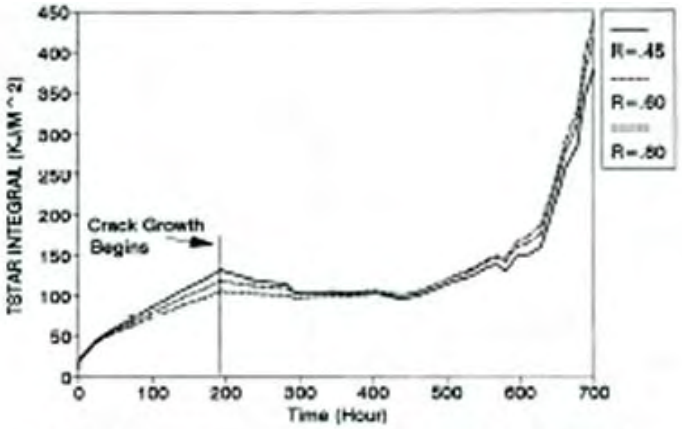

Fig. 19a. T^*-integral versus time for several definitions of path size, R.

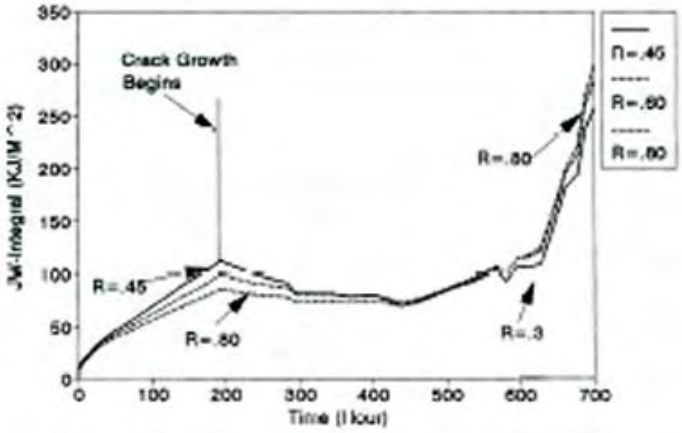

Fig. 19b. J_a-integral versus time for several definitions of path size, R.

The resistance curves are plotted in Figs 20a–20c for $R = 0.45$ and 0.8 mm. Note the nearly constant value that the T^*- and J_0-integral resistance curves maintain during crack growth. The J_M-integral, on the other hand (Fig. 20c), continually increases during crack growth at a nearly constant rate (especially for $R = 0.8$ mm). After about 628 h, the curves become unstable, suggesting that unstable creep failure is predicted. The predicted

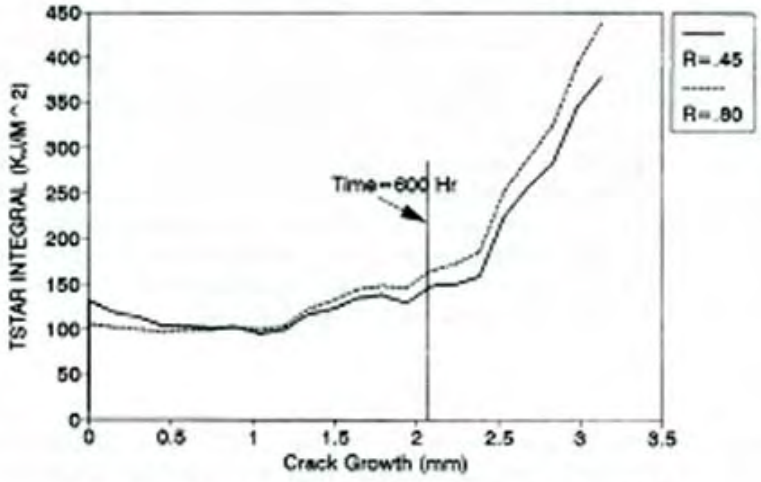

Fig. 20a. T^*-resistance curves. Instability begins after about 600 h.

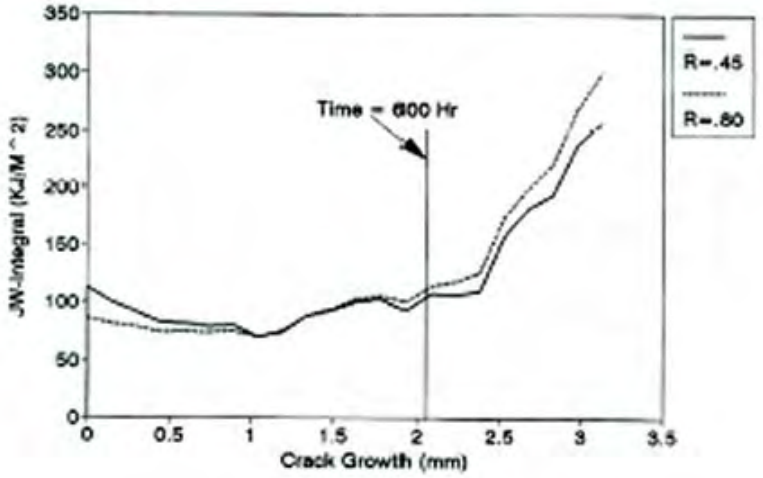

Fig. 20b. J_w-resistance curve.

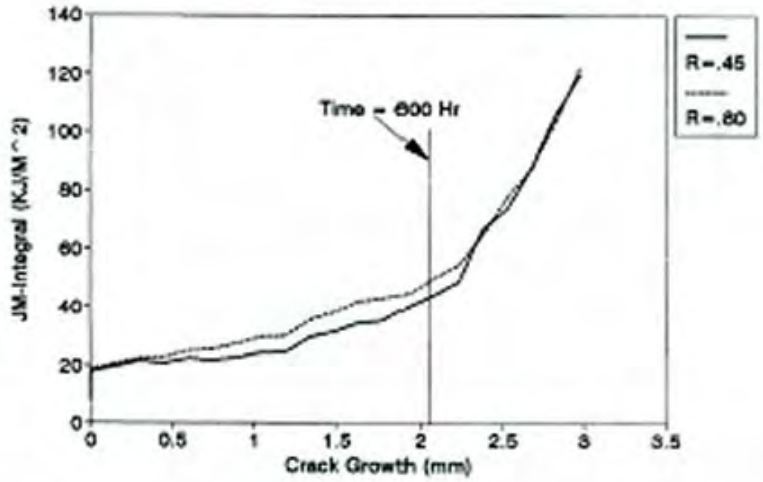

Fig. 20c. J_M-resistance curve.

instability point for this analysis compares reasonably well with the experimental results, especially considering the two-dimensional nature of the analysis.

The nearly constant saturation values for T^* and J_W during crack growth suggest that these parameters may be used as a creep fracture parameter for cyclic creep. The fact that they are not perfectly uniform is due to three-dimensional crack-growth effects and the plane-stress assumption. Moreover, errors in crack growth measurements can certainly affect results. However, this suggests that these integrals may be used to predict crack initiation as well as growth by using the value at initiation throughout the history. In addition, creep crack nucleation and reinitiation may also be predicted. The J_M-integral may likewise be used, with its resistance curve continually increasing. However, because the T^*-integral has a physical interpretation, it may be the most useful of the parameters. Crack nucleation or crack reinitiation during history dependent loading would be predicted by using this constant value of the resistance curve of Fig. 20a.

5. CONCLUSIONS

The subject of creep-crack growth behavior under variable load conditions was investigated here. The importance of large creep strain rates which develop after stress reversals was shown to have a strong influence on the deformation response of a cracked creep

specimen. Classical creep-crack approaches for variable load creep-fatigue conditions were critically examined. It was determined that such approaches, which are based on obtaining the strength of asymptotic crack tip fields, may not be sufficiently general because the fields appear to break down and change as the number of load cycles increases. The possibility of using alternative integral fracture parameters for characterizing the variable load creep-crack growth process was examined. While certainly not conclusive, the potential for using these alternative parameters for characterizing this complex process of crack behavior appears promising. Further work is necessary, is ongoing, and will be reported in the near future.

Acknowledgements—This work was supported by the U.S. Department of Energy, Office of Basic Engineering Sciences, under Grant No. DE-FG02-90ER14135. The author thanks Dr O. Manley and S. Datta for their support. The author would also like to thank Dr Bhaskar Majumdar for directing the experimental efforts.

REFERENCES

Atluri, S. N. (1982). Path independent integrals in finite elasticity and inelasticity, with body forces, inertia, and arbitrary crack-face conditions. *Engng Fract. Mech.* **16**, 341–364.

Bassani, J. L. and McClintock, F. A. (1981). Creep relaxation of stress around a crack tip. *Int. J. Solids Structures* **17**, 479–492.

Blackburn, W. S. (1972). Path independent integrals to predict onset of crack instability in an elastic plastic material. *Int. J. Fract.* **8**, 343–346.

Brust, F. W. and Atluri, S. N. (1986). Studies on creep crack growth using the T^* integral. *Engng Fract. Mech.* **23**, 551–574.

Brust, F. W. and Leis, B. N. (1992). A new model for characterizing primary creep damage. *Int. J. Fract.* **54**, 45–63.

Brust, F. W. and Majumdar, B. S. (1994). Load history effects on creep-crack growth. *Engng Fract. Mech.*

Brust, F. W., Nishioka, T., Atluri, S. N. and Nakagaki, M. (1985). Further studies on elastic–plastic stable fracture utilizing T^*-integral. *Engng Fract. Mech.* **22**, 1079–1103.

Brust, F. W., McGowan, J. J. and Atluri, S. N. (1986). A combined numerical/experimental study of ductile crack growth after a large unloading using T^*, J, and CTOA criteria. *Engng Fract. Mech.* **23**, 537–550.

Brust, F. W., Nakagaki, M. and Springfield, C. W. (1989). Integral parameters for thermal fracture. *Engng Fract. Mech.* **33**, 561–579.

Brust, F. W., Krishnaswamy, P. and Majumdar, B. S. (1993). Further studies of history-dependent loading in the creep-crack growth regime. In *Fracture Mechanics—Applications and New Materials* (PVP-Vol. 260), pp. 49–58. American Society of Mechanical Engineers, New York, NY, USA.

Cherepanov, G. P. (1967). Crack propagation in continuous media. *Appl. Math. Mech.* **31**, 467–488.

Cherepanov, G. P. (1989). A remark on the dynamic invariant or path-independent integral. *Int. J. Solids Structures* **25**, 1267–1269.

Gittus, J. (1975). *Viscoelasticity and Creep Fracture in Solids*. Applied Science, London.

Giovanola, J. H. and Kirkpatrick, S. W. (1992). Advances in Fracture/Damage Models for the Analysis of Engineering Problems (ASME Publication AD-Vol. 137), pp. 285–303.

Goldman, N. L., and Hutchinson, J. W. (1975). Fully-plastic crack problems: the center cracked strip under plane strain. *Int. J. Solids Structures* **11**, 575–592.

Inoue, T. *et al.* (1991). Evaluation of inelastic constitutive models under plasticity-creep interaction condition. *Nucl. Engng Des.* **126**, 1–11.

Janke, C. E. (1984). Topical report on damage accumulation by crack growth under creep and fatigue, Ph.D. thesis, Ohio State University, USA (also Department of Energy Report for Contract No. W-7405-ENG-92-131).

Kim, K. S. and Orange, T. W. (1988). A review of path-independent integrals in elastic–plastic fracture mechanics. In *Fracture Mechanics: Eighteenth Symposium* (ASTM STP 945), American Society for Testing and Materials, Philadelphia, PA, USA, pp. 713–729.

Kim, K. S. and van Stone, R. H. (1992). Elevated temperature crack growth, NASA Final Report, NASA CR-189191.

Kishimoto, K., Aoki, S. and Sakata, M. (1980). On the path independent integral. *J. Engng Fract. Mech.* **13**, 841–850.

Krishnaswamy, P., Brust, F. W. and Ghadiali, N. D. (1993). Finite element analysis of history dependent damage in time dependent fracture mechanics. *ASME J. Press. Vessel Technol.* **115**, 339–347.

Krishnaswamy, P., Brust, F. W. and Ghadiali, N. D. (1994). A finite element algorithm to study creep crack growth based on the creep hardening surface. *Int. J. Num. Meth. Engng*, in print.

Lemaitre, J., and Chaboche, J. L. (1990). *Mechanics of Solid Materials*. Cambridge University Press, Cambridge, UK.

Leung, C. P., McDowell, D. L. and Saxena, A. (1988). Influence of primary creep in the estimation of C_t parameter. *Int. J. Fract.* **36**, 275–289.

McClintock, F. A. (1971) in *Fracture* 3 (Edited by H. Liebowitz), Academic Press.

Moran, B. and Shih, C. F. (1987). Crack tip and associated domain integrals from momentum and energy balance. *Engng Fract. Mech.* **27**, 615–62.

Murakami, S. and Ohno, N. (1982). A constitutive equation of creep based on the concept of a creep hardening surface. *Int. J. Solids Structures* **18, 67,** 597–609.

Nicholas, T. and Weerasooriya, T. (1985). A model for creep fatigue interactions in alloy 718 (ASTM STP 868), pp. 167–180. American Society for Testing and Materials, Philadelphia, PA, USA.

Nicholas, T. and Weerasooriya, T., (1986). Hold-time effects in elevated temperature fatigue crack propagation (ASTM STP 905), pp. 167–180. American Society for Testing and Materials, Philadelphia, PA, USA.

Nishioka, T. and Atluri, S. N. (1983). Path independent integrals, energy release rates, and general solutions of near-tip fields in mixed-mode dynamic fracture mechanics, *Engng Fract. Mech.* **18,** 1–22.

Ohno, N., Murakami, S. and Ueno, T. (1985). A constitutive model of creep describing creep recovery and material softening caused by stress reversals. *J. Engng Mater. Technol.* **107,** pp. 1–6.

Rice, J. R., Drugan, W. J. and Sham, T. L. (1980). Elastic–plastic analysis of growing cracks (ASTM STP 700) pp. 189–221. American Society for Testing and Materials, Philadelphia, PA, USA.

Riedel, H. (1981). Creep deformation at crack tips in elastic–viscoplastic solids. *J. Mech. Phys. Solids* **29,** 35–49.

Riedel, H. (1987). *Fracture at High Temperatures.* Springer-Verlag, Berlin, Germany.

Riedel, H. and Rice, J. R. (1980). Tensile cracks in creeping solids. In *Fracture Mechanics: Twelfth Conference* (ASTM STP 700), pp. 112–130. American Society for Testing and Materials, Philadelphia, PA, USA.

Saxena, A. and Han, J. (1986). Evaluation of crack tip parameters for characterizing crack growth behavior in creeping materials. ASTM Task Group Report E24.08.07IE.24.04.08.

Saxena, A. (1991). Creep crack growth in high temperature ductile materials. *Engng Fract. Mech.* **40,** 721–736.

Shih, C. F. and German, M. D. (1981). Requirements for a one parameter characterization of crack tip fields by the HRR singularity. *Int. J. Fract.* **17,** 27–43.

Watanabe, K. (1985). The conservation law related to path independent integral and expression of crack energy density by path independent integral, *Bull. Japan Soc. Mech. Engrs* **28,** 26–33.

Willis, J. R. (1975). Equations of motion for propagating cracks. In *The Mechanics and Physics of Fracture*, pp. 57–67. The Metal Society.

Yokobori, T. and Yokobori, A. T., Jr (1984). Some notes to the high temperature crack growth rates and probabilistic fracture mechanics approach, respectively. In *Proceedings of ICF6*, New Delhi, India, 4–10 December, pp. 273–284.

Final Technical Report

to

ASME Standards Technology, LLC

Gen IV/NGNP Materials Project: Task 8

Task 8: Creep and Creep-Fatigue Crack Growth at Structural Discontinuities and Welds

Part II Task Report – Draft Rules

to

Mr. Jim Ramirez
Vice President, Business Development
ASME Standards Technology, LLC
Three Park Avenue
New York, NY 10016

from

Dr. F. W. Brust
Dr. G. M. Wilkowski
Dr. P. Krishnaswamy
Mr. Keith Wichman
Engineering Mechanics Corporation of Columbus (Emc^2)
3518 Riverside Drive, Suite 202
Columbus, OH 43221-1735

January 27, 2010

1.0 Introduction

The subsection ASME NH high temperature design procedure does not admit crack-like defects into the structural components. The US NRC identified the lack of treatment of crack growth within NH as a limitation of the code and thus this effort was undertaken. This effort is broken into two parts. The Part 1 final report, summarized in [1], involved examining all high temperature creep-fatigue crack growth codes being used today and from these, the task objective was to choose a methodology that is appropriate for possible implementation within NH. The second part of this task, which is summarized here, is to develop design rules for possible implementation within NH. This second part is a challenge since all codes require step-by-step analysis procedures to be undertaken in order to assess the crack growth and life of the component. Simple rules for design do not exist in any code at present. The codes examined in this effort included R5, RCC-MR (A16), BS 7910, API 579, and ATK (and some lesser known codes).

After examining the pros and cons of all these methods, the R5 code was chosen as the most up-to-date and validated high temperature creep and creep fatigue code currently used in the world at present. R5 is considered the leader because the code: (i) has well established and validated rules, (ii) has a team of experts continually improving and updating it, (iii) has software that can be used by designers, (iv) extensive validation in many parts with available data from BE resources as well as input from Imperial college's database, and (v) was specifically developed for use in nuclear plants.

R5 was specifically developed for use in gas cooled nuclear reactors which operate in the UK and much of the experience is based on materials and temperatures which are experienced in these reactors. If the next generation advanced reactors to be built in the US used these same materials within the same temperature ranges as these reactors, then R5 may be appropriate for consideration of direct implementation within ASME code NH or Section XI. However, until more verification and validation of these creep/fatigue crack growth rules for the specific materials and temperatures to be used in the GEN IV reactors is complete, ASME should consider delaying this implementation. With this in mind, it is this authors opinion that R5 methods are the best available for code use today.

The focus of this work was to examine the literature for creep and creep-fatigue crack growth procedures that are well established in codes in other countries and choose a procedure to consider implementation into ASME NH. It is very important to recognize that all creep and creep fatigue crack growth procedures that are part of high temperature design codes are related and very similar. This effort made no attempt to develop a new creep-fatigue crack growth predictive methodology. Rather examination of current procedures was the only goal. The uncertainties in the R5 crack growth methods and recommendations for more work are summarized here also.

Finally, it is important to recognize that R5 was developed as an 'assessment' procedure. A high temperature assessment procedure is used to assess or determine the effect of cracks on safety and performance of high temperature components. As such, it is not really used for design.

2.0 Overview of Task 8, Part I

ASME Standards Technology, LLC is leading efforts to conduct research in support of the Generation IV/NGNP Materials project. A number of tasks have been completed and many efforts are ongoing in this program. These programs are a continuation of an existing Cooperative Agreement between ASME Standards Technology, LLC and The U.S. Department of Energy in support of the Generation IV/NGNP programs. The scope includes development of technical basis documents necessary to update and expand codes and standards for application in next generation reactor systems that operate at elevated temperatures. This is a multi-year agreement. A project structure is already in place that includes a Steering Committee, and subcontracted Task Investigators and Technical Advisors.

The GEN IV reactor concepts require structural components to operate at high temperatures in a regime where creep damage may occur and cracks may grow. The US Nuclear Regulatory Commission (NRC) has identified the lack of a quantitative methodology for evaluating creep and creep crack growth as a shortcoming of the ASME Subsection NH (Class 1 Components in Elevated Temperature Service) standard [2]. The development of elastic-plastic fracture mechanics methods and the concepts of leak-before-break (LBB) were led by the needs of the nuclear industry. These crack assessment methods are now well established and used routinely in PWR and BWR plant extension applications and new designs. Quantitative creep and creep-fatigue crack growth assessment procedures are now needed for these GEN IV developments.

The subsection ASME NH high temperature design procedure does not admit crack-like defects into the structural components. In fact, design codes generally consider defect free structures while assessment codes address flaws and their treatment. Therefore, from a code design perspective, the need for creep and creep-fatigue crack growth procedures within NH is not warranted. However, there are several reasons that the capability for assessing cracks in high temperature nuclear components is desirable. These include:

- Some components that are part of GEN IV reactors may have geometries that have sharp corners – which are essentially cracks. For instance, some of the heat exchanger designs consist of micro-process technology, which are diffusion bonded sheets with hole patterns strategically placed so as to make thousands of small passages and features. Due to the fabrication procedure, the features have sharp corners. Design of these components within the traditional ASME NH procedure is quite challenging. It is natural to ensure adequate life design by modeling these features as cracks within a creep-fatigue crack growth procedure.
- Workmanship flaws in welds sometimes occur. It can be convenient to consider these as flaws when making a design life assessment.
- Non-destructive Evaluation (NDE) and inspection methods after fabrication are limited in the size of the crack or flaw that can be detected. In fact, it can be said that every nuclear component has crack like defects of some size that cannot be detected due to limitations in NDE technology. It is often convenient to perform a life assessment using a flaw of a size that represents the maximum size that can elude detection.
- Flaws that are observed using in-service detection methods often need to be addressed as plants age. Shutdown inspection intervals can only be designed using creep and creep-fatigue crack growth techniques. While NH is meant to be a design procedure rather than a service assessment procedure, methods for crack growth analysis can be useful.
- The use of crack growth procedures can aid in examining the seriousness of creep damage in structural components. How cracks grow can be used to determine the ultimate or limit load of a component and margins on safety.

The focus of this work was to examine the literature for creep and creep-fatigue crack growth procedures that are well established in codes in other countries and choose a procedure to consider

implementation into ASME NH. The currently established engineering methods for predicting creep and creep fatigue crack growth at discontinuities and welded components was thoroughly reviewed. For the most part, these procedures were developed in Europe and have been implemented into European codes. *It is very important to recognize that all creep and creep fatigue crack growth procedures that are part of high temperature design codes are related and very similar.* The differences, which are pointed out later, are mainly in how to estimate the appropriate creep crack growth parameters. As such, the choice of the procedure to implement within ASME NH is made based on applicability to nuclear components, validation data bases, ongoing support for the methods, maturity of the procedures, options for computer codes to apply the methods, among others.

These procedures examined in this effort include:

- British R5. The R5 standard [3], which was an extension of the low temperature crack assessment procedure R6, is the oldest and most established code procedure available. The procedures were developed in the 1980's in response to the need for high temperature crack assessment of UK reactor designs which operate at higher temperatures compared with the US PWR and BWR designs. R5 also has a crack initiation procedure, called Time Dependent Failure Assessment Diagram (TPFAD approach) also since crack initiation can be important for minimal fatigue conditions.
- The French RCC-MR (A-16) procedure [4]. This method, which is quite similar in concept to the R5 method and appears to have followed the philosophy of R5 from the beginning, has seen extensive development in the 1990's. The main difference to R5 is the methods used to estimate the reference stress methods used.
- API 579 approach. The API fitness for service (FFS) standard provides guidance for conducting FFS assessments using methods specifically prepared for equipment in the refining and petrochemical industry, although they are used in other industries as well [5]. The specific approach for creep and creep-fatigue crack growth has recently been implemented and a computer code has been developed for FFS assessment for both time dependent and time independent crack growth. The methods again are similar to the other approaches.
- BS-7910 code. The BS-7910 code, which is an advanced creep-fatigue crack growth assessment approach [6] similar to R5 and A16 (in fact many portions come from the R5 code), provides assessment and remaining life estimation procedure that can be used at the design stage and for in service situations.
- The German KTA method. KTA does not appear as well established as R5 or A16 as a creep-fatigue crack growth assessment code. The 2-criterion method regards crack initiation as the most important factor in life assessment and does not deal with the crack growth regime [7]. The flat-bottom-hole approach (FBH) represents a crack detection and characterization method. The approaches used in Germany follow along the lines the R5 and A16 approaches, and are not discussed further here. It is important to note that crack incubation time can take up to 70% of the life, especially under conditions where fatigue is not important.
- Several other code approaches exist in other countries, many of which are summarized and compared in [8], also are available. However, these approaches either follow R5 or A16 or do not consider crack growth explicitly.

Damage based methods used in some industries such as the Omega Method can be quite valuable for creep-fatigue life assessment as well. The creep-crack code procedures discussed above are related to each other. Most currently established methods use variations of K, C* (C_t), and reference stress, all of which will be discussed. An engineering approach based on these parameters is natural since estimates

are based on extensions of methods and solution handbooks on well-established elastic-plastic fracture. Hence, new users of the NH crack growth code that are familiar with elastic-plastic methods should adjust rather quickly. It is anticipated that a step-by-step procedure will be recommended for code implementation.

3.0 NH Creep-Fatigue Crack Growth Recommendations

Creep fatigue crack growth methods are complicated to use and require a fair amount of training for a user to make an assessment. An extensive attempt was made to develop code rules that are simple to use that would be useful within Section III, NH. However, because the methods are complicated, the development of simple rules would make the creep crack growth analysis procedure so conservative that it may not be useful for design. Moreover, there is some controversy within the design and research communities as to the general nature of such approaches. These concerns were clearly pointed out within the Part I report (reference [1]). As such, a decision was made to require the full R5 type approach as a starting point. Moreover, it is not certain that this assessment procedure belongs within NH. Rather, section XI may be a better home.

The R5 code is detailed and does not permit a simple assessment approach. This is also true for API 579, which essentially follows the R5 procedure with some merger of the Omega approach estimate material properties. As such, after much thought and consultation with R5 developers, it has been decided that a simple NH code procedure is not warranted.

The R5 procedure is an engineering approach to predict creep-fatigue crack growth in components which operate at high temperature. Here we provide a summary of the R5 approach, the material property needs and requirements, and a short summary of the process. An example problem is provided in the next section. Some of the description below is part of the R5 code (presented with permission of BE, Inc.).

3.1 The R5 Method

The procedure of R5 [3] is concerned with estimating the remaining safe life of a structure which is subject to creep-fatigue loading and which contains a crack or a postulated crack (for design purposes). The ASME NH code procedure does not permit a crack to be in the structural component being designed. The question then is how can this procedure be implemented within NH even if it was considered appropriate? This question is being addressed with the 2nd part of this program entitled 'ASME NH Code Implementation'. Essentially, there are several reasons why a creep-fatigue creep crack growth assessment might be desirable. These include (i) some GEN IV components may have unavoidable sharp corners (or crack like defects) from fabrication, (ii) workmanship flaws may be assumed (iii) it may be desirable to perform a life assessment with an initial flaw size defined by the maximum size non-detectable flaw that can persist after inspection, (iv) address in service observed flaws, (v) determine crack growth failure mode, and (vi) determine the amount of crack growth over a given operating period.

For the R5 approach, only Mode I loading is considered; mixed modes are not taken into account. The procedure concentrates components which operate within the global creep shakedown limit. The cyclic modes of crack propagation which occur during load changes and crack growth during dwell periods due to creep mechanisms are considered. However an indication of the approach for more extensive cyclic plastic deformation can also be accounted for. The R5 procedures were originally developed for austenitic and ferritic steels at but they have been used in recent years for super alloy materials. Some potential Gen IV materials include In 617 and other nickel base alloys. Experimental and finite element validation for a range of these materials is given in the Appendices of the R5 documentation. Defects are assumed to be in homogeneous parent or weld metal or in non-homogeneous weldments.

Crack behavior under both load-controlled and combined load- and displacement-controlled stress systems is considered. Particular advice is given in an Appendix for the cases of displacement control due to a constant applied displacement and for thermal loads acting alone. R5 does not address leak-before-break procedures for pressurized components so that LBB considerations would have to be developed separately by NRC, if desired in the future. However, LBB arguments may be constructed using, as a basis, using the failure assessment diagram procedure in an Appendix of R5.

Before proceeding it is important to point out that GEN IV applications are likely outside the validation range of R5 applications. Before R5 could be used with confidence within the ASME code framework, more validation is necessary for GEN IV applications. Section 6 will deal with this in more detail.

3.2 The ASME Draft Rules Recommendations: Step by Step Approach

Here a step-by-step procedure is set out whereby a component containing a known or postulated defect can be assessed under creep-fatigue loading. The general 13 step approach is provided in Figure 1. Both continuum damage accumulation and crack growth are addressed. The cases of insignificant creep and insignificant fatigue are included as special cases. The procedure may be applied to a component in the design stage, or where it has already experienced high temperature operation, as in an operating plant where damage has been observed or is postulated. In the case of addressing an aging nuclear component advice if given on the effect of the time at which the defect is assumed to form. Continuum damage failure (creep rupture) of an un-cracked body may be considered as a special case by omitting the steps covering crack growth and cyclic loading. However, ASME NH already addresses this. The steps in the procedure are listed below with a description. Please refer to reference [3] for the complete details of the R5 method, where many examples are provided. These rules are also similar to those for creep crack growth in API 579 [5], which are described within a 19 step framework and incorporate some concepts of the Omega method and different estimates of material parameters (compared to R5) if data is not available.

Before summarizing the creep-fatigue crack growth evaluation steps, note that there are a number of appendices which can aid the user in the assessment. Appendix I summarize the basic equations to use for the assessment. Appendix A lists uniaxial material data needed for the assessment for a number of different materials. Appendix B and C summarizes statistical uniaxial creep and creep rupture test data, respectively. Appendix D provides test formula for creep test specimen analysis (if the user plans to develop their own crack growth data). And Appendix E lists creep crack growth data for a number of different materials. Hence, some material data for analysis is provided here. More data is provided in references summarized in the appendices and reference [3]. We emphasize that new data for different materials operating under different conditions will be needed for GEN IV applications.

STEP 1 - Establish the Expected or Actual Cause of Cracking and Characterize Initial Defect.

Establish the cause of the cracking to ensure that the procedures of this volume are applicable. The defect type, position and size should be identified. For a creep-fatigue design crack growth assessment, the expected crack size and location can be determined from the stress analysis where the highest stresses occur. The size would be the limit on the NDE confidence. For defects found in service, this process may require the advice of materials and non-destructive testing experts, particularly for the case of defects in weldments. Suitable sensitivity studies (Step 12) should be performed to address uncertainties. The detected defect should be characterized by a suitable bounding profile amenable to analysis. Defects which are not of simple Mode I type should be resolved into Mode I orientation.

STEP 2 - Define Service Conditions for the component

Resolve the load history into cycle types suitable for analysis. This includes all design cycles or for in service assessment, the historical operation and the assumed future service conditions. The service life should be defined. For the case of a component which is defect-free at the start of high-temperature

operation, an estimate of the time at which the defect formed (or the crack nucleation time) can be determined. It is conservative to neglect this time. Suitable sensitivity studies should be performed to address uncertainty in the time of defect formation.

STEP 3 - Collect Materials Data

The material data needs to be defined and collected. The details of the material data necessary will be discussed in the next section. Define the materials relevant to the assessed feature including, in the case of weldments, the weld metal and heat-affected zone structures. The material properties must be appropriate over temperature range and in the correct cyclically-conditioned state. The effects of thermal ageing may also need to be considered for some materials – especially cast stainless steel. In practice, the requirements are influenced by the outcome of the tests for significant creep or fatigue in Step 6 below. Time-independent material properties are required for the stability analyses performed in Steps 5 and 11. It should be noted in particular that fracture toughness properties are required for creep-damaged material, if available. If not available, they must be estimated from creep undamaged material. It is important to mention that some materials that may be used for GEN IV applications may not have been validated for R5 assessment yet. This will need to occur before R5 can be used in NH. Appendices A to E provide material data for some materials at some temperatures.

STEP 4 - Perform Basic Stress Analysis

Elastic stress analyses of the un-cracked feature should be performed for the extremes of the service cycles. In the case of cyclic loading, a shakedown assessment of the un-cracked feature should then be performed. The type of shakedown assessment is quite similar to NH and could be performed using NH procedures. It should be determined if the feature satisfies strict or global shakedown or not. In the case that shakedown cannot be demonstrated, it is necessary to justify the use of the methods of this volume using. For example, inelastic analysis methods, including finite element analysis, may be required. If shakedown is demonstrated, the crack depth should be such that the compliance of the structure is not significantly affected.

STEP 5 - Check Stability under Time-Independent Loads

The cracked component must be checked to ensure time-independent mechanisms under fault or overload load conditions at the initial defect size does not occur. R5 suggests using R6 [36]. However, for ASME NH purposes and the US NRC, this can be performed using Section XI procedures or a J-Tearing assessment. If failure occurs due to time independent effects alone at this step, then the assumptions in the analysis should be revisited and remedial design action taken. Only if sufficient margins can be justified is it permissible to continue to Step 6 to justify future service life or the design. J-resistance curve data for this assessment must be obtained elsewhere. Alternatively, the crack assessment procedure in Section XI, based on limit load with Z-factor correction may be used.

STEP 6 - Check Significance of Creep and Fatigue

The checks for insignificant creep should be made using ASME NH or R5 procedures. If creep is insignificant then the assessment becomes one of fatigue loading alone and Steps 7 and 10 below are omitted. Conversely, if fatigue is judged to be insignificant then the assessment becomes one of steady creep loading alone and further consideration of cyclic loading is not required. A further test determines if creep-fatigue interaction is significant. If it is not, simplified summation rules for combining creep and fatigue crack growth increments may be adopted (Step 9).

STEP 7 - Calculate Rupture Life based on the Initial Defect Size

The time to continuum damage failure (creep rupture) must be calculated based on the initial crack size from Step 1. If this is less than the required service life, it may not be necessary to perform crack

Step 1) Establish cause of cracking or expected cracking

- Define defect type, bounding size, incubation Mode I required

Step 2) Define service conditions

- Resolve loads into cycle blocks, desired service life (loads, temperatures, etc)

Step 3) Define materials and properties

- cyclic, creep crack growth, temperatures collect appropriate data

Step 4) Basic stress analysis (operating extremes)

- Shakedown assessment If shakedown not established, inelastic analysis necessary

Step 5) Check time independent stability

- Time independent fracture analysis (section XI type) failure predicted stop here

Step 6) Check significance of creep and fatigue

- Rules are checked to determine insignificance of creep or fatigue Check if creep-fatigue interaction is important

Step 7) Calculate rupture life based on initial defect size

- Rupture life calculated based on cracked limit load stress Ductility exhaustion methods may be needed

Step 8) Calculate crack incubation time

- Conservative to ignore this

Step 9) Calculate crack growth for the desired life time

- Integrate creep and fatigue crack growth expressions Note both affect each other Changes in reference stress during crack growth should be included

Step 10) Recalculate rupture life for final crack size (Step 7)

- Continuum damage prediction after crack growth Conservative to base this final crack size

Step 11) Time independent stability check for final crack size

- This is actually performed during crack growth analysis in practice

Step 12) Assess significance of results

- R5 does not prescribe margins ASME may require this

Step 13) Report results

- Prescribe inspection intervals, etc

Figure 1 Draft Step by Step Procedure (13 steps)

growth calculations and the NH procedure alone suffices. The estimate of rupture life is based on a calculated limit load reference stress (discussed in the appendices) and, for predominately primary loading, the material's creep rupture data. For damage due to cyclic relaxation and due to the relaxation of welding residual stresses, ductility exhaustion methods are more appropriate. The particular requirements for defects in weldments are also addressed. For the case of short defects close to stress concentrations such as notch radii or weld toes, special considerations must be followed to ensure that the reference stress is conservatively calculated.

STEP 8 - Calculate Crack Nucleation or Incubation Time

Typically it takes some time for a crack in a nuclear component to begin growing. For some components, crack initiation may consume the bulk of the life and when crack growth commences, failure occurs quickly. The crack nucleation or incubation time is the time from the start of the of high-temperature operation to crack growth start. Depending on the cause of cracking, its location within a weldment and the type of loading it may be possible to calculate a non-zero incubation time. *It is always conservative to ignore this period and assume that crack growth occurs on first loading*. The cause of cracking will influence the determination of an incubation time. For example, a naturally-occurring creep defect, such as some weld defects, may not experience an incubation period prior to macroscopic crack growth. There are several procedures for calculating crack incubation time within R5 including TDFAD and the two criteria approach (similar to A16).

STEP 9 - Calculate Crack Growth for the Desired Life Time

The crack size at the end of the design period of operation is calculated, following the procedures of R5 based on K, C*, reference stress, and the appropriate estimation schemes laid out. Finite element analysis can also be used. This is done by integrating the appropriate creep and fatigue crack growth expressions. This incremental process is simplified in some cases, depending on the outcomes of the significance creep and fatigue tests determined in Step 6. Changes in reference stress due to crack growth should be included in the calculations. Integration is required because all parameters (K, C*, C(t)) and reference stress change with time as the crack proceeds. Required material data may be found in Appendices A, B, C, and E.

STEP 10 - Re-Calculate Rupture Life after Crack Growth

The time to continuum damage failure should be re-calculated taking into account the increased crack size from Step 9. Crack growth calculations should not be performed in practice beyond an acceptable rupture life. It is conservative to base the estimate of rupture life on the final crack size as this neglects slower accumulation of creep damage when the crack size is smaller during growth.

STEP 11 - Check Stability under Time-Independent Loads after Crack Growth

In practice, this step is carried out in conjunction with the crack size calculations of Step 9. The crack growth calculations of that step should not be performed beyond a crack size at which failure by time-independent mechanisms is conceded at fault or overload load levels. For ASME purposes, this assessment could be made using ASME section XI methods.

STEP 12 - Assess Significance of Results

The uncertainties in loads, material properties, defined crack location, etc., need to be assessed. Margins against failure are not prescribed in R5 and are left to the user to set. The sensitivity of the results of the preceding steps to realistic variations in loads, initial flaw size and location, and material properties should be assessed as part of a sensitivity study. The various modeling assumptions made can also be revisited with a view to reducing conservative assumptions in the analysis if unacceptable margins are determined. If this still fails to result in an acceptable crack growth life the options of new design, or for service assessment, of reducing future service conditions, or repair or replacement of the defective

components should be considered. For NRC needs, this may require placing the procedure within a probabilistic framework.

An alternative to the quantitative assessment of margins using the deterministic approach of this section is to use probabilistic methods to directly determine failure probabilities. A procedure for doing this is set out in one of the Appendices but requires estimates of the distributions of variable quantities.

STEP 13 - Report Results

The results of the assessment, including margins determined, and the details of the materials properties, flaw size, loads, stress analysis calculations, etc, used in the assessment should be comprehensively reported. This facilitates both verification of the particular assessment and repeatability in future assessments. Each of these steps is summarized in great detail within the large volume of material provided within R5. This includes some material data along with extensive examples of the use of the method. A simple example calculation of the procedure is provided in the Section 6 of the Part I report (reference [1]).

3.3 Comments on R5 Application for ASME

From the flow chart description and 13 step procedure described above, it must appear that there are a number of judgments, interpretations and supporting properties data required to sort through the various behavioral regimes and to make an eventual design assessment. For near term HTGR applications as described above, it is not possible to narrow down the options and simplify the procedure. To do so would make the assessments too conservative to be used as a practical design tool within NH. Also, the goal of Code design rules is to have requirements that can be implemented consistently such that the design assessment will not be dependent on the individual/organization doing the assessment. To ensure that the creep/fatigue assessment procedures are properly applied, organizations using the procedure must ensure that the staff is properly trained. The use of the procedure (and all other methods) requires an experienced user. Therefore, the R5 procedure may not be ready for generally applicable design rules within NH but may be more suitable to regulatory requirements and licensing review. This last point requires further discussion and cannot be answered at this point.

3.4 The R5 Material Data Requirements

The material requirements for R5 crack growth analyses were summarized reference [1]. The material data testing requirements are well established. In addition to the typical high temperature properties required for an ASME NH design life assessment, the following material data is needed.

1. Creep rate material properties and the constitutive law. The constitutive law could be a classical law (power law) or other type of law depending on the material and temperature (including hyperbolic laws and even tertiary laws). Appendices A and B provide data for some materials.
2. Creep crack growth constants are required to predict the creep crack growth portion of the analysis (Appendix E). *It is very important to note that this data can be estimated using a simple procedure within R5 if creep crack growth data is not available. This estimate is based only on knowledge of the tensile creep properties and the estimates are made to be conservative. These simple estimates were discussed in [1] and are also summarized in Appendix I.*
3. Fatigue crack growth constants are needed as spelled out in R5. This data is obtained at the temperature of interest using one of a number of fracture specimens including the compact tension type specimen. Again, a power law relationship between crack growth per cycle and the change in stress intensity factor (ΔK) is generally obtained.
4. Creep ductility properties along with elastic and elastic-plastic fracture properties at temperature.

Many of the high temperature materials within NH are included in R5 and have been validated for creep-fatigue crack growth using the R5 approach. Figure 2 provides a comparison of materials that are

supported within NH and those within R5. From Figure 2 it is seen that both NH and R5 support 2 1/4Cr-1Mo steels across nearly the same temperature ranges. For stainless steels, R5 has not been used much for temperatures higher than about 650 C while NH goes to 815C. However, R5 has been used for a larger variety of austenitic steels, including 347. BE says that R5 has been used outside this temperature range, but only on a spot basis, and it is not possible to document the specifics here. From the middle of Figure 7 it is seen that R5 has not been used for alloy 800H. As noted in Figure 7 though, it has been used for some other super alloys for a steel similar to IN 617. Also, 9Cr-1Mo-V steel has not been used, mainly since these steels are not used in any BE plants. Because of the success of R5 for other Cr-Mo steels, there is no reason to suspect that R5 cannot perform for this steel. At the bottom of Figure 2 some steels that have been supported by R5 are listed which are not supported within ASME NH.

NH:	2 1 4Cr-1Mo steel (Grade 22 Class 1) Stress intensity values to 1100F (575C) for 300,000 h
R5:	21 4 CrMoV, 1 2CrMoV and 1CrMoV in the range 500-565C
NH:	304H stainless steel Stress intensity values to 1500F(815C) for 300,000 h
NH:	316H stainless steel Stress intensity values to 1500F (815C) for 300,000 h
R5:	Various stainless steels and weldments (304, 316, 316H, 321, 347 weld, 316 weld) in the range 525-650C
NH:	Alloy 800H Stress intensity values to 1400F (750C) for 300,000 h
R5	No Alloy 800 H However, BE has used R5 for super alloys up to 800C (similar to IN617)
NH:	9Cr-1Mo-V steel (Grade 91) Stress intensity values to 1200F (650C) for 300,000 h
R5:	No 9Cr-1Mo-V steel (Grade 91)
R5:	CMn steels in the range 360-390C
R5:	P22, P91 and some P92 ferritic steels

Figure 2 Comparison of materials within NH and R5 BE has used R5successfully outside these temperature ranges also – to lower and higher temperatures especially in austenitic steels

3.5 Summary of The Material Data

Some of the material data required is summarized in the appendices. Sources for data are available in the literature. BE (Ainsworth) and Imperial College (Nikbin) can compile this data into a coherent library and this should be considered by ASME. The current sources for data needed for R5 assessments are:

In summary, a large data base exists but much of it proprietary. Methods exist for estimating crack growth law without the necessary data. This is convenient and provides conservative estimates of

the properties. Material data required creep/fatigue crack growth assessments using R5 is not available for some GEN IV materials.

4.0 NH Theoretical Concerns and Issues for GEN IV

The critical issue with creep crack growth is the creeping solid in the creep plastic zone. Fracture toughness and also pure fatigue crack growth are mainly dominated by plastic effects (dislocation movement). Within the creep plastic zone the whole time dependent creep mechanisms (from power law break-down to pure diffusion creep) can happen. The exponents in a power law-type approach change from 1 (diffusion) to 50 and higher (power law break-down) in a small volume element. Formation of a creep crack which can propagate follows micro-structural laws rather than continuum mechanics. therefore, incubation period or crack initiation phase are important. The situation is comparable with fatigue crack growth close to the threshold value where it is well accepted today that micro-structurally short cracks can grow well below the threshold because a continuum approach is not the appropriate description. These micro-structural aspects need to be considered for future concepts. Micro-structural effects are also extremely important in case of creep-fatigue interactions. All of these concerns are ignored with the current methods for predicting creep and creep-fatigue crack growth in real structures. Please keep this in mind while reading the rest of this section.

The state of the art engineering creep and creep-fatigue crack growth predictive methodologies are based on characterizing the crack growth rates using parameters (K, C*, C(t)) that measure, in theory, the strength of the asymptotic crack tip fields, as discussed in reference [1]. There are a number of theoretical concerns regarding this approach. Perhaps the main concern is that the asymptotic crack tip fields can only be developed for simple creep constitutive laws (such as power law types). Moreover, the methods formally break down once crack growth occurs, non-proportional stressing occurs, and cyclic loads are experienced when a creep crack grows in service.

For a creep/fatigue crack growth predictive methodology to be valid, the measured values of the parameters (here C*, C(t)) must be related to crack growth events. Experiments on fracture specimen are performed by measuring far field parameters (load, load point displacement (or crack opening displacement), and crack size). These parameters are then properly integrated to obtain the crack characterizing parameters. A fundamental question that must be answered in any fracture mechanics based approach is whether these far field measurements can properly characterize the near crack field events. Traditionally, with fracture mechanics, this characterization is made because the asymptotic crack tip fields, which characterize growth, can be related to far field measurements. For instance, with elastic-plastic fracture, far field events can be related to near crack tip field fracture events through the use of a path independent integral (J-integral). For creep crack growth, this relationship is only strictly valid for full scale creep for a stationary crack and for simplistic constitutive laws. When crack growth occurs, or more importantly, when both crack growth and cyclic loading occur, the asymptotic interpretation of the crack tip events to far field measurements, breaks down. *In fact, for cyclic loading of a stationary crack, the asymptotic crack tip fields depend strongly on the form of the constitutive law being used and these fields can change for each cycle of loading [7].* This makes establishing the link between near field crack events, which drive crack growth and fracture, and far field events (where measurements are made to characterize material properties) quite challenging. Today, despite the fact that engineering creep/fatigue crack growth procedures based on R5 type methods have been used with success for years, controversy over the general nature of the methods persists. Indeed, while R5 has been established and validated for materials and operating conditions within BE plants, it is not certain whether these methods will carry over in a straight forward fashion to GEN IV conditions. Hence, even if R5 approaches were implemented within NH, validation under GEN IV conditions is necessary. This issue is discussed further in reference [1].

The engineering creep-fatigue methods used in all codes today, including R5, are used outside their range of validity. Despite this, the methods have shown to provide reasonable predictions of creep-

fatigue life, albeit conservative – perhaps sometimes too conservative. Most of this summary comes from the R5 manual [3], Ainsworth's book [8]. It is this author's belief that continued development of more fundamentally sound creep-fatigue life predictive methods must continue while we continue to use the engineering approaches in R5.

Essentially, the theory behind the R5 engineering method (and all other methods) is summarized in the book by Webster and Ainsworth [8] and it is based on earlier asymptotic solutions for creep emanating from an initially elastic field (or plastic HRR field) within a creeping zone (both primary, secondary, and combined primary and secondary creep). Herman Riedel, in his classic treatise in 1987 [9], summarizes all of this. Riedel bases his work on earlier work when he was working with Rice, Bassani and colleagues work, etc (see [10 – 14]. So a firm theoretical foundation based on the asymptotic interpretation of crack tip fields does exist and it is clear.

In practice though, these conditions are violated - often severely. The creep response very near the crack tip (high stresses) cannot be represented by power laws. Once the crack grows beyond a small amount, the asymptotic interpretation becomes unclear, and we can go on and on. As Hoffelner points out, the linear life fraction rules used in NH today have no real basis. However, from an applications standpoint all these simplified rules and laws do a very good job for design provided you build in the necessary safety margins. The same can be said for R5. Nothing would ever be built if we kept waiting for the perfect theory. There are no perfect theories in the fracture field. The conservatisms built into the methods were done so with these issues in mind. They were then validated with mock-ups, and service experience over the years. As such, we must start with the R5 approach, see how well it performs for GEN IV conditions, and improve on these methods or develop new methods as required. We must keep in mind, that in practice, J-Tearing theory for elastic-plastic fracture is used far beyond its theoretical validity routinely - with success and it can guarantee conservative results.

5.0 Discussion of GEN IV and R5

The R5 creep/fatigue life cycle crack growth prediction code represents the state-of-the-art procedure for assessing the life of cracked components operating in the creep regime. The method has a theoretical foundation which is based on rather simple constitutive laws and in practice, these assumptions are violated. This is not uncommon in the fracture mechanics field. J-tearing theory, which is used for predicting elastic-plastic fracture, likewise has a theoretical basis that is routinely violated in practice and is used far beyond its basis, with success. The success is possible by obtaining confidence in the procedures through validation with mock-up tests and service experience. Likewise, the success with R5 is based on a similar series of mock-up validations and service experience – mainly for the materials and operating conditions within British Energy HTGC reactors.

As such, the R5 procedure is a semi-empirical procedure (as is ASME NH) that needs qualification for materials and operating conditions that will be experienced in GEN IV. Certainly, the stainless steels and Cr-Mo steels are qualified for creep/fatigue crack growth assessment for a range of operating conditions in R5. We cannot recommend implementation of R5 procedures outside this range until further qualification for GEN IV materials is made. R5 is an assessment procedure rather than a design procedure in its present form. An assessment procedure attempts to accurately predict crack growth response while a design procedure involves built-in safety factors and conservatism. This is the case with all creep/fatigue crack growth procedures. Hence, if R5 were implemented to the high temperature design procedure of NH in the future, safety factors would have to be introduced.

Fracture mechanics methods have proven a valuable practical tool to predict life of structures which develop cracks. The aerospace industry has adopted a 'damage tolerant' design approach which permits the presence of cracks. The structures are maintained by specifying sufficient inspection intervals so that a crack will not grow to a critical length between inspection intervals. Despite the fact that ASME does not permit cracks, they will be present and a procedure for assessing them is important to have.

Some of the statements below must be kept in mind as we consider R5 for possible implementation into NH in the future.

In conclusion, in future HTGRs the influence of stress raisers like notches, production flaws, welding defects, developing cracks etc. should be considered for safety and/or NDE purpose, a fracture mechanics concept (for creep, fatigue and creep-fatigue) is needed. It is certainly a valid approach to use the methods, procedures and data developed within the R5 for that purpose, certainly as a starting point until the procedures are qualified for GEN IV conditions. Either the complete R5 procedure or only parts of it should be used depends on the demands and NRC's requirements and concerns.

6.0 Summary, Conclusion and Suggestions for Additional Work.

The subsection ASME NH high temperature design procedure does not admit crack-like defects into the structural components. The US NRC identified the lack of treatment of crack growth within NH as a limitation of the code and thus this effort was undertaken. This effort is broken into two parts. Part 1, summarized here, involved examining all high temperature creep-fatigue crack growth codes being used today and from these, choose a methodology that is appropriate for possible implementation within NH. The second part of this task is to develop design rules for possible implementation within NH. This second part is a challenge since all codes require step-by-step analysis procedures to be undertaken in order to assess the crack growth and life of the component. Simple rules for design do not exist in any code at present. The codes examined in this effort included R5, RCC-MR (A16), BS 7910, API 579, and ATK (and some less known codes).

After examining the pros and cons of all these methods, the R5 code was chosen for consideration. R5 was chosen because the code: (i) has well established and validated rules, (ii) has a team of experts continually improving and updating it, (iii) has software that can be used by designers, (iv) extensive validation in many parts with available data from BE resources as well as input from Imperial college's database, and (v) was specifically developed for use in nuclear plants. Further reasons for the choice of R5 are listed in [1].

There are several reasons that the capability for assessing cracks in high temperature nuclear components is desirable. These include:

- Some components that are part of GEN IV reactors may have geometries that have sharp corners – which are essentially cracks. Design of these components within the traditional ASME NH procedure is quite challenging. It is natural to ensure adequate life design by modeling these features as cracks within a creep-fatigue crack growth procedure. Figure 16 illustrates some types of components that may be part of GEN IV that fall into this category.
- Workmanship flaws in welds sometimes occur. It can be convenient to consider these as flaws when making a design life assessment.
- Non-destructive Evaluation (NDE) and inspection methods after fabrication are limited in the size of the crack or flaw that can be detected. It is often convenient to perform a life assessment using a flaw of a size that represents the maximum size that can elude detection.
- Flaws that are observed using in-service detection methods often need to be addressed as plants age. Shutdown inspection intervals can only be designed using creep and creep-fatigue crack growth techniques.
- The use of crack growth procedures can aid in examining the seriousness of creep damage in structural components. How cracks grow can be used to assess margins on components and lead to further safe operation.

The focus of this work was to examine the literature for creep and creep-fatigue crack growth procedures that are well established in codes in other countries and choose a procedure to consider implementation into ASME NH. It is very important to recognize that all creep and creep fatigue crack growth procedures that are part of high temperature design codes are related and very similar. This effort made no attempt to develop a new creep-fatigue crack growth predictive methodology. Rather, examination of current procedures was the only goal.

The overwhelming majority of data was gained with ferritic/bainitic, ferritic/martensitic and austenitic (basically 316) steels. Nickel-base super alloys are covered insufficiently with R5 and other creep crack growth approaches. The restricted slip in fcc metals together with M23C6 carbides along grain boundaries acting as preferred points for void nucleation my change the creep, and creep-fatigue crack growth significantly. Such questions need to be addressed in the future when an application to 617, 230, Hast X(R), 800H etc. would be seriously considered. Even a simple da/dt-K approach can correlate creep crack growth data for such alloys in some cases. Creep-fatigue crack growth procedures for super alloys needs to be verified and developed.

The critical issue with creep crack growth is the creeping solid in the creep plastic zone. Fracture toughness and also pure fatigue crack growth are mainly dominated by plastic effects (dislocation movement). Within the creep plastic zone the whole time dependent creep mechanisms (from power law break-down to pure diffusion creep) can happen. The exponents in a power law-type approach change from 1 (diffusion) to 50 and higher (power law break-down) in a small volume element. Formation of a creep crack which can propagate follows micro-structural laws rather than continuum mechanics. therefore, incubation period or crack initiation phase are important. The situation is comparable with fatigue crack growth close to the threshold value where it is well accepted today that micro-structurally short cracks can grow well below the threshold because a continuum approach is not the appropriate description. These micro-structural aspects need to be considered for future concepts. Micro-structural effects are also extremely important in case of creep-fatigue interactions. All of these concerns are ignored with the current methods for predicting creep and creep-fatigue crack growth in real structures. Such effects need to be considered in future efforts.

Subcritical crack growth considerations (fatigue, creep, environment and interactions) should be used for condition assessments, safety assessments, definition of NDE intervals or definition of locations needing specific design or NDE attention. Definition of allowable stresses or loads based on crack growth in terms of a design code would not be an attractive approach for design. Flaw-tolerant design always needs definitions of initial flaw sizes and geometries. This would make the design dependent on available NDE methodology.

Based on the fact that a the quality of ultrasonic information from coarse grained austenite (including nickel-base) is much worse than that from fine grained ferritic steels it is fair to say that the establishment of material independent design rules would be either not possible or extremely conservative. Adding uncertainties of flaw detection and flaw sizing together with procedural uncertainties concerning materials, fracture mechanics parameters and concepts would lead to a very vaguely defined design space.

In conclusion: We strongly support fracture mechanics considerations for safety assessments of components and in this sense guess that this report is an excellent starting point for further work. However, this work should in my view be directed rather toward condition assessments within Section XI.

Acknowledgements

The author would like to thank ASME and DOE for funding the study presented within this report. In particular, Mr. James Ramirez of ASME and Ken Balkey of Westinghouse (DOE program manager) are thankfully acknowledged. Dr. Sam Sham of Oak Ridge National Laboratory, and Mr. Robert Jetter, ASME NH chair, and Dr. Wolfgang Hoffelner of PSI, Switzerland provided excellent comments of the draft report which were implemented into this final version. Dr. Hoffelner also provided excellent review and comments for this final report version. Useful discussions with Dr. Bilal Dogan of EPRI are thankfully acknowledged as well. Finally, the authors would like to express sincere thanks to Dr. R. Ainsworth of British Energy, and Prof. K. Nikbin of Imperial College for all their help. They graciously provided many comments and supported the authors throughout this effort. Moreover, much of the appendices were provided by them via a contract from ASME.

7.0 References

1. Brust, F. W., Wilkowski, G., Krishnaswamy, P., and Wichman, K., *Creep and Creep-Fatigue Crack Growth at Structural Discontinuities and Welds - Review and Assess Current Methodologies and Recommend NH Implementation, February, 2009.*
2. ASME, *Case of ASME Boiler and Pressure Vessel Code*, 3NH Class 1 Components in Elevated Temperature Service, 2004, New York: American Society of Mechanical Engineers.
3. BEGL, *An Assessment Procedure for the High Temperature Response of Structures*, British Energy Generation Ltd., R5 Issue 3, 2008.
4. RCC-MR, *Design and Construction Rules for Mechanical Components of FBR Nuclear Islands and High Temperature Applications, Appendix A16: Guide for Leak Before Break Analysis and Defect Assessment*, AFCEN, Appendix A16, 2002.
5. API, *Recommended Practice for Fitness-For-Service*, American Petroleum Institute, Washington, D. C., 2008.
6. British Standard, *BS 7910: Guide on Methods for Assessing the Acceptability of Flaws in Metallic Structures*, BSI, London, 1999.
7. Brust, F. W., "Investigations Of High Temperature Damage And Crack Growth Under Variable Load Histories," *International Journal Of Solids And Structure*, Vol. 32, No. 15, pp. 2191-2218, 1995.
8. Ainsworth, R. A., 'Flaw Analysis in the French RSE_M and RCC-MR code appendices', five papers presented in special issue of *The International Journal of Pressure Vessels and Piping*, S. Marie et al authors, Vol. 84, 2007, pp 589-695.
9. Riedel, H., in *Creep in Structures*, Proceedings of the 3rd IUTAM-Symposium, Leicester, UK, 1980, Ponter and Hayhurst (eds.), Springer-Verlag, p 504-519, 1981.
10. Hui, C. Y., ASTM STP 803, American Society for Testing and Materials, Shih and Gudas (eds.), p. I-573 - I-593, 1983.
11. Bassani, J. L., in *Creep and Fracture of Engineering Materials and Structures*, B. Wilshire and D.R.J. Owen (eds), Pineridge Press, p. 329-344, 1981
12. Chang, T. C., Popelar, C. H., and Staab, G. H., "A Damage Model for Creep Crack Growth", *International Journal of Fracture*, **32**, p. 157-168, 1987.
13. Wu, F. H. Bassani, J. L., and Vitek, V., "Transient Crack Growth Under Creep Conditions Due to Grain-Boundary Cavitation", *J of Mechanics and Phys of Solids*, **34** (5), p. 455-475, 1986.
14. Chung, J. O., Yu, J., and Hong, S. H., "Steady State Creep Crack Growth by Continually Nucleating Cavities", *J Mechanics and Phys of Solids*, **38** (1), p. 37-53, 1990.

Appendices

Originally Compiled by K. Nikbin and R. Ainsworth, and modified by F. Brust

Appendix I

GUIDELINES FOR DEVELOPMENT OF ASME BASED REMAINING LIFE DEFECT ASSESSMENT PROCEDURE

Introduction

This document is aimed at analysis methods for remaining life assessment of components, containing cracks, at elevated temperatures. Thus the methods are not generally used to produce the initial design criteria except in the case of analyzing the behavior of postulated defects to produce a defect tolerant design. The methods are also relevant for designing components, which cannot be inspected during their operational life. The report presents guidelines for assessing the structural design, relevant failure criteria under creep and fatigue and the significance of defects in components. The procedures will need to contain methodology for dealing with failure by net section rupture, incremental crack growth or some combination of both processes. The influence of creep and fatigue and the onset of brittle or ductile fracture in determining tolerable defect size need to be considered.

Information should be included for specifying loading conditions under normal and abnormal operating conditions and methods suggested for characterizing defects. The calculations will make use of limit analysis methods and fracture mechanics concepts. Several levels of complexity need to be discussed depending on the criticality of the problem and the materials properties data available. Approximations should be presented for dealing with cracked components when only some data are available. In essence various means of analysis and detailed advice should be available to the user in the document to deal with the problem irrespective of the amount of data available. The level of safety factors used will need to be determined from available data and its extent of scatter.

The inclusion of probabilistic methods to indicate confidence limits in design and life assessment is also recommended. Where this is not possible sensitivity analyses should be performed. In some cases, due to setting levels of safety factors, new tests may need to be performed to validate the decisions. Finally the document should refer wherever possible to the source of the information or data it has used in order to further assist the user in reaching a design criterion or in making a life assessment decision.

General requirements for a procedure

The defect assessment procedure may be applied to components containing planar defects, including cracking or lack of fusion. It may be applied, subject to restrictions, to defects, which are actually discovered during pre-service or in-service inspection (where possible). The objective is to decide whether the defect is innocuous and will never affect the integrity of the structure, whether remedial action can be deferred until sometime in the future or whether repairs are needed immediately. The procedure may also be applied at the design stage, subject to the same restrictions, to hypothetical defects, in order to set inspection sensitivity or to check that a proposed component is tolerant to defects.

The procedure should be applicable to defects, which are caused by time-dependent environmental phenomena where the degraded material property is available and can be used in performing the life assessment analysis set out.

Cracks in welds are a further complication in the analysis step and need special treatment. In most cases the measurement of residual stresses is not a practical solution and factors on stress level may need to be considered. In addition properties of the heat affected zone and the weld metal usually differ from

those of the parent material and the local residual stress may need to be taken into account. However the interactions between these regions are not always clear or well documented. Therefore tests may be needed to deal with weld properties for the relevant components.

The Document should suggest safety factors where the design of the component is the objective. Factors of safety need to be adjusted to suit the circumstances of the case under investigation. A number of points need to be considered in choosing factors of safety. These are

- The level of safety that is attributed to the structure
- The availability and the amount and the extent of scatter of relevant data
- The consideration of unexpected loads during operation in the structure
- Factors due to residual stresses that may exist due to welding and loading processes.
- The ability or otherwise of being able to perform NDT after fabrication and in-service inspection
- The degradation of the material and the available material properties for the degraded material
- Advice and statistical data on expected failure rates and safety factors to be available to the user

However the code should not suggest a factor of safety, which could be applied to life predictions due to crack initiation, growth and final failure. The decision about this must be left to the discretion of the assessor or from expert advice given in the document. The value chosen will depend on the degree of pessimism introduced into the input data and on the results of sensitivity analyses. The introduction of sensitivity analysis and probabilistic methods in the assessment procedure will to some measure assist the user in determining remaining lifetimes in the operating structures.

Cracking behavior at high temperatures

Under high temperature operating conditions creep or fatigue could be the primary mechanism in initiating and growing a crack in components. Crack propagation can continue until structural failure takes place at some stage. Local plastic damage or creep damage may build up ahead of the crack over a time period due to thermal or cyclic loading. Alternatively the net section may fail through a short-term phenomenon - plastic collapse if the material is ductile or fast fracture if the material is brittle. Various conditions such as knowing the crack opening displacement at initiation and using the right definition of the collapse loads need to be calculated.

In addition following the initial loading of the component, the crack may blunt and, in these circumstances, there will be an incubation period before a further short crack forms and propagation initiates. Where such blunting does not occur, crack propagation may be assumed to start immediately on loading. The crack grows, in all cases, by a fracture mechanics controlled mechanism. Where new plant is under consideration, it may be possible to benefit from the incubation period, starting the crack growth calculations at the end of this period. Various conditions such as knowing the crack opening displacement at initiation and using the right definition of the creep strain versus time at the relevant stress and temperature need to be met in order that the incubation period is calculated.

When a defect has been discovered after the component has been in service, the conservative assumption should be made that the crack initiated earlier in life, unless there is strong evidence to the contrary. In this case it is also current practice to discount time to crack initiation where fatigue is the mode of failure.

Application of procedure

The Procedure is implemented in a series of well-defined steps, which should be shown as a flow chart. The chart (see for example Fig.1) and the detailed descriptions of the individual steps could refer to

- A component before it enters service, containing a postulated defect or one found during inspection.
- To a defect, which has been discovered after a component has been in service for a period of time?

These choices are noted in the text of the chart, as appropriate. An important point in the flow chart is the variations and choices available to the user in accordance with their level of expertise and the level of information available on the component under consideration. Furthermore the chart and the document should show the importance of the need for sensitivity and/or probabilistic analyses in performing the assessment task.

Initial investigations to establish cause of cracking

Prior to performing calculations, an initial investigation should be carried out to identify the most likely cause of cracking. For postulated defect sizes, the minimum crack size should be established to taken into account the NDT limits relevant to the structure. This may include a combination of non-destructive testing, visual examination and metallurgical examination, as appropriate. Also, if possible, a dimensional check should be carried out on the component to establish if there has been any significant distortion during fabrication and in the case of remaining life assessment during its operational life.

Significant plasticity away from the crack tip, particularly if accompanied by distortion of the component, is often an indication that there has been local overloading due to primary or secondary stresses, or some form of over-stressing and that the material is nearing the end of its safe working life. Any crack propagation and failure calculations which are carried out must take into account the properties (both static and fatigue) of the material in its damaged state.

Leaving aside overheating in the fabrication and operational stage, over-stressing and environmental effects, crack growth in the structure is most likely to be associated with a pre-existing defect which has not been detected by pre-service inspection or with a crack which has been initiated by some form of fatigue loading. The document should give guidance for both cases. Pre-existing defects often occur in welds and certain precautions should be described in the defect characterization section before applying the assessment procedure.

Definition of previous plant history and future operational requirements

The service loads, possible presence of residual stresses and service temperatures for the component should be established for each operating condition. The previous history of the plant can usually be obtained from operating records. At the design stage it should be stipulated that these records should be kept. Where service stresses and service temperatures depend on plant output, the previous history should be broken down into a series of blocks, during which the stress and temperature are sensibly constant.

In addition to tabulating the total time at each of the steady operating conditions, any events likely to contribute to fatigue damage must also be taken into account. Where vibration or thermal fluctuations occur during periods of nominally constant load operation, an estimate of the frequency and magnitude of the fluctuations is required. Where transient thermal or mechanical loads occur at start up or shut down or with change with plant output, the number of load cycles and their magnitude must be established.

Establishment of relevant stress

The relevant stresses to be used in the assessment should be those, which would exist in the local region of the defect if the body were un-cracked. They should not include stress intensification effects due to the defect itself, as the Assessment Procedure naturally takes these into account.

It is sometimes necessary to separate the stresses into different categories. This can follow the principles of the ASME Boiler and Pressure Vessel Code, Section III, NB 3000 and of Appendix A of BS 5500:1991, R6, A16 and BS7910. However special care is needed in dealing with the secondary and peak stresses. All stresses which are induced by internal pressure and external loads must be categorized as Primary. In the case of peak stresses, it is necessary to distinguish between those, which are due to internal pressure and external load, and those, which are brought about by secondary stresses resulting from thermal loading or residual stresses in welds.

In carrying out the stress categorization, it is important to take into account any elastic follow up effect due to the spring action of adjacent parts of the structure. Unless it can be demonstrated to the contrary, long range thermal and residual stresses must be categorized as Primary.

The definitions of stress category, which could be used in the document, are thus:

P - Primary stress, which includes all stresses arising from internal pressure and external loads and which includes some stresses classified as Secondary by ASME Section III and Appendix A of BS 5500:1991. The primary stress category also includes long-range thermal and residual stresses, unless there is conclusive evidence to the contrary.

Q - Secondary stress, arising from thermal loading and residual stresses due to manufacturing processes, including welding.

F - Peak stresses, usually associated with local stress raising features.

Thus the stress intensity factor K_I^P is calculated using the stresses, which are categorized as *P*. The portion of the *F* stresses which are induced by internal pressure and external loads are added to the *P* stresses if the crack tip is situated in the *F* stress region.

The stress intensity factor $K_I^{(P+Q)}$ is calculated using the sum of the *P* and the *Q* stresses. The F stresses arising from all causes are added if the crack tip is situated in the F stress region.

These should be presented and categorized in a linearized format and referred to in figures similar to BS 7910. It should be noted that many of the difficulties inherent in stress categorization and in simplification and linearization can be avoided, for more complex structures if a detailed finite element analysis is performed to calculate the stresses in the vicinity of the defect. However this is not feasible for every situation. Stress intensity factors can be evaluated using a weight function method or by using a post processor program. There are handbooks available that contain solutions for some structures and R6 contains a number of practical solutions, for example. Two calculations will generally be required. In the first, used to evaluate K_I^P the component is subjected only to those loads, which contribute to plastic collapse, including, where necessary, long-range thermal and residual stresses. In the second calculation, to evaluate $K_I^{(P+Q)}$ the calculation is carried out for the total loading to which the structure is subjected, i.e. internal pressure and external loads plus both long range and localized thermal and residual stresses.

It is important to tabulate the relevant loading, stress intensity factors and reference stresses for the important components, which are of most concern. This task will need a comprehensive literature search and FE numerical analysis in order to be complete.

Numerous creep crack growth studies that have been performed have shown that the results of a nonlinear analysis must be used otherwise the stress state in time will be greatly over-estimated. For example, when looking a crack-like flaws near a nozzle, if the stresses at the junction are computed

elastically, peak values will be reached, and subsequent linearization and classification will result in high stress intensity factors and associated C* values. Hence the use of the elastic driving force will give results that are too conservative. In many cases, reference stress formulations based on limit load solutions, such as those in a compendium in R6, adequately describe the non-linear effects. In other cases, an elastic-plastic-creep assessment is suggested.

Therefore in general, calculating C* using linear elastic stress analysis, especially at shell junctions, is a bad model, and applying a probabilistic approach to a model like this will not correct the deficiency. With the rapid increase in computing power and improved software that can be run on parallel processing inelastic analysis is less difficult. An alternative to reference stress techniques is to compute C* from the stress and strain results of an inelastic analysis of the un-cracked body. This will accurately account for stress relaxation/redistribution. A more rigorous analysis where the crack is introduced directly into the FEA analysis is also possible. However available software, such as in ABAQUS, to calculate C* directly in 3-D cases, needs to be verified for accuracy.

Characterizing defects

Defects are generally of irregular shape. The maximum depth and maximum length are used in this instance. The method to determine the size and to circumscribe the shape, such as a rectangle or ellipse, is available in BS 7910 and could be implemented in the procedure. The relevant section also provides the method for characterizing and assessing the interaction of multiple defects. For multiple cracks, which are at close proximity, weaker material property in the intermediate ligaments may need to be considered. For the case of ligament failure re-characterization may be necessary. The procedure should refer to figures detailing the methods for characterizing defects.

An elliptical defect, inscribed within a rectangle, is often used for the purpose of calculation. In BS7910, the length is defined as *2l* and the depth as *2a*. It should be noted that the depth of a semi-elliptical surface breaking defect is taken as *a*.

Where there is doubt about the accuracy of the size of defect established by the inspection procedure, it may be necessary to assume a larger defect for the purpose of assessment in order to ensure a safe assessment. It is the intention of this document that upper bound sizes for defects should always be used. Where the plane of the defect is not aligned with a plane of principal stress further consideration is needed. The code places rigid restrictions in such cases and suggests that specialist advice should be sought.

Establishment of material properties

The basic materials data required for the assessment comprise the following, which must be in the relevant range of stresses and temperatures taking into account the material condition (e.g. new or damaged due to service condition)

- Yield stress/0.2% proof stress
- Creep strain versus time curves
- Stress versus time to rupture curves
- Ultimate tensile stress
- Fatigue threshold
- Fatigue S-N curve data
- Fatigue crack propagation rates
- Creep crack initiation and propagation data
- Fracture toughness properties

Allowance needs to be made for any deterioration (if any), which may occur during service, due to ageing and environmental effects. Allowance should also be made for any reduction in fracture toughness and any increase in creep and fatigue crack propagation rates, which may occur in material, which has suffered significant bulk creep damage.

It is preferable to use data, which are derived from the material actually used in the component. Often these are not available. The code should provide the information on the more commonly used materials. It is important to undertake a sensitivity analysis, when using the data of the parent material, to allow for the possible presence of poorer material in the component. In making a preliminary assessment, "worst case" material data can be used in the analysis; for example, upper bound data for fatigue crack growth rate and lower bound data for fracture toughness and tensile properties. However, care needs to be taken to guard against excessive pessimism. When the "worst case" assumption does not provide satisfactory margins, a more thorough investigation may need to be carried out.

Fracture Toughness

The code suggests that data should preferably be obtained on the materials actually used in the component. Where these are not available, the lower and upper bound values as appropriate should be provided for a range of temperatures in a table. They can never be too comprehensive and it may be necessary to look for the relevant material data from outside databases. It is necessary to check that these data are applicable to the heat treatment and manufacturing procedure used for the component. A check should also be made regarding any allowances for ageing of the material, and for the presence of welds.

Procedures for checking the fatigue component

Before proceeding further, it is necessary to check whether fatigue loading can be neglected. Otherwise, the assessment must be modified according to the requirements of code. The methods of BS 7910 could be used to evaluate fatigue crack propagation. The value of D*K*, the stress intensity factor range, may be evaluated from the relevant stress intensity equations or by using validated expressions for the component or where unavailable using finite elements. *P* and *Q* stresses must be included in the evaluation of *K*. *F* stresses must be included if the crack tip is located in the *F* stress region.

Performing defect assessment

The principal steps in the defect assessment that are recommended are as follows:

- Determine margin against fast fracture, assuming an initial defect size or a measured defect dimension, using various levels of the Failure Assessment Diagram (FAD), by the elastic plastic method proposed in R6, FITNET and BS7910
- Evaluate fatigue threshold and crack propagation rates and estimate amount of crack growth at intervals during the future life of a component
- Determine creep rupture life of component, using initial defect dimensions
- Evaluate crack propagation rates and estimate amount of crack growth at intervals during the future life of a component
- Check that steady creep conditions apply at the crack tip; if not, revise crack growth estimates
- Determine crack dimensions at the end of each interval
- Repeat calculation of margin against fast fracture, by the elastic-plastic methods proposed in R6, FITNET and BS7910, using the new crack dimensions at the end of each interval
- If end of life margin against fast fracture is satisfactory, no remedial action is needed
- If end of life margin against fast fracture is unsatisfactory, the intermediate calculations can be used to establish the time at which this margin ceases to be acceptable and to define when remedial action is necessary

The method of performing the calculations should be given in detail in the code and a summary will be given here. It should be noted that it is often possible to demonstrate that the component has adequate future life by making conservative assumptions about stress level, temperatures and material properties. Where such calculations do not give satisfactory margins, a more thorough investigation should be performed.

Fatigue Crack Propagation Rates

The fatigue crack propagation rate is defined by the equation

$$(da/dN)_f = C(\Delta K)^m \qquad (1)$$

where $(da/dN)_f$ is the crack extension per cycle due to fatigue (mm/Cycle) and ΔK is the range of stress intensity factor arising from the cyclic loading. A mean, upper bound and lower bound to crack propagation data for the relevant steels used in the component should be obtainable in the procedure. There is information available in the literature for many cases however for a specific temperature range and specific steels of interest additional tests may be needed.

Further data should be available in appendices and in some cases References given in the code. It should be noted that the rate of growth in the depth *a* of the crack may differ from the rate of growth in the length l of the crack. This arises because of a possible difference in ΔK in the two positions. Therefore this should also be considered. Where R-ratios are negative, allowance for crack closure may be made by using an effective stress intensity factor range in eqn (1) as set out in R5.

Concepts of High Temperature Fracture Mechanics

The arguments for high temperature fracture mechanics essentially follow those of non-linear elastic fracture mechanics for room temperature applications. For creeping situations where elasticity dominates the stress intensity factor may be sufficient to predict crack growth. However as creep is a non-linear time dependent mechanism even in situations where small-scale creep may exist linear elasticity may not be the answer. J estimation procedures have been used in developing methods for estimating the fracture mechanics parameter C^*.

Numerical method to calculate J

Although the numerical methods to analyze the *J* integral are becoming easier to apply, owing to improvements in computer performance and software, including pre/post-processing systems, simplified methods are still desired for engineering. Because the problem is non linear, it is generally difficult to obtain the *J* integral by analytical methods. Analytical solutions for only very simple cases are available, for example a 2-D crack in an infinite plate with power law plasticity. Therefore, solutions for *J* integrals for various geometries and material properties have to rely on numerical calculations. The simplified methods are usually, themselves, based on previous numerical solutions. One engineering approach for calculating the *J* integral is based on the GE / EPRI method. In this method, the elastic-plastic material property is expressed by a Ramberg-Osgood type of formula as;

$$E\varepsilon = \sigma + \alpha\left(\frac{|\sigma|}{\sigma_0}\right)^{n-1}\sigma \qquad (2)$$

where E is Young's modulus, α, σ_0 and n are material constants. The first term expresses the elastic component, and the second term is the plastic component. As the simplest combination of an elastic part and a plastic part, the J integral is calculated by summation of the elastic J_{el} and the plastic J_{pl} integrals.

$$J = J_{el} + J_{pl} \tag{3}$$

The J_{el} is the same as the energy release rate G and can be calculated from the stress intensity factor K. The plastic part of J_{pl} is given by;

$$J_{pl} = \alpha \sigma_0 \varepsilon_0 c h_1 \left(\frac{P}{P_0}\right)^{n+1} \tag{4}$$

where $\varepsilon_0 = \sigma_0/E$ and c is characteristic length, usually taken as the uncracked ligament length. The P and P_0 are an applied load and characterizing load, respectively. h_1 is a non dimensional function of geometryand n and has been tabulated for specific values of P_0 . Any P_0 value can be used, but to give relatively constant h_1 values against the material constant n, usually the P_0 is taken as plastic collapse load or limit load.

This method (called the GE/EPRI) is applicable to simple geometries like a fracture mechanics test specimens of pipe components. However, if a fracture mechanics estimate for other geometry is required, numerical calculations are required using fully plastic material properties to make new h_1 tables. Some further calculations have been made to extend the h_1 tables, especially for 3 dimensional surface cracks that are realistic defects in actual components.

Crack Driving Force Parameter in Creep

A simplified expression for stress dependence of creep is given by a power law equation which is often called the Norton's creep law and is comparable to the power law hardening material giving;

$$\varepsilon = A\sigma^N \tag{5}$$

and by analogy for a creeping material

$$\dot{\varepsilon} = C\sigma^n \quad \text{or} \quad \frac{\dot{\varepsilon}}{\dot{\varepsilon}_0} = \left(\frac{\sigma}{\sigma_0}\right)^n \tag{6}$$

where A, N, C, n, ε_0 and σ_0 are material constants. Eqn. 6 is used to characterize the steady state (secondary) creep stage where the hardening by dislocation interaction is balanced by recovery processes. The typical value for n is between 3 and 10 for most metals. When $N=n$ for creep and plasticity the assumption is that the state of stress is characterized in the same manner for the two conditions. The stress fields characterized by K in elasticity will be modified to the stress field characterized by the J integral in plasticity in the region around the crack tip. In the case of large scale creep where stress and strain rate determine the crack tip field the C^* parameter is analogous to J. The C^*

integral has been widely accepted as the fracture mechanics parameter for this purpose. The definition of the *C** integral is obtained by substituting strain rate and displacement rate for strain and displacement in the *J* integral leading to

$$C^* = \int_\Gamma \left[W_s^* dy - T_i (\delta \dot{u}_i / \delta_x) ds \right] \tag{7}$$

where *W** is strain energy density rate,

$$W_s^* = \int_o^{\dot{\varepsilon}_{ij}^c} \sigma_{ij} d\dot{\varepsilon}_{ij}^c \tag{8}$$

$(\dot{u}_i = du_i / dt)$ where is displacement rate. The other notations are the same as in the *J* integral definition. As the *J* integral characterizes the stress and strain state, the *C** integral also characterizes the stress and strain rate around a crack. Due to the analogy between non-linear elasticity and non-linear creep, the stress and strain rate in materials following Norton's creep law by equation (6) are given as;

$$\sigma_{ij} = \sigma_o \left(\frac{C^*}{I_n \sigma_o \dot{\varepsilon}_o r} \right)^{1/(n+1)} \tilde{\sigma}_{ij}(\theta, n) \tag{9}$$

$$\dot{\varepsilon}_{ij} = \dot{\varepsilon}_o \left(\frac{C^*}{I_n \sigma_o \dot{\varepsilon}_o r} \right)^{n/(n+1)} \tilde{\varepsilon}_{ij}(\theta, n) \tag{10}$$

Therefore the stress and strain rate fields of non-linear viscous materials are also HRR type fields with $\tilde{\sigma}_{ij}(\theta, n)$ $\tilde{\varepsilon}_{ij}(\theta, n)$ as before. Using eqns. (5, 6), the ratio of strain rate or displacement rate for a steady creep condition, and strain or displacement in a fully plastic analysis is *C/ A*. Hence by substitution, the relationship, at steady state, between *C** and *J* is obtained as follows.

$$C^* = \frac{C}{A} J \tag{11}$$

Equation (11) suggests that only a *J* calculation for fully plastic behavior is required to calculate the *C** integral for steady state creep conditions.

GE/EPRI method applied to Creep

In the case of a power law material, there exists the simple relationship in eqn.(11) between *J* and steady state *C** as mentioned above. Therefore, the GE/EPRI method introduced as an engineering approach for calculating the *J* integral, is also applicable for calculating *C**. When power law plasticity is used, the plastic *J* integral can be expressed using a non-dimensional factor h_1 and material constants. When the creep exponent is the same as the plastic exponent *n*, the *C** integral can be obtained using strain rate instead of strain as follows;

$$C^* = \sigma_o \dot{\varepsilon}_o c h_1 \left(\frac{P}{P_o} \right)^{n+1} \tag{12}$$

where h_1 is common between the C^* and J integrals. This method is useful for engineering applications of the C^* integral because it does not require a non-linear stress and strain analysis. However the same limitation exists, as for the J integral, and it is necessary to have the non-dimensional factor h_1 for a specific geometry and material constant n.

Reference stress method for *J* and *C**

Another engineering approach to calculate the J integral has been proposed using reference stress procedures. The reference stress has been also utilized for estimating the non-linear fracture mechanics parameters. The reference stress is defined by,

$$\sigma_{ref} = \sigma_y \frac{P}{P_{LC}} \quad (13)$$

where P is the applied load, and P_{LC} is the plastic collapse load of the cracked body made of elastic perfect plastic material with yield stress σ_y. This reference stress concept has been extended to non-linear fracture mechanics estimations. The reference stress method was originally developed for un-cracked bodies. Its extension to estimate J and C* for cracked structures was verified by comparison with the GE/EPRI technique mentioned earlier. A stress σ_r is defined by

$$\sigma_r = \sigma_0 \left(\frac{P}{P_0} \right) \quad (14)$$

to produce a plastic strain component ε_r from eqn. (2).

$$\varepsilon_r = \alpha \varepsilon_0 \left(\frac{P}{P_0} \right)^n \quad (15)$$

Substituting eqns. (14) and (15), equation (4) becomes;

$$J = \sigma_r \varepsilon_r c h_1 \quad (16)$$

If an appropriate P_0^* is chosen instead of P_0 for eqn. (14), then h_1 values become approximately independent of the material constant n.

$$h_{1,n} = h_{1,1} \quad (17)$$

where the second subscripts n and 1 show the values of the power law exponent. For elastic $n = 1$ condition, the J integral is related to stress intensity factor K, so that eqns. (15) and (16) give;

$$\frac{K^2}{E'} = \sigma_r \varepsilon_r c h_{1,1} \quad (18)$$

where $E' = E$ for plane stress , $E' = E/(1- \nu 2)$ for plane strain. Since ε_r is also related to σ_r for the elastic case by;

$$\varepsilon_r = \sigma_r / E \quad (19)$$

the following relationship is obtained.

$$ch_{1,n} = ch_{1,1} = \frac{K^2}{E'\sigma_r \varepsilon_r}$$
$$= \frac{K^2}{\sigma_r^2} \quad \text{for plane stress}$$
$$= \frac{(1-\nu^2)K^2}{\sigma_r^2} \quad \text{for plane strain} \quad (20)$$

Using this relation in eqn. (16) gives;

$$J = \mu \sigma_r \varepsilon_r \left(\frac{K}{\sigma_r}\right)^2$$

$\mu = 1$ for plane stress

$\mu = (1 - \nu^2) = 0.75$ for plane strain (21, 22))

To obtain the relations above, an appropriate P_0 value must be chosen. It has been concluded that the plastic collapse load P_{LC} is a good approximation of P_0^* for examining the dependence of h_1 values on n for several geometries. Substituting P_{LC} for P_0, the stress σ_r becomes σ_{ref}, then the J integral is calculated using the reference stress as;

$$J = \mu \sigma_{ref} \varepsilon_{ref} \left(\frac{K}{\sigma_{ref}}\right)^2 \quad (23)$$

where ε_{ref} is the uniaxial strain corresponding to the reference stress σ_{ref}. It should be noted that, as the reference stress estimation is an approximate solution, the effect of μ is relatively small compared to other factors and often ignored.

There are advantages of the reference stress method over the original GE/EPRI method. Power law fitting of actual plastic behavior is not necessary since is not easy to fit a power law equation to an actual stress and strain curve on wide range of plastic behavior. The GE/EPRI eqn. (4) has a strong dependency on the plastic exponent n and hence the J integral. The reference stress method can use actual stress and strain relationships. Also the reference stress method does not require the h_1 values that are specific to individual geometries and material properties and need to be derived using numerical methods whereas the reference stress method only needs plastic collapse loads of the specific geometries. Collapse loads solutions are available for a number of geometries and loading in the literature. Consequently, the reference stress method is easier to employ for flaw assessments in general structures.

Following the arguments linking plasticity and creep a reference stress method for C^* calculation is also easily obtained by analogy with that for the J integral introduced earlier. The only difference is the

strain ε_{ref} is replaced by the reference strain rate at a reference stress σ_{ref}. The C^* formulation using the reference stress method becomes

$$C^* = \mu\sigma_{ref}\dot{\varepsilon}_{ref}\left(\frac{K}{\sigma_{ref}}\right)^2 \quad (24)$$

The μ and K have the same definitions as previously. This method is particularly useful in industrial applications where information may only be available for material rupture properties. This method is identified in various codes of practice as an appropriate way to evaluate C^*. This method has been validated and verified for a number of components as discussed later.

The accuracy of this method is dependent on the consistency with which the reference stress is calculated for different cracked components. A compendium of limit load and reference stress solutions over a range of crack lengths has been developed within R6 using numerical, experimental and limit analysis methods to accurately identify the appropriate reference stresses for relevant components.

Transient Creep

A fracture mechanics parameter C_t for describing the transient creep stage has been proposed by Saxena. However, another parameter $C(t)$ characterizes the stress and strain rate fields around a crack tip for the transient creep condition and is therefore another possible parameter for describing the transient creep stage. The C_t parameter was introduced based on energy concepts but in practice is calculated from the expansion rate of a creep zone or from displacement rate measurements. For the steady state condition, C^* has both its characterizing role and its energy interpretation. During transient creep C_t is given by the energy expression,

$$C_t = \frac{1}{B}\frac{dU^*}{da} \quad (25)$$

but an approximate expression for Ct at short times is

$$C_t = \left[1 + \left(\frac{t_T}{t}\right)^{\frac{n-3}{n-1}}\right] C^* \quad (26)$$

A method for estimating C_t is identified in ASTM E1457 as the method of evaluating cracking rate as a material property in laboratory specimens in the transient region. However it has not been extended any further to relate it to creep crack growth in creep ductile components in any comprehensive way as compared to the reference stress method which has been developed for estimating C(t). As generally C(t) > C_t it is conservative to use C(t) rather than C_t to estimate creep crack growth during the transient regime.

Primary effects can be taken into account by employing the appropriate material property for the primary and the secondary region. This is used in reference stress method to estimate creep cracking where primary creep is a first order effect. This may become relevant under low frequency cyclic loading when the primary effects occurring at the start of each cycle or at the start of the first cycle might affect creep crack initiation and growth.

Creep Crack Propagation Rate

Creep crack propagation data, defining material property, are derived in accordance with ASTM E1457 high temperature testing standard. Crack growth rate is thus defined as

$$\dot{a}_c = A(C^*)^q \quad (27)$$

Where crack propagation data are not available for the material used in the component, estimates can be obtained, for a number of materials in procedures giving approximate bounds to eqn. (27). Both mean and upper bound data are presented in the procedures. Use of the upper bound data introduces conservatism into the estimates of remaining life. It should be noted that, for components more than about 100mm thick, crack propagation rates may be higher due to crack tip constraint effects and specialist advice should be sought about the appropriate values to be used.

For materials not covered by the procedure, two methods are available to estimate crack propagation rates, although the results may not be upper bound.

Where the creep rupture ductility of the material is known, a guide to crack propagation rates can be obtained by taking q as 0.85 and deriving A from the equation (27) in m/h

$$A = 0.003/\varepsilon_f \quad (28)$$

where ε_f is the creep rupture ductility of the material in a uniaxial test at σ_{ref} (Note that the fractional strain is used, not the percentage strain). Creep rupture ductility's for certain steels are given in References quoted in the code. Where the creep rupture ductility is not known, a guide to propagation rates can be obtained from the equation

$$\dot{a}_c = 0.005[\ (K_a^p)^2 / (\sigma_{ref} \cdot t_{R(ref)})\ ]^{0.85} \quad (29)$$

where K_a^p is the elastically calculated stress intensity factor at maximum depth for a crack characterized by the dimensions a and l. σ_{ref} is the reference stress; and $t_{R(ref)}$ is the time to rupture at the reference stress. A similar calculation should be made for growth in the l direction using K_l^p.

Creep/Fatigue interaction

From the literature and extensive work carried out in this field it has been concluded that a linear summation of the time dependent creep and the time independent fatigue portions of crack growth adequately describe the high temperature failure under most cyclic loading. R5 identifies the special cases where this does not apply. The crack growth per cycle of creep-fatigue loading is estimated by summing the crack propagation due to creep and due to fatigue calculated independently.

The crack growth rate due to creep is calculated, as in eqn. 27. The crack extension due to creep in a single fatigue cycle, $(da/dN)_c$, is thus

$$(da/dN)_c = \frac{\dot{a}_c}{(3600.f)} \quad (30)$$

The crack growth per cycle due to fatigue is calculated from Eqn. 1. The predictions made using these equations may be over conservative where the stresses at one end of the cycle are compressive. Thus total crack growth per cycle, *(da/dN)*, is given by

$$(da/dN) = (da/dN)_c + (da/dN)_f \quad (31)$$

This linear summation combines creep and creep/fatigue components. If failure by excessive crack growth is indicated within the required service life, or if the sensitivity analysis gives unacceptable results, then remedial action is required, such as repair of the component or removal of the defect.

Alternatively, a change in service parameters (load, temperature, desired service life) may be made and the assessment procedure repeated either to demonstrate acceptance or to estimate at what time repair will be necessary. Finally, it may be possible to obtain data on the material actually used in the component to remove pessimism in the assessment resulting from the use of bounding data. The sensitivity analysis is particularly useful for indicating which material properties may significantly influence the assessment. For example, if remedial action is required because the desired service life exceeds the rupture life calculated, there is no point in generating creep crack growth in an attempt to improve the assessment.

Incubation period

The Incubation period is an important period for development of damage ahead of the macro crack. There are a number of criteria for defining initiation. Invariably the level of accuracy in measuring a small amount of crack growth from a planar crack could be set as an engineering initiation period. There are four approaches that could be considered for evaluating initiation times. It should be noted that where fatigue is present most codes suggest that there should be no account taken for an initiation time. The four methods that have been proposed are as follows;

COD Method: Where data are not available for the material used in the component, the incubation period can be estimated from the eqn (32). The incubation time is calculated using

$$t_I = 0.0025\left[\frac{\sigma_{ref} t_{R(ref)}}{\left(K_a^p\right)^2}\right]^{0.85} \quad (32)$$

Where experimental data are available and the crack opening displacement at initiation of creep crack growth, δ_I is known, then provided that the creep strain versus time curve for the material, at the relevant stress and temperature, can be represented by an equation of the form

$$\varepsilon_c = D\,\sigma^n\, t^p \quad (33)$$

Then t_I can be obtained from the equation

$$t_I = \left[\frac{(\delta_I / R')^{n/n+1} - \sigma_{ref} / E}{D \sigma_{ref}^n} \right]^{\frac{1}{p}} \quad (34)$$

where $R' = (K_p / \sigma_{ref})2$. Where incubation time data are available from test specimens, the incubation time for the component can be obtained from the following equations, provided that both specimen and component are in the secondary stage of creep

$$\left(\frac{t_{I\,comp}}{t_{I\,spec}} \right) = \left(\frac{C^*_{spec}}{C^*_{comp}} \right)^{n/n+1} \quad (35)$$

where subscript *comp* refers to the component and *spec* refers to specimen.

Sigma σ_D approach: The principle is based on calculating damage accumulation by creep and fatigue in a cracked structure and this method is an extension of the same methodology for un-cracked structures with the exception that a specific stress σ_D is defined at a specific distance from the crack tip. The method is to determine strain ranges $\Delta\varepsilon$, the stress σ (accounting for elastic + plastic strains +creep strains) at a distance *D,* which is material dependent and usually taken as 50 μm, from the crack tip. Fatigue damage is determined by calculating strain ranges for all cycles in the life *N*. Number of cycles to failure at each strain range is determined from fatigue endurance data.

Finally all ratios of the numbers of cycles experienced at each strain range over the maximum number of cycles at that strain range are summed. Calculation of the creep damage is the same as for fatigue but damage calculation includes elastic, plastic, and creep strains. Creep damage is determined for all cycles and rupture time used up is determined from the fraction as the sum over all ratios of numbers of cycles. If the fatigue and creep fraction points lie within a specified fatigue-creep interaction diagram no initiation occurs. If initiation did occur then the initiation time is determined through an iterative procedure. The last point at the intersection boundary to initiation determines the timed cycles to initiation. A detailed approach is set out in R5 and has recently been the subject of an independent peer review in the UK.

Two criteria approach: This method is only relevant to creep initiation and does not consider fatigue. Initiation is given if the point lies in the specific two criteria diagram, which depends on material or at least material group properties. It compares ligament damage R_σ against crack tip damage R_K where

$$R_{\mathrm{K}} = \frac{K}{K_{\mathrm{I}}} \text{ and } R_\sigma = \frac{\sigma_{\mathrm{no}}}{R_{\mathrm{mt}}} \quad (36)$$

and where σ_{no} is the nominal stress in the far-field of a pre-cracked component (fully redistributed stresses), $P_{\mu\tau}$ is the creep rupture strength of a smooth tensile specimen (function of time, e.g. taken at 10^4 h), *K* is elastic *K*-value at the crack tip of the component and K_I is *K*-value at creep crack initiation experimentally determined as a function of time, (e.g. taken at 10^4h). If fatigue is present then initiation time is taken as zero. A detailed approach is set out in the FITNET creep section.

Transient method: This method also uses creep fracture mechanics principles to determine the time taken for creep damage to accumulate at the crack tip starting from first initial elastic loading. Essentially the steady state creep crack growth ratę can be correlated satisfactorily in terms of *C** by the relation in

Eqn. 27. Bounds on initiation times t_i can be obtained by representing cracking rate by its initial value and its steady state value. The initial cracking rate can be approximated to the steady state rate in by

$$\dot{a}_0 = \dot{a}_s /(n+1) \quad (37)$$

The value of n for most engineering materials is usually in the range 5-10, which suggest that $_o\dot{a}$ is approximately an order of magnitude less than its steady state value. Thus for steady state conditions a lower bound incubation period of

$$t_{iL} = \Delta a / DC^{*\phi} \quad (38)$$

is indicated or using the approximate Eqn. 28

$$t_{iL} = \frac{\Delta a \varepsilon_f^*}{3C^{*0.85}} \quad (39)$$

Tentatively if the incubation period is calculated from the initial transient cracking rate a_o determined from Eqn. 37 the approximate upper-bound t_{iU} to the initiation time becomes

$$t_{iU} = \frac{(n+1)\Delta a\ \varepsilon_f^*}{3C^{*0.85}} \quad (40)$$

In eqns. (38-40) the incubation period is proportional to Δa. The limit of reliable crack detection is at best $\pm 100\ \mu m$ (which is the level set for standard CT testing in ASTM E1457-98) and can sometimes be as large as 0.5 mm. In reality the engineering initiation time should be set as the level of accuracy of the NDE method.

Special considerations for welds

Many of the defects found in high temperature steam generating plant are associated with weldments. These defects may arise during fabrication, post-weld heat treatment or in service. Furthermore, since weldments contain wide metallurgical and mechanical property variations, the defects are often located in non-homogeneous material, which has a significant effect on crack growth.

Defects in austenitic and ferritic weldments, including Type IV cracking can be assessed using the methods described in this document. However, dissimilar metal weldments, where cracking occurs at the interface between the austenitic weld metal and ferritic parent metal, need special consideration. Specialist advice is contained in R5 for assessing such weldments.

The properties of the weld metal and the heat affected zone are usually considerably different from those of the parent material, in terms of creep strength, crack propagation rate and fracture toughness. It is important to identify the part of the weld in which the crack is situated and then to use properties appropriate to that location.

Residual stresses in the vicinity of a weld can have a significant influence on crack propagation and failure and must be considered in the assessment. Localized residual stresses are classified *Q*. Long range residual stresses, arising for example from lack of fit during fabrication, must be classified as P. Typical residual stress distributions in some commonly used types of weld are provided in R6 and BS7910. For other configurations, in the absence of data to the contrary, it should be assumed that a tensile membrane stress of yield point magnitude is present.

Where it can be confirmed that the component has been subjected to a post weld heat treatment, which reduces the residual stresses to a negligible level, they can be ignored in the assessment. It may also be possible to take credit for a reduction in residual stress when a component has been in service for a sufficiently long period at a sufficiently high temperature. R5 provides methods for assessing this stress relaxation.

PERFORMING THE DEFECT ASSESSMENT

Once all aspects of input are satisfied, the procedure should be implemented in a series of well-defined steps, which should be shown as a flow chart. For example, the chart in Figure 3 represents a detailed description of the individual steps, which could refer to a component before it enters service, containing either a postulated defect or one discovered during inspection or to a defect, which has been discovered after a component, has been in service for a period of time.

These choices are noted in the text of the chart, as appropriate. Important points in the flow chart are the variations and choices available to the user in accordance with their level of expertise and the level of information available on the component under consideration. Furthermore the chart and the document should show the importance of the need for sensitivity analyses in performing the assessment task.

The principal steps in the defect assessment that are recommended are as follows:

- Determine margin against fast fracture, assuming an initial defect size or a measured defect dimension, using various levels of the Failure Assessment Diagram (FAD), by the elastic-plastic method proposed for example in R6, FITNET or BS7910.
- Evaluate fatigue threshold and crack propagation rates and estimate amount of crack growth at intervals during the future life of a component
- Determine creep rupture life of component, using initial defect dimensions
- Evaluate crack initiation and propagation rates and estimate amount of crack growth at intervals during the future life of a component.
- Check that steady creep conditions apply at the crack tip; if not, revise crack growth estimates
- Determine crack dimensions at the end of each interval
- Repeat calculation of margin against fast fracture, by the elastic-plastic methods proposed in R6 or BS7910, using the new crack dimensions at the end of each interval.
- If end of life margin against fast fracture is satisfactory, no remedial action is needed.
- If end of life margin against fast fracture is unsatisfactory, the intermediate calculations can be used to establish the time at which this margin ceases to be acceptable and to define when remedial action is necessary.

The method of performing the calculations should be given in detail in the code and a summary will be given here. It should be noted that it is often possible to demonstrate that the component has adequate future life by making conservative assumptions about stress level, temperatures and material properties. Where such calculations do not give satisfactory margins, a more thorough investigation should be performed.

Remedial Action

If failure by excessive crack growth is indicated within the required service life, or if the sensitivity analysis gives unacceptable results, then remedial action is required, such as repair of the component or removal of the defect.

Alternatively, a change in service parameters (load, temperature, desired service life) may be made and the assessment procedure repeated either to demonstrate acceptance or to estimate at what time repair will be necessary. Finally, it may be possible to obtain data on the material actually used in the component to remove pessimism in the assessment resulting from the use of bounding data. The sensitivity analysis is particularly useful for indicating which material properties may significantly influence the assessment.

For example, if remedial action is required because the desired service life exceeds the rupture life calculated, there is no point in generating creep crack growth in an attempt to improve the assessment.

Sensitivity Analysis and Life assessment using probabilistic methods

Assuming the final defect size gives an acceptable end-of-life safety margin, a sensitivity analysis should be recommended. This analysis is not considered in detail in this document, but reference may be made to BS7910, R6 and R5, which describes the principles. The sensitivity analysis should consider the effects of different assumptions (e.g. stress levels, material properties and defect size). The UK codes stress the fact that a sensitivity analysis is an important factor in the life assessment procedure since only then should the user finds confidence in the calculations that he has performed.

Given the importance that the codes attach to sensitivity analyses the use of probabilistic method is the natural next step in the development of the procedures. This aspect of defect assessment is relatively new and has been set out in some derail in the FITNET creep document and in R5. Essentially data are statistically filled to find its relevant distribution. In variably where there is insufficient set of dada to consider a log-normal distribution is assumed. Then the calculations are performed many times over with randomly generated material properties data (within the constraints set by the expert, the data distribution and the model). The output will then need to be analyzed with different confidence levels according to the design levels set for the component.

Recent Developments in Creep Fracture Assessment Methods

Treatment of Combined Mechanical and Secondary Loading

Recently, it has been demonstrated that practical creep defect assessments may be extended to cases involving combined loading, creep crack growth, stress relaxation and complex creep laws. The methods involve evaluation of C(t) by reference stress methods allowing for relaxation of the secondary stresses either by creep, crack growth or a combination of both. Validation of these extended methods has been obtained by comparisons with finite element analyses. Some of these extended methods were incorporated into the creep part of the FITNET procedure and are shortly to be included more comprehensively in the R5 document.

Elastic Follow-up

For combined loading, relaxation of the secondary stresses may be associated with elastic follow-up. Finite element analyses have been performed for a number of component geometries (mostly cylinders), crack sizes and loading types to evaluate the elastic follow-up factor as a function of these parameters. The rate of relaxation has also been determined in terms of a corresponding redistribution time that can be related to reference stress methods (time for creep strain at the reference stress to equal the elastic-plastic strain at the reference stress). This will lead to improved advice on simplified estimation of elastic follow-up.

Use of non-standard test specimens

A recently completed European project (CRETE) examined the use of non-standard specimens (i.e. not deeply cracked bend) for obtaining creep crack growth data. Relevant factors to determine C* from experimental load-line and mouth opening displacement rates were evaluated and used to develop a testing procedure that is more flexible than current testing standards.

Within the FITNET project, there was work on development of probabilistic methods for assessing creep rupture and crack growth in cracked components. There is also developing advice in R5 as such methods are used in applications. An important aspect is that the different material properties are not independent (for example, creep crack growth rates are known to be approximately inversely proportional to material ductility) so that the effects of correlations between input parameters needs to be treated. Approaches to treat such correlations have been developed within Failure Assessment Diagram methods for creep crack growth assessment.

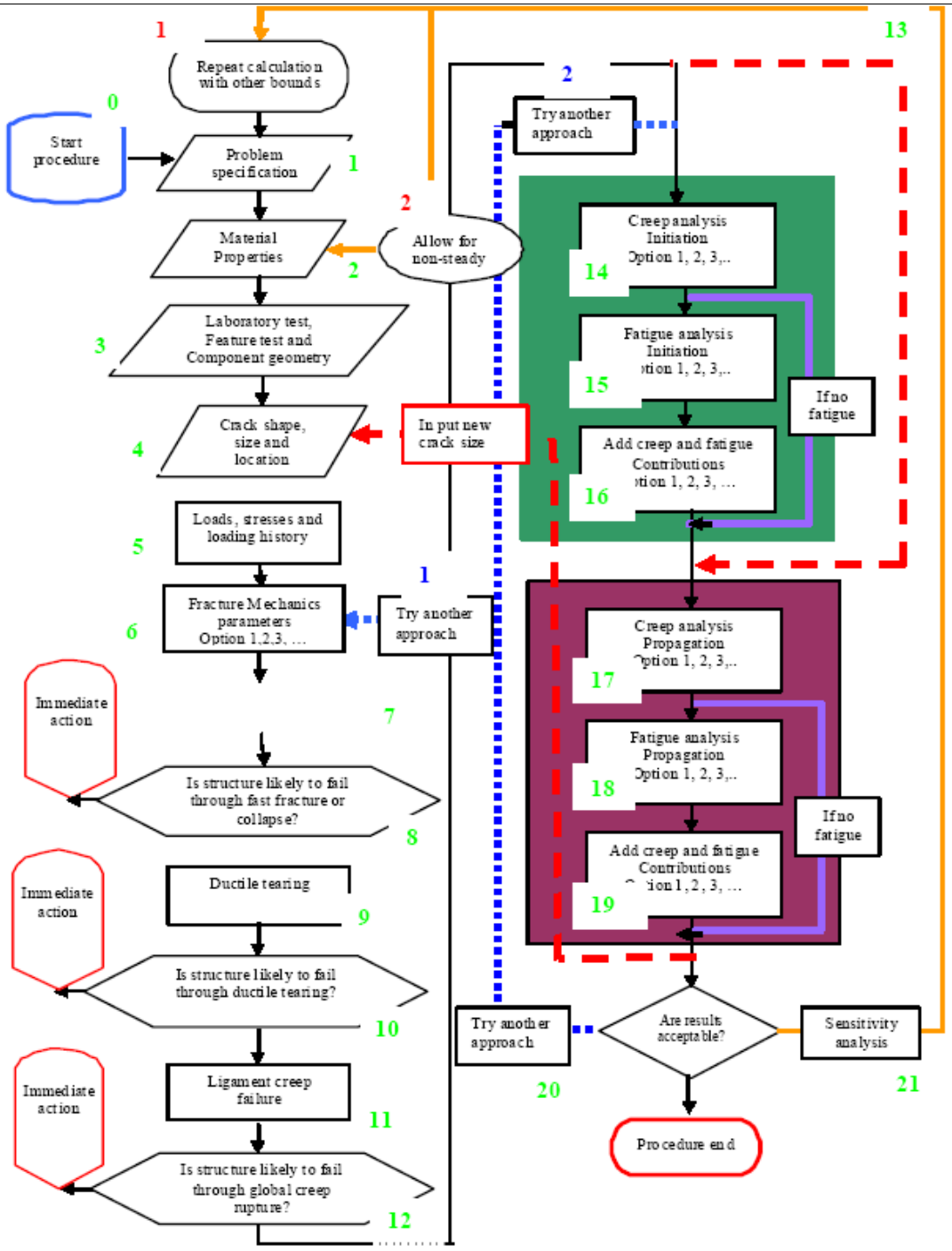
1
Repeat calculation with other bounds
0
Start procedure
Problem specification
1
Material Properties
2
2
Allow for non-steady
3
Laboratory test, Feature test and Component geometry
4
Crack shape, size and location
Input new crack size
5
Loads, stresses and loading history
6
Fracture Mechanics parameters Option 1,2,3, ...
1
Try another approach
Immediate action
7
Is structure likely to fail through fast fracture or collapse?
8
Immediate action
Ductile tearing
9
Is structure likely to fail through ductile tearing?
10
Immediate action
Ligament creep failure
11
Is structure likely to fail through global creep rupture?
12
13
2
Try another approach
Creep analysis Initiation Option 1, 2, 3,..
14
Fatigue analysis Initiation Option 1, 2, 3,..
15
If no fatigue
Add creep and fatigue Contributions Option 1, 2, 3, ...
16
Creep analysis Propagation Option 1, 2, 3,..
17
Fatigue analysis Propagation Option 1, 2, 3,..
18
If no fatigue
Add creep and fatigue Contributions Option 1, 2, 3, ...
19
Try another approach
20
Are results acceptable?
Sensitivity analysis
21
Procedure end

Part II: COMPENDIUM OF RELEVANT DATA OF ENGINEERING STEELS FOR USE IN FRACTURE MECHANICS BASES LIFE ASSESSMENT PROCEDURES

THIS SECTION IS FOR ASME USE ONLY

Summary
In this part reference is made for the need to have valid test data for use in life assessment codes. Where there are little or no data available the codes do in some cases contain generic material data and models to predict behavior in order that the user can obtain approximate assessment. However it would be preferable and is recommended that for a detailed assessment material data for the specific batch should be available. The Appendices A-D contain a range of data for low alloy, ferritic and austenitic steels that are available in the open literature. A more detailed analysis would be needed to identify the optimum data and information for each material.

Need for validated Test Data

Manufacturer's recommendations and their past experience have usually been the basis for the design of vital engine components such as turbine blades, vanes and discs and in critical engineering components such as gas or steam pipes, pressure vessels and in weldments which might contain pre-existing defects. In recent times however crack growth initiation and failure analyses have become more acceptable as an independent design and remaining life assessment methodology. The development of high temperature fracture mechanics concepts, through which the time dependent effects of creep could be modeled, uses experimental uniaxial and crack growth data from simple laboratory tests specimens in order to predict failure times under operating conditions. Furthermore the improvement in non-destructive inspections and testing methods (NDT) has allowed smaller and smaller defects to be detected and the need for more reliable methods for predicting crack initiation/incubation periods and steady crack growth rates.

Figure 2 shows a schematic of the overall relationship between testing and component assessment showing the circular link between developing test methods and applying it to life assessment which in turn feeds information back into improving testing methods. The main objective of developing testing procedures is to improve the reliability of design and life assessment codes, which use material basis data for their calculations. In developing a testing standard methodology for laboratory specimens a first step was taken to improve life prediction procedures of components. However life extension calculations of components requires a validated fracture mechanics model for crack initiation and growth as well as detailed knowledge of component non-linear time dependent stress analysis, past service records and postulated future operations together with 'appropriate' mechanical properties. It therefore seemed appropriate to develop a testing method for components and integrate it with life assessment codes for creep and creep/fatigue of components.

Relevance of Testing Methods to Life Assessment Codes

Components in the power generation and petro-chemical industry operating at high temperatures are almost invariably submitted to static and/or combined cycle loading. They may fail by net section rupture, crack growth or a combination of both. The development of codes in different countries has moved in similar directions and in many cases the methodology has been borrowed from a previously available code in another country. The early approaches to high temperature life assessment used methodologies that were based on defect-free assessment codes. For example ASME Code Case N-47 and the French RCC-MR, which have many similarities, are based on lifetime assessment of un-cracked structures. The

materials properties data that are used for these codes is usually uniaxial properties and S-N curves for fatigue.

More recent methods make life assessments based on the presence of defects in the component. The codes dealing with defects vary in the extent of the range of failure behaviour they cover. Essentially fracture mechanics solutions dealing with creep and creep/fatigue interaction in initiation and growth of defects are covered. In terms of creep crack growth all propose similar approaches but can use different formulae which are likely to affect the predictive solutions. In such codes material properties, dealing with crack growth data that are needed are more complex compared to uniaxial data both in terms of testing methods and derivation.

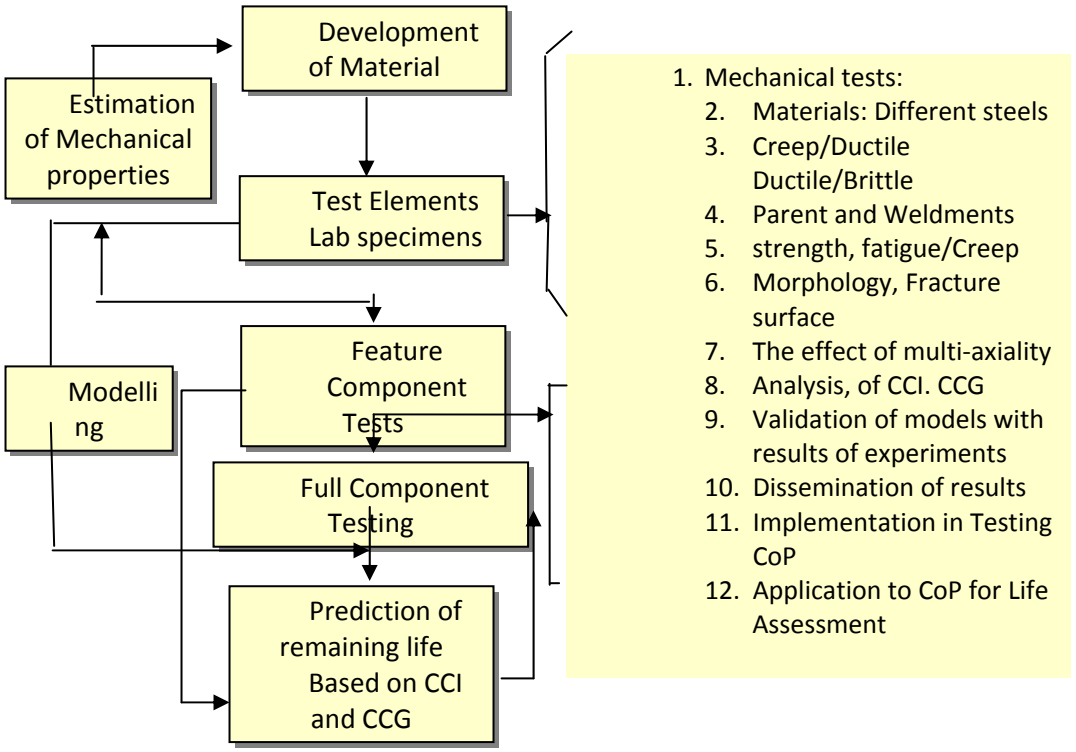

Figure 2: Schematic of the objectives in high temperature testing procedures.

Relation between laboratory tests and Component Assessment Codes

Generally defect assessment problems can be divided into two regions. Firstly the initiation region whose limit can be determined either from micro-mechanical models or from NDT limits and secondly the steady crack growth region which can be described using the fracture mechanics parameters such as K, reference stress $_{ref}$ and C^*. The more recent defect assessment procedures mentioned in Part I are based on experimental and analytical models to assess crack initiation and growth and to determine the remaining useful life of such components. These codes base their analysis on tests taken from laboratory specimens, which are invariably derived from small specimens at short test times. Therefore there is little direct verification of the predicted results with very long-term component tests or behaviour. This is an important point since size and geometry differences impose various degrees of constraint, which affects crack growth and initiation. Furthermore the development of residual stresses during fabrication and loading history which may be non-existent in small laboratory testing will need to be considered for components.

In addition it is clear from these assessment methods that the correct evaluation of the relevant fracture mechanics parameters, for which the lifetime prediction times are dependent upon, are extremely important.

The codes attempt to deal comprehensively with assessment and remaining life estimation procedures that can be used at the design stage and for in service situations. The Codes' approach allows the expert to make decisions based on predictions made using the methodology in relation to the operating circumstances of the component. The concept implies that the codes need to show they are both reliable and understandable over a range of material and loading conditions that may not have been previously examined or validated by the code developer. This is particularly important as new higher strength steels, which have little or no long-term material properties database, are developed or used by the power industry.

Further factors involved in the joint development of assessment codes and material data

Figure 2 highlights the importance of research in the improvement and extension of industrial codes. The trend in the development of the codes suggests that, in addition to verification of data between laboratory tests and component tests the following factors need to be considered

1. The available material property data for the analysis can be insufficient or crude and since they are usually taken from either historical data, results from different batches of material or tested in different laboratories with insufficient number of tests specimens they are likely to contain a large scatter.
2. The scatter and sensitivity in creep properties inherently produce a large variation in the calculations. Upper and lower bounds are therefore introduced which can give widely different life prediction results.
3. Improvements in the evaluation of the relevant parameters such as K, limit load concepts, reference stress $_{ref}$ and C^*. Use of 3D non-linear FE methods would help in this task.
4. The uses of short-term small laboratory data for use in long-term component life predictions further increases the possibilities of a wrong prediction. The relationship between short and long term behavior needs to be quantified.
5. Difficulty in ascertaining the level of crack tip constraint and multiaxiality effects in the component could reduce the accuracy of crack growth predictions Use of 3D FE modeling would assist in this task.
6. Unknowns in modeling the actual loading history, component system stresses and additional unknowns such as little or no knowledge of past service history, residual stresses also act as sources of error in predictions.
7. Non-destructive examination methods (NDE) of measuring defects in components, during operation and/or shutdown and insufficient crack measurement data during operation, are likely to add to errors involved in life-time assessment.
8. Probabilistic assessment of data and the predictions are required to deal with the material properties sensitivity to the models, test data scatter and unknowns in the parameters and predictive models.

Furthermore similarities of the approaches in the various codes do not necessarily imply that calculations by the different methods will give the same predictions. It may be possible that under certain controlled and validated circumstance the predictions can be optimized. It is clear that a critical comparison is only possible when the same method is used on another material and condition or the same test cases are examined by the different codes.

Validation of the methods in R5

Validation of the methods in R5 has been addressed in a number of different ways. These are briefly summarised below.

Validation of C calculations by comparisons with experiments on test specimens*

For test specimens, values of C* during a test are obtained from the measured load-line (or mouth opening) displacement rate and the measured crack length. These values have been compared with reference stress estimates of C* for a number of cases. Some of these results are set out in detail in R5 for 5 cases, as summarised in Tables 1,2.

Table 1-2: Summary of materials, geometries and dimensions for the validation tests

Case	Specimen type	Notes
1	CT	Thickness 12.5 and 25 mm
2	CT	Thickness 5-100mm; width 40-200 mm
3	CT	Thickness 5-50mm; width 40-100mm
4	CT	Various sizes
5	CT and DENT	Various sizes

Case	Material	Temperature
1	C-Mn weld	360 and 390°C
2	½ CrMoV (N&T)	565°C
3	½ CrMoV (Coarse grain bainite)	565°C
4	1 CrMoV	Various within the creep range
5	Type 316 stainless steel	600°C

To apply the reference stress method, instantaneous creep strain rates are required as a function of stress and accumulated creep strain. The materials considered include those for which the creep deformation data are adequately described by a steady state law and those requiring a more complete description of the primary stage.

Detailed results are given in R5. In summary, the examples of validation given above show that for a wide range of steels, plane stress reference stress estimates of C^* in CT specimens are conservative compared with experimental values.

Finite element validation of C* estimates obtained using reference stress techniques.

R5 presents comparisons of estimates of the C^* and C(t) parameters, obtained using reference stress techniques, with numerical solutions from detailed finite element analyses. The creep rates are described by a simple power law. The results demonstrate that the simplified reference stress methods result in good or conservative estimates of the crack tip parameter C(t) for a range of geometries (compact tension, single edge notch, centre cracked plate, externally circumferentially cracked cylinder) and loading types (pure mechanical, pure thermal, combined mechanical/thermal and displacement controlled loadings) for linear elastic/secondary creep behaviour.

Finite element analyses reported in the literature have also demonstrated accuracy for a range of creep laws for primary loading cases. More recently, finite element results to be reported shortly confirm the accuracy of the reference stress method for complex creep laws for complex loading (combined primary

loads and welding residual stress) involving stress relaxation. It has also been shown that an accurate estimate of an equivalent power-law exponent (n) is not needed to obtain an accurate estimate of the creep characterising parameter.

Features Tests

The R5 procedures have been applied to a number of features or component tests to demonstrate that they provide a conservative assessment of the observed creep or creep-fatigue crack growth. The results of some of these studies are summarised here.

The first example is a cyclically loaded wide plate of Type 316L(N) stainless steel with a semi-elliptical starter defect (a=7.9mm, c=43.6mm) tested at 650°C. The assessment was performed using best estimate, cast specific data throughout so that it should be expected that doing this will not necessarily produce a conservative answer, but should give a fairly accurate representation of the real, experimentally measured crack growth. The prediction in the through thickness direction was accurate and fell slightly on the conservative side. Predictions of crack growth along the surface were not so well predicted but use of bounding data, which are recommended for assessment purposes, gave conservative results for both the through thickness and surface crack growth directions.

Crack growth assessments have been carried out on a number of fatigue, creep and creep-fatigue crack growth tests in Type 347 weld material and Type 316H steel compact tension specimens at 650°C under displacement and load controlled creep, fatigue and creep-fatigue loading (with dwell periods of 24 and 192 hours). The predicted crack growth has been compared to that obtained experimentally. Based on the recommended fatigue and creep crack growth material data, conservative predictions of crack growth have been obtained.

Tests have been performed on a number of CMV vessels as summarised in the table 3 below. Some of these have extended to very long testing times (>50,000h). The failure mechanism (rupture or crack growth has been correctly identified and predicted using the R5 methods.

Table 4 below summarises austenitic features tests to which the crack growth procedures in R5 have been applied. Again, the procedures have been shown to be applicable and conservative.

Table 3:Summary of CMV vessel tests to which the crack growth procedures in R5 have been applied

TEST DESCRIPTION	CMV VESSEL TEST CONDITIONS					
	MATERIAL	STARTER CRACK(S)	TEMP. (C)	LOADING	DURATION (h)	DATA FORMAT
MEL Vessel FM1 R_i = 115mm t = 60mm	0.5CrMoV parent	Various circ. notches.	565	p = 62.5 MPa	1.6kh (total failure at site of deepest fully circ. notch)	Creep strain • Strain gauges • Notch CMOD Crack size • DCPD • Ultrasonics • Post test exam.
MEL Vessel FM2 R_i = 115mm t = 60mm	0.5CrMoV parent 2.25Cr1Mo welds (AW & SR)	Various defects spark machined in circ. welds (HAZ & Type IV zones).	565	p = 35 MPa	46kh (steam leak)	Creep strain • Creep pips • Strain gauges Crack size • Ultrasonics • Post test exam.
MEL Vessel FM2A R_i = 115mm t = 60mm	0.5CrMoV parent 2.25Cr1Mo welds (AW & SR)	Various defects spark machined in circ. welds (HAZ & Type IV zones).	565	p = 35 MPa	54kh (steam leak)	Creep strain • Creep pips • Strain gauges Crack size • Ultrasonics • Post test exam.

Table 4: Summary austenitic features tests to which the crack growth procedures in R5 have been applied

TEST DESCRIPTION	AUSTENITIC VESSEL AND FEATURES TEST CONDITIONS					
	MATERIAL	STARTER CRACK(S)	TEMP. (C)	LOADING	DURATION (h)	DATA FORMAT
BRITE 2147 Vessel 2 R_i = 75mm t = 40mm	316L(N) parent and welds (AW & SR)	Various defects spark machined in centre line of circ. welds	510-620	p = 63 MPa	11.5 kh (stopped – increase in hoop strain at SR weld but NDT did not reveal any cracking)	Creep strain • Creep pips • Strain gauges Crack size • Ultrasonics
Superheater Header R_i = 152.4mm T = 63.5mm r_i = 51.6mm t = 62.7mm (tapered)	316H parent and weld (AW) Ex-service	Reheat crack Max depth ~ 20mm	550	p = 18.8 MPa Nozzle end load = 15.4 kN Thermal Shocks (510-330C in 1h) every 500 h	8.8 kh + 17 thermal shocks (stopped)	Creep strain • Strain gauges Crack size • Ultrasonics • Post test exam.
Superheater Header Pressure Only R_i = 152.4mm T = 63.5mm r_i = 51.6mm t = 62.7mm (tapered)	316H parent and weld (AW) Ex-service	Reheat crack	550	p = 18.8 MPa	20 kh (planned)	Creep strain • Strain gauges Crack size • Ultrasonics • Post test exam.

Full scale tube feature test.	347 Casting 347 Weld 321 Tube	EDM in centre of weld	T_{min}=20 T_{max}=650 50 cycles:-transient 120 hr creep dwell 10 elastic cycles	6 khrs approx. (50 x 120 hrs)	Crack size • acpc • destructive examination

Acknowledgements: This document has made use of relevant information and data in procedures such as R6, R5, BS7910, FITNET and A16 to develop a common methodology for use in high temperature defect assessment procedures. Additional information has come from the ASTM E08, ESIS TC11 and previous VAMAS TWA 11, 19, 25 committees as well as from four European Union sponsored projects called

1. **'CCG in CMn', EU Project, 1993-1997, 'CCG in Carbon-Manganese at 320-400'**
2. **'HIDA', EU Project, 1996-2000, 'High Temperature Defect Assessment'**
3. **'LICON', EU Project, 1997-2001, 'Accelerated Test Methods for Advanced Steels'**
4. **'CRETE', EU Project 2001-2004, 'Creep Crack Growth Testing for an EU CoP'**

REFERENCES – Relevant International Standards and Codes

The following standards are useful references to this document. These documents can provide additional advice to the user on specific subjects. All standards are subject to revision, and parties to agreements based on this International Standard are encouraged to investigate the possibility of applying the most recent editions of the standards indicated below. Members of ASTM, BS, ESIS, IEC and ISO maintain registers of current valid version of these standards.

1. E 4 Practices for Force Verification of Testing Machines
2. E 74 Practice for Calibration of Force-Measuring Instruments for Verifying the Force Indication of Testing Machines
3. E 83 Practice for Verification and Classification of Extensometers
4. E 139 Practice for Conducting Creep, Creep-Rupture, and Stress-Rupture Tests of Metallic Materials
5. E 220 Method for Calibration of Thermocouples by Comparison Techniques
6. E 399 Test Method for Plane-Strain Fracture Toughness of Metallic Materials
7. E 647 Test Method for Measurements of Fatigue Crack Growth Rates
8. ASTM E 813 Standard Test Method for JIC, A Measure of Fracture Toughness
9. E 1457 Standard for Creep Crack growth Testing
10. E 1820 Standard Test Method for Measurement of Fracture Toughness
11. E 1823 Terminology Relating to Fracture Testing
12. British Energy Generation Ltd. Procedure R5 Issue 2, 2001.
13. British Standards- 7910: 1999, BSI, London, 1999.
14. ESIS Procedure for Determining the Fracture Behaviour of Materials, ESIS P2-92, 1992BS 0, A standard for standards, 1980
15. BS 160, Methods for load verification of testing machines, 1986
16. BS 3846, Methods for calibrating and grading of extensometers, 1970
17. BS 3500, Creep and rupture testing of metals, 1969.
18. BS 5500, Specification for unfired fusion welded pressure vessels
19. BS 5447 : 1977, Method of test for plane strain fracture toughness (K_{1c})of metallic materials
20. ISO 204, Metallic materials - Uninterrupted uniaxial creep testing in tension - Method of test
21. ISO/IEC Directives, Part 2, Rules for the structure and drafting of International Standards, 2001

22. ISO/IEC TR 10000-1, Information technology — Framework and taxonomy of International Standardized Profiles — Part 1: General principles and documentation framework
23. ISO 10241, International terminology standards — Preparation and layout
24. ISO 128-30, Technical drawings — General principles of presentation — Part 30: Basic conventions for views
25. ISO 128-34, Technical drawings — General principles of presentation — Part 34: Views on mechanical engineering drawings
26. ISO 128-40, Technical drawings — General principles of presentation — Part 40: Basic conventions for cuts and sections
27. ISO 128-44, Technical drawings — General principles of presentation — Part 44: Sections on mechanical engineering drawings
28. ISO 31 (all parts), Quantities and units
29. IEC 60027 (all parts), Letter symbols to be used in electrical technology
30. ISO 1000, SI units and recommendations for the use of their multiples and of certain other units
31. ISO 690, Documentation — Bibliographic references — Content, form and structure
32. ISO 690-2, Information and documentation — Bibliographic references — Part 2: Electronic documents or parts thereof ISO 204:1997, Metallic materials – Uninterrupted uniaxial creep testing in tension – Method of test.
33. ISO 12737:1996, Metallic materials – Determination of plane–strain fracture toughness.
34. ISO 7500-1:1986, Metallic materials – Verification of static uniaxial testing machines – Part 1: Tensile testing machines.
35. ISO 7500-2:1996, Metallic materials – Verification of static uniaxial testing machines – Part 2: Tensile creep testing machines – Verification of the applied load.
36. ISO 9513:1989, Metallic materials – Verification of extensometers used in uniaxial testing.

REFERENCES – Relevant Publications for further information

1. Nikbin, K. M., Webster, G. A., and Turner, C. E., "Relevance of Nonlinear Fracture Mechanics to Creep Cracking," Cracks and Fracture, ASTM STP 601, ASTM, 1976, pp. 47-62.
2. Landes, J. D. and Begley, J. A., "A Fracture Mechanics Approach to Creep Crack Growth," Mechanics of Crack Growth, ASTM STP 590, ASTM, 1976, pp. 128-148.
3. Saxena, A., "Evaluation of C* for the Characterization of Creep Crack Growth Behavior in 304 Stainless Steel," Fracture Mechanics: Twelfth Conference, 1980 ASTM STP 700, ASTM, pp. 131-151.
4. Saxena, A., "Creep Crack Growth under Non Steady-State Conditions," Fracture Mechanics: Seventeenth Volume, ASTM STP 905, ASTM, Philadelphia, 1986, pp. 185-201.
5. Hui, C.Y., "Steady-State Crack Growth in Elastic Power Law Creeping Materials", Elastic-Plastic Fracture, Vol. 1, ASTM STP 803, ASTM, Philadelphia, 1983, pp 573-593.
6. Riedel, H. and Rice, J. R., "Tensile Cracks in Creeping Solids," Fracture Mechanics: Twelfth Conference, ASTM STP 700, ASTM, 1980, pp. 112-130.
7. Bassani, J.L., Hawk, D.E. and Saxena, A., "Evaluation of the Parameter for Characterizing Creep Crack Growth Rate in the Transient Regime", Nonlinear Fracture Mechanics: Time-Dependent Fracture Mechanics, Vol. I, ASTM STP 995, ASTM, Philadelphia, 1989, pp 7-29.
8. Nikbin, K. M., Smith, D. J. and Webster, G. A., 'Prediction of Creep Crack Growth from Uniaxial Data'. Proceedings of the Royal Society of London, A396, 1984, pp. 183 – 197.
9. Webster, G.A. and Ainsworth, R.A., 'High Temperature Component Life Assessment'. Chapman and Hall, 1994.
10. Saxena, A., "Evaluation of Crack Tip Parameters for Characterizing Crack Growth: Results of the ASTM Round-Robin Program", Materials at High Temperatures, Vol.10, 1992, pp 79-91.
11. Schwalbe, K. H., Ainsworth, R. H., Saxena, A. and Yokobori, T., 'Recommendations for Modifications of ASTM E1457 to Include Creep-Brittle Materials', Engineering Fracture Mechanics, Vol. 62, 1999, pp123-142.
12. Saxena, A. and Yokobori, T. editors, "Crack Growth in Creep-Brittle Materials" special issue of Engineering Fracture Mechanics, Vol. 62, No.1, 1999.
13. Nikbin, K. M., Smith, D. J., and Webster, G. A., "An Engineering Approach to the Prediction of Creep Crack Growth," Journal of Engineering Materials and Technology, Trans. ASME, Vol. 108, 1986, pp. 186-191
14. Yokobori, A. T., Jr., Engineering Fracture Mechanics, 62, (1999), pp.61-78
15. Tabuchi, M., Kubo, K., Yagi, K., Yokobori, A.T., and Fuji, A., "Results of the Japanese Round-Robin on Creep Crack Growth Evaluation Methods for Ni-Base Superalloys, Engineering Fracture Mechanics, Vol. 62, 1999, pp 47-60.
16. Kwon, O., Nikbin, K. M., Webster, G. A., and Jata, K. V. "Crack Growth in the Presence of Limited Creep Deformation", Engineering Fracture Mechanics, Vol. 62, 1999, pp 33-46.
17. Fuji, A, Tabuchi, M, Yokobori, A. T., Jr., and Yokobori, T., Engineering Fract. Mechanics vol. 62, 1999, pp. 23-32.
18. Hall, D.E., McDowell, D.L. and Saxena, A., "Crack Tip Parameters for Creep-Brittle Crack Growth", Fatigue and Fracture of Engineering Materials and Structures, Vol. 21, 1998, pp 387-402.
19. Ainsworth, R. A., Fatigue and Fracture of Engineering Materials and Structures, Vol. 10, 1987, pp. 115- 127.
20. Winstone, M.R., Nikbin, K.M. and Webster, G.A., 'Modes of failure under creep/fatigue loading of a nickel-based superalloy'. J. Mat. Sci., 20, 1985, pp. 2471 – 2476.
21. Webster, G. A, Nikbin, K. M., Chorlton, M. R., Célard, N. J. C. and Ober, M. 'Comparison of High Temperature Defect Assessments Methods'; Material at High Temperature; Vol. 15: pp. 337-346, 1998.

22. Nikbin, K. M., 'Comparison between Crack Growth in Fracture Mechanics Specimens and Feature Component Tests Carried out in a Low Alloy Steel', ASME Pressure Vessels and Piping June 1998
23. Nikbin, K. M., 'Fatigue and Fracture', Section on 'Fracture and Fatigue', Published in the 'Encyclopaedia of Physical Sciences', USA, 2001.
24. Nikbin, K. M., Foreward, 'Creep Crack Growth in Components', Guest Editor, 'International Journal of Pressure Vessels and Piping, 2003 Elsevier Ltd., Volume 80, Issues 7-8, Pages 415-595 (July - August 2003)
25. Bettinson, A, Nikbin, K. M., N. O'Dowd, N, Webster, G. A., 'The influence of Constraint on Creep Crack Growth in 316H Stainless Steel', 'Structural Integrity in the 21st Century- The Lifetime of plant', Eds. J. H. Edwards et.al., Pub. EMAS. 219-22, Sept. Cambridge, pp. 149-159, 2000
26. B. Dogan, M. Horstmann, 'Laser Scanner Displacement Measurement at High Temperatures' , Int. J. Press. Ves. & Piping, Vol. 80, pp427-434, 2003
27. Nikbin, K. M., 'A unified approach to a European High Temperature Defect Assessment in High Temperature Plant', International Journal of Pressure Vessels and Piping, Volume 78, Issue 5, May 2001, pp. 33-50
28. Hutchinson, J.W., 'Singular Behaviour at the End of a Tensile Crack in a Hardening Material'. Journal of the Mechanics and Physics of Solids, 16, 1968, pp. 13 – 31.
29. P. J. Budden, 'Validation of the High-Temperature Structural Integrity Procedure R5 By Component Testing', Vol- 8-9, July, 2003.
30. British Energy (2003), 'R5 Assessment Procedure for the High Temperature Response of Structures'. Report R5, Issue 3 Nuclear Electric Ltd, UK.
31. British Energy, 'R6 Assessment of the Integrity of Structures Containing Defects'. Report R6, Revision 4, UK, with amendments (2009).
32. A16: 'Guide for Defect Assessment and Leak before Break Analysis'. Third Draft, Commissariat A L'Energie Atomique, 31/12/96.
33. B. Drubay, S.Marie, S.Chapuliot, Mh Lacire, 'A16: Guide for Defect Assessment at Elevated Temperature', Vol- 8-9, July, 2003.
34. BS7910,"Guide on Methods for Assessing the Acceptability of Flaws in Fusion Welded Structures", London, BSI, 2005.
35. API RP-579-Recommended Practice (RP) " standardized fitness-for-service assessment techniques for pressurized equipment used in the petrochemical industry' American Petroleum Inst. 2004
36. ASME Boiler & Pressure Vessel Code, Section XI, 1998.
37. AFCEN, 'Design and Construction Rules for Mechanical Components of FBR Nuclear Islands' RCC-MR, APPENDIX A16, AFCEN, Paris, 1985.
38. Wasmer, K., Nikbin, K. M. and Webster, G. A., 'Creep Crack Initiation and Growth in Thick Section Steel Pipes Under Internal Pressure', International Journal of Pressure Vessels and Piping, Volume 80, Issues 7-8, (July - August 2003), Pages 489-498.
39. Biglari, F., Nikbin, K.M., Goodall, I.W., Webster, G.A., `Determination of Fracture Mechanics Parameters J and C^* by Finite Element and $_{ref}$ Methods for a Semi-Elliptical Flaw in a Plate', Int. J. of Fracture, Vol- 8-9, July, 2003.
40. Wasmer, K., Davies, C. M., Nikbin, K, M., O'Dowd, N. P. and Webster, G. A., "A Sensitivity Study of Creep Initiation and Growth Prediction in Welded P22 Pipes", Paper presented at the 2nd International Conference on Integrity of High Temperature Welds, November 2003.
41. K. B. Yoon, T. G. Park and A. Saxena, 'Creep Crack Growth Analysis of Elliptical Surface Cracks in Pressure Vessels', Vol- 8-9, July, 2003.
42. B.Dogan and U.Ceyhan, "High Temperature Failure Assessment of Weldments", ECF16, due 3-7.7.2006, Alexandroupolis, Greece. Conf. Proc. CD, Track:2T26, Paper No. 585, pp.1-11.
43. ECCC Recommendations- Vol. 3 Part IV, (Issue 2), Testing Practices for Creep Crack Initiaiton, Ed. A. Klenk, 15.08.2005.

44. B. Dogan and K-H. Schwalbe: "Creep Crack Growth Behaviour of Ti-6242.",ASTM Symposium Proc. ASTM STP 1131,H.A.Ernst, A.Saxena and D.L.McDowell, Eds. Philadelphia,1992,pp.284-296.
45. B.Dogan, A.Saxena, K.-H.Schwalbe: "Creep Crack Growth in Creep-Brittle Ti-6242 Alloys", Materials at High Temperatures,Vol 10, No 2, May 1992,pp 138-143.
46. A.Saxena,B.Dogan and K.-H.Schwalbe: "Evaluation of the Relationship between C^*, $_5$ and $_t$ During Creep Crack Growth", Proc.ASTM 24th Symp. on Fracture Mechanics. ASTM-STP 1207, 1994, pp.510-526.
47. B.Dogan and B.Petrovski, 'Creep Crack Growth of High Temperature Weldments', Int.Journal of Pressure Vessels and Piping, Vol.78, 2001, pp.795-805.
48. B.Dogan and M. Horstmann, "Laser scanner displacement measurement at high temperatures", Int. Journal of Pressure Vessels and Piping, Vol.80, 2003, pp.427-434.
49. Yokobori, A.T. Jr., Yokobori, T, 'New Concept to Crack Growth at High Temperature Creep and Fatigue', Advances in Fracture Research, Proc., ICF7, Edds. K. Salama, K. Ravi-Chandar, D.M.R. Taplin and P.Rama Rao, Perbammon Press, Vol.12, 1989, 1723-1735
50. Tabuchi, M., Adachi, T., Yokobori, A.T., Jr., Fuji, A., Ha, J., Yokobori, T., 'Evaluation of Creep Crack Growth Properties using Circular Notch Specimens', Vol. 8-9, July 2003.
51. Yokobori Jr. AT, Uesugi T, Yokobori T, Fuji A, Kitagawa M, Yamaya I, Tabuchi M, Yagi K. Estimation of Creep Crack Growth rate in IN100 based on the *Q** Parameter Concept. Journal of Materials Science 1998, 33, 1555-1562.
52. Adachi, T., Yokobori,A.T.Jr., Tabuchi,M., Fuji,A, Yokobori,T and Nikbin,K., The Proposal of Q* Parameter and derivation of the Law of Creep Crack Growth Life for a round bar Specimen With a circular Notch for Cr-Mo-V Steel, Materials at High Temperatures, vol.21 (2004) 95.
53. Yokobori Jr. AT, Takamori S, Yokobori T, Hasegawa Y, Kubota K, Hidaka K. The characteristics of creep crack growth rate and life for W added 9-12Cr steels. Transaction of the Annual Meeting of the Japanese Society for Strength and Fracture of Materials 2000, 33, 11-16. (in Japanese)
54. Tan, M., Celard, N.J.C., Nikbin, K., Webster, G.A., 'Comparison of creep crack initiation and growth in four steels tested in HIDA', Int. J. PVP, pp 2001, 737-747
55. Newman, J.C. and Raju, I.S., 'An Empirical Stress Intensity Factor Eqn. for the Surface Crack'. Engineering Fracture Mechanics, 15, No. 1-2, pp. 185–192, 1981.
56. Rooke, D.P. and Cartwright, D.J., 'Compendium of Stress Intensity Factors' by. HMSO, London, 1976.
57. Zahoor, A., 'Closed Form Expressions for Fracture Mechanics Analysis of Cracked Pipes', Journal of Pressure Vessel Technology, 107, pp. 203 – 205, 1985.
58. Tada, H., 'Stress Analysis of Cracks Handbook'. Paris Productions Incorporated, 2nd edition, 1985.
59. Kumar, V., German, M.D. and Shih, C.F., 'Estimation Techniques for the Prediction of Elastic-Plastic Fracture of Structural Components of Nuclear Systems'. EPRI report SRD-80-094, EPRI, Palo Alto, CA, June 1981.
60. J. Baker, M. P. O'Donnell and D. W. Dean, 'Use of the R5 Volume 4/5 Procedures to Assess Creep-Fatigue Crack Growth in a 316L (N) Cracked Plate at 650^{o}C', Vol- 8-9, July, 2003.
61. C. M. Davies, N. P. O'Dowd, D. W. Dean+, K. M. Nikbin, R. A. Ainsworth, 'Failure Assessment Diagram Analysis of Creep Crack Initiation in 316H Stainless Steel', Vol- 8-9, July, 2003.
62. J. Fookes and D. J. Smith, 'The Influence of Plasticity in Creep Crack Growth in Steels', Vol- 8-9, July, 2003.
63. Davies, C., Nikbin, K. M., O'Dowd, N. P., 'Experimental Evaluation of the *J or C** Parameter for a Range of Cracked Geometries', ASTM STP 1480, to be published in the Int. J. of ASTM., Feb., 2006
64. Wasmer, K., Nikbin, K. M. and Webster, G. A. 'A Sensitivity Study of Creep Crack Growth in Pipes'; ASME 2002, Vancouver, 2002.
65. Yatomi, M., Nikbin, K. M., 'Life Management in Creep/Fatigue using Deterministic and Probabilistic Modelling', EPRI- int. Conf. on Advances in Life Assessment and Optimization of Fossil Power Plants, March 11-13, 2002, Orlando, Florida.

66. M. Yatomi, K. M. Nikbin, `Sensitivity analysis of Creep Crack Growth Prediction Using the Statistical Distribution of Uniaxial Data', HIDA3 Conf. Cambridge, Sept. 2004.
67. M. Yatomi, A. Nyilas, A. Portone, C. Sborchia, N. Mitchell, and K. Nikbin, Application of Probabilistic Fracture Mechanics in Structural Design of Magnet Components Parts Operating Under Cyclic Loads at Cryogenic Temperatures", Probabilistic Aspects of Life Prediction, ASTM STP 1450, W.S. Johnson and B.M. Hillberry, Eds., ASTM International, West Conshohocken, PA, 2003.
68. Nikbin, K. M., Yatomi, M., Wasmer, K. and Webster, G. A., 'Probabilistic Analysis of Creep Crack Initiation and Growth in Pipe Components', International Journal of Pressure Vessels and Piping, Elsevier Ltd., Volume 80, Issues 7-8, (July - August 2003), Pages 565-571.
69. Nikbin, K. M., Yatomi, M., Wasmer, K. and Webster, G. A., 'Comparison between Monte Carlo Simulation and Deterministic Method of Predicting Creep Crack Initiation and Growth in Pipe Components' Probabilistic Aspects of Life Prediction, ASTM STP 1450, W.S. Johnson and B.M. Hillberry, Eds., ASTM International, PA, 2003.
70. Yokobori, A.T., Jr, Yokobori, T.,'Comparative study on Characterisation Parameters for High Temperature Creep Crack Growth, with special emphasis on on dual value behaviour of crack growth rate', Eng. Fract. Mech., 55, 1966.
71. Haigh, J.R. and Richards, C.E., 'Yield Point Loads and Compliance Functions of Fracture Mechanics Specimens'. CERL RD/L/M461, June 1974.
72. Miller, A. G. Review of Limit Loads of Structures Containing Defects. International Journal of Pressure Vessel and Piping, 1988, 32, pp. 197-327.
73. Yun-Jae Kim, Do-Jun Shim, K. M. Nikbin, Young-Jin Kim, Seong-Sik Hwang And Joung-Soo Kim, 'FE Based Plastic Limit Loads For Cylinders With Part-Through Surface Cracks Under Combined Loading', Vol- 8-9, July, 2003.
74. Goodall, I. W. and Webster, G. A. 'Theoretical Determination of Reference Stress for Partially Penetrating Flaws in Plates'; International Journal of Pressure Vessels and Piping; Vol. 78:pp. 687-695, 2001.
75. B.Dogan, U.Ceyhan, K.M.Nikbin, B.Petrovski and D.W.Dean, "European Code of Practice for Creep Crack Initiation and Growth Testing of Industrially Relevant Specimens", Journal of ASTM International, February 2006, Vol. 3, No. 2, Paper ID JAI13223. Available online at www.astm.org , Published in ASTM STP 1480, 2007.
76. N. O'Dowd, C. Davies, K. Nikbin, ` Validation of the Experimental Evaluation of the C* parameter for a range of Crack Geometries`, Fifth Int. ASTM/ESIS Symp. on Fatigue and Fracture Mechanics, Journal of ASTM International, February 2006, Vol. 3, No. 2, Available online at www.astm.org, Published in ASTM STP 1480, 2007.
77. A.T. Yokobori Jr., T. Yokobori and T. Yamaoku, 'An alternative Correlating Parameter for Creep Crack Growth and its Application': Derivation of *Q**, Materials at High Temp., Vol. 10, (1992), 108, ERRATA, 10(1992) 224.
78. Yokobori,A.T.Jr., Yokobori,T, Kuriyama,T and Kakō,T., Advances in Fracture Research, Proc. of the 6th ICF (1984) 2181. Eds. S.R.Valluri et.al. Pergamon Press "RNOD concept for Crack Initiation in High Temperature Time Dependent Fracture"
79. Yokobori,A.T.Jr. and Yokobori,T, "A New Concept on High Temperature Creep Crack Initiation, Growth and Creep Fracture Life", Creep and Fracture of Engineering Materials and Structures, Proc. of the fifth Int. Conf. Eds B.Wilshire and R.W.Evans. 1993, p.81
80. R.Piques, Ph.Bensussan and A.Pineau, Proc. Mechamet, Int. Seminar on High Temperature Fracture Mechanisms and Mechanics, Eds. Bensussan. P et al., 1987, pp.53-70
81. R A Ainsworth, Some observations on creep crack growth, Int J Fracture **20**, 147-159 (1982).
82. R A Ainsworth, The initiation of creep crack growth, Int J Solids Structures **18**, 873-881 (1982).
83. R A Ainsworth and I W Goodall, Defect assessments at elevated temperature, ASME J Pres Ves Tech **105**, 263-268 (1983).

84. R A Ainsworth, The assessment of defects in structures of strain hardening material, Engng Fract Mech **19**, 633-642 (1984).
85. R A Ainsworth and M C Coleman, Example of an application of an assessment procedure for defects in plant operating in the creep range, Fatigue Fract Engng Mater Struct **10**, 129-140 (1987).
86. R A Ainsworth and P J Budden, Crack tip fields under non-steady creep conditions- I. estimates of the amplitude of the fields, Fatigue Fract Engng Mater Struct **13** (3), 263-276 (1990).
87. R A Ainsworth and P J Budden, Crack tip fields under non-steady creep conditions- II. estimates of associated crack growth, Fatigue Fract Engng Mater Struct **13** (3), 277-285 (1990).
88. R A Ainsworth, The use of a failure assessment diagram for initiation and propagation of defects at high temperatures, Fatigue Fract Engng Mater Struct **16**, 1091-1108 (1993).
89. R A Ainsworth, R5 procedures for assessing structural integrity of components under creep and creep-fatigue conditions, Int Materials Reviews **51** (2), 107-126 (2006).

APPENDIX A

♦ European Collaborative Round Robin Uniaxial Data - Analyses and Results

In this appendix information and data from the following EU projects that could be relevant to R5 analysis are presented. The projects are as follows

- Project HIDA (High-Temperature Defect Assessment), 1996-2000
- HIDA applicability G1RD-CT-2002-00730 Probabilistic and Sensitivity of Crack Assessment in High Temperature Plant and Applicability of HIDA Procedure 2002-2005
- LICON (Life Conditioning methods in advanced steels), (1998-2002)
- CRETE' (Creep crack growth standardisation in Industrial specimens), CRETE (2000-2003)
- International collaborative programme; Versailles Agreement for Advanced Materials and Standards (VAMAS) Technical Working Area (TW25, TWA31) covering Creep/fatigue crack growth of components in parent and welded materials.

Data analysis for the laboratory uniaxial tests on the HIDA materials

Uniaxial data analysis

The stress and temperature dependence during the secondary stage of creep curve is considered. Minimum strain rate, also known as steady state or secondary creep rate, is defined as the lowest value of strain rate under constant load uniaxial test as seen from Figure A1 below:

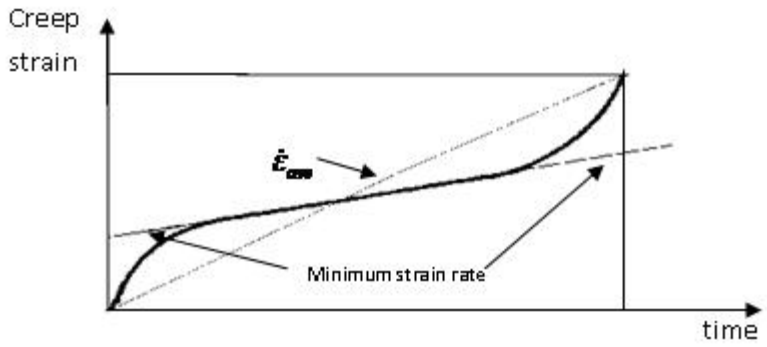

Figure A1: Schematic figure of the time v strain in creep uniaxial tests.

It is usually expressed as a function of stress when temperature is constant and its mathematical derivation is represented by the Norton's law equation as:

$$\dot{\varepsilon}_{\min} = A_{\min}\sigma^{n_{\min}} \qquad \text{(A1)}$$

where A_{min} and n_{min} are material constants at a specific temperature.

In cases where secondary data does not exist an average creep rate is used such as

$$\dot{\varepsilon}_{ave} = A_{ave}\sigma^{n_{ave}} \qquad \text{(A2)}$$

When the average creep strain rate $\dot{\varepsilon}_{ave}$ is introduced then the results take into account the three stages of creep. It can be calculated from the rupture strain ε_f and the rupture time t_r as following:

$$\dot{\varepsilon}_{ave} = \frac{\varepsilon_f}{t_r} \qquad \text{(A3)}$$

which enables the creep law to be written as:

$$\dot{\varepsilon}_{ave} = \dot{\varepsilon}_{0ave}\left(\frac{\sigma}{\sigma_0}\right)^{n_{ave}} = A_{ave}\sigma^{n_{ave}} \qquad \text{(A4)}$$

where again, A_{ave}, n_{ave}, σ_0 and $\dot{\varepsilon}_0$ (at 1/hour) are material constants at a specific temperature. The results were obtained indirectly by using the 'ZRATE' data analysis program. These properties can be found in Tables later in the text.

The choice of an "average creep rate" proposed here can certainly not be taken as a seriously defined parameter. The only reason for using this choice is when strain data is lacking. This becomes fully understandable when one knows that the bulk of historical creep tests were pure stress rupture tests which only reported stress, temperature, rupture time and rupture elongation (determined "post-mortem"). The whole scatter of rupture elongation fully affects the average creep rate which tells something about the quality of such a parameter. In contrast to our ongoing discussion concerning "steady state" or "minimum" creep rates and the validity of the Norton law the average creep rate approach is must be used with caution.

The rupture time is expressed as a function of stress at constant temperature:

$$t_r = \frac{\varepsilon_{f0}}{\dot{\varepsilon}_0}\left(\frac{\sigma_0}{\sigma}\right)^{\nu} \qquad \text{(A5)}$$

where ε_{f0} is the uniaxial creep rupture strain at stress σ_0. The constant ν, is a material constant that can be obtained when rupture times are plotted on a log-log scale. By using thereafter a power law fit, the slope of the line is equal to the $-1/\nu$, as seen in the figure below:

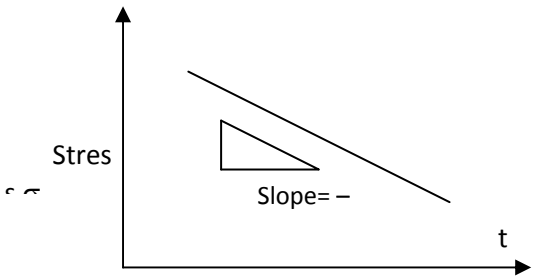

Figure A2: Variation of stress against time at constant temperature for uniaxial tests

The values of ν obtained from the different tests are also tabulated later in the main text. Finally, the average ductility ε_f for each material was obtained by averaging rupture strains at different stresses. Details of plots of the data received from different institutions were shown in figures.

Results

The uniaxial creep data of the following materials are analysed:

- P22 base metal with longitudinal orientation
- P22 base metal service exposed with circumferential orientation
- P22 service exposed material weld with cavities
- P22 service exposed weld without cavities
- P22 service exposed parent material
- P91 base metal with longitudinal orientation
- P91 base metal with circumferential orientation
- P91 cross weld metal with longitudinal orientation
- 316L(N) stainless steel base material
- 1CrMoV cast base material
- 1CrMoV forged base material

Materials

Figure A3 shows the type and pedigree of the materials tested. Table A1 shows the material composition for the parent material and Table A2 shows the room temperature uniaxial properties of the four parent material. Tables A3-A8 show the uniaxial results for the above materials. It should be noted that the results are derived from limited numbers of tests and the statistical analysis identifies the level of variability in the test results. Below is a description of the individual materials tested in the programmes.

P22 material

Two institutions (ENEL, SIMR) performed a series of uniaxial tests on the $2^{1/4}$Cr1Mo steel (P22). New materials as well as service exposed were used for testing purposes: a seamless pipe of ASTM A335 (216 mm outer diameter, 50 mm thickness) was purchased for the manufacture of laboratory test specimens. To prepare the weld specimens, appropriate pieces were welded longitudinally and circumferentially according to the test geometry specified and by using the same welding procedures at every instance. On the other hand, to assess the properties of material subjected to service exposure, creep specimens were taken from a T-shape piece, which had been in service for 110,000hrs at 530 ^{o}C and 60MPa hoop stress.

P91 Material

Data received from EDF were used to obtain the creep properties of P91 steel. Base metal specimens together with cross welded ones, were tested in order to investigate the material's behavior. The base metal specimens were manufactured from a P91 pipe (295 mm in outer diameter, 55mm wall thickness and 12m long) which was bought from Mannesman (Germany) in accordance with the specifications set in ASTM A 335 for pipes.

Once again, the orientation of the specimen had no effect in both 'minimum strain rate vs stress' and 'stress to rupture' graphs. However, the cross welded material appears to creep faster than the base one by a factor of 6 due to reduced ductility following the welding process. In addition, the drop in strength on the welded material may arise from the high composition in Chromium, which in turn leads to worse weldability compared to the low alloy steels.

In conclusion, it can be stated that the base metal is very close to the mean value for grade 91 steel and although the filler metal seems to be weaker, it is also within the ECCC scatted-band.

1CrMoV Material

Two types of 1%Cr MoV were examined in Germany by MPA and SPG. Both materials were parent metals and the only difference between them, was the way in which they were produced. Thus, 1CrMoV cast steel together with 1CrMoV forged steel were used for experimental purposes:

316(LN) Stainless Steel Material

Stainless steel 316L(N) parent metal was tested at Imperial College and the results obtained were used to compare different batches of the above material. A single geometry was tested and the 'minimum strain rate vs stress' and 'stress vs time to rupture' graphs were used to derive the properties. The creep curves of the tests performed show no special features and they exhibit all the three stages for a typical creep curve. The 316L(N) batch SD tested at IC creeps faster than the other batches by a factor of 1.4 to 2. However the stress to rupture correlation for all batches is very close. After the end of the experimental stage, a comparison of creep ductility with other batches was made and some important characteristics were revealed:

- multiple necking was observed in the specimens and it can be justified by the fact that the specimen was uniformly heated along its gauge length.
- An oxide layer was observed along the length of the specimen
- and the reduction of area at the point of fracture was approximately 60%

Comparison of the HIDA Materials at their typical operating temperature range

Although the testing temperature varies in the different alloys an attempt to compare uniaxial properties of all five materials is made in this section. Although, they are not tested at the same temperatures and their geometries are not similar, a comparison, as to their behavior, can still be obtained. Initially, the creep exponent and average failure ductility's of the different base materials range from 8-12 and the creep ductility's range from 20-60%.

For the stress to rupture graphs again the 1CrMoV steels appear to have good strength characteristics at its operating temperature with the forged type showing higher strength compared to the cast material. The 316L(N) stainless steel also shows good strength at 650 ^{o}C whereas the P91 and P22 steels seem to have similar strengths at their operating temperatures.

With respect to the welded materials, data for P91 and P22 steels were received and the comparison was made between these two. The new material creeps at comparatively lower rates than the other materials whereas the service exposed creeps much faster. Finally, the stress to rupture of cross weld specimens are stronger that the specimens of P91. This can be explained by the fact that P91 high alloy steels exhibit medium weldability due to the high content in Chromium, in contrast with P22 steels which show excellent welding characteristics.

Figure A3(a): P22 - material A tested at 565 ^{o}C

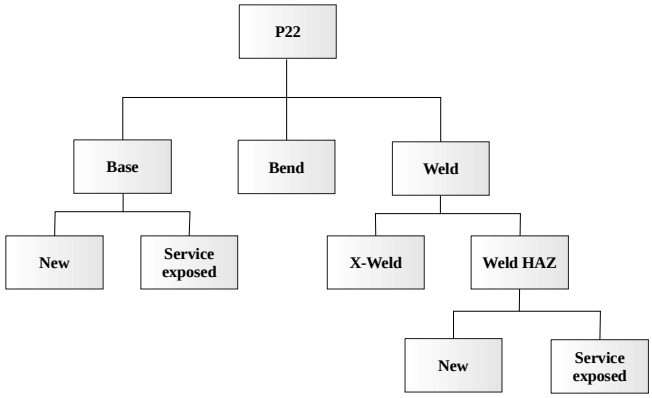

Figure A3(b): 316 L(N) - material B tested at 650 ^{o}C

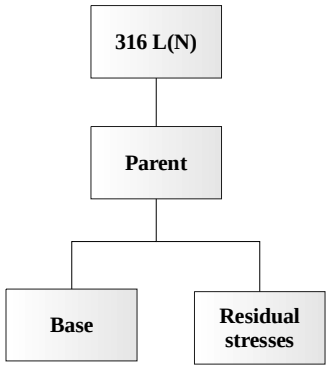

Figure A3(c): P91 - material C tested at 625 ^{o}C

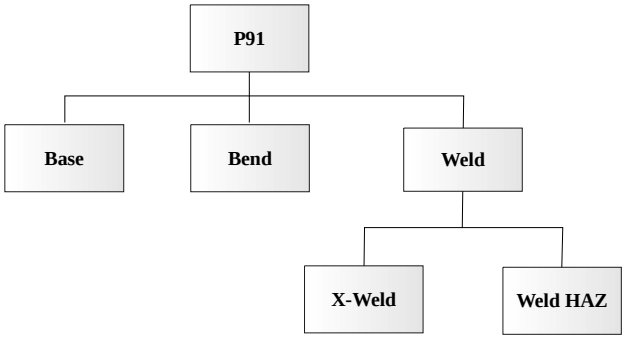

Figure A3(d): 1CrMoV - material D tested at 530 ^{o}C

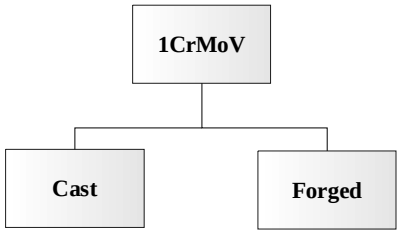

Figure A3: Categories of material conditions tested in HIDA

Table A1(a): Chemical composition Material A - P22

	C	Mn	Si	S	P	Cr	Ni	Mo	V	N	Al
P22	0.1 01	0.443	0.206	0.015	0.024	2.070	0.099	0.939	0.180	0.013	<0.01

Table A1(b): Material B - 316 L(N) batch SD

C	Mn	Si	S	P	Cr	Ni	Mo	Ti	Nb	N	Cu
0.038	1.830	0.313	0.02	0.036	17.3	11.9	2.46	<0.01	<0.01	0.067	0.27

Table A1(c): Material C - P91

	C	Mn	Si	S	P	Cr	Ni	Mo	V	Cu	N	Al
P91	0.091	0.409	0.369	0.013	0.028	8.440	0.270	0.920	0.240	0.040	0.038	0.070

Table A1(d):Material D - 1CrMoV

	C	Mn	Si	S	P	Cr	Ni	Mo	V	Ti	Cu	Al
Cast	0.158	0.660	0.398	0.004	0.007	1.370	0.280	1.030	0.237	0.029	0.060	<0.005
Forged	0.290	0.390	0.318	0.002	0.007	1.760	0.300	1.130	0.294	0.014	0.070	<0.005

Table A2: Room temperature properties monotonic tensile tests

Material (parent)	Orientation	Young's modulus GPa	0.2% yield point MPa	UTS MPa	R.A.
A	L	218	349	558	20
	T-L	213	352	557	22
B					
C	L	245	538	688	19
	T-L	237	539	687	19
D_ca	L	198	504	636	17
	T-L	225	502	636	16
D_fo	L	217	653	794	16
	T-L	387	654	792	15

Table A3: Uniaxial material properties for HIDA materials

Material	Type	Material Condition	Orientation	Temp. ^oC	A_{min}	σ_{omin}	n_{min}	A_{ave}	$\sigma_{o\ ave}$	n_{ave}	σ/rupture Constant	ν	ε_f	Red. of Area *RA*
P91	Base	New	cr	625	5E-23	391.9	8.6	1E-29	247.0	12.1	288.1	7.8	0.19	0.68
P91	Base	New	ln	625	6E-23	411.5	8.5	1E-25	279.4	10.2	283.3	8.6	0.21	0.79
P91	Bend	New	n/a	625	1E-31	253.0	12.9	2E-34	198.2	14.7	218.9	11.5	0.32	0.55
P91	wm	New	n/a	625	5E-28	260.6	11.3	4E-29	179.4	12.6	442.3	18.0	0.15	0.70
P91	XW	New	n/a	625	4E-19	463.8	6.9	8E-17	534.9	5.9	117.2	18.9	0.03	0.19
P22	Base	New	ln	565	3E-27	302.8	10.69	2E-24	290.7	9.6	269.0	9.2	0.31	0.66
P22	Base	New	cr	565	1E-25	318.1	9.99	2E-24	280.7	9.7	317.3	8.4	0.32	0.64
P22	Base	XS	n/a	565	2E-23	259.9	9.4	4E-20	246.5	8.1	253.8	10.0	0.48	0.89
P22	Bend	New	n/a	565	6E-37	217.2	15.5	4E-32	211.7	13.5	235.9	7.8	0.49	0.89
P22	wm	New	N/a	565	2e-35	260.6	14.4	5e-29	250.3	11.8	196.3	10.0	0.22	0.76
P22	wwc	XS	n/a	565	9E-14	1063.8	4.31	8E-14	877.3	4.5	0.0	0.0	0.07	0.08
P22	wwoc	XS	n/a	565	2E-37	147.1	16.93	3E-40	134.4	18.6	395.7	5.0	0.07	0.12
P22	XW	New	n/a	565	3E-27	308.5	10.65	4E-26	306.4	10.2	159.7	10.9	0.02	0.19
1CrMoV_ca	Cast	New	n/a	530	2E-23	910.9	7.67	6E-31	440.6	11.4	202.9	11.0	0.12	0.66
1CrMoV_fo	Forged	New	n/a	530	1E-34	652.5	12.08	2E-30	552.4	10.8	429.4	9.4	0.18	0.70
316L(N)	Base	New	n/a	650	9E-24	436.3	8.73	2E-22	383.0	8.4	298.6	7.4	0.60	0.64

σ/rupture Constant taken at t=1h

XW = cross weld

n/a= not applicable

bs=base material

ln =longitudinal direction

cr= circumferential direction

cs=cast

fo = forged

wwc= weld with cavity

wwoc= weld without cavities

XS=ex-service

Uniaxial Test Tables and Results

Uniaxial Test Matrices and Results

Given below are the tables of uniaxial test matrices performed under the HIDA and LICON projects by the different partners. The tests conditions and global results are contained in these tables.

Notation:

Instit. : Institution which carried out the test
Temp. : Temperature
σ_{net} : Net section stress
$\dot{\varepsilon}_s$: Secondary or minimum strain rate
$\dot{\varepsilon}_{Ave}$: Average strain rate
ε_f : Creep failure strain
R. A. : Reduction of area at failure

Table A-4: Uniaxial results for 316L(N)

Project	Insist.	Test name	Material condition	Gauge diameter [mm]	Gauge length [mm]	Temp. [°C]	σ_{net} [MPa]	Test duration [h]	$\dot{\varepsilon}_s$ [h^{-1}]	$\dot{\varepsilon}_{Ave}$ [h^{-1}]	ε_f [%]	R.A. [%]	Status
HIDA	IC	CR1	PM	7.89	33.60	650	190	373.0	6.04E-04	1.55E-03	57.63	61.10	Failed
HIDA	IC	CR2	PM	7.95	33.60	650	153	1562.0	9.19E-05	3.33E-04	52.00	59.30	Failed
HIDA	IC	CR3	PM	7.89	33.60	650	190	28.0	6.12E-04	-	-	-	Stopped
HIDA	IC	CR4	PM	7.89	33.60	650	170	277.5	2.62E-04	-	-	-	Stopped
HIDA	IC	CR5	PM	7.89	33.60	650	210	105.5	2.00E-03	6.06E-03	63.90	70.20	Failed
HIDA	IC	CR7	PM	7.89	33.60	650	160	935.8	2.03E-04	6.31E-04	59.06	62.10	Failed
HIDA	IC	CR8	PM	7.89	33.60	650	170	900.7	1.79E-04	7.39E-04	66.61	68.70	Failed

Table A-5: Uniaxial results for P22

Project	Insist.	Test name	Material condition	Gauge diameter [mm]	Gauge length [mm]	Temp. [°C]	σ_{net} [MPa]	Test duration [h]	$\dot{\varepsilon}_s$ [h^{-1}]	$\dot{\varepsilon}_{Ave}$ [h^{-1}]	ε_f [%]	R.A. [%]	Status
HIDA	ENEL	6365-1L	PM	8.00	33.58	565	160	141.2	8.22E-04	2.58E-03	36.38	81.34	Failed
HIDA	ENEL	6366-1C	PM	8.00	33.55	565	160	98.1	1.49E-03	4.56E-03	44.69	83.24	Failed
HIDA	ENEL	6367-1C	PM	8.00	33.58	565	120	2058.0	4.97E-05	1.47E-04	30.32	54.34	Failed
HIDA	ENEL	6368-2L	PM	8.00	33.65	565	120	1424.0	7.95E-05	2.72E-04	38.73	72.44	Failed
HIDA	ENEL	7010-3C	PM	6.99	33.52	565	105	6277.4	7.77E-06	3.09E-05	19.42	54.60	Failed
HIDA	ENEL	7013-3L	PM	6.99	33.52	565	95	11212.2	2.89E-06	2.17E-05	24.32	52.81	Failed
HIDA	ENEL	7014-4L	PM	6.97	33.53	565	110	4640.3	1.37E-05	5.46E-05	25.35	56.10	Failed
HIDA	ENEL	H10	WM	6.99	34.73	565	120	1509.0	2.19E-05	1.78E-04	26.86	82.31	Failed
HIDA	ENEL	H11	WM	7.00	34.73	565	110	2938.0	6.35E-06	5.71E-05	16.78	68.96	Failed
HIDA	ENEL	H6	XW	7.00	33.78	565	85	6726.5	1.79E-06	2.99E-06	2.01	17.97	Failed
HIDA	ENEL	H7	XW	6.99	33.78	565	100	2998.3	4.59E-06	6.91E-06	2.07	19.28	Failed
HIDA	ENEL	H8	XW	6.99	34.53	565	100	3757.0	6.33E-06	1.65E-05	6.18	36.05	Failed
HIDA	ENEL	H9	XW	7.00	33.53	565	120	931.0	4.34E-05	8.66E-05	8.06	28.24	Failed

Table A-6: Uniaxial results for E911

Project	Insist.	Test name	Material condition	Gauge diameter [mm]	Gauge length [mm]	Temp. [°C]	σ_{net} [MPa]	Test duration [h]	$\dot{\varepsilon}_s$ [h^{-1}]	$\dot{\varepsilon}_{Ave}$ [h^{-1}]	ε_f [%]	R.A. [%]	Status
LICON	MFI	SE1	HAZ	6.00	60.00	625	125	1052.0	2.67E-05	2.76E-04	29.00	88.60	Failed
LICON	MFI	SE2	HAZ	6.00	60.00	625	110	2544.0	1.02E-05	1.26E-04	32.10	80.50	Failed
LICON	MFI	SE3	HAZ	6.00	60.00	650	95	504.0	1.29E-04	7.66E-04	38.60	87.90	Failed
LICON	MFI	SE4	HAZ	6.00	60.00	650	83	770.0	5.54E-05	5.56E-04	42.80	84.80	Failed
LICON	MFI	SE5	HAZ	6.00	60.00	650	83	–	–	–	3.00	–	Stopped
LICON	MFI	SE6	HAZ	6.00	60.00	650	83	–	–	–	2.50	–	Stopped
LICON	MFI	SE7	HAZ	6.00	60.00	650	83	–	–	–	2.00	–	Stopped
LICON	MFI	SE8	HAZ	6.00	60.00	650	83	–	–	–	1.00	–	Stopped
LICON	LE	16342	PM	6.00	30.0	680	75	2260.0	1.55E-06	7.04E-05	15.90	42.00	Failed
LICON	LE	16343	PM	6.00	30.0	700	75	521.0	3.46E-05	5.34E-04	27.80	73.00	Failed
LICON	LE	16344	PM	6.00	30.0	710	75	146.0	2.68E-04	1.71E-03	24.90	86.00	Failed
LICON	LE	16345	PM	6.00	30.0	670	75	2299.0	6.19E-07	9.48E-05	21.80	73.00	Failed
LICON	LE	16346	PM	6.00	30.0	690	75	1869.0	1.64E-05	1.15E-04	21.40	45.00	Failed
LICON	MFI	E1	PM	6.00	30.0	650	110	1616.0	2.55E-05	1.02E-04	16.48	59.30	Failed
LICON	MFI	E2	PM	6.00	30.0	650	95	5703.0	6.62E-06	1.73E-05	9.84	23.30	Failed
LICON	MFI	E3	PM	6.00	30.0	650	83	6812.0	6.49E-06	2.00E-05	13.62	31.80	Failed
LICON	MFI	E4	PM	6.00	30.0	625	110	13190.0	–	4.70E-06	6.20	14.30	Failed
LICON	MFI	E5	PM	6.00	30.0	650	83	–	–	–	2.50	–	Stopped
LICON	MFI	E6	PM	6.00	30.0	650	83	–	–	–	3.00	–	Stopped
LICON	MFI	E7	PM	6.00	30.0	650	83	–	–	–	2.00	–	Stopped
LICON	MFI	E8	PM	6.00	30.0	650	83	–	–	–	1.00	–	Stopped
LICON	MFI	E9	PM	6.00	30.0	625	140	1865.0	2.21E-05	1.23E-04	23.00	79.40	Failed
LICON	MFI	E10	PM	6.00	30.0	625	125	2151.0	1.37E-05	8.51E-05	18.30	79.60	Failed
LICON	MFI	E11	PM	6.00	30.0	625	150	532.0	6.35E-05	4.46E-04	23.73	86.30	Failed
LICON	MFI	E12	PM	6.00	30.0	650	120	256.0	2.35E-04	9.14E-04	23.40	86.00	Failed
LICON	LE	16393	XW	6.00	60.00	680	75	13.0	N/A	3.08E-03	4.00	81.00	Failed
LICON	LE	16394	XW	6.00	60.00	660	75	322.0	N/A	1.12E-04	3.60	47.00	Failed
LICON	LE	16395	XW	6.00	60.00	670	75	192.0	N/A	8.33E-05	1.60	59.00	Failed
LICON	LE	16396	XW	6.00	60.00	650	75	406.0	N/A	1.31E-04	5.30	32.00	Failed
LICON	LE	16398	XW	6.00	60.00	645	75	2011.0	N/A	N/A	N/A	N/A	Failed
LICON	MBEL	98-035	WM	6.00	60.00	625	145	773.0	N/A	1.31E-04	10.10	22.00	Failed
LICON	MBEL	98-033	WM	6.00	60.00	625	135	1671.0	N/A	5.15E-05	8.60	24.00	Failed
LICON	MFI	LIE1	XW	6.00	60.00	625	150	431.0	N/A	2.04E-04	8.80	36.00	Failed
LICON	MFI	LIE2	XW	6.00	60.00	625	110	2898.0	N/A	9.32E-06	2.70	10.00	Failed
LICON	MFI	LIE3	XW	6.00	60.00	650	120	165.0	N/A	8.36E-04	13.80	58.00	Failed
LICON	MFI	LIE4	XW	6.00	60.00	650	83	897.0	N/A	5.57E-05	5.00	17.00	Failed
LICON	MFI	LIE5	XW	6.00	60.00	625	140	752.0	N/A	7.98E-05	6.00	24.00	Failed
LICON	MFI	LIE6	XW	6.00	60.00	625	125	1007.0	N/A	4.37E-05	4.40	14.00	Failed
LICON	MFI	LIE7	XW	6.00	60.00	650	110	233.0	N/A	3.09E-04	7.20	32.00	Failed
LICON	MFI	LIE8	XW	6.00	60.00	650	95	595.0	N/A	8.40E-05	5.00	22.00	Failed

Table A-7: Uniaxial results for P91

Project	Insist.	Test name	Material condition	Gauge diameter [mm]	Gauge length [mm]	Temp. [°C]	σ_{net} [MPa]	Test duration [h]	$\dot{\varepsilon}_s$ [h^{-1}]	$\dot{\varepsilon}_{Ave}$ [h^{-1}]	ε_f [%]	R.A. [%]	Status
LICON	MFI	SP1	HAZ	N/A	N/A	600	135	110.0	7.21E-04	3.07E-03	33.80	92.80	Failed
LICON	MFI	SP2	HAZ	N/A	N/A	600	120	270.0	2.71E-04	1.15E-03	31.10	92.30	Failed
LICON	MFI	SP3	HAZ	N/A	N/A	625	97	121.0	9.40E-03	4.07E-03	49.20	94.00	Failed
LICON	MFI	SP4	HAZ	N/A	N/A	625	85	489.0	1.85E-03	8.59E-04	42.00	92.30	Failed
LICON	MFI	SP5	HAZ	N/A	N/A	625	85	53.0	–	–	2.00	–	Stopped
LICON	MFI	SP6	HAZ	N/A	N/A	625	85	55.0	–	–	2.50	–	Stopped
LICON	MFI	SP7	HAZ	N/A	N/A	625	85	24.0	–	–	1.50	–	Stopped
LICON	MFI	SP8	HAZ	N/A	N/A	625	85	25.0	–	–	1.00	–	Stopped
HIDA	EdF	1545	PM	7.95	36.01	625	120	907.4	3.83E-05	1.76E-04	15.95	75.00	Failed
HIDA	EdF	1546	PM	7.95	36.13	625	120	916.2	3.52E-05	1.51E-04	13.77	68.00	Failed
HIDA	EdF	1547	PM	7.95	35.96	625	120	878.0	4.11E-05	1.92E-04	16.90	80.00	Failed
HIDA	EdF	1548	PM	7.95	36.14	625	120	791.6	4.11E-05	1.33E-04	10.50	84.00	Failed
HIDA	EdF	1549	PM	7.95	36.08	625	110	1826.4	1.58E-05	7.49E-05	13.69	73.00	Failed
HIDA	EdF	1573	PM	7.95	36.02	625	100	3831.2	7.87E-06	2.54E-05	9.75	40.00	Failed
HIDA	EdF	1574	PM	7.95	36.04	625	100	3765.2	7.49E-06	1.93E-05	7.26	18.00	Failed
HIDA	EdF	1575	PM	7.95	36.02	625	110	1666.2	1.48E-05	7.53E-05	12.55	61.00	Failed
HIDA	EdF	1702	PM	7.95	36.06	625	90	6972.1	3.76E-06	9.26E-06	6.46	N/A	Failed
LICON	LE	16350	PM	N/A	N/A	680	75	1928.0	1.13E-05	3.01E-05	5.80	31.00	Failed
LICON	LE	16351	PM	N/A	N/A	700	75	112.0	2.10E-03	2.10E-03	23.50	93.00	Failed
LICON	LE	16352	PM	N/A	N/A	710	75	32.0	1.12E-04	8.19E-03	26.20	95.00	Failed
LICON	LE	16354	PM	N/A	N/A	675	75	1131.0	3.05E-05	1.13E-04	12.80	48.00	Failed
LICON	LE	16355	PM	N/A	N/A	690	75	194.0	1.65E-04	1.69E-03	32.70	90.00	Failed
LICON	LE	16356	PM	N/A	N/A	665	75	1066.0	1.70E-05	2.60E-04	27.70	71.00	Failed
LICON	MFI	P1	PM	N/A	N/A	600	120	4361.0	5.96E-06	2.62E-05	11.42	50.60	Failed
LICON	MFI	P2	PM	N/A	N/A	625	85	9857.0	N/A	7.81E-06	7.70	20.30	Failed
LICON	MFI	P3	PM	N/A	N/A	625	85	7146.0	–	–	2.50	–	Stopped
LICON	MFI	P5	PM	N/A	N/A	600	150	417.0	1.03E-04	5.20E-04	21.67	89.40	Failed
LICON	MFI	P6	PM	N/A	N/A	600	135	2945.0	1.12E-05	8.00E-05	23.56	80.50	Failed
LICON	MFI	P7	PM	N/A	N/A	625	120	303.0	1.57E-04	9.45E-04	28.63	90.20	Failed
LICON	MFI	P8	PM	N/A	N/A	625	105	1672.0	2.41E-05	1.10E-04	18.47	60.50	Failed
LICON	MFI	P9	PM	N/A	N/A	600	145	817.0	5.63E-05	2.80E-04	22.87	77.80	Failed
LICON	MFI	P10	PM	N/A	N/A	625	97	3556.0	9.63E-06	5.38E-05	19.13	54.50	Failed
LICON	MFI	P13	PM	N/A	N/A	625	85	6696.0	–	–	2.00	–	Stopped
LICON	MFI	P14	PM	N/A	N/A	625	85	6912.0	–	–	1.50	–	Stopped
LICON	MFI	P15	PM	N/A	N/A	625	85	4728.0	–	–	1.00	–	Stopped
HIDA	EdF	1631	WM	7.95	36.02	625	100	853.2	2.17E-05	6.15E-05	5.25	N/A	Failed
HIDA	EdF	1646	WM	7.95	36.11	625	80	7949.2	1.66E-06	4.17E-06	3.31	4.70	Failed
LICON	ISQ	91U1	WM	N/A	N/A	600	145	1625.0	N/A	5.54E-05	9.00	22.00	Failed
LICON	ISQ	91U2	WM	N/A	N/A	600	135	2925.0	N/A	1.71E-05	5.00	6.00	Failed
LICON	ISQ	91U3	WM	N/A	N/A	625	105	1892.0	N/A	2.11E-05	4.00	9.00	Failed
LICON	ISQ	92U8	WM	N/A	N/A	625	140	1066.0	N/A	6.57E-05	7.00	22.00	Failed
HIDA	EdF	1632	XW	7.95	36.03	625	100	323.2	4.27E-05	8.59E-05	2.78	N/A	Failed
HIDA	EdF	1647	XW	7.95	36.03	625	60	3906.1	1.18E-06	3.81E-06	1.49	19.30	Failed
HIDA	EdF	1671	XW	7.95	36.06	625	80	10492.0	2.98E-07	1.57E-06	1.64	N/A	Failed
HIDA	EdF	1700	XW	7.95	36.02	625	80	1996.1	3.26E-06	8.44E-06	1.69	N/A	Failed
LICON	LE	16385	XW	N/A	N/A	680	75	10.0	N/A	1.13E-02	11.30	77.00	Failed
LICON	LE	16386	XW	N/A	N/A	660	75	186.0	N/A	2.63E-04	4.90	69.00	Failed
LICON	LE	16387	XW	N/A	N/A	650	75	429.0	N/A	1.07E-04	4.60	60.00	Failed
LICON	LE	16388	XW	N/A	N/A	670	75	95.0	N/A	6.32E-04	6.00	70.00	Failed
LICON	LE	16390	XW	N/A	N/A	640	75	552.0	N/A	5.25E-05	2.90	59.00	Failed

LICON	LE	16391	XW	N/A	N/A	640	75	629.0	N/A	6.04E-05	3.80	69.00	Failed
LICON	LE	16392	XW	N/A	N/A	675	75	35.0	N/A	1.74E-03	6.10	78.00	Failed
LICON	LE	16428	XW	N/A	N/A	660	75	3860.0	N/A	7.77E-06	3.00	24.00	Failed
LICON	LE	16429	XW	N/A	N/A	665	75	621.0	N/A	6.92E-05	4.30	33.00	Failed
LICON	MFI	LIP1	XW	N/A	N/A	600	150	344.0	N/A	4.27E-04	14.70	74.00	Failed
LICON	MFI	LIP2	XW	N/A	N/A	600	120	1926.0	N/A	1.82E-05	3.50	27.00	Failed
LICON	MFI	LIP3	XW	N/A	N/A	625	120	153.0	N/A	6.27E-04	9.60	64.00	Failed
LICON	MFI	LIP4	XW	N/A	N/A	625	85	1326.0	N/A	2.19E-05	2.90	21.00	Failed
LICON	MFI	LIP5	XW	N/A	N/A	600	145	419.0	N/A	4.25E-04	17.80	88.00	Failed
LICON	MFI	LIP6	XW	N/A	N/A	600	135	1068.0	N/A	7.21E-05	7.70	44.00	Failed
LICON	MFI	LIP7	XW	N/A	N/A	625	105	417.0	N/A	8.87E-05	3.70	33.00	Failed
LICON	MFI	LIP8	XW	N/A	N/A	625	97	527.0	N/A	6.45E-05	3.40	24.00	Failed

Table A-8: Uniaxial results for P92

Project	Insist.	Test name	Material condition	Gauge diameter [mm]	Gauge length [mm]	Temp. [°C]	σ_{net} [MPa]	Test duration [h]	$\dot{\varepsilon}_s$ [h^{-1}]	$\dot{\varepsilon}_{Ave}$ [h^{-1}]	ε_f [%]	R.A. [%]	Status
LICON	ISQ	92U5	HAZ	N/A	N/A	625	140	343.0	N/A	5.54E-04	19.00	85.00	Failed
LICON	CESI	1	PM	N/A	N/A	625	125	7037.0	1.14E-06	1.71E-05	12.04	82.09	Failed
LICON	CESI	2	PM	N/A	N/A	650	95	8609.0	1.49E-06	1.04E-05	8.95	25.02	Failed
LICON	GECA	S9750	PM	N/A	N/A	625	150	936.0	3.95E-05	2.67E-04	25.00	83.00	Failed
LICON	LE	16411	PM	N/A	N/A	710	75	184.0	1.36E-03	1.55E-03	28.50	76.00	Failed
LICON	LE	16412	PM	N/A	N/A	700	75	447.0	8.53E-05	4.34E-04	19.40	71.00	Failed
LICON	LE	16413	PM	N/A	N/A	680	75	2075.0	5.36E-05	9.83E-05	20.40	58.00	Failed
LICON	LE	16414	PM	N/A	N/A	690	75	2544.0	1.01E-05	5.07E-05	12.90	40.00	Failed
LICON	LE	16415	PM	N/A	N/A	675	75	3278.0	6.48E-06	7.47E-05	24.50	61.00	Failed
LICON	MBEL	98_060	PM	N/A	N/A	625	145	1432.0	1.68E-05	1.46E-04	20.90	80.00	Failed
LICON	MBEL	98_061	PM	N/A	N/A	650	130	249.0	1.64E-04	9.52E-04	23.70	87.00	Failed
LICON	MBEL	98_068	PM	N/A	N/A	625	135	4102.0	5.50E-06	4.02E-05	16.50	72.00	Failed
LICON	MBEL	98_069	PM	N/A	N/A	650	112	2943.0	8.67E-06	6.93E-05	20.40	68.00	Failed
LICON	MBEL	98_070	PM	N/A	N/A	650	120	1448.0	1.89E-05	1.44E-04	20.90	77.00	Failed
LICON	MBEL	99_004	PM	N/A	N/A	625	155	504.0	7.79E-05	4.44E-04	22.40	83.00	Failed
LICON	MBEL	99_005	PM	N/A	N/A	625	122	7161.0	2.20E-06	2.21E-05	15.80	59.00	Failed
LICON	MBEL	99_006	PM	N/A	N/A	650	94	7492.0	2.90E-06	2.11E-05	15.80	52.00	Failed
LICON	CESI	A	WM	N/A	N/A	650	120	436.0	5.36E-05	2.53E-04	11.03	41.02	Failed
LICON	CESI	B	WM	N/A	N/A	650	112	609.0	3.33E-05	1.59E-04	9.71	24.54	Failed
LICON	CESI	4	XW	N/A	N/A	650	135	86.1	1.50E-04	1.30E-03	11.20	82.09	Failed
LICON	CESI	5	XW	N/A	N/A	650	120	563.5	5.00E-06	1.34E-04	7.56	57.14	Failed
LICON	CESI	6	XW	N/A	N/A	650	112	688.4	1.30E-05	7.36E-05	5.07	24.39	Failed
LICON	CESI	7	XW	N/A	N/A	650	95	2220.0	2.80E-06	1.39E-05	3.08	19.57	Failed
LICON	LE	16427	XW	N/A	N/A	680	75	169.0	N/A	1.66E-04	2.80	16.00	Failed

Appendix B

Statistical Analyses of Uniaxial Creep Tests Results

Given below are the tables of statistical analyses of creep strain rates results from uniaxial tests performed under the HIDA and LICON projects by the different partners as well as the uniaxial tests provided by British Energy Generation Ltd. on 316L(N), P91 and P92 [Lehmann, 1995; ECCC, 1995; ECCC, 1998].

Notation:

Orient. : Orientation
Temp. : Temperature
Log(A_s) : Logarithm base 10 of A in the Norton law for the secondary creep strain rate
SE A_s : Standard error of A_s in logarithm base 10
n_s : Creep exponent in the Norton law for the secondary creep strain rate
SE n_s : Standard error of n_s
SD $\dot{\varepsilon}_s$: Standard deviation of the error of the secondary creep strain rate
Log(A_{Ave}) : Logarithm base 10 of A in the Norton law for the average creep strain rate
SE A_{Ave} : Standard error of A_{Ave} in logarithm base 10
n_{Ave} : Creep exponent in the Norton law for the average creep strain rate
SE n_{Ave} : Standard error of n_{Ave}
SD $\dot{\varepsilon}_{Ave}$: Standard deviation of the error of the average creep strain rate
r^2_{STAT} : Coefficient of determination

Tests on 316 Stainless Steel in Longitudinal Direction

Material	Material condition	Casts	Temp. [°C]	N° of tests	Log(A_s)	$SE\ A_s$	n_s	$SE\ n_s$	$SD\ \dot{\varepsilon}_s$	r^2_{STAT}	N° of tests	Log(A_{Ave})	$SE\ A_{Ave}$	n_{Awe}	$SE\ n_{Ave}$	$SD\ \dot{\varepsilon}_{Ave}$	r^2_{STAT}
316L(N)	PM	All	500	10	-48.94	15.21	16.59	5.84	0.41	0.50	11	-34.86	9.77	11.68	3.76	0.34	0.52
316L(N)	PM	20541	500	7	-47.43	15.86	15.95	6.09	0.42	0.58	7	-45.48	8.02	15.68	3.08	0.21	0.84
316L(N)	PM	All	550	110	-30.21	1.92	10.15	0.76	0.43	0.75	127	-33.25	1.58	11.74	0.63	0.38	0.74
316L(N)	PM	428	550	5	-32.35	4.39	10.97	1.76	0.32	0.93	4	-37.07	6.08	13.16	2.40	0.25	0.94
316L(N)	PM	612	550	13	-30.91	2.37	10.51	0.96	0.33	0.92	8	-39.04	4.68	14.06	1.85	0.32	0.91
316L(N)	PM	636	550	5	-36.53	4.90	12.59	1.97	0.19	0.93	5	-32.81	2.00	11.47	0.80	0.08	0.99
316L(N)	PM	929	550	6	-28.33	1.22	9.50	0.52	0.14	0.99	4	-24.76	2.53	8.28	1.03	0.12	0.97
316L(N)	PM	20528	550	7	-24.02	3.67	7.91	1.47	0.30	0.85	8	-39.21	4.51	14.37	1.80	0.29	0.91
316L(N)	PM	20540	550	7	-38.38	6.30	13.57	2.53	0.45	0.85	7	-39.86	5.24	14.60	2.10	0.38	0.91
316L(N)	PM	20541	550	8	-40.27	6.20	14.04	2.43	0.40	0.85	8	-48.36	6.16	17.67	2.42	0.40	0.90
316L(N)	PM	All	600	126	-25.02	0.75	8.76	0.32	0.39	0.86	124	-24.82	0.95	8.96	0.40	0.34	0.81
316L(N)	PM	424	600	3	-21.64	6.47	7.38	2.76	0.16	0.88	8	-22.48	1.79	8.03	0.77	0.10	0.95
316L(N)	PM	428	600	10	-22.76	2.31	7.66	1.03	0.44	0.87	2	-19.24	0.00	6.57	0.00	0.00	1.00
316L(N)	PM	527	600	0	–	–	–	–	–	–	5	-31.03	7.74	11.57	3.31	0.26	0.80
316L(N)	PM	612	600	7	-25.56	2.31	8.99	1.00	0.23	0.94	5	-28.86	2.28	10.67	0.96	0.13	0.98
316L(N)	PM	636	600	4	-21.10	1.00	7.00	0.42	0.04	0.99	4	-25.13	1.24	9.00	0.52	0.05	0.99
316L(N)	PM	929	600	6	-31.04	1.57	11.43	0.70	0.16	0.99	4	-19.27	2.66	6.60	1.16	0.12	0.94
316L(N)	PM	10123	600	10	-30.68	3.42	11.41	1.48	0.28	0.88	10	-29.34	2.75	11.03	1.19	0.23	0.92
316L(N)	PM	10125	600	7	-27.99	1.26	10.15	0.56	0.16	0.99	4	-31.03	2.02	11.69	0.85	0.14	0.99
316L(N)	PM	20528	600	8	-26.13	0.95	9.47	0.41	0.13	0.99	11	-28.58	0.89	10.78	0.38	0.10	0.99
316L(N)	PM	20540	600	8	-30.14	1.36	11.10	0.57	0.16	0.98	7	-28.03	1.41	10.47	0.59	0.12	0.98
316L(N)	PM	20541	600	18	-29.53	1.69	10.54	0.69	0.27	0.94	18	-25.95	1.64	9.41	0.68	0.26	0.92
316L(N)	PM	All	650	87	-22.34	0.72	8.27	0.32	0.38	0.88	82	-19.68	0.79	7.37	0.35	0.34	0.85
316L(N)	PM	HIDA	650	7	-23.61	1.98	8.97	0.88	0.10	0.95	5	-21.72	2.32	8.35	1.03	0.12	0.96
316L(N)	PM	428	650	6	-29.98	0.67	8.03	0.32	0.09	0.99	1	–	–	–	–	–	–
316L(N)	PM	612	650	6	-21.63	0.30	7.98	0.14	0.04	1.00	4	-19.66	0.40	7.37	0.18	0.03	1.00
316L(N)	PM	636	650	5	-23.16	0.39	8.65	0.18	0.03	1.00	5	-16.73	1.41	5.96	0.65	0.10	0.97
316L(N)	PM	929	650	0	–	–	–	–	–	–	4	-19.25	1.24	7.15	0.56	0.09	0.99

Material	Material condition	Casts	Orient.	Temp. [°C]	N° of tests	Log(A_s)	*SE* A_s	n_s	*SE* n_s	*SD* $\dot{\varepsilon}_s$	r^2_{STAT}	N° of tests	Log(A_{Ave})	*SE* A_{Ave}	n_{Ave}	*SE* n_{Ave}	*SD* $\dot{\varepsilon}_{Ave}$	r^2_{STAT}
316L(N)	PM	10125	Long	650	7	-23.27	1.12	8.76	0.53	0.22	0.98	4	-21.80	1.37	8.35	0.62	0.12	0.99
316L(N)	PM	20528	Long	650	7	-20.66	1.21	7.78	0.56	0.23	0.98	9	-19.26	0.96	7.42	0.45	0.18	0.98
316L(N)	PM	20540	Long	650	6	-22.28	0.36	8.41	0.16	0.05	1.00	6	-20.83	0.54	8.06	0.25	0.08	1.00
316L(N)	PM	20541	Long	650	16	-26.66	0.76	10.15	0.33	0.13	0.99	14	-21.82	0.90	8.35	0.39	0.15	0.97
316L(N)	PM	All	Long	700	23	-17.28	0.94	6.63	0.46	0.36	0.91	24	-15.22	0.81	5.98	0.39	0.28	0.91
316L(N)	PM	20528	Long	700	6	-16.66	0.94	6.48	0.46	0.17	0.98	8	-15.68	1.24	6.29	0.61	0.20	0.95
316L(N)	PM	20540	Long	700	6	-14.32	1.70	5.25	0.84	0.32	0.91	5	-16.89	3.89	6.85	1.87	0.49	0.82
316L(N)	PM	20541	Long	700	11	-20.01	0.37	7.83	0.17	0.10	1.00	11	-15.13	0.51	5.86	0.25	0.14	0.98
316L(N)	PM	All	Long	750	15	-14.33	0.71	5.78	0.37	0.26	0.95	15	-13.74	0.41	5.78	0.21	0.15	0.98

Table B-1: Statistical results of 316L(N) uniaxial tests

P22	PM	HIDA	Long	565	4	-27.49	2.90	11.15	1.40	0.23	0.97	4	-23.75	2.26	9.64	1.09	0.18	0.98
P22	PM	HIDA	Cr	565	3	-30.71	1.65	12.69	0.79	0.10	1.00	3	-29.13	0.42	12.19	0.20	0.03	1.00
P22	PM	HIDA	Ave	565	7	-28.76	1.65	11.76	0.79	0.17	0.98	7	-25.69	1.64	10.57	0.79	0.17	0.97
P22	WM	HIDA	Cr	565	2	-31.45	0.00	12.88	0.00	0.00	1.00	2	-28.36	0.00	11.84	0.00	0.00	1.00
P22	XW	HIDA	Long	565	4	-24.62	2.54	9.71	1.27	0.13	0.97	4	-25.38	4.04	10.23	2.01	0.20	0.93

Table B-2: Statistical results of P22 uniaxial tests

E911	HAZ	LICON	N / A	625	2	-21.29	–	7.99	–	0.10	–	2	-31.78	–	13.56	–	0.22	–
E911	PM	LICON	N / A	625	3	-21.66	6.32	7.99	2.95	0.17	–	4	-32.84	6.05	13.56	2.86	0.29	0.92
E911	WM	LICON	N / A	625	0	–	–	–	–	–	–	2	-33.17	–	13.56	–	0.01	–
E911	XW	LICON	N / A	625	0	–	–	–	–	–	–	4	-33.00	–	13.56	–	0.26	–
E911	HAZ	LICON	N / A	650	2	-23.14	–	9.78	–	0.15	–	2	-23.11	–	10.18	–	0.32	–
E911	PM	LICON	N / A	650	3	-23.21	6.69	9.78	3.34	0.41	0.81	4	-24.52	7.20	10.18	3.59	0.44	0.80
E911	XW	LICON	N / A	650	0	–	–	–	–	–	–	4	-24.13	–	10.18	–	0.23	–

Table B-3: Statistical results of E911 uniaxial tests

Tests results on P91

Material	Material condition	Casts	Orient.	Temp. [°C]	N° of tests	Log(A_s)	$SE\ A_s$	n_s	$SE\ n_s$	$SD\ \dot{\varepsilon}_s$	r^2_{STAT}	N° of tests	Log(A_{Ave})	$SE\ A_{Ave}$	n_{Ave}	$SE\ n_{Ave}$	$SD\ \dot{\varepsilon}_{Ave}$	r^2_{STAT}
P91	PM	All	N / A	500	0	–	–	–	–	–	–	11	-55.02	2.29	20.81	0.92	0.14	0.98
P91	PM	All	N / A	550	0	–	–	–	–	–	–	110	-36.31	2.03	13.87	0.87	0.54	0.70
P91	PM	DE.05.1	N / A	550	0	–	–	–	–	–	–	5	-40.52	3.79	15.48	1.61	0.24	0.97
P91	PM	DE.05.2	N / A	550	0	–	–	–	–	–	–	4	-34.00	4.04	12.71	1.73	0.25	0.96
P91	PM	DE.05.4	N / A	550	0	–	–	–	–	–	–	4	-30.17	1.85	11.06	0.79	0.12	0.99
P91	PM	DE.05.6	N / A	550	0	–	–	–	–	–	–	4	-30.54	1.09	11.12	0.46	0.05	1.00
P91	PM	DE.05.7	N / A	550	0	–	–	–	–	–	–	4	-41.31	1.89	16.08	0.80	0.12	1.00
P91	PM	DE.05.8	N / A	550	0	–	–	–	–	–	–	4	-43.47	0.72	16.95	0.31	0.05	1.00
P91	PM	DE.05.12	N / A	550	0	–	–	–	–	–	–	4	-30.65	2.19	11.39	0.95	0.09	0.99
P91	PM	GB.02.5	N / A	550	0	–	–	–	–	–	–	4	-52.44	3.49	21.16	1.52	0.08	0.99
P91	PM	IT.03.4	N / A	550	0	–	–	–	–	–	–	12	-45.58	2.17	17.77	0.93	0.12	0.97
P91	PM	JN.00.5	N / A	550	0	–	–	–	–	–	–	4	-35.95	7.13	13.88	3.02	0.30	0.91
P91	PM	JN.00.7	N / A	550	0	–	–	–	–	–	–	4	-39.00	1.80	15.27	0.76	0.11	0.99
P91	PM	JN.00.26	N / A	550	0	–	–	–	–	–	–	4	-38.79	2.42	15.12	1.03	0.11	0.99
P91	PM	All	N / A	580	13	-23.79	4.56	8.81	2.03	0.33	0.63	15	-23.43	3.83	8.97	1.71	0.28	0.71
P91	PM	Aged	N / A	580	6	-33.06	2.11	13.11	0.95	0.09	0.98	6	-29.99	2.13	12.03	0.96	0.09	0.98
P91	PM	New	N / A	580	7	-36.88	2.84	14.49	1.25	0.12	0.96	7	-35.38	2.29	14.15	1.01	0.09	0.98
P91	HAZ	LICON	N / A	600	2	-31.06	0.00	12.89	0.00	0.00	1.00	2	-30.76	0.00	13.30	0.00	0.00	1.00
P91	PM	All	N / A	600	8	-33.52	3.38	13.51	1.57	0.18	0.93	238	-24.00	0.81	9.41	0.38	0.42	0.72
P91	PM	LICON	N / A	600	4	-32.13	6.38	12.89	2.99	0.22	0.90	4	-31.91	3.32	13.30	1.55	0.12	0.97
P91	PM	RANTALA	N / A	600	4	-35.42	4.57	14.36	2.13	0.19	0.96	4	-30.57	4.30	12.53	2.00	0.17	0.95
P91	PM	BE.01.4	N / A	600	0	–	–	–	–	–	–	5	-24.14	4.19	9.71	2.00	0.33	0.89
P91	PM	CH.02.AZ	N / A	600	0	–	–	–	–	–	–	10	-15.89	1.39	5.41	0.65	0.15	0.89
P91	PM	CH.02.W1	N / A	600	0	–	–	–	–	–	–	7	-14.30	1.58	4.58	0.75	0.13	0.88
P91	PM	CH.02.W2	N / A	600	0	–	–	–	–	–	–	10	-15.42	2.25	5.24	1.06	0.25	0.85
P91	PM	CH.02.W3	N / A	600	0	–	–	–	–	–	–	7	-15.91	2.38	5.39	1.12	0.20	0.82
P91	PM	DE.05.1	N / A	600	0	–	–	–	–	–	–	5	-27.93	1.37	11.12	0.63	0.16	0.99
P91	PM	DE.05.2	N / A	600	0	–	–	–	–	–	–	5	-23.51	1.19	9.15	0.55	0.14	0.99

Material	Material condition	Casts	Orient.	Temp. [°C]	N° of tests	Log(A_s)	$SE\ A_s$	n_s	$SE\ n_s$	$SD\ \dot{\varepsilon}_s$	r^2_{STAT}	N° of tests	Log(A_{Ave})	$SE\ A_{Ave}$	n_{Ave}	$SE\ n_{Ave}$	$SD\ \dot{\varepsilon}_{Ave}$	r^2_{STAT}
P91	PM	DE.05.5	N / A	600	0	–	–	–	–	–	–	4	-19.38	5.06	7.08	2.30	0.39	0.83
P91	PM	GB.02.5	N / A	600	0	–	–	–	–	–	–	5	-13.66	2.87	4.66	1.38	0.13	0.79
P91	PM	IT.01.1	N / A	600	0	–	–	–	–	–	–	5	-30.49	1.10	12.35	0.51	0.03	1.00
P91	PM	IT.03.4	N / A	600	0	–	–	–	–	–	–	12	-22.67	1.84	8.81	0.87	0.18	0.91
P91	PM	IT.03.6	N / A	600	0	–	–	–	–	–	–	8	-28.67	3.77	11.61	1.77	0.18	0.88
P91	PM	JN.00.5	N / A	600	0	–	–	–	–	–	–	5	-27.05	0.69	10.83	0.32	0.05	1.00
P91	PM	JN.00.7	N / A	600	0	–	–	–	–	–	–	9	-32.47	1.93	13.50	0.66	0.13	0.98
P91	PM	JN.00.25	N / A	600	0	–	–	–	–	–	–	12	-31.61	1.91	13.05	0.87	0.16	0.96
P91	PM	JN.00.26	N / A	600	0	–	–	–	–	–	–	4	-32.48	2.40	13.35	1.11	0.19	0.99
P91	WM	LICON	N / A	600	0	–	–	–	–	–	–	2	-33.05	0.00	13.30	0.00	0.00	1.00
P91	XW	LICON	N / A	600	0	–	–	–	–	–	–	4	-30.76	4.56	13.30	2.11	0.13	0.96
P91	HAZ	LICON	N / A	625	2	-28.26	–	13.21	–	0.03	–	2	-29.45	–	13.66	–	0.08	–
P91	PM	All	N / A	625	12	-22.95	2.90	8.96	1.42	0.21	0.90	37	-21.96	2.43	8.94	1.19	0.22	0.92
P91	PM	HIDA	Ave	625	9	-21.86	0.80	8.38	0.39	0.05	0.99	9	-25.20	1.12	10.30	0.55	0.07	0.98
P91	PM	HIDA	Cr	625	3	-22.56	0.84	8.72	0.41	0.03	1.00	3	-28.12	1.50	11.70	0.73	0.05	1.00
P91	PM	HIDA	Long	625	4	-21.64	1.24	8.26	0.61	0.06	0.99	4	-24.39	1.71	9.91	0.84	0.09	0.99
P91	PM	LICON	N / A	625	3	-31.28	1.32	13.21	0.65	0.04	1.00	4	-31.48	1.60	13.66	0.80	0.09	0.99
P91	WM	All	N / A	625	2	-22.71	–	8.96	–	0.17	–	4	-22.64	–	8.93	–	0.55	–
P91	WM	HIDA	Ave	625	2	-21.58	–	8.38	–	0.21	–	2	-24.90	–	10.30	–	0.12	–
P91	WM	LCION	Ave	625	0	–	–	–	–	–	–	2	-32.90	–	13.66	–	0.86	–
P91	XW	All	N / A	625	2	-22.57	–	8.96	–	0.73	–	8	-21.98	–	8.93	–	0.42	–
P91	XW	HIDA	Ave	625	4	-24.48	–	8.38	–	0.87	–	4	-24.60	–	10.30	–	0.84	–
P91	XW	LICON	N / A	625	4	–	–	–	–	–	–	4	-31.43	–	10.30	–	0.44	–
P91	PM	All	N / A	650	0	–	–	–	–	–	–	145	-19.06	0.49	7.98	0.25	0.32	0.87
P91	PM	CH.02.W2	N / A	650	0	–	–	–	–	–	–	6	-20.55	1.70	8.76	0.91	0.16	0.96
P91	PM	DE.05.1	N / A	650	0	–	–	–	–	–	–	5	-20.00	0.75	8.36	0.38	0.12	0.99
P91	PM	DE.05.2	N / A	650	0	–	–	–	–	–	–	5	-21.45	0.57	9.06	0.29	0.09	1.00
P91	PM	DE.05.4	N / A	650	0	–	–	–	–	–	–	4	-18.81	3.42	7.84	1.73	0.26	0.91
P91	PM	GB.02.4	N / A	650	0	–	–	–	–	–	–	6	-19.41	1.11	8.37	0.61	0.13	0.98
P91	PM	GB.02.5	N / A	650	0	–	–	–	–	–	–	6	-16.48	1.33	6.98	0.73	0.16	0.96
P91	PM	GB.02.6	N / A	650	0	–	–	–	–	–	–	4	-18.77	0.51	8.03	0.27	0.03	1.00
P91	PM	IT.01.1	N / A	650	0	–	–	–	–	–	–	5	-14.32	2.45	5.47	1.27	0.12	0.86
P91	PM	IT.03.4	N / A	650	0	–	–	–	–	–	–	18	-19.45	0.67	8.19	0.35	0.14	0.97

Material	Material condition	Casts	Orient.	Temp. [°C]	N° of tests	Log(A_s)	SE A_s	n_s	SE n_s	SD $\dot{\varepsilon}_s$	r^2_{STAT}	N° of tests	Log(A_{Ave})	SE A_{Ave}	n_{Ave}	SE n_{Ave}	SD $\dot{\varepsilon}_{Ave}$	r^2_{STAT}
P91	PM	IT.08.2	N / A	650	0	–	–	–	–	–	–	4	-23.27	2.97	9.90	1.49	0.19	0.96
P91	PM	JN.00.5	N / A	650	0	–	–	–	–	–	–	7	-20.29	0.54	8.61	0.28	0.07	1.00
P91	PM	JN.00.6	N / A	650	0	–	–	–	–	–	–	5	-24.51	1.18	10.67	0.60	0.16	0.99
P91	PM	JN.00.7	N / A	650	0	–	–	–	–	–	–	14	-23.61	0.49	10.30	0.25	0.11	0.99
P91	PM	JN.00.21	N / A	650	0	–	–	–	–	–	–	4	-20.95	0.25	8.85	0.13	0.02	1.00
P91	PM	JN.00.23	N / A	650	0	–	–	–	–	–	–	4	-20.87	1.80	8.81	0.92	0.14	0.98
P91	PM	JN.00.26	N / A	650	0	–	–	–	–	–	–	4	-24.85	0.62	10.82	0.32	0.06	1.00
P91	PM	All	N / A	700	0	–	–	–	–	–	–	13	-14.96	0.48	6.71	0.27	0.16	0.98
P91	PM	JN.00.6	N / A	700	0	–	–	–	–	–	–	4	-15.50	0.48	7.06	0.28	0.08	1.00
P91	PM	JN.00.7	N / A	700	0	–	–	–	–	–	–	6	-15.41	0.57	7.00	0.34	0.13	0.99

Table B-4: Statistical results of P91 uniaxial tests

P92	PM	All	Ave	550	0	–	–	–	–	–	–	56	-49.53	1.98	19.13	0.82	0.31	0.91
P92	PM	All	Long	550	8	-49.38	4.79	18.62	1.97	0.35	0.94	49	-49.15	2.03	18.97	0.83	0.30	0.92
P92	PM	JN.00.DDF	Long	550	0	–	–	–	–	–	–	4	-70.58	9.32	27.74	3.78	0.23	0.96
P92	PM	JN.00.E	Ave	550	0	–	–	–	–	–	–	9	-51.47	1.85	20.09	0.76	0.13	0.99
P92	PM	JN.00.E	Cr	550	0	–	–	–	–	–	–	4	-55.83	3.15	21.97	1.31	0.11	0.99
P92	PM	JN.00.E	Long	550	0	–	–	–	–	–	–	5	-50.13	2.45	19.53	1.00	0.14	0.99
P92	PM	JN.00.EPP	Long	550	5	-45.24	0.93	16.81	0.39	0.06	1.00	17	-47.03	2.64	17.99	1.08	0.23	0.95
P92	PM	JN.00.YAP	Long	550	3	-43.94	2.89	16.56	1.17	0.08	0.99	6	-46.31	1.26	17.87	0.52	0.08	1.00
P92	PM	JN.00.YAP2	Long	550	0	–	–	–	–	–	–	6	-50.44	1.45	19.57	0.60	0.07	1.00
P92	PM	JN.00.YBP	Long	550	0	–	–	–	–	–	–	5	-51.78	1.65	20.07	0.68	0.09	1.00
P92	PM	JN.02.1	Tr	550	0	–	–	–	–	–	–	3	-34.91	12.71	12.86	5.33	0.17	0.85
P92	PM	All	Ave	600	39	-38.14	1.81	14.88	0.81	0.40	0.90	125	-40.13	1.06	16.15	0.47	0.40	0.91
P92	PM	All	Long	600	24	-40.88	2.30	16.13	1.01	0.35	0.92	84	-41.82	0.95	16.90	0.42	0.29	0.95
P92	PM	DE.07.CMS	N / A	600	8	-26.43	2.05	9.41	0.92	0.17	0.94	5	-30.25	3.64	11.47	1.62	0.12	0.94
P92	PM	DE.07.CQM	N / A	600	7	-33.66	3.47	12.85	1.61	0.23	0.93	3	-35.46	7.28	14.07	3.30	0.26	0.95
P92	PM	DE.08.1	N / A	600	0	–	–	–	–	–	–	7	-32.09	4.68	12.64	2.07	0.32	0.88
P92	PM	IT.01.1	Long	600	5	-49.41	2.55	20.07	1.14	0.08	0.99	5	-41.29	3.71	16.81	1.66	0.12	0.97
P92	PM	IT.01.2	Long	600	5	-47.72	2.23	19.32	1.03	0.08	0.99	5	-40.48	1.34	16.44	0.60	0.04	1.00
P92	PM	JN.00.DDF	Long	600	0	–	–	–	–	–	–	5	-40.19	2.67	16.13	1.17	0.16	0.99
P92	PM	JN.00.E	Ave	600	0	–	–	–	–	–	–	15	-40.31	1.16	16.37	0.50	0.19	0.99

Material	Material condition	Casts	Orient.	Temp. [°C]	N° of tests	$\mathrm{Log}(A_s)$	$SE\ A_s$	n_s	$SE\ n_s$	$SD\ \hat{\varepsilon}_s$	r^2_{STAT}	N° of tests	$\mathrm{Log}(A_{Ave})$	$SE\ A_{Ave}$	n_{Ave}	$SE\ n_{Ave}$	$SD\ \hat{\varepsilon}_{Ave}$	r^2_{STAT}
P92	PM	JN.00.E	Cr	600	0	–	–	–	–	–	–	8	-39.24	1.41	15.90	0.62	0.17	0.99
P92	PM	JN.00.E	Long	600	0	–	–	–	–	–	–	7	-41.85	2.08	17.04	0.91	0.22	0.99
P92	PM	JN.00.EPP	Long	600	11	-44.41	1.34	17.53	0.58	0.16	0.99	23	-44.71	0.79	18.03	0.34	0.15	0.99
P92	PM	JN.00.YAP	Long	600	3	-42.51	1.70	16.95	0.73	0.07	1.00	7	-42.87	1.26	17.43	0.55	0.10	1.00
P92	PM	JN.00.YAP	Long	600	4	-32.99	0.57	13.72	0.26	0.04	1.00	10	-28.07	0.84	11.86	0.40	0.16	0.99
P92	PM	JN.00.YAP2	Long	600	0	–	–	–	–	–	–	8	-43.12	2.93	17.54	1.28	0.23	0.97
P92	PM	JN.00.YBP	Long	600	0	–	–	–	–	–	–	7	-44.38	1.21	18.03	0.53	0.12	1.00
P92	PM	JN.02.1	Tr	600	0	–	–	–	–	–	–	3	-40.49	0.70	16.14	0.31	0.02	1.00
P92	PM	All	Ave	625	10	-42.81	4.14	17.64	1.94	0.28	0.91	25	-34.46	2.03	14.19	0.94	0.29	0.91
P92	PM	JN.00.EPP	Long	625	0	–	–	–	–	–	–	8	-36.17	0.72	14.88	0.33	0.07	1.00
P92	PM	LICON	N / A	625	6	-40.15	4.05	16.41	1.89	0.18	0.95	6	-33.13	2.95	13.59	1.38	0.13	0.96
P92	PM	All	Ave	650	31	-28.50	1.29	11.56	0.62	0.35	0.92	130	-28.14	0.53	11.81	0.25	0.32	0.94
P92	PM	All	Long	650	14	-27.69	1.71	11.23	0.80	0.35	0.94	88	-27.98	0.55	11.76	0.26	0.28	0.96
P92	PM	DE.07.CMS	N / A	650	5	-25.49	2.53	9.91	1.22	0.16	0.96	5	-30.78	3.27	12.86	1.74	0.23	0.95
P92	PM	DE.07.CQM	N / A	650	7	-30.00	2.25	12.37	1.10	0.28	0.96	7	-28.51	1.66	12.00	0.81	0.21	0.98
P92	PM	DE.08.1	N / A	650	0	–	–	–	–	–	–	5	-20.09	1.70	7.66	0.85	0.21	0.96
P92	PM	IT.01.1	Long	650	5	-18.00	2.40	6.49	1.19	0.15	0.91	5	-15.72	2.14	5.80	1.06	0.13	0.91
P92	PM	JN.00.DDF	Long	650	0	–	–	–	–	–	–	5	-23.45	2.36	9.62	1.13	0.20	0.96
P92	PM	JN.00.E	Ave	650	0	–	–	–	–	–	–	13	-28.04	0.81	11.94	0.39	0.18	0.99
P92	PM	JN.00.E	Cr	650	0	–	–	–	–	–	–	6	-27.74	0.68	11.79	0.32	0.09	1.00
P92	PM	JN.00.E	Long	650	0	–	–	–	–	–	–	7	-28.20	1.50	12.03	0.70	0.25	0.98
P92	PM	JN.00.EPP	Long	650	5	-30.03	2.11	12.18	0.98	0.25	0.98	24	-28.41	0.85	11.87	0.39	0.27	0.98
P92	PM	JN.00.YAP	Long	650	4	-32.99	0.57	13.72	0.26	0.04	1.00	10	-28.07	0.84	11.86	0.39	0.16	0.99
P92	PM	JN.00.YAP2	Long	650	0	–	–	–	–	–	–	7	-29.98	0.77	12.77	0.37	0.12	1.00
P92	PM	JN.00.YBP	Long	650	0	–	–	–	–	–	–	7	-30.20	1.14	12.81	0.53	0.19	0.99
P92	PM	JN.02.1	Ave	650	0	–	–	–	–	–	–	8	-26.07	1.60	10.63	0.77	0.12	0.97
P92	PM	JN.02.1	Tr	650	0	–	–	–	–	–	–	5	-27.04	1.83	11.09	0.88	0.11	0.98
P92	PM	LICON	N / A	650	5	-26.31	4.85	10.50	2.37	0.30	0.97	5	-28.27	3.99	11.84	1.96	0.24	0.92
P92	WM	LICON	N / A	650	2	-25.99	–	10.50	–	0.09	–	2	-28.12	–	11.84	–	0.11	–
P92	XW	LICON	N / A	650	4	-26.05	–	10.50	–	0.14	–	4	-28.31	–	11.84	–	0.17	–

Material	Material condition	Casts	Orient.	Temp. [°C]	N° of tests	$Log(A_s)$	$SE\ A_s$	n_s	$SE\ n_s$	$SD\ \dot{\varepsilon}_s$	r^2_{STAT}	N° of tests	$Log(A_{Ave})$	$SE\ A_{Ave}$	n_{Ave}	$SE\ n_{Ave}$	$SD\ \dot{\varepsilon}_{Ave}$	r^2_{STAT}
P92	PM	All	Ave	700	10	-20.02	0.79	8.53	0.40	0.17	0.98	70	-18.37	0.38	8.13	0.20	0.24	0.96
P92	PM	All	Long	700	9	-19.96	0.86	8.51	0.44	0.18	0.98	64	-18.33	0.40	8.11	0.21	0.25	0.96
P92	PM	JN.00.DDF	Long	700	0	–	–	–	–	–	–	4	-16.73	1.34	7.31	0.70	0.16	0.98
P92	PM	JN.00.E	Ave	700	0	–	–	–	–	–	–	9	-19.67	0.51	8.85	0.26	0.08	0.99
P92	PM	JN.00.E	Cr	700	0	–	–	–	–	–	–	4	-19.73	1.37	8.87	0.70	0.13	0.99
P92	PM	JN.00.E	Long	700	0	–	–	–	–	–	–	5	-19.52	0.48	8.78	0.24	0.06	1.00
P92	PM	JN.00.EPP	Long	700	5	-20.02	0.63	8.49	0.32	0.10	1.00	18	-19.00	0.76	8.32	0.39	0.26	0.97
P92	PM	JN.00.YAP	Long	700	4	-20.83	1.68	9.01	0.86	0.20	0.98	7	-17.35	1.04	7.64	0.56	0.23	0.97
P92	PM	JN.00.YAP2	Long	700	0	–	–	–	–	–	–	10	-18.20	0.54	8.10	0.29	0.17	0.99
P92	PM	JN.00.YBP	Long	700	0	–	–	–	–	–	–	5	-20.88	0.35	9.49	0.18	0.07	1.00
P92	PM	All	Long	750	3	-16.01	0.72	7.35	0.39	0.03	1.00	8	-13.83	0.71	6.74	0.40	0.17	0.98

Table B-5: Statistical results of P92 uniaxial tests

Appendix C

Statistical Analyses of Uniaxial Creep Failure Results

Given below are the tables of statistical analyses of creep rupture results from uniaxial tests performed under the HIDA and LICON projects by the different partners as well as the uniaxial tests provided by British Energy Generation Ltd. on 316L(N), P91 and P92 [Lehmann, 1995; ECCC, 1995; ECCC, 1998].

Notation:

Orient. : Orientation
Temp. : Temperature
Log*(H)* : Logarithm base 10 of *H* in the rupture law
SE H : Standard error of *H* in logarithm base 10
v : Creep exponent in the rupture law
SE v : Standard error of *v*
SD t_R : Standard deviation of the error of the failure times
r^2_{STAT} : Coefficient of determination

Table C-6: Statistical results of 316L(N) uniaxial rupture data

Material	Material condition	Casts	Orient.	Temp. [°C]	N° of tests	Log(*H*)	*SE H*	*v*	*SE v*	*SD* t_R	r^2_{STAT}
316L(N)	PM	All	Long	500	11	26.80	9.25	-8.78	3.56	0.33	0.40
316L(N)	PM	20541	Long	500	7	34.40	9.59	-11.63	3.68	0.25	0.67
316L(N)	PM	All	Long	550	127	30.25	1.42	-10.79	0.57	0.35	0.74
316L(N)	PM	428	Long	550	4	33.59	4.26	-11.97	1.68	0.18	0.96
316L(N)	PM	612	Long	550	8	37.03	3.06	-13.47	1.21	0.21	0.95
316L(N)	PM	636	Long	550	5	35.92	0.56	-12.90	0.22	0.02	1.00
316L(N)	PM	929	Long	550	4	26.57	3.56	-9.34	1.45	0.17	0.95
316L(N)	PM	20528	Long	550	8	39.04	3.88	-14.49	1.56	0.25	0.94
316L(N)	PM	20540	Long	550	7	34.56	4.14	-12.70	1.66	0.30	0.92
316L(N)	PM	20541	Long	550	8	44.37	5.09	-16.32	1.99	0.33	0.92
316L(N)	PM	All	Long	600	127	25.39	0.87	-9.38	0.37	0.32	0.84
316L(N)	PM	424	Long	600	8	27.79	1.47	-10.49	0.63	0.08	0.98
316L(N)	PM	428	Long	600	2	22.66	0.00	-8.14	0.00	0.00	1.00
316L(N)	PM	527	Long	600	5	34.78	4.21	-13.35	1.80	0.14	0.95
316L(N)	PM	612	Long	600	5	30.00	1.91	-11.27	0.80	0.10	0.99
316L(N)	PM	636	Long	600	4	26.73	0.84	-9.78	0.35	0.03	1.00
316L(N)	PM	929	Long	600	4	20.59	0.32	-7.33	0.14	0.01	1.00
316L(N)	PM	10123	Long	600	10	26.15	3.92	-9.82	1.70	0.33	0.81
316L(N)	PM	10125	Long	600	4	31.13	1.70	-11.92	0.72	0.12	0.99
316L(N)	PM	20528	Long	600	11	27.72	1.00	-10.53	0.42	0.11	0.98
316L(N)	PM	20540	Long	600	7	29.34	1.38	-11.17	0.58	0.11	0.99
316L(N)	PM	20541	Long	600	18	26.55	1.29	-9.83	0.53	0.21	0.95
316L(N)	PM	All	Long	650	84	19.51	0.70	-7.42	0.31	0.30	0.87
316L(N)	PM	HIDA	Long	650	5	20.65	2.30	-7.97	1.02	0.12	0.95
316L(N)	PM	428	Long	650	1	–	–	–	–	–	–
316L(N)	PM	612	Long	650	4	20.27	0.83	-7.74	0.38	0.05	1.00
316L(N)	PM	636	Long	650	5	18.14	1.16	-6.69	0.54	0.08	0.98
316L(N)	PM	929	Long	650	4	18.10	0.59	-6.76	0.27	0.05	1.00
316L(N)	PM	10125	Long	650	4	19.63	1.46	-7.52	0.66	0.13	0.99
316L(N)	PM	20528	Long	650	9	18.70	1.18	-7.24	0.55	0.22	0.96
316L(N)	PM	20540	Long	650	6	19.82	1.22	-7.70	0.56	0.17	0.98
316L(N)	PM	20541	Long	650	16	22.01	0.94	-8.55	0.41	0.16	0.97
316L(N)	PM	All	Long	700	24	15.63	0.72	-6.26	0.35	0.25	0.94
316L(N)	PM	20528	Long	700	8	16.11	0.89	-6.52	0.44	0.15	0.97
316L(N)	PM	20540	Long	700	5	17.28	3.91	-7.12	1.88	0.50	0.83
316L(N)	PM	20541	Long	700	11	15.31	0.47	-6.05	0.23	0.13	0.99
316L(N)	PM	All	Long	750	15	13.05	0.36	-5.47	0.19	0.13	0.99

Table C-7: Statistical results of P22 uniaxial rupture data at 565°C

Material	Material condition	Casts	Orient.	Temp. [°C]	N° of tests	Log(*H*)	*SE H*	*v*	*SE v*	*SD* t_R	r^2_{STAT}
P22	PM	HIDA	Long	565	4	21.49	1.28	-8.80	0.62	0.10	0.99
P22	PM	HIDA	Cr	565	3	24.57	0.68	-10.26	0.32	0.04	1.00
P22	PM	HIDA	Ave	565	7	22.63	0.94	-9.35	0.45	0.09	0.99
P22	WM	HIDA	Cr	565	2	17.61	0.00	-6.94	0.00	0.00	1.00
P22	XW	HIDA	Long	565	4	15.53	1.58	-6.02	0.79	0.08	0.97

Table C-8: Statistical results of E911 uniaxial rupture data

Material	Material condition	Casts	Orient.	Temp. [°C]	N° of tests	Log(*H*)	*SE H*	*v*	*SE v*	*SD* t_R	r^2_{STAT}
E911	HAZ	LICON	N/A	625	2	22.41	–	-9.28	–	0.16	–
E911	PM	LICON	N/A	625	4	23.00	4.35	-9.28	2.06	0.21	0.91
E911	WM	LICON	N/A	625	2	22.95	–	-9.28	–	0.25	–
E911	XW	LICON	N/A	625	4	22.65	–	-9.28	–	0.09	–
E911	HAZ	LICON	N/A	650	3	19.44	–	-8.54	–	0.22	–
E911	PM	LICON	N/A	650	4	20.42	5.25	-8.54	2.62	0.32	0.85
E911	XW	LICON	N/A	650	4	19.91	–	-8.54	–	0.27	–

Table C-9: Statistical results of P91 uniaxial rupture data

Material	Material condition	Casts	Orient.	Temp. [°C]	N° of tests	Log(*H*)	*SE H*	*v*	*SE v*	*SD* t_R	r^2_{STAT}
P91	PM	All	N/A	500	11	55.48	1.68	-21.22	0.68	0.10	0.99
P91	PM	All	N/A	550	112	33.37	1.65	-12.89	0.71	0.46	0.75
P91	PM	DE.05.1	N/A	550	5	37.32	3.50	-14.46	1.49	0.22	0.97
P91	PM	DE.05.2	N/A	550	4	34.12	2.91	-13.07	1.25	0.18	0.98
P91	PM	DE.05.4	N/A	550	4	27.74	2.40	-10.30	1.02	0.15	0.98
P91	PM	DE.05.6	N/A	550	4	31.77	2.09	-11.94	0.88	0.09	0.99
P91	PM	DE.05.7	N/A	550	4	38.07	2.70	-15.00	1.15	0.17	0.99
P91	PM	DE.05.8	N/A	550	4	40.72	0.55	-16.10	0.23	0.03	1.00
P91	PM	DE.05.12	N/A	550	4	27.02	1.32	-10.11	0.57	0.05	0.99
P91	PM	GB.02.5	N/A	550	4	48.39	0.71	-19.65	0.31	0.02	1.00
P91	PM	IT.03.4	N/A	550	12	44.14	1.89	-17.41	0.81	0.10	0.98
P91	PM	JN.00.5	N/A	550	4	33.17	8.24	-12.91	3.49	0.35	0.87
P91	PM	JN.00.7	N/A	550	5	37.53	1.66	-14.87	0.70	0.10	0.99
P91	PM	JN.00.26	N/A	550	4	37.29	2.70	-14.70	1.14	0.12	0.99
P91	PM	All	N/A	580	15	20.58	4.23	-7.97	1.89	0.31	0.62
P91	PM	Aged	N/A	580	6	29.74	1.86	-12.21	0.84	0.08	0.98
P91	PM	New	N/A	580	7	32.69	1.36	-13.22	0.60	0.05	0.99
P91	HAZ	LICON	N/A	600	2	18.28	0.00	-7.62	0.00	0.00	1.00
P91	PM	All	N/A	600	242	21.96	0.67	-8.73	0.31	0.31	0.77
P91	PM	LICON	N/A	600	4	25.24	6.11	-10.33	2.86	0.21	0.87
P91	PM	RANTALA	N/A	600	4	27.49	4.19	-11.33	1.95	0.17	0.17
P91	PM	BE.01.4	N/A	600	5	23.33	3.92	-9.52	1.87	0.31	0.90
P91	PM	CH.02.AZ	N/A	600	10	14.31	1.42	-4.97	0.67	0.16	0.87
P91	PM	CH.02.W1	N/A	600	7	12.98	1.18	-4.26	0.56	0.10	0.92
P91	PM	CH.02.W2	N/A	600	10	14.15	1.77	-4.94	0.83	0.19	0.85
P91	PM	CH.02.W3	N/A	600	7	14.08	1.96	-4.84	0.92	0.16	0.85
P91	PM	DE.05.1	N/A	600	5	23.73	2.04	-9.55	0.94	0.23	0.97
P91	PM	DE.05.2	N/A	600	5	21.27	1.93	-8.42	0.89	0.22	0.97
P91	PM	DE.05.5	N/A	600	4	17.71	5.55	-6.61	2.52	0.42	0.77
P91	PM	GB.02.5	N/A	600	5	11.03	1.55	-3.67	0.74	0.07	0.89
P91	PM	IT.01.1	N/A	600	5	26.49	2.11	-10.83	0.98	0.07	0.98
P91	PM	IT.03.4	N/A	600	12	21.49	1.77	-8.51	0.84	0.18	0.91
P91	PM	IT.03.6	N/A	600	8	25.12	2.76	-10.22	1.30	0.13	0.91
P91	PM	JN.00.5	N/A	600	5	24.55	0.92	-9.91	0.43	0.06	0.99
P91	PM	JN.00.7	N/A	600	9	29.65	1.36	-12.42	0.63	0.12	0.98
P91	PM	JN.00.25	N/A	600	12	29.16	1.37	-12.14	0.63	0.11	0.97
P91	PM	JN.00.26	N/A	600	4	30.62	2.60	-12.74	1.20	0.21	0.98
P91	WM	LICON	N/A	600	2	20.99	0.00	-8.26	0.00	0.00	1.00

P91	XW	LICON	N/A	600	4	19.98	2.62	-8.01	1.23	0.09	0.95
P91	HAZ	LICON	N/A	625	2	22.10	0.00	-10.07	0.00	0.00	1.00
P91	PM	All	N/A	625	41	19.85	1.83	-8.23	0.90	0.39	0.91
P91	PM	HIDA	Ave	625	9	18.61	0.54	-7.53	0.27	0.03	0.99
P91	PM	HIDA	Cr	625	3	19.13	0.09	-7.78	0.05	0.00	1.00
P91	PM	HIDA	Long	625	4	18.25	0.88	-7.36	0.43	0.04	0.99
P91	PM	LICON	N/A	625	4	23.50	1.92	-10.07	0.96	0.10	0.98
P91	WM	All	N/A	625	4	19.89	–	-8.23	–	0.55	–
P91	WM	HIDA	Ave	625	2	18.12	–	-7.53	–	0.17	–
P91	WM	LICON	Ave	625	2	24.14	–	-10.07	–	0.71	–
P91	XW	All	N/A	625	8	19.06	–	-7.53	–	0.41	–
P91	XW	HIDA	Ave	625	4	17.64	–	-7.53	–	0.69	–
P91	XW	LICON	N/A	625	4	22.67	–	-10.07	–	0.36	–
P91	PM	All	N/A	650	145	17.34	0.42	-7.37	0.22	0.28	0.89
P91	PM	CH.02W2	N/A	650	6	16.47	1.15	-6.88	0.62	0.11	0.97
P91	PM	DE.05.1	N/A	650	5	17.83	0.77	-7.62	0.38	0.12	0.99
P91	PM	DE.05.2	N/A	650	5	19.35	1.07	-8.34	0.53	0.17	0.99
P91	PM	DE.05.4	N/A	650	4	16.27	3.04	-6.81	1.54	0.23	0.91
P91	PM	GB.02.4	N/A	650	6	15.32	0.73	-6.48	0.41	0.09	0.98
P91	PM	GB.02.5	N/A	650	6	14.14	0.46	-5.98	0.25	0.05	0.99
P91	PM	GB.02.6	N/A	650	6	15.68	0.79	-6.65	0.43	0.09	0.98
P91	PM	IT.01.1	N/A	650	5	15.31	1.02	-6.35	0.53	0.05	0.98
P91	PM	IT.03.4	N/A	650	18	17.78	0.64	-7.59	0.33	0.14	0.97
P91	PM	IT.08.2	N/A	650	4	21.34	0.25	-9.28	0.13	0.02	1.00
P91	PM	JN.00.5	N/A	650	7	17.90	0.20	-7.60	0.10	0.03	1.00
P91	PM	JN.00.6	N/A	650	5	21.56	1.30	-9.41	0.67	0.18	0.99
P91	PM	JN.00.7	N/A	650	14	21.36	0.44	-9.41	0.23	0.10	0.99
P91	PM	JN.00.21	N/A	650	4	19.51	0.04	-8.35	0.02	0.00	1.00
P91	PM	JN.00.23	N/A	650	4	19.88	1.77	-8.57	0.90	0.14	0.98
P91	PM	JN.00.26	N/A	650	4	22.96	1.01	-10.13	0.51	0.10	1.00
P91	PM	All	N/A	700	13	14.04	0.37	-6.48	0.21	0.12	0.99
P91	PM	JN.00.6	N/A	700	4	14.56	0.28	-6.76	0.16	0.05	1.00
P91	PM	JN.00.7	N/A	700	6	13.55	0.27	-6.20	0.16	0.06	1.00

Table C-10: Statistical results of P92 uniaxial rupture data

Material	Material condition	Casts	Orient.	Temp. [°C]	N° of tests	Log(*H*)	*SE H*	*v*	*SE v*	*SD* t_R	r^2_{STAT}
P92	PM	All	Ave	550	56	48.25	1.94	-18.84	0.80	0.30	0.91
P92	PM	All	Long	550	49	47.77	1.97	-18.63	0.81	0.29	0.92
P92	PM	JN.00.DDF	Long	550	4	70.30	6.22	-27.85	2.54	0.15	0.98
P92	PM	JN.00.E	Ave	550	9	50.38	1.18	-19.85	0.47	0.08	1.00
P92	PM	JN.00.E	Cr	550	4	52.71	1.67	-20.84	0.69	0.06	1.00
P92	PM	JN.00.E	Long	550	5	49.68	1.73	-19.58	0.71	0.10	1.00
P92	PM	JN.00.EPP	Long	550	17	45.29	2.71	-17.52	1.11	0.23	0.94
P92	PM	JN.00.YAP	Long	550	6	44.66	1.41	-17.43	0.58	0.09	1.00
P92	PM	JN.00.YAP2	Long	550	6	48.56	0.94	-19.02	0.38	0.05	1.00
P92	PM	JN.00.YBP	Long	550	5	50.82	1.42	-19.91	0.58	0.07	1.00
P92	PM	JN.02.1	Tr	550	3	38.56	10.39	-14.63	4.36	0.14	0.92
P92	PM	All	Ave	600	125	36.31	0.91	-14.76	0.40	0.35	0.91
P92	PM	All	Long	600	85	39.11	0.84	-15.97	0.37	0.25	0.96
P92	PM	DE.07.CMS	N/A	600	5	24.06	3.10	-9.06	1.38	0.10	0.94
P92	PM	DE.07.CQM	N/A	600	4	34.07	5.28	-13.72	2.40	0.19	0.94

P92	PM	DE.08.1	N/A	600	7	26.92	4.67	-10.48	2.08	0.32	0.84
P92	PM	IT.01.1	Long	600	5	41.94	2.53	-17.39	1.13	0.08	0.99
P92	PM	IT.01.2	Long	600	5	38.72	2.52	-15.92	1.13	0.08	0.99
P92	PM	JN.00.DDF	Long	600	5	38.25	2.74	-15.55	1.20	0.16	0.98
P92	PM	JN.00.E	Ave	600	15	37.98	0.98	-15.60	0.43	0.16	0.99
P92	PM	JN.00.E	Cr	600	8	36.65	1.16	-15.02	0.51	0.14	0.99
P92	PM	JN.00.E	Long	600	7	39.99	1.56	-16.46	0.68	0.16	0.99
P92	PM	JN.00.EPP	Long	600	23	40.84	0.87	-16.63	0.37	0.16	0.99
P92	PM	JN.00.YAP	Long	600	7	41.42	1.09	-17.03	0.47	0.09	1.00
P92	PM	JN.00.YAP	Long	600	10	25.85	1.00	-11.09	0.47	0.18	0.99
P92	PM	JN.00.YAP2	Long	600	8	39.86	2.71	-16.37	1.18	0.22	0.97
P92	PM	JN.00.YBP	Long	600	7	41.17	1.20	-16.88	0.52	0.11	1.00
P92	PM	JN.02.1	Tr	600	3	32.13	2.59	-12.73	1.15	0.06	0.99
P92	PM	All	Ave	625	25	29.29	1.39	-12.11	0.65	0.20	0.94
P92	PM	JN.00.EPP	Long	625	8	32.08	0.83	-13.31	0.38	0.08	1.00
P92	PM	LICON	N/A	625	6	27.17	2.31	-11.13	1.08	0.10	0.96
P92	PM	All	Ave	650	130	24.52	0.47	-10.40	0.23	0.28	0.94
P92	PM	All	Long	650	88	25.06	0.52	-10.66	0.25	0.27	0.96
P92	PM	DE.07.CMS	N/A	650	5	22.62	2.36	-9.24	1.13	0.15	0.96
P92	PM	DE.07.CQM	N/A	650	7	25.33	1.88	-10.79	0.92	0.23	0.96
P92	PM	DE.08.1	N/A	650	6	18.81	0.87	-7.49	0.43	0.11	0.99
P92	PM	IT.01.1	Long	650	5	14.58	1.81	-5.56	0.89	0.11	0.93
P92	PM	JN.00.DDF	Long	650	5	22.76	1.81	-9.55	0.87	0.16	0.98
P92	PM	JN.00.E	Ave	650	13	24.25	0.87	-10.42	0.41	0.19	0.98
P92	PM	JN.00.E	Cr	650	6	23.87	0.91	-10.22	0.44	0.13	0.99
P92	PM	JN.00.E	Long	650	7	24.41	1.51	-10.51	0.71	0.25	0.98
P92	PM	JN.00.EPP	Long	650	24	24.74	0.91	-10.44	0.43	0.29	0.96
P92	PM	JN.00.YAP	Long	650	10	25.85	1.00	-11.09	0.47	0.18	0.99
P92	PM	JN.00.YAP2	Long	650	7	26.13	0.11	-11.22	0.50	0.16	0.99
P92	PM	JN.00.YBP	Long	650	7	27.98	1.40	-12.05	0.65	0.23	0.99
P92	PM	JN.02.1	Ave	650	8	20.37	1.09	-8.23	0.53	0.08	0.98
P92	PM	JN.02.1	Tr	650	5	20.55	0.92	-8.33	0.44	0.05	0.99
P92	PM	LICON	N/A	650	5	22.95	3.69	-9.61	1.81	0.22	0.90
P92	WM	LICON	N/A	650	2	22.55	–	-9.61	–	0.10	–
P92	XW	LICON	N/A	650	4	22.50	–	-9.61	–	0.17	–
P92	PM	All	Ave	700	70	16.55	0.35	-7.46	0.18	0.22	0.96
P92	PM	All	Long	700	64	16.50	0.37	-7.43	0.19	0.23	0.96
P92	PM	JN.00.DDF	Long	700	4	16.13	0.97	-7.26	0.51	0.11	0.99
P92	PM	JN.00.E	Ave	700	9	18.77	0.36	-8.63	0.18	0.06	1.00
P92	PM	JN.00.E	Cr	700	4	18.02	0.46	-8.24	0.23	0.04	1.00
P92	PM	JN.00.E	Long	700	5	19.21	0.50	-8.85	0.25	0.06	1.00
P92	PM	JN.00.EPP	Long	700	18	17.18	0.64	-7.67	0.33	0.22	0.97
P92	PM	JN.00.YAP	Long	700	7	15.53	1.05	-6.95	0.57	0.23	0.97
P92	PM	JN.00.YAP2	Long	700	10	15.47	0.61	-6.96	0.33	0.19	0.98
P92	PM	JN.00.YBP	Long	700	5	18.45	0.84	-8.53	0.43	0.16	0.99
P92	PM	All	Long	750	8	12.53	0.71	-6.23	0.40	0.17	0.98

In this appendix, a summary of the main statistical analyses tabulated in Appendices D and E is given. In fact, this summary contains only the statistical analyses from all batches combined. The uniaxial results presented here can be seen as references values of $\mathrm{Log}(A_s)$, n_s, $SD\ \dot{\varepsilon}_s$, $\mathrm{Log}(A_{Ave})$, n_{Ave}, $SD\ \dot{\varepsilon}_{Ave}$, $\mathrm{Log}(H)$, v and $SD\ t_R$, when very little or no information is available for the five materials. The notation is similar to the one defined in Appendices D and E.

Table C-6: Summary of the principal statistical results of uniaxial for secondary creep strain rate

Material	Material condition	Casts	Orient.	Temp. [°C]	N° of tests	Log(A_s)	*SE* A_s	n_s	*SE* n_s	*SD* $\dot{\varepsilon}_s$	r^2_{STAT}
316L(N)	PM	All	Long	550	110	-30.21	1.92	10.15	0.76	0.43	0.75
316L(N)	PM	All	Long	600	126	-25.02	0.75	8.76	0.32	0.39	0.86
316L(N)	PM	All	Long	650	87	-22.34	0.72	8.27	0.32	0.38	0.88
316L(N)	PM	All	Long	700	23	-17.28	0.94	6.63	0.46	0.36	0.91
316L(N)	PM	All	Long	750	15	-14.33	0.71	5.78	0.37	0.26	0.95
P22	PM	HIDA	Ave	565	7	-28.76	1.65	11.76	0.79	0.17	0.98
P91	PM	Aged	N/A	580	6	-33.06	2.11	13.11	0.95	0.09	0.98
P91	PM	New	N/A	580	7	-36.88	2.84	14.49	1.25	0.12	0.98
P91	PM	All	N/A	625	12	-22.95	2.90	8.96	1.42	0.21	0.90
P92	PM	All	Ave	600	39	-38.14	1.81	14.88	0.81	0.40	0.90
P92	PM	All	Long	600	24	-40.88	2.30	16.13	1.01	0.35	0.92
P92	PM	All	Ave	625	10	-42.81	4.14	17.64	1.94	0.28	0.91
P92	PM	All	Ave	650	31	-28.50	1.29	11.56	0.62	0.35	0.92
P92	PM	All	Long	650	14	-27.69	1.71	11.23	0.80	0.35	0.94
P92	PM	All	Ave	700	10	-20.02	0.79	8.53	0.40	0.17	0.98
P92	PM	All	Long	700	9	-19.96	0.86	8.51	0.44	0.18	0.98
P92	PM	All	Long	750	3	-16.01	0.72	7.35	0.39	0.03	1.00

Table C-7: Summary of the statistical results of uniaxial for average creep strain rate

Material	Material condition	Casts	Orient.	Temp. [°C]	N° of tests	Log(A_{Ave})	*SE* A_{Ave}	n_{Ave}	*SE* n_{Ave}	*SD* $\dot{\varepsilon}_{Ave}$	r^2_{STAT}
316L(N)	PM	All	Long	550	127	-33.25	1.58	11.74	0.63	0.38	0.74
316L(N)	PM	All	Long	600	124	-24.82	0.95	8.96	0.40	0.34	0.81
316L(N)	PM	All	Long	650	82	-19.68	0.79	7.37	0.35	0.34	0.85
316L(N)	PM	All	Long	700	24	-15.22	0.81	5.98	0.39	0.28	0.91
316L(N)	PM	All	Long	750	15	-13.74	0.41	5.78	0.21	0.15	0.98
P22	PM	HIDA	Ave	565	7	-25.69	1.64	10.57	0.79	0.17	0.97
P91	PM	All	N / A	500	11	-55.02	2.29	20.81	0.92	0.14	0.98
P91	PM	All	N / A	550	110	-36.31	2.03	13.87	0.87	0.54	0.70
P91	PM	Aged	N/A	580	6	-29.99	2.13	12.03	0.96	0.09	0.98
P91	PM	New	N/A	580	7	-35.38	2.29	14.14	1.01	0.09	0.98
P91	PM	All	N / A	600	238	-24.00	0.81	9.41	0.38	0.42	0.72
P91	PM	All	N / A	625	37	-21.96	2.43	8.94	1.19	0.22	0.92
P91	PM	All	N / A	650	145	-19.06	0.49	7.98	0.25	0.32	0.87
P91	PM	All	N / A	700	13	-14.96	0.48	6.71	0.27	0.16	0.98
P92	PM	All	Ave	550	56	-49.53	1.98	19.13	0.82	0.31	0.91
P92	PM	All	Long	550	49	-49.15	2.03	18.97	0.83	0.30	0.92
P92	PM	All	Ave	600	125	-40.13	1.06	16.15	0.47	0.40	0.91
P92	PM	All	Long	600	84	-41.82	0.95	16.90	0.42	0.29	0.95
P92	PM	All	Ave	625	25	-34.46	2.03	14.19	0.94	0.29	0.91
P92	PM	All	Ave	650	130	-28.14	0.53	11.81	0.25	0.32	0.94
P92	PM	All	Long	650	88	-27.98	0.55	11.76	0.26	0.28	0.96
P92	PM	All	Ave	700	70	18.37	0.38	8.13	0.20	0.24	0.96
P92	PM	All	Long	700	64	-18.33	0.40	8.11	0.21	0.24	0.96
P92	PM	All	Long	750	8	-13.83	0.71	6.74	0.40	0.17	0.98

Table C-8: Summary of the principal statistical results of uniaxial for rupture data

Material	Material condition	Casts	Orient.	Temp. [°C]	N° of tests	Log(*H*)	*SE H*	*v*	*SE v*	*SD* t_R	r^2_{STAT}
316L(N)	PM	All	Long	550	127	30.25	1.42	-10.79	0.57	0.35	0.74
316L(N)	PM	All	Long	600	127	25.39	0.87	-9.38	0.37	0.32	0.84
316L(N)	PM	All	Long	650	84	19.51	0.70	-7.42	0.31	0.30	0.87
316L(N)	PM	All	Long	700	24	15.63	0.72	-6.26	0.35	0.25	0.94
316L(N)	PM	All	Long	750	15	13.05	0.36	-5.47	0.19	0.13	0.99
P22	PM	HIDA	Ave	565	7	22.63	0.94	-9.35	0.45	0.09	0.99
P91	PM	All	N/A	500	11	55.48	1.68	-21.22	0.68	0.10	0.99
P91	PM	All	N/A	550	112	33.37	1.65	-12.89	0.71	0.46	0.75
P91	PM	All	N/A	600	242	21.96	0.67	-8.73	0.31	0.31	0.77
P91	PM	All	N/A	625	41	19.85	1.83	-8.23	0.90	0.39	0.91
P91	PM	All	N/A	650	145	17.34	0.42	-7.37	0.22	0.28	0.89
P91	PM	All	N/A	700	13	14.04	0.37	-6.48	0.21	0.12	0.99
P92	PM	All	Ave	550	56	48.25	1.94	-18.84	0.80	0.30	0.91
P92	PM	All	Long	550	49	47.77	1.97	-18.63	0.81	0.29	0.92
P92	PM	All	Ave	600	125	36.31	0.91	-14.76	0.40	0.35	0.91
P92	PM	All	Long	600	85	39.11	0.84	-15.97	0.37	0.25	0.96
P92	PM	All	Ave	625	25	29.29	1.39	-12.11	0.65	0.20	0.94
P92	PM	All	Ave	650	130	24.52	0.47	-10.40	0.23	0.28	0.94
P92	PM	All	Long	650	88	25.06	0.52	-10.66	0.25	0.27	0.96
P92	PM	All	Ave	700	70	16.55	0.35	-7.46	0.18	0.22	0.96
P92	PM	All	Long	700	64	16.50	0.37	-7.43	0.19	0.23	0.96
P92	PM	All	Long	750	8	12.53	0.71	-6.23	0.40	0.17	0.98

Appendix D

Fracture Mechanics Formulae for Laboratory Specimens

In this appendix the formulae for evaluating laboratory specimen data are given. They include, for the CT and the C-ring specimens, the non-dimensional geometry function (Y) in the stress intensity factor solutions, the different reference stress solutions, σ_{ref}, and the factor relating J to the area under the load-line displacement curve in the plastic regime, η_{pl} which is used to calculate the experimental creep fracture parameter C^*.

CT specimen [Miller, 1988; Webster 1994; Commissariat à l'Energie Atomique, 1995; Charlton, 1998 and ASTM, 2001b and 2001d]

$$Y^{CT} = \frac{\left(2+\frac{a}{W}\right)\cdot\left(0.866+4.64\cdot\left(\frac{a}{W}\right)-13.32\left(\frac{a}{W}\right)^2+14.72\cdot\left(\frac{a}{W}\right)^3-5.6\cdot\left(\frac{a}{W}\right)^4\right)}{\sqrt{\pi\cdot\frac{a}{W}}\cdot\left(1-\frac{a}{W}\right)^{3/2}} \qquad \text{(E-1)}$$

$$\sigma^{CT}_{p\sigma,VM} = \frac{P}{B\cdot W}\cdot\frac{1}{-\left(1+\gamma\cdot\frac{a}{W}\right)+\sqrt{\left(1+\gamma\cdot\left(\frac{a}{W}\right)^2\right)\cdot(1+\gamma)}} \qquad \text{(E-2)}$$

where $\gamma = 2/\sqrt{3}$

$$\sigma^{CT}_{p\sigma,Tresca} = \frac{P}{B\cdot W}\cdot\frac{1}{-\left(1+\frac{a}{W}\right)+\sqrt{\left(2+2\cdot\left(\frac{a}{W}\right)^2\right)}} \qquad \text{(E-3)}$$

$$\sigma^{CT}_{p\varepsilon,VM} = \frac{P}{B\cdot W}\cdot\frac{1}{\frac{2}{\sqrt{3}}\left[-\left(1+\gamma\cdot\frac{a}{W}\right)+\sqrt{(1+\gamma)\cdot\left\{1+\gamma\cdot\left(\frac{a}{W}\right)^2\right\}}\right]} \qquad \text{(E-4)}$$

where $\gamma = 1.702$

$$\sigma^{CT}_{p\varepsilon,Tresca} = \frac{P}{B\cdot W}\cdot\frac{1}{\left[-\left(1+\gamma\cdot\frac{a}{W}\right)+\sqrt{(1+\gamma)\cdot\left\{1+\gamma\cdot\left(\frac{a}{W}\right)^2\right\}}\right]} \qquad \text{(E-5)}$$

where $\gamma = 1.702$

$$\eta_{pl}^{CT} = 2 + 0.522 \cdot \left(1 - \frac{a}{W}\right) \tag{E-6}$$

C specimen [Miller, 1988;Charlton, 1998 and ASTM, 2001b]

$$Y^C = \sqrt{\frac{W}{\pi \cdot a}}\left[3.4 + 1.1 \cdot \left(\frac{a}{W}\right)\right]\left[1 + 0.25 \cdot \left(1 - \frac{a}{W}\right)^2 \cdot \left(1 - \frac{R_i}{R_o}\right)\right] \cdot \frac{(a/W)^{1/2}}{(1 - a/W)^{3/2}} \times \left\{3.74 - 6.30 \cdot \left(\frac{a}{W}\right) + 6.32 \cdot \left(\frac{a}{W}\right)^2 - 2.43 \cdot \left(\frac{a}{W}\right)^3\right\} \tag{E-7}$$

$$\sigma_{p\sigma,VM}^C = \frac{P}{B \cdot W} \cdot \frac{1}{-\gamma \cdot \left(\frac{1}{2} + \frac{a}{W}\right) - \frac{3}{2} + \sqrt{\frac{1}{4}\left[\gamma \cdot \left(1 + 2 \cdot \frac{a}{W}\right) + 3\right]^2 + \left(1 - \frac{a}{W}\right)^2}} \tag{E-8}$$

where $\gamma = 2/\sqrt{3}$

$$\sigma_{p\varepsilon,VM}^C = \frac{P}{B \cdot W} \cdot \frac{1}{\frac{2 \cdot 1.26 \cdot}{\sqrt{3}}\left\{-\gamma\left(\frac{1}{2} + \frac{a}{W}\right) - \frac{3}{2} + \sqrt{\frac{1}{4}\left[\gamma\left(1 + 2\frac{a}{W}\right) + 3\right]^2 + \left(1 - \frac{a}{W}\right.\right.}} \tag{E-9}$$

where $\gamma = 2/\sqrt{3}$

$$\eta_{pl}^C = -\left\{-\gamma \cdot \left(\frac{1}{2} + \frac{a}{W}\right) - \frac{3}{2} + \sqrt{\frac{1}{4} \cdot \left[\gamma \cdot \left(1 + 2 \cdot \frac{a}{W}\right) + 3\right]^2 + \gamma \cdot \left(1 - \frac{a}{W}\right)^2}\right\}^{-1} \times \left\{-\gamma + \frac{1}{2} \cdot \left[\frac{1}{4} \cdot \left\{\gamma \cdot \left(1 + 2 \cdot \frac{a}{W}\right) + 3\right\}^2 + \gamma \cdot \left(1 - \frac{a}{W}\right)\right]^{-1/2}\left[\gamma \cdot (\gamma + 1) \cdot \left(1 + 2 \cdot \frac{a}{W}\right)\right]\right\} \tag{E-10}$$

Appendix E

Creep Crack Growth Experimental Results

The key materials property data for a high temperature fitness-for-service assessment are creep strain, creep rupture and creep and fatigue crack growth information. Given below are the tables (E1-E4) of creep crack growth test matrices performed or collated under the HIDA, LICON and FITNET projects by the different partners. The test conditions and global results are contained in these tables and statistically analyzed. It should be noted that in some cases there are only few tests performed and therefore the degree of confidence in the properties would be lower.

Notation:

Orient. : Orientation
Spec. : Specimen size

Temp. : Temperature
Log(D) : Logarithm base 10 of D in the creep crack growth law
SE D : Standard error of D in logarithm base 10
ϕ : Creep exponent in the rupture law
SE ϕ : Standard error of ϕ
SD $\dot{a}_{ss}$: Standard deviation of the error of the creep crack growth rate
Log(D_i) : Logarithm base 10 of D_i in the initiation law
SE D_i : Standard error of D_i in logarithm base 10
ϕ_i : Creep exponent in the initiation law
SE ϕ_i : Standard error of ϕ_i
SD t_i : Standard deviation of the error of the initiation times
r^2_{STAT} : Coefficient of determination
Instit. : Institution which carried out the test
P : Applied load on the specimen
W : Width of the specimen
B : Thickness of the specimen
B_N : Net thickness of the specimen
a_{ini} : Initial crack length
a_{fin} : Final crack length
$da/dt=DC^{*\phi}$: Creep crack growth rate relationship versus C*
CCG Creep Crack Growth Rate
CCI Creep Crack Initiation at 0.2mm crack extension $a_i=D_iC^{*\phi i}$

Statistical Analyses of CCG and CCI Experimental Results

Given below are the tables (E1-E3) which can be used as reference values of Log(D), ϕ, *SD* $\dot{a}_{ss}$, Log(D_i), ϕ_I and *SD* t_i, in the *CCG and CCI* when very little or no information is available for the five materials. Table E4 gives an average summary of the results for the relationship $da/dt=DC^{*\phi}$

Table E-1: Statistical results of Creep Crack Growth (CCG) tests

Material	Material condition	Casts	Orient.	Spec.	Temp. [°C]	N° of tests/points	Log(D)	$SE\ D$	ϕ	$SE\ \phi$	$SD\ \dot{a}_{ss}$	r^2_{STAT}
316L(N)	PM	HIDA	N/A	CT25	650	2 / 21	0.013	0.035	0.672	0.010	0.073	0.995
316L(N)	PM	HIDA	N/A	CT50	650	3 / 36	0.381	0.108	0.735	0.038	0.226	0.914
316L(N)	PM	PROFIS	N/A	CT50	650	2 / 33	1.124	0.091	1.085	0.024	0.072	0.984
316L(N)	PM	All	N/A	CT	650	7 / 90	0.438	0.093	0.834	0.028	0.300	0.910
P22	HAZ	HIDA	Cr	CT25	565	2 / 41	1.277	0.054	0.883	0.010	0.089	0.992
P22	HAZ	HIDA	Long	CT25	565	2 / 35	1.323	0.073	0.813	0.013	0.091	0.983
P22	HAZ	HIDA	All	CT25	565	4 / 76	1.340	0.089	0.874	0.022	0.187	0.955
P22	PM	HIDA	Cr	CT25	565	5 / 91	0.550	0.048	0.695	0.012	0.133	0.975
P22	PM	HIDA	Long	CT25	565	2 / 24	0.125	0.061	0.588	0.014	0.054	0.987
P22	PM	HIDA	All	CT25	565	7 / 115	0.510	0.043	0.684	0.011	0.126	0.973
P22	PM	HIDA	Cr	CT50	565	1 / 19	0.785	0.092	0.733	0.026	0.085	0.979
P22	PM	HIDA	All	CT	565	8 / 134	0.556	0.040	0.692	0.010	0.127	0.973
E911	PM	LICON	N/A	C25	625	2 / 32	1.700	0.113	0.917	0.024	0.074	0.980
E911	PM	LICON	N/A	C25	625	2 / 50	2.227	0.092	0.979	0.021	0.094	0.978
E911	PM	LICON	N/A	C25	625	2 / 101	2.353	0.079	0.985	0.020	0.083	0.962
P91	HAZ	HIDA	N/A	CT25	625	2 / 29	5.162	0.682	1.512	0.127	0.262	0.839
P91	HAZ	ELSAM	All	CT50	580	2 / 32	1.578	0.167	0.917	0.048	0.114	0.923
P91	PM	HIDA	Cr	CT25	625	3 / 23	0.116	0.313	0.659	0.075	0.255	0.783
P91	PM	HIDA	Long	CT25	625	2 / 22	-0.170	0.366	0.496	0.085	0.172	0.792
P91	PM	HIDA	All	CT25	625	5 / 34	-0.091	0.319	0.577	0.075	0.301	0.644
P91	PM – Aged	ELSAM	N/A	CT50	580	2 / 52	0.400	0.046	0.662	0.014	0.059	0.979
P91	PM - New	ELSAM	N/A	CT50	580	3 / 49	0.355	0.127	0.684	0.036	0.134	0.886
P91	PM	ELSAM	N/A	CT50	580	5 / 101	0.432	0.071	0.688	0.020	0.118	0.919
P91	PM	LICON	N/A	C25	600	6 / 109	0.694	0.083	0.698	0.018	0.160	0.932
P91	WM	ELSAM	N/A	CT50	580	3 / 58	1.443	0.143	0.880	0.038	0.143	0.904
P91	XW	LICON	N/A	C25	600	2 / 22	1.629	0.111	0.843	0.025	0.093	0.983
P92	PM	LICON	N/A	C25	625	2 / 47	0.929	0.055	0.750	0.015	0.113	0. 982
P92	XW	LICON	N/A	C25	625	1 / 6	3.228	0.226	1.207	0.053	0.032	0.992

Table E-2: Statistical results of Creep Crack Initiation (CCI) tests for Δa = 0.2 mm

Material	Material condition	Casts	Orient.	Spec.	Temp. [°C]	N° of tests	Log(D_i)	$SE\ D_i$	ϕ_i	$SE\ \phi_i$	$SD\ t_i$	r^2_{STAT}
316L(N)	PM	HIDA	N/A	CT50	650	3	-1.011	0.785	0.815	0.294	0.308	0.885
P22	PM	HIDA	Cr	CT25	565	6	-1.429	0.722	0.847	0.145	0.177	0.985
E911	XW	LICON	N/A	C25	625	3	-5.436	0.040	1.551	0.008	0.007	0.999
P91	PM	PROFIS	N/A	CT50	580	3	-0.650	1.243	0.673	0.320	0.320	0.816
P91	PM	HIDA	Cr	CT25	625	3	0.556	2.056	0.430	0.457	0.745	0.470
P91	PM	LICON	N/A	C25	600	9	-1.312	1.469	0.849	0.279	0.249	0.568
P91	WM	PROFIS	N/A	CT50	580	3	0.085	0.715	0.406	0.181	0.116	0.834

Table E-3: Statistical results of Creep Crack Initiation (CCI) tests for Δa = 0.5 mm

Material	Material condition	Casts	Orient.	Spec.	Temp. [°C]	N° of tests	Log(D_i)	SE D_i	$-\phi_i$	SE ϕ_i	SD t_i	r^2_{STAT}
316L(N)	PM	HIDA	N/A	CT50	650	3	0.137	1.540	0.466	0.494	0.648	0.470
P22	PM	HIDA	Cr	CT25	565	6	0.146	0.565	0.602	0.117	0.157	0.869
E911	PM	LICON	N/A	C25	625	3	2.147	6.275	0.187	1.221	0.239	0.023
E911	XW	LICON	N/A	C25	625	3	-4.668	1.059	1.472	0.225	0.175	0.977
P91	PM	PROFIS	N/A	CT50	580	3	-0.951	0.383	0.833	0.097	0.096	0.987
P91	PM	HIDA	Cr	CT25	625	3	-0.632	0.227	0.749	0.050	0.057	0.996
P91	PM	LICON	N/A	C25	600	6	0.714	1.030	0.525	0.193	0.160	0.648
P91	WM	PROFIS	N/A	CT50	580	3	-0.918	0.630	0.749	0.154	0.111	0.959

Table E4: Summarized average best estimate creep crack growth properties from all tests

Material	Condition	Temp ^oC	ε_f	D	ϕ
P22	parent	565	0.37	5.2	0.85
P22	weld	565	0.07	3.5	0.64
P91	parent	-	0.13	1.8	0.63
P91	weld	-	0.02	20	0.80
1Cr_cast	parent	530	0.22	4.2	0.72
1Cr_forged	parent	540-550	0.17	2.5	0.69
316SS	parent	550.625	-	2.3	0.74
316HAZ	parent	510,525,560	-	2.4	0.69

Where ε_f is the uniaxial ductility

Using $da/dt=DC^{*\phi}$ where C^* is in $MJ/m^2\ h$ and is in mm/hour

Assessments of the type described above have been performed for a range of materials and data were collated during the FITNET project as illustrated in Table E4 for creep crack growth data. More recently, long-term creep crack growth data have been obtained from tests lasting several years and these indicate that data are approximately inversely proportional to material ductility as suggested by the models discussed in the main text. Thus, where materials are known to have low long-term ductility, caution must be exercised in using creep crack growth data from short-term tests in which the representative ductility is higher, possibly because the failure mechanism differs at long times.

Table E4. Typical Creep crack growth data collated during the FITNET project. Constants are those in eqn (27) with $\dot{a}$ in units of m/h and C* in units of MPa m/h.

Material	Temperature (°C)	Upper Bound		Mean	
		A	q	A	q
Plain C steels	482 - 538	0.015	1.0	0.006	1.0
½CrMoV, wrought and cast	500 - 600	0.06	0.80	0.006	0.80
½CrMoV, Type IV	540 - 565	0.15	0.80	0.007	0.80
½CrMoV, coarse HAZ	565	0.30	0.80	0.10	0.80
1CrMo	450-600	0.02	0.84	0.006	0.84
1CrMoV	538 - 594	0.015	0.75	0.005	0.79
2¼Cr1Mo weld metal	540 - 565	0.015	0.647	0.003	0.647
2¼Cr1Mo wrought	550 - 600	0.006	0.80	0.004	0.83
Type 304 and Type 304H	650 - 760	0.035	1.0	0.007	1.0
Type 304, service exposed	760	0.10	0.85	0.05	0.85
Type 321, wrought	650	0.02	0.90	0.005	0.90
Type 316 and 316H, Wrought					
short term	500 - 550	0.021	0.81	0.005	0.81
Medium term	500 - 550	0.007	0.62	.001	0.54
Long term	500 - 550	0.22	0.89	0.088	0.89
Type 316 weld	600 - 650	0.06	0.876	0.01	0.876
Inconel 800H	800	0.08	0.90	0.025	0.90
In 939	850	0.20	1.0	0.04	1.0
Modified 9Cr	580 - 593	0.005	0.65	0.003	0.70
Aluminium alloy RR 58	150	2.5	0.85	1.5	0.85
Aluminium alloy 2519 - T851	135	0.35	0.90	0.175	0.90
Astroloy API	700	0.124	0.78	0.054	0.79

New R5 Proposed Equations for 316H data

The proposed new equations for predicting long-term creep crack growth rates in Type 316H steel, as summarised in the table above, are given in more detail below. Mean (E1-E3) and upper bound (E4-E6) creep crack growth rates are:

$da/dt = 0{:}088C^{*0{:}891}$ $C^* \leq 3\text{x}10^{-6}$ MPa mh^{-1} (E1)

$da/dt = 0.0011C^{*.543}$ $3\text{x}10^{-6} < C^* < 3\text{x}10^{-3}$ MPa mh^{-1} (E2)

$da/dt = 0.005C^{*0{:}.811}$ $C^* \geq 3\text{x}10^{-3}$ MPa mh^{-1} (E3)

$da/dt = 0.221C^{*0:891}$ $C^* \leq 3x10^{-6}$ MPa mh^{-1} (E4)

$da/dt = 0.007C^{*0:618}$ $3x10^{-6} < C^* < 3x10^{-3}$ MPa mh^{-1} (E5)

$da/dt = 0.021C^{*0:811}$ $C^* \geq 3x10^{-3}$ MPa mh^{-1} (E6)

These new proposals as shown in equations E1-E6 update the creep crack growth data for ex-service Type 316H materials at 525 and 550 C. The proposals provide a significantly improved description of the creep crack growth data, particularly in the low C^* regime.